Climate Variability in Tasmania Based on Dendroclimatic Studies of *Lagarostrobos Franklinii*

by

Brendan M. Buckley, BSc, MA

Submitted in fulfilment

of the requirements

for the degree of

Doctor of Philosophy

Institute of Antarctic and Southern Ocean Studies

University of Tasmania

Hobart

Australia

March, 1997

Declaration

This is to certify that this thesis contains no material which has been accepted for a degree or diploma by the University or any other institution, except by way of background information and duly acknowledged in the thesis, and to the best of my knowledge and belief no material previously published or written by another person except where due acknowledgement is made in the text of the thesis.

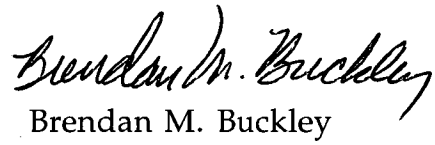

Brendan M. Buckley

Authority of Access

This thesis may be made available for loan and limited copying in accordance with the Copyright Act 1968.

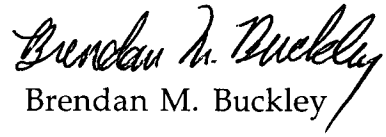

Brendan M. Buckley

ABSTRACT:

Four new Huon pine ring-width chronologies complete a seven-chronology network from western Tasmania, and span an elevationial range from 200 to 950 metres above sea level. The new chronologies are from relict stands in the Frenchmans Cap area of western Tasmania, and range from 451 to 1925 years in length. Two are from rare subalpine sites above 800 metres, and two are from 550 and 700 metres, respectively. The sample depth in the earliest portion of the 950 metre-high chronology from Mt. Read, from which a 2792 year reconstruction of warm season temperature was previously derived, is substantially improved through the inclusion of several subfossil logs. The crossdating of ring sequences, and the climatic responses of the three earlier chronologies is confirmed. The chronology network enables a more complete analysis of Huon pine's climatic response throughout much of its latitudinal and elevational range. An improved temperature time-series (a composite of 9 coastal or near-coastal records surrounding Tasmania) is used for the calibration and verification of the climate response. Response function analyses clearly define the seasonal influence of temperature and preciptiation on Huon pine growth. An elevation dependence of the temperature response is revealed, reflecting the stratification of the climate in mountainous western Tasmania. This vertical structure is due to the effects of orographic uplift of westerly and southwesterly airflow, combined with a persistent subsidence-inversion layer above 700 metres. Apparent changes in the mean height of a persistent cloud zone (from 820 - 930 metres) are coincident with recent warming in the region. These changes appear to be associated with a poleward migration of the mean latitude of the Subtropical High Pressure Belt, and slackened zonal circulation. New reconstructions of temperature help define the regional extent of the climate signal from this region. Several unique qualities make Huon pine a valuable resource for palaeoenvironmental research, in particular the tremendous preservation properties of its wood which can survive for many thousands of years. The abundance of subfossil logs at most sites allows for great sample depth through time. Very long ring sequences allow for the preservation of low-frequency signals in the chronology indices, normally not afforded by dendroclimatological reconstructions. Such low-frequency signals are critical for the detection of natural climate variability on timescales of centuries to millennia, and allow for a more accurate assessment of recent trends in regional climate.

Acknowledgements

I wish to offer my gratitude to more people than I can possibly mention here, and to those whose names I have forgotten I can only offer my sincerest apologies, along with my thanks. Firstly, I wish to thank my supervisors at the University of Tasmania, Dr. Andrew McMinn (IASOS) and Dr. Guus Van de Geer (Geography). Thanks to my "unofficial" supervisor, Dr. Edward Cook from Lamont-Doherty Earth Observatory in the USA. I can never fully repay the mountains of assistance, inspiration, and patience I have received over the past 7 years of working for, and with him. I would never have seen Huon pine were it not for Ed, and this project would not have been possible without his constant support and encouragement. To my good friends and colleagues, Dr. Mike Barbetti from the University of Sydney, and Dr. Roger Francey, from CSIRO in Aspendale, I am eternally grateful for the confidence they have shown in me, and the sound scientific and personal support over the past 4 years. In Tasmania there are several people whose expertise and assistance were critical to the success of this project. Foremost among them are Trevor Bird from the Forests & Forest Industry Council of Tasmania, and Mike Peterson from Forestry Tasmania. Their vast local knowledge and expertise, and their great mateship, has left me forever in their debt. To the many who assisted with the often difficult fieldwork I owe a huge thanks, with the hope that I might someday return the favour; Garn Cooper, Rob Wilson, Annie Wong, Kathy Allen, Rob Argent, Adrian Lewis, Daryl Mummery, Paul Krusic, and Dave Stahle. I thank David Pepper from the University of Sydney for sharing his hard-earned meteorological data from Mt. Read, and thanks to Anne La Sala, from CSIRO Forestry in Hobart, for helping us get the AWS up there in the first place. Thanks to the folks at the Department of Parks, Wildlife & Heritage for their support and assistance with the field work, and to Pasminco and Telecom for permission to use the road to access the field site on Mt. Read. Dr. Mike Pook, Dr. Tim Gibson, and Dr. Andrew Ruddell (from the Antarctic CRC, Hobart) reviewed a related manuscript, and offered important discussions and comments regarding this research. And finally, my biggest thanks are reserved for my best friend and companion Annie, to whom my gratitude for simply being able to tolerate me for so long where others have failed, can never be properly expressed. This project was funded through a grant from the National Greenhouse Advisory Committee of the Commonwealth of Australia.

TABLE OF CONTENTS

LIST OF PLATES

LIST OF FIGURES

LIST OF TABLES

DEFINITIONS AND ABREVIATIONS

AMSL = Above mean sea level

AR = Autoregression

HAR = Harman River Huon pine site

LJH = Lake Johnston Huon pine site

LMH = Lake Marilyn High Huon pine site

LML = Lake Marilyn Low Huon pine site

LVH = Lake Vera Huon pine site

PCA = Principal Component Analysis

RCYBP = Radiocarbon years before present

SLP = Sea level pressure

SRT = Stanley River Huon pine site

SST = Sea surface temperature

TTRP = Tasmanian Tree-Ring Project, refers to the following body of published work on Huon pine in Tasmania: Cook *et al.*, 1991; 1992; 1995a; 1996a; 1996b.

DEDICATION

This thesis is dedicated to the memory of my father, Robert A. Buckley.

CHAPTER 1: INTRODUCTION

1.1 Preamble

Relatively little is known about the variability of climate in the Southern Hemisphere, compared to the Northern Hemisphere. Instrumental records from south of the equator seldom cover more than the past 100 years (Barry, 1978; Jones and Briffa, 1992). Southern Hemisphere records are also poorly represented in a spatial sense, due to the paucity of landmass in the temperate zone. Therefore, proxy climate records obtained from ice cores, tree rings, corals, marine and terrestrial sediments are critical for the supplementation of instrumental and historical records of climate. At present, the best sources for long, high-resolution records from the Southern Hemisphere are derived from Antarctic ice cores and tree rings from temperate zone conifers in South America, New Zealand and Tasmania. The best source for long, annually-resolved proxy records of climate in the temperate zone is from tree-rings.

Dendroclimatic research in the Southern Hemisphere has been limited by the lack of land mass, particularly in the temperate zone between 30° and 60° S, where suitable trees are most likely to be located (Hughes *et al.*, 1982). Eighty percent of the Southern Hemisphere is comprised of ocean, and only 10% of that total land mass falls within the temperate zone. This paucity of land also accounts for the scarcity of detailed meteorological data from south of the equator (Salinger, 1979; 1982a; 1982b), which in turn contributes to the difficulties involved in verifying and calibrating tree-growth/climate relationships.

The Tasmania/New Zealand sector of the Southern Ocean (Figure 1.1) is one region which has experienced warming over recent decades (e.g., Salinger and Gunn, 1975; Bindoff and Church, 1992; Cook *et al.*, 1992; D'Arrigo *et al.*, 1995; Rudell, 1995). This region may be important for the early detection of any accelerated warming related to anthropogenic

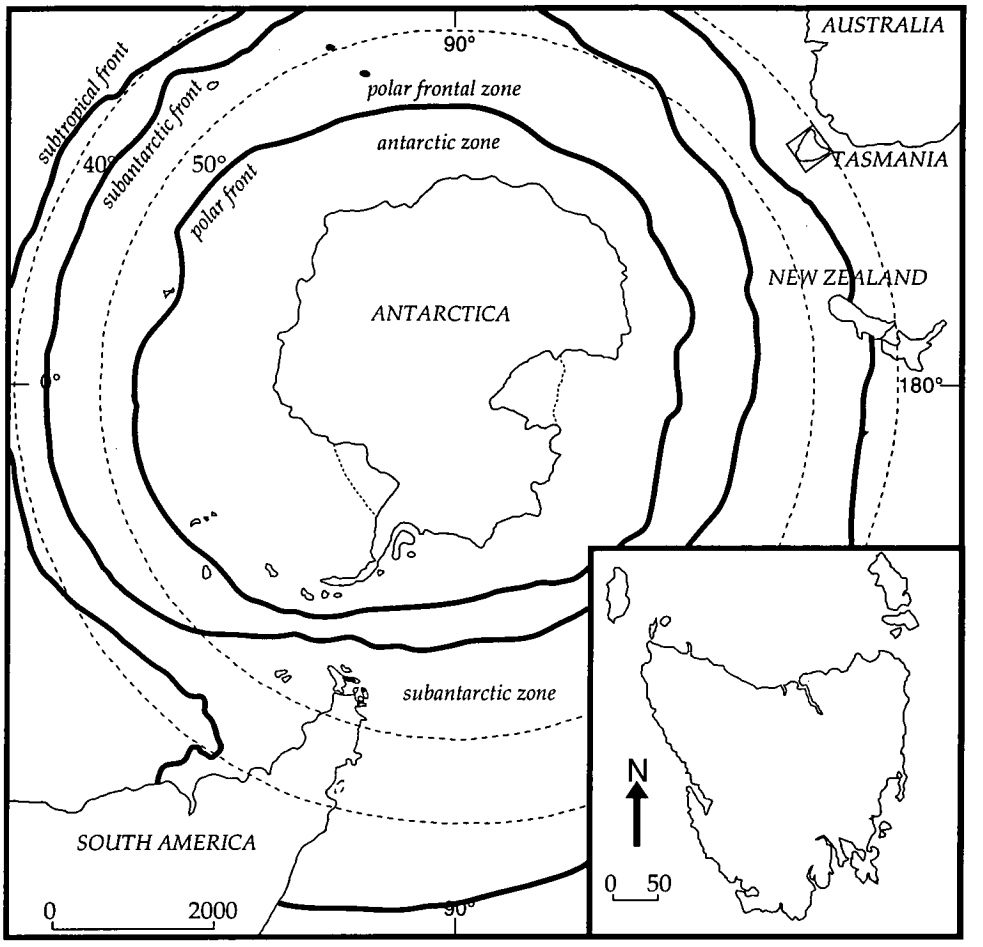

Figure 1.1. The three major oceanographic boundaries and regions of the Southern Ocean, showing Tasmania's location adjacent to the Subtropical Front. (Adapted from Nowlin and Klinck, 1986)

production of greenhouse gases, due to its proximity to the Subtropical Front and the Subantarctic Zone of Nowlin and Klinck (1986), and its apparent sensitivity to climate variability on decadal or greater timescales (Cook *et al.*, 1995a). This region is also located in a poorly represented part of the International Geosphere-Biosphere Project's (IGBP) Past Global Changes (PAGES) Pole Equator Pole (PEP) II transect, which seeks to analyse climate variability along a longitudinal transect from pole to pole through Australasia. Seven Tasmanian Huon pine chronologies are used for this study, and collectively span the past few millennia. This increase in temporal coverage is particularly important for assessing recent trends

in climate, such as the warming noted above, within the context of the natural variability of the climate system.

1.2 The Study Premise

The primary aim of this study is to assess the value of the Tasmanian endemic conifer, Huon pine (*Lagarostrobos franklinii* [Hook f.] C.J. Quinn), for the purpose of dendroclimatic reconstruction. Four Huon pine chronologies were developed for this study, completing a seven-chronology network of sites ranging from 200 to 950 metres above mean sea level (AMSL) (Figure 1.2). An existing chronology, the 2,792 year LJH ring-width series from a 950 metre site on Mt. Read, has been substantially improved through an increase in sample depth in the earliest portion. A previous body of dendroclimatic research on Huon pine by Cook *et al.* (1991; 1992; 1995a; 1996a; 1996b), will henceforth be referenced collectively as the Tasmanian Tree-Ring Project (TTRP). This ongoing research effort has produced a warm-season temperature reconstruction for most of the past 3 millennia, based on the LJH chronology from Mt. Read. The research undertaken for this thesis analyses the representativeness of the LJH temperature reconstruction with respect to a regional climate signal. Detailed response function analyses were applied to all seven chronologies, in order to reveal the relative influence of seasonal climate (i.e., temperature and precipitation) over annual radial growth, with respect to an elevational and latitudinal gradient. A rotated Principal Component Analysis of the seven chronologies was also employed, in order to test for a clustering of sites by elevation or region. New reconstructions of warm season temperatures were developed from the highest-elevation chronologies, allowing a reassessment of temperature changes in the Tasmanian sector of the Southern Ocean over the past three millennia.

This study was built around the following questions:

1.) What is the regional representativeness of the TTRP's Mt. Read Huon pine temperature reconstruction? Buckley *et al.* (1993) found little agreement between ring-width sequences from Mt Read Huon pine from LJH with two lower elevation chronologies from 200 and 500 metres, respectively. They hypothesised that the strong, direct response to growing season temperature for LJH was related to its subalpine location, where temperature is expected to be the factor most limiting to growth (*sensu* Fritts, 1976). The lack of signal in common with the two lower chronologies was thought to be related to different controlling factors due to the different climate regimes experienced at high and low elevations in western Tasmania. This leads to the second question:

2.) Is Huon pine's temperature response elevation dependent? Climate-response modelling by Cook *et al.* (1991; 1992) and Buckley *et al.* (1993) suggests this is so, demonstrating a far more robust response to temperature for the 950 metre high Mt. Read LJH trees than for either of two low elevation chronologies mentioned above. The development of an elevational transect was, therefore, a critical step for assessing the hypothesis that the colder temperatures at subalpine sites would be directly limiting to growth through the inhibition of photosynthesis and related physiological functions. Other subalpine sites were expected to exhibit strong crossdating of ring-width sequences with the Mt. Read chronology, as well as a similarly strong, direct response to warm season temperature.

3.) What is the most appropriate temperature time series for the calibration of the seven Huon pine chronologies used for this study? The temperature time series used for calibrating the Mt. Read temperature reconstruction was a composite of three low-elevation stations from the

eastern half of the island (locations shown in Figure 1.2). Is it appropriate to compare these data with a subalpine tree-ring site from the West Coast Ranges more than 100 km distant and *ca.* 900 m higher? The requirement for the longest possible time series for calibration necessitates the use of such distant sites, since west coast station records are generally of much shorter length, and in some cases of dubious quality (Torok, 1996). An exploration of Tasmanian temperature regimes is presented in Chapter 5.2.1, along with a new, more geographically-representative time series of warm season temperature for calibration.

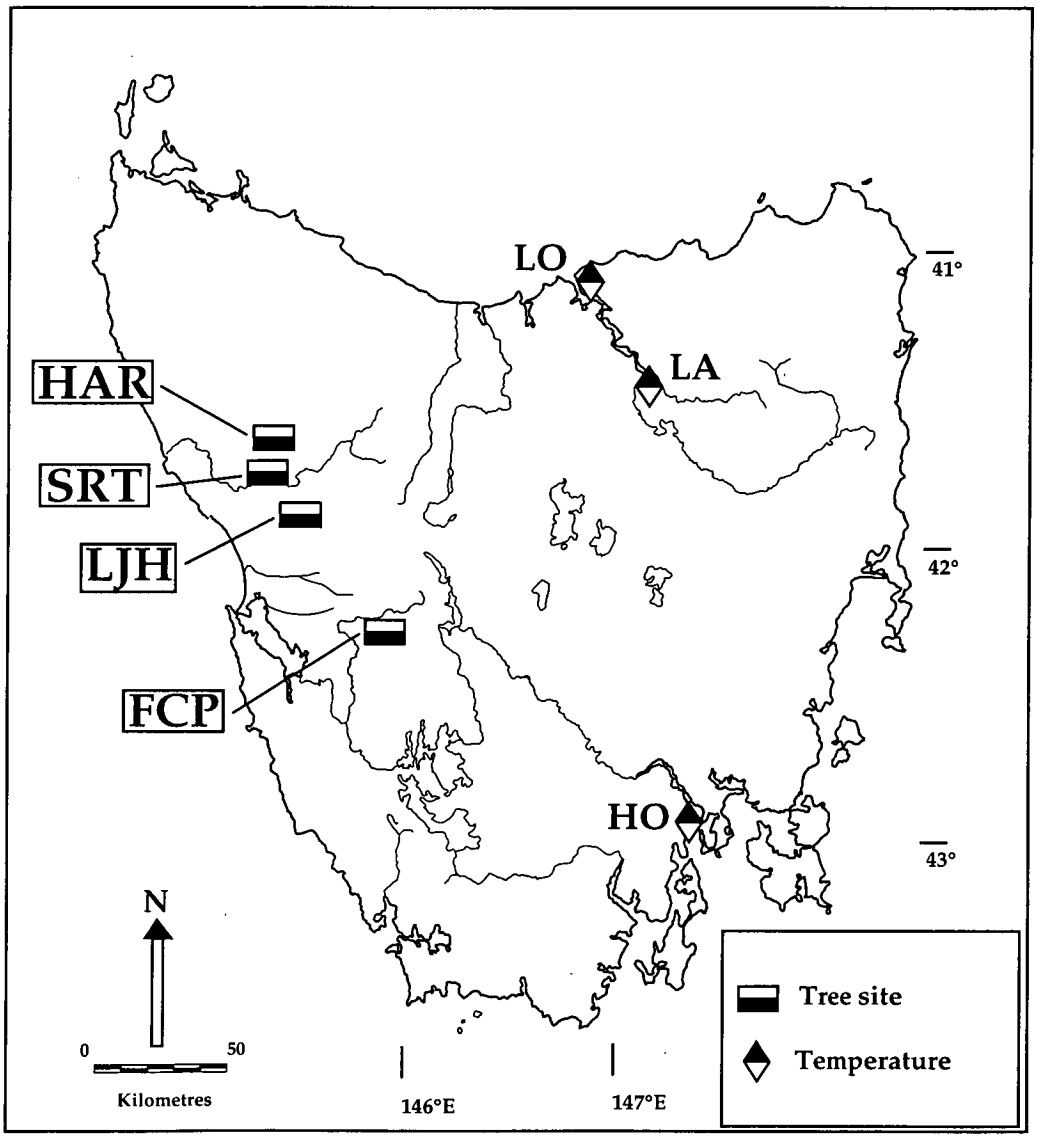

Figure 1.2. Huon pine sampling locations. HAR = Harman River, SRT = Stanley River, LJH = Lake Johnston site on Mt. Read, and FCP= Frenchmans Cap region where four new chronologies were developed for this research. The locations of three meteorological stations (HO = Hobart, LA = Launceston, and LO = Low Head) are also shown.

1.3 Objectives of the Research

The main objectives of this research project were:

1.) To confirm or refute the crossdating (i.e., the temporal control) of three previous Tasmanian Huon pine ring-width chronologies.

2.) To explore the possibility of an elevational dependence of Huon pine's response to temperature.

3.) To develop a new Tasmanian temperature reconstruction, based on a detailed response functions analysis of the seven-chronology network.

4.) To reassess the TTRP's Mt. Read temperature reconstruction, paying particular attention to key climatic periods of the past 3 millennia.

The success of this study was dependent upon replication of tree-ring chronologies, particularly from subalpine stands. One major obstacle was the scarcity of known Huon pine stands from elevations greater than 800 metres, many of which were either too difficult to access or were off limits to sampling due to their location within World Heritage Areas. In spite of the exclusion of some potentially important sites, the project objectives were fulfilled with subalpine sites from the Frenchmans Cap region of central western Tasmania (Figure 1.2). The importance of accounting for climate variability across space and time necessitated the establishment of the most robust temporal and spatial coverage possible. Therefore, Huon pine sites were selected covering a range of elevations and over as broad a region of Tasmania as possible. The inclusion of subfossil logs afforded greater sample depth in the earliest parts of some chronologies, enabling a more robust estimation of the regional climate through time. Efforts were made to maximise the length of individual time series in each chronology to preserve as much low frequency variance as possible.

Important climatic features of the Northern Hemisphere (e.g., the Little Ice Age and Medieval Warm Period) were investigated in the Tasmanian records to examine the possibility of more global signatures. Regional features, such as Tasmania's warming of the past three decades and the anomalous cooling at the turn of the last century, were also examined.

1.4 Structure of the Thesis

This thesis is divided into 7 Chapters; the first 4 consist of the introductory and background information, materials and methods. Chapter 5 presents the tree-ring chronologies and meteorological data sets used for the study. Chapters 6 and 7 include the results, discussion, conclusions, and the direction of future research. Since the history and basic principles of dendrochronology are well-documented in the literature (e.g., Stokes and Smiley, 1968; Fritts, 1976; Hughes *et al.*, 1982; Cook and Kairiukstis, 1990), only those concepts that relate specifically to this study are discussed in Chapter 2. This research makes use of several study sites, with large numbers of subfossil logs and living trees of great age. Therefore, it is appropriate to discuss at length the methods used in deriving the final, standardised chronologies used for climatic reconstruction, and their strengths and limitations. The difficult nature of standardisation, the removal of non-climatic growth trends and preservation of low-frequency variance in long chronologies are discussed in Chapter 4. An appendix to this thesis includes the actual warm season temperature data used for climate reconstruction, and the estimated warm-season temperatures from two reconstructions back to AD 1000.

CHAPTER 2: BACKGROUND

2.1 Basis for Dendroclimatology

2.1.1 Introduction: the annual growth ring

The annual growth layer or "tree ring" (Figure 2.1) is central to dendrochronology. It can be described as a growth band in the xylem of a tree or shrub with anatomically-definable boundaries, and is formed during a single annual period of cambial activity (Esau, 1977; Salisbury and Ross, 1992). Multiple, annual-growth bands may occur under certain conditions but there are no documented cases of consistent, systematic multiple-banding in any species, from any region of the world (Hughes *et al.*, 1982).

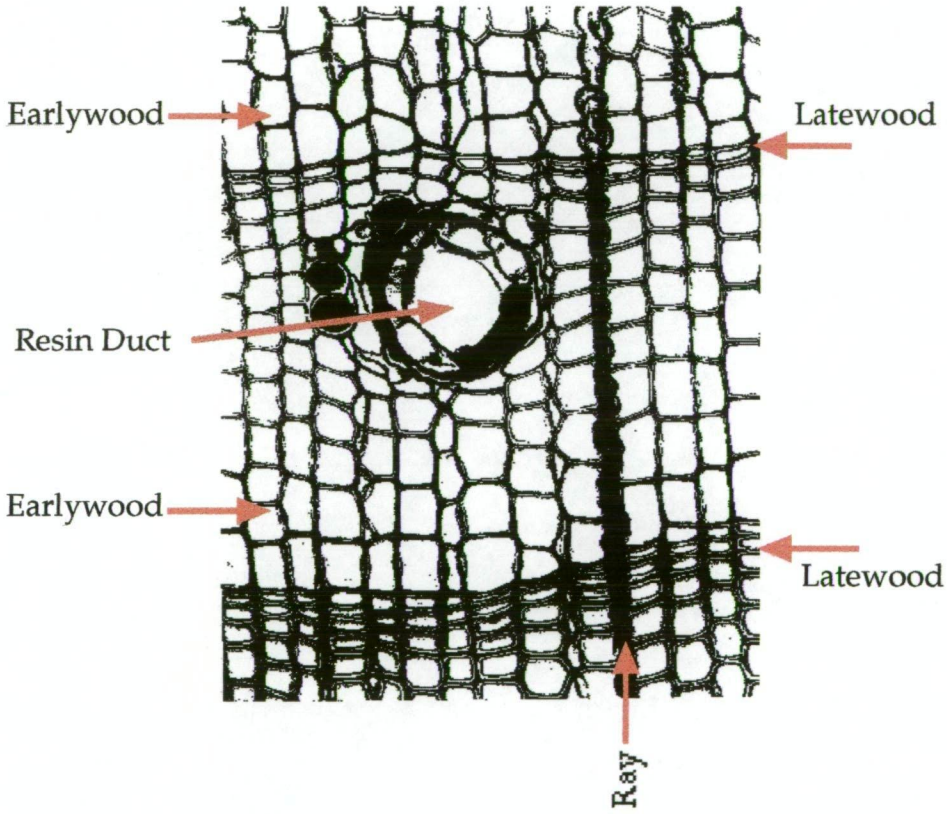

Figure 2.1. Typical conifer growth rings and associated features. This transverse view reveals the tracheids and some parenchyma cells which comprise the annual growth ring, while the rays contain only parenchyma cells. The individual cells are divided into two general types; earlywood and latewood. The earlywood cells form at the beginning of the growth season and are usually larger, thinner-walled, and far less-dense than latewood cells due to a lesser degree of lignification. The latewood cells form near the end of the growth season as part of the "hardening off" period before dormancy. It is the delineation between these two cellular types that allows for the identification of annual growth rings in some trees, and hence crossdating of annual ring sequences (Adapted from Fritts, 1976).

Growth rings in trees are sheaths of cells generated in the vascular cambium, and appear as concentric rings in a cross section of the stem. Each ring is the result of an annual flush of cambial growth which usually begins in the spring following a period of cambial rest or dormancy, and terminates in the latter part of summer or early autumn (Esau, 1977). Initiation of cambial activity in the spring appears to be related to the resumption of bud growth, while its termination is likely correlated with the cessation of shoot extension (Digby and Wareing, 1966). While initial cambial activity has been linked to the downward movement of growth substances from the expanding buds, continued cambial growth is driven by a local source of auxin which is probably supplied by the differentiating xylem (Samish, 1954; Sheldrake, 1968; 1971).

During cambial activity, the newly-formed cells differentiate into phloem and xylem. The phloem forms on the bark side of the cambium and serves as a conduit for transporting photosynthate downward from the leaves, while the xylem grows on the inner side of the cambium and transports water and nutrients upward (Nobel, 1974; Shigo, 1984). In some sense, each new ring can be viewed as a whole new functioning tree that completely envelops and replaces the previous year's growth flush (Shigo, 1984). A distinct boundary appears between annual rings because cells formed during the beginning of the growth season, known as *earlywood*, are larger and have thinner walls than those formed at the end of the cycle which are known as *latewood*. While there is some interaction between the latest, active growth rings and their predecessors, growth rings become effectively non-functional with time (Esau, 1977; Shigo, 1984).

When annual growth rings are formed in trees, it is likely that those layers reflect the environmental conditions under which they were formed (Douglass, 1914; Fritts, 1966). Annual variability in the width (or

some other characteristic such as density) of such rings, when synchronous in many trees within a region, indicates a common set of external factors that are influencing tree growth within that region. Such external forcing factors, particularly where they are spatially-extensive, are most likely related to climate, as no other external factors are likely to act over a similar range in the space, time and frequency domains (Fritts, 1976; Hughes *et al.*, 1982). It should therefore be possible to extract the climatic "signal" from the annual record of tree growth in such instances, and it is this objective that forms the underlying basis for dendroclimatological research.

2.1.2 Factors affecting tree growth

Tree growth, in an absolute sense, is an integration of all aspects of the operational environment. Climate is arguably one of the most important factors controlling overall growth. However, annual radial growth is also strongly influenced by stand dynamics effects, related to the competition for light, water, and nutrients. Other factors which influence growth include the type, texture and mineral content of soils; the drainage, latitude, elevation, slope and aspect of the site; and the amount of solar radiation, available moisture and average temperature during the growing season and, perhaps, previous seasons (Fritts, 1976). Natural disturbances such as earthquakes and landslides, snow avalanches, fire, volcanic eruptions and ash fall, and herbivorous insect attack, can all influence tree growth for one or more seasons. Anthropogenic factors, such as air and ground water pollution, fire, and nearby disturbances, which in turn may affect drainage or the availability of light, may also play a role.

In addition to the effects of external factors, there are several internal factors which may influence growth. These include availability of nutrients, minerals, growth regulators, enzymes, and water (Nobel,

1974; Fritts, 1976; Salisbury and Ross, 1992). Such internal factors are, however, influenced by external forcing from temperature and moisture availability, making it difficult to clearly isolate a specific response. The genetics of a given species may be important in regulating these internal factors in a general sense. However, external variables (particularly those related to climate) may be more important on a year-to-year basis and are therefore reflected in the *annual variability* of ring width that makes crossdating possible (Fritts, 1966). The genetic component, or phenology, of a species may have a more important role in dendroclimatology with regards to the autocorrelative component or "memory" inherent in most tree-ring time-series (Fritts, 1976). Annual growth rings in some species of trees may partially reflect antecedent conditions from prior seasons, and this must be carefully considered during standardisation of tree ring time-series and the construction of chronology indices (Chapter 4.3).

2.1.3 Growth response to temperature

It is well-established that plant growth is sensitive to temperature, and that differences of just a few degrees can lead to noticeable changes in growth rate (Salisbury and Ross, 1992). Each species of plant has its own "response window" with regard to temperature; minimum and maximum temperatures beyond which it will not grow, and an optimum temperature range in which maximum growth is achieved (Fritts, 1976). The response window for a given species may be dependant upon several factors such as the age of the plant, moisture and nutrient availability, light levels, CO_2 concentration in the ambient air, and other environmental factors. Figure 2.2 shows temperature response windows for seven Tasmanian rainforest endemics acclimatised to three different temperatures, while Figure 2.3 illustrates the relationship between annual growth of several North American conifers, and temperature as a function of elevation and season.

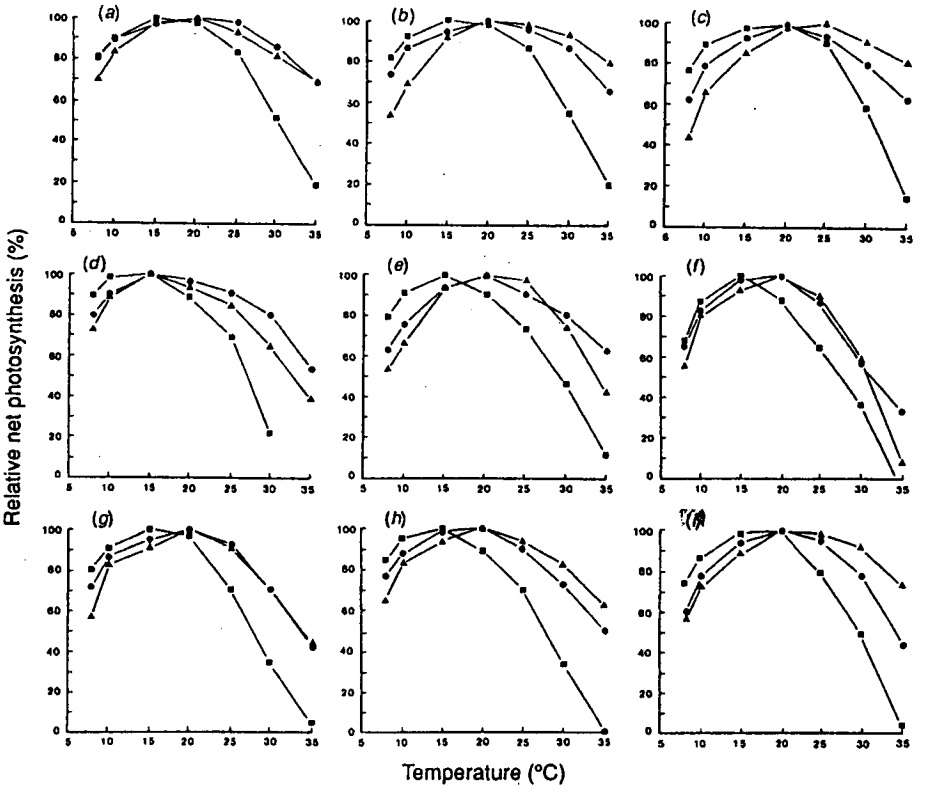

Figure 2.2. Temperature response windows for 7 Tasmanian endemic tree species. The plots show the response of net photosynthesis to instantaneous temperatures in foliage acclimatised to 8°C (square), 20°C (circle), and 29°C (triangle). The rates of net photosynthesis are expressed as a percentage of the P_{max} rate recorded for that acclimation temperature, and each value is the mean of five replicates. (a) = *Nothofagus cunninghamii* (from 980 m), (b) = *N. cunninghamii* (700 m), (c) = *N. cunninghamii* (80 m), (d) = *Athrotaxis selaginoides* (980 m), (e) = *N. gunnii* (980 m), (f) = *Atherosperma moschatum* (700 m), (g) = *Eucryphia lucida* (700 m), (h) = *Phyllocladus asplenifolius* (700 m), and (i) = *Lagarostrobos franklinii* (80 m). (From Read and Busby, 1990).

A plant's response to temperature is not simply linear, and while a positive response is generally experienced as temperature goes from the minimum to the optimum range, certain processes are actually promoted as temperature decreases towards freezing (Thompson, 1953; Samish 1954). Often the promotion of flowers, for instance, may be dependant upon a reversion to normal temperature subsequent to an extended period of cold. Autumn decreases in temperature may cause or contribute to the development of dormancy in seed, buds, or underground organs (Chouard, 1960), while low winter temperatures may initiate the breaking of dormancy in these same organs the following

spring (Salisbury and Ross, 1992). Such "positive" responses to cold temperatures are not well understood, especially for many species of trees used in dendroclimatology.

Plants may exhibit a direct response to temperature up to a point, but may become dormant, or even die, if temperature increases too far beyond the maximum temperature of the species tolerance (Salisbury and Ross, 1992). Since dendroclimatic research typically involves empirical relationships between tree growth and climate for the derivation of transfer functions for the reconstruction of climate, it is likely that such poorly understood processes, and their delayed effects, may be responsible for some of the classic, prior-season response functions that show significant relationships opposite to those seen in the year of growth (Chapter 4.4.2).

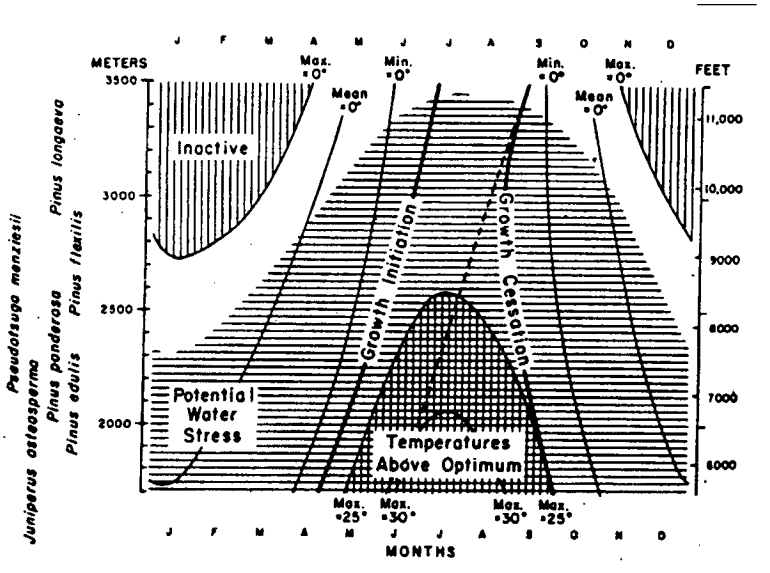

Figure 2.3. Temperature thresholds for several North American conifers. Plotted are the elevations and the approximate dates when maximum, mean, and minimum air temperatures are at 0°C; when maximum temperatures are at 25°C and 30°C; and when the period of growth begins and ends. The data are related to six conifers growing at latitudes between 34° - 38° N in western North America. The elevations and the times when water stress is most likely to be limiting to growth are shaded with horizontal lines. The vertical lines show the photosynthetically-inactive period when maximum temperatures are generally below 0°C. The area shaded with both horizontal and vertical lines represents the dates and elevations when the average maximum temperatures are above 25°C. The heavy dashed line indicates the earliest date that growth would be expected to cease due to severe water stress. The approximate elevational ranges of the six dendrochronologically proven conifers are shown on the left margin. (From Fritts, 1976. Drawn by M. Huggins).

2.1.4 Importance of site selection

Dendroclimatic research can only be successful if the trees selected are sensitive to climate (Fritts, 1976; Hughes *et al.*, 1982). There are two basic principles of dendrochronology underlying climatic sensitivity in trees, and which therefore relate directly to site selection: the principle of limiting factors, and the principle of ecological amplitude (Fritts, 1976).

The principle of limiting factors states that a biological process such as growth cannot proceed faster than is allowed by its most limiting factor. Although the same factors may limit growth to some extent in all years, the degree and duration of their limiting influence may vary annually (Figure 2.4). When one factor is no longer limiting (e.g., when adequate moisture is available to drought-stressed trees) growth will systematically increase until another factor becomes limiting (Fritts, 1976). This becomes important in dendrochronology because tree rings can only be crossdated when one or more environmental factor, such as temperature, is *uniformly* limiting to growth across time and space. Very harsh environmental conditions, such as those experienced by krummholz trees at the alpine timberline, may also result in trees that are unworkable.

The principle of ecological amplitude refers to a species' range of potential habitats (Figure 2.5). Every species may grow and reproduce over a certain range of habitats, dependant upon certain hereditary factors which determine its phenotype (Fritts, 1976). Species that thrive on a wide range of habitats are said to have a large ecological amplitude, while those restricted to very specific habitat requirements have a small ecological amplitude. Near the center of its ecological amplitude a species may be found on the widest range of sites, and climate may only rarely be limiting to growth. Near the margins, however, it may be restricted to very specific habitats, and it is in these marginal zones where climate is

likely to be the most growth-limiting factor, and the most climatically-sensitive trees will be found (Fritts, 1976; Hughes *et al.*, 1982).

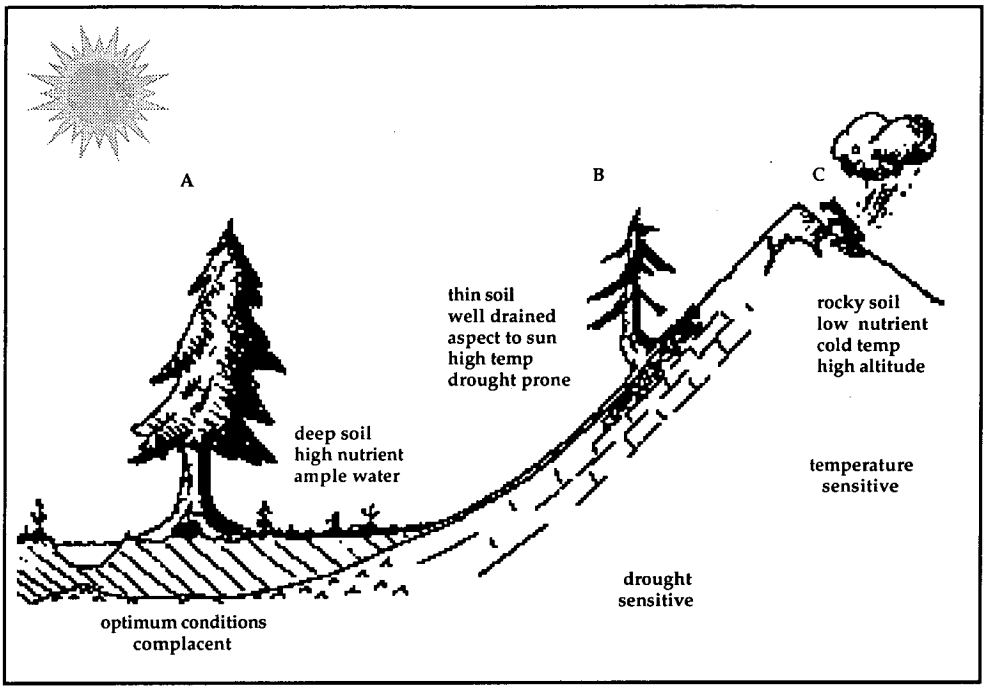

Figure 2.4. The principle of limiting factors. Tree A has optimum conditions for growth; deep soil, access to the water table, and adequate temperature for photosynthesis. Its ring-width sequences would exhibit relative complacency due to a lack of annual variability compared with B; growing on thin, rocky soils on a steep slope, with an aspect facing the direct rays of the sun. This tree is totally dependent upon rainfall for its moisture needs. It would be prone to drought stress which would be reflected in a sensitive ring-width series. C is growing at high altitude away from the direct rays of the sun, where temperature and wind stress would limit its growth. Trees with such krummholz form often exhibit excessive sensitivity to environmental stress, such that its ring sequences may not be able to be crossdated.

Site selection, therefore, becomes a matter of maximising the desired climatic signal by sampling trees on sites where that parameter is likely to be growth limiting. In a dendroclimatic study of rainfall, such trees might be found in areas of steep slope, with well-drained, rocky soils, and an aspect facing the direct rays of the sun (Stokes and Smiley, 1968). It would also be advantageous to search for a species growing near the limits of its ecological amplitude, with regard to its need for moisture. If the aim of the study is to reconstruct temperature, trees should be sampled from the altitudinal or latitudinal limits of the species range where temperature should be the factor most limiting to growth.

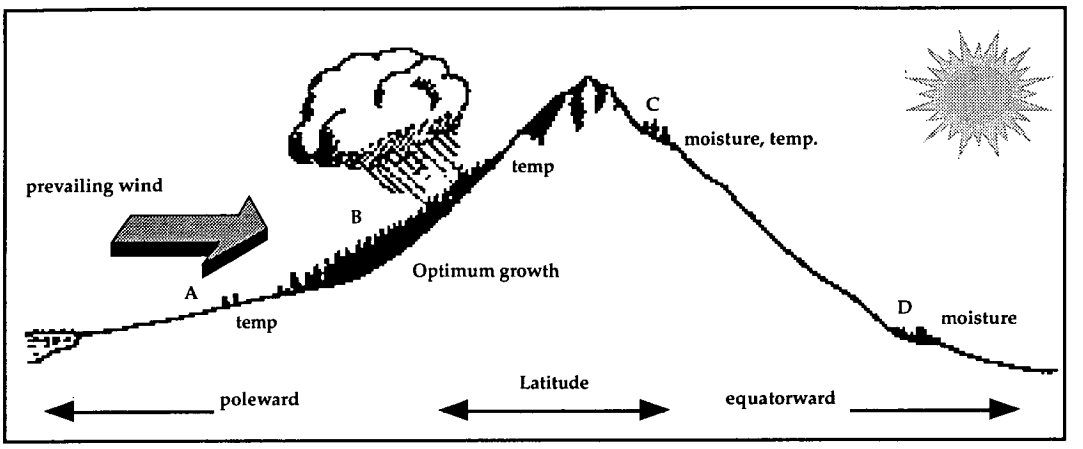

Figure 2.5. The principle of ecological amplitude. A, trees growing at their latitudinal limits limited by temperature; B, optimal conditions for growth regarding temperature and moisture; C, leeward site at altitudinal limits of species, aspect towards direct rays of the sun, showing both temperature and moisture sensitivity; D, trees at the lower latitudinal and altitudinal limits of the species showing drought sensitivity.

STRATEGY	ANN. RING	LIMITING FACTORS	CLIMATIC RESPONS.	SENS. & XDATING	CIRCUIT UNIFORM	REPET.
Regional selection	+++	+++	+	0	0	0
Species selection	+++	+	+++	+++	+	0
Site selection	+	+++	+++	+++	+	0
Sample size estimation	0	0	+	+	+++	+++
Tree & radius estimation	0	0	0	0	+++	+++

Table 2.1. Influence of dendrochronological concepts on sampling strategy. The concept categories are; Annual Ring, Limiting Factors, Climatic Responsiveness, Sensitivity and Crossdating, Circuit Uniformity, and Repetition or sample depth. Strong influence is indicated by +++, moderate influence by +, and little or no influence by 0. (Adapted from LaMarche, 1982).

2.1.5 Conditions for dendroclimatological success

Based on the discussion in the previous sections of this chapter, dendroclimatological studies in a given region can only be successful if the following conditions are met:

1.) There must be quantifiable variability in some aspect of the climate in the region of interest. For example, there must be a distinct wet

and dry, or warm and cold, phase of the annual cycle. There must also be measurable annual variability within these seasons.

2.) There must be at least one tree species available within the study region that exhibits distinct, annual growth rings with reasonable circuit uniformity. In some regions of the world, such as in the tropics, there are few species with distinct annual growth boundaries, and some may also exhibit intra-annual banding, where more than one growth ring is formed in some or all years (Mariaux, 1981; Jacoby, 1989; Worbes, 1985). Some species may also exhibit poor circuit uniformity, with circumferential variability of ring width exceeding annual variability (e.g., Buckley *et al.*, 1995).

3.) Some definable aspect of annual growth (e.g., ring width or latewood density) must be uniformly variable in all trees at the site, so that sequences of wide and narrow, or dense and less dense, rings can be matched between trees. This "crossdating" of annual ring sequences assures the temporal control that is central to dendrochronology (Chapter 4.3.1).

4.) The researcher must be able to link the common, synchronous variability in growth of all trees at a site, to some recorded climatic parameter (e.g., rainfall, temperature, or mean sea-level pressure). If the climate/tree growth link is significantly strong, then a reconstruction of the selected climatic parameter can be considered (Chapter 4.4).

2.2 Dendroclimatic Research in the Southern Hemisphere

2.2.1 Overview

Dendrochronological research in the Southern Hemisphere was initiated in the 1950's by visiting Northern Hemisphere researchers; Schulman in South America and Bell in New Zealand. While Schulman succeeded in publishing the first Southern Hemisphere chronologies from two Argentinian species (Schulman, 1956), Bell was led to a more pessimistic view of such research in New Zealand (Bell, 1958). By the

1970s however, dendroclimatic reconstructions had been accomplished in both regions.

LaMarche (1975) presented a preliminary reconstruction of precipitation from tree rings, back to A.D. 1010 for Santiago, Chile. This led to a major sampling effort producing 32 chronologies from 3 species from Chile and Argentina (LaMarche *et al.*, 1979a; 1979b). During the same period in New Zealand, researchers were producing a network of 21 chronologies from seven conifer species (LaMarche *et al.*, 1979c; Dunwiddie, 1979). Since that time both regions have seen much activity by local as well as outside researchers.

There are more than 150 tree-ring chronologies available from South America at present (Boninsegna and Villalba, 1996). Millennia-length reconstructions of temperature from tree rings have been produced from Chile and Argentina (Villalba, 1990; Lara and Villalba, 1993; Villalba, 1994). Most important among these is from the 3,620 year old *Fitzroya cuppressoides* chronology from Lenca, Chile (Lara and Villalba, 1993). This site is located near 43° S, at about the same parallel as Tasmania. There is, however, an apparent lack of agreement between the Lenca series and the Mount Read temperature reconstruction. For example, the recent warming trend indicated for Tasmania is absent from the Lenca reconstruction. More will be said about the disparity between these two reconstructions in Chapter 6.3.

New Zealand has several climate reconstructions which cover many hundreds of years. Subsequent to the work of LaMarche in the 1970's, more than 30 chronologies have been reported by Ahmed and Ogden (1985), Palmer (1982), and Norton (1983a; 1983b). Many of LaMarche's chronologies from the North and South Islands have been recently updated by J. Murphy (pers. comm.) and by R. D'Arrigo (pers. comm.). Norton *et al.* (1989) reconstructed summer temperature back to 1730 AD using chronologies from two *Nothofagus* species from the South

Island. More recently, D'Arrigo *et al.* (1995) produced several temperature-sensitive chronologies of pink pine (*Halocarpus biformis*) growing on Stewart Island, the first such chronologies to be developed from the southernmost of New Zealand's main islands. Salinger *et al.* (1994) presented a reconstruction of New Zealand climate indices back into the 1700s using ring width chronologies from five species and three genera, and this reconstruction is discussed further in Chapter 6.3.

A number of important "floating" chronologies from subfossil material have also been published for New Zealand, including Bridge and Ogden's (1986) chronology of *Agathis australis* which spanned the interval from 3500 - 3000 calibrated radiocarbon years before present (RCYBP), and Palmer's (1989) floating chronology from buried logs of *Phyllocladus trichomanoides* covering the interval from 2200 - 1800 RCYBP.

Besides South America, New Zealand and Australia, the only other land mass in the temperate zone of the Southern Hemisphere is southern Africa. Lilly (1977) and Dyer (1982) revealed an apparent lack of suitable trees for dendrochronological research in South Africa, where only about 12% of the virgin forests remained at the turn of the century, much of which has since been exploited (Palmer and Pitman, 1972). Furthermore, many of the tree species in the region exhibit multiple, intra-annual bands, ring wedging, and indistinct ring boundaries, however, LaMarche (1979e) suggested the potential of two conifer genera, *Podocarpus* and *Widdringtonia*. Only the latter has so far proven successful, yielding a 413 year chronology from *W. cedarbergensis* which displayed statistically significant links with spring and early-summer precipitation (Dunwiddie and LaMarche, 1980a).

Mainland Australia has seen limited success in dendrochronological research. The most common genera of Australian tree, *Eucalyptus*, has shown limited potential for crossdating and

chronology building (Ogden, 1978). The exception is the subalpine *E. pauciflora* which has exhibited limited potential (Ogden, 1982). Lamarche *et al.* (1979d) published two chronologies from the very short-lived *Callitris* which revealed an apparent dependence on precipitation (Dunwiddie and LaMarche, 1980b). Some attempts were made to pursue dendrochronology in the Australian tropics (Ash, 1983a; 1983b; Ogden, 1981; T. Bird, pers. comm.). While certain species were noted as having potential, little has been accomplished as of this writing.

2.2.2 Previous Research in the study region

In the 1970's LaMarche undertook a sampling trip to Australia which resulted in several published chronologies (LaMarche *et al.*, 1979d). This led to the first dendroclimatic reconstructions from Tasmania, including a 199-year reconstruction of stream flow based on 11 chronologies from several species; one each of *Nothofagus gunnii* and *Athrotaxis selaginoides*, two of *A. cupressoides*, and seven *Phyllocladus aspleniifolius* chronologies (Campbell, 1982). LaMarche and Pittock (1982) used these same 11 chronologies to generate the first Southern Hemisphere temperature reconstruction. As there are substantial differences between this reconstruction and the Mt. Read warm season temperature reconstruction, these will be discussed in Chapter 6.3.1.

Ogden (1978) concluded that the Tasmanian conifers were the most suitable species for dendroclimatological research in Australia. Among them, he included *Lagarostrobos* (then *Dacrydium*) *franklinii*, but he specifically highlighted the potential of *Phyllocladus asplenifolious* (celery top pine) and the two *Athrotaxis* species (*A. selaginoides* and *A. cuppressoides*; King Billy and pencil pine, respectively). The potential for Huon pine to exceed 2,000 years in age was recognised but the species was thought to be too complacent, and therefore unsuitable for dendroclimatic research (Ogden, 1978; T. Bird, pers. comm.). At that time

it was not known that Huon pine grew at altitudes higher than 700 metres, where temperature would be severely limiting to growth.

Ogden developed several Tasmanian chronologies from celery top, King Billy and pencil pine. Most of the early research on Huon pine, however, was pursued by Bird who produced a number of lowland chronologies from around the island, including the Stanley River in the west, the Picton River in the east, and Bathurst Harbour in the southwest (Francey *et al.*, 1984; T. Bird, pers. comm.). These efforts only reinforced the assessment that Huon pine was a long-lived, but complacent, species that would have limited usefulness for dendroclimatic reconstruction.

2.2.3 Dendroclimatic research with Huon pine

The discovery of high-elevation Huon pine stands on Mt. Read in 1987 (M. Peterson, pers. comm.), and in the Frenchman's Cap area (Hickey and Felton, 1988), is among the most important developments in Tasmanian dendrochronology. The TTRP research forms the baseline of research upon which this study is built. The principal development from the TTRP research is the nearly 3,000 year reconstruction of warm season (November to April) temperature from western Tasmania, first presented by Cook *et al.* (1992). This reconstruction is derived from a well-replicated, ring-width chronology from a stand growing at 950 metres near the summit of Mt. Read, which is discussed in Chapter 3.5.1.

The Mt. Read chronology explains 37% of the variance in warm-season temperature, and is presently among the longest and most well-replicated chronologies from the Southern Hemisphere (Cook *et al.*, 1996b). The recent 100 year period exhibits both anomalously cold and warm 25-year periods, which are among the most unusual of the entire record. While the recent temperature increase is unusual (i.e., at least 4.5 standard errors above the mean) it is not statistically unprecedented. Any links to an hypothesised "Greenhouse" warming are premature and

equivocal at best. It is clear, however, that the recent period of warm temperature has not been exceeded in Tasmania for at least the past 1200 years (Cook *et al.*, 1996b).

Oscillatory behaviour in the original temperature reconstruction was detected, at frequencies of about 30, 56, 80, and 180 years (Cook *et al.*, 1995a). No specific forcing factors were implicated, however the most likely influences were thought to be related to the internal dynamics of the ocean-atmosphere-cryosphere system (Cook *et al.*, 1995a). When the chronology was extended to more than 2000 years through the inclusion of subfossil logs, the four oscillatory modes (now at 31, 57, 77, and 200 years) collectively accounted for 12% of the overall variance in the reconstructed temperature series, and 41% of the variance on time scales greater than a decade (Cook *et al.*, 1995a; 1996a). It was noted that 51% of the mean anomalous warming of the past 3 decades could be accounted for by the mean aggregate of these four oscillations (Figure 2.6a).

Cook *et al.* (1996a) discussed the possibility of forecasting climate change in the Tasmanian sector of the Southern Ocean, and any masking effects these internal oscillatory modes might have on a CO_2-induced warming over the next few decades (Figure 2.6b). Based on the mean aggregate of the four oscillations, substantial cooling could be projected to take place over the next 3 decades. The authors described a plausible scenario where any warming over that same time span would be masked by the forcing of the internal oscillatory modes driving temperature down, making Greenhouse warming difficult to detect.

Tasmanian Huon pine offers perhaps the greatest potential for the development of Holocene-length chronologies in the Southern Hemisphere. Research over the past two decades has led to the near completion of the first such time-series from the Stanley River in western Tasmania. Well-preserved, radiocarbon-dated logs, spanning nearly the entire Holocene period (i.e., the past 10,000 years), have been

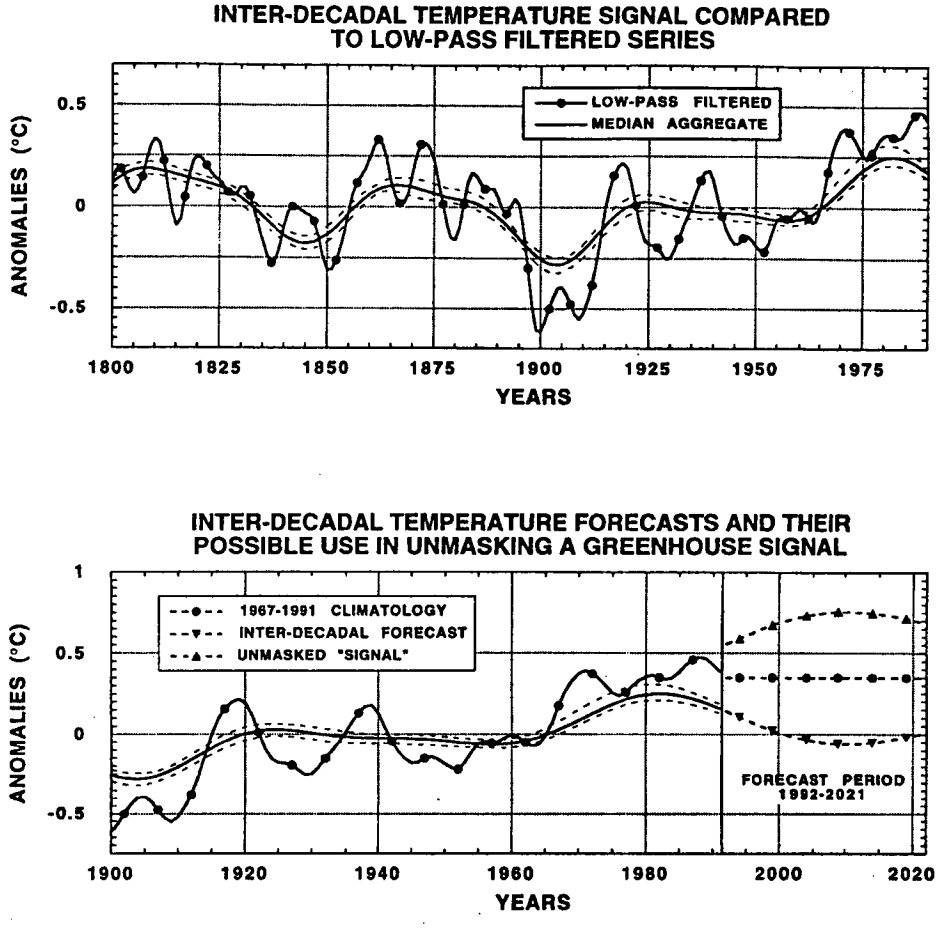

Figure 2.6. Oscillatory behaviour in the Tasmanian warm-season temperature reconstruction, as revealed from Singular Spectral Analysis. The top plot shows the median aggregate waveform of the four greater-than-decadal oscillations since AD 1800, with the approximate 95% confidence limits superimposed upon the low-pass filtered series. The aggregate accounts for approximately 12% of the overall variance in the estimate of annual temperature, and 41% of the variance at frequencies greater than a decade. Much of the post-1965 warming trend can be explained by the trend in these four waveforms, as can the cool period at the turn of the last century. The bottom plot illustrates a potential *masking* effect by natural climate variability with regards to detection of an hypothesised, anthropogenic-induced warming. A statistical forecasting technique based on the aggregate, was compared against a similar forecast using the mean of the climate data for the 1967 - 1991 period, which represents a continuation of the anomalous warming period of the past few decades. The two forecasts, which extend out to the year 2021, are at odds with each other, having a potentially neutralising effects that could effectively mask any real warming, were it to continue into the next few decades. (From Cook *et al.*, 1996a).

excavated from the river's flood plain (McPhail *et al.*, 1983; Francey *et al.*, 1984; 1985; Barbetti *et al.*, 1992; 1995). This site serves a central role in the calibration of the radiocarbon curve for the Southern Hemisphere, as well as for the inter-hemisphere comparison of ^{14}C production (M. Barbetti pers. comm.). Francey *et al.* (1984) used Stanley River Huon pine for

isotopic studies, and (1985) for analysing the physiological influences on carbon isotope discrimination in Huon pine. Subfossil Huon pine logs have been recovered from many parts of the state, and have been noted at each of the sites used in this study. It is not unreasonable to anticipate the development of several chronologies spanning most of the past 10,000 years or more.

CHAPTER 3: THE ENVIRONMENT OF THE STUDY REGION:

3.1 Physiography

The island of Tasmania is located between 40° and 44° S, and 144° and 149° E (Figure 1.1), and covers approximately 64,000 square kilometres. Tasmania, along with its adjacent islands, is a detached portion of the eastern highlands of Australia, presently separated from mainland Australia by the *ca.* 200 kilometre expanse of the Bass Strait. The terrain is mostly mountainous with more than 60 peaks exceeding 915 metres. The island can be broadly divided into four physiographic regions (Figure 3.1): The Western Highlands; the Central Plateau; the Eastern Highlands, and the Midlands.

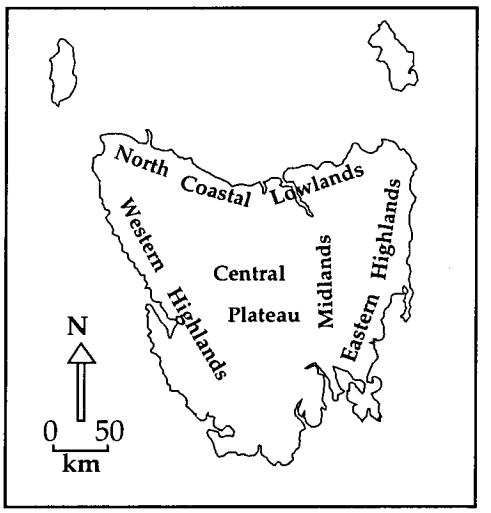

Figure 3.1. The physiographic regions of Tasmania. (Adapted from Davies, 1965).

The Western Highlands is a region of northwest-southeast trending mountain ranges which in places exceed 1,500 metres in altitude. Deep valleys have been formed along the strike of less resistant rocks such as limestone, while the more resistant quartzites and conglomerates of the region have been left to form steep ridges and high peaks. The Western Highlands are comprised mostly of folded pre-Carboniferous rocks which have subsequently been stripped of their post-Carboniferous cover by repeated glaciations and other erosional processes (Davies, 1965). There are expressions of at least three Cainozoic glaciations on the present

Tasmanian landscape, the most recent of which was active from approximately 30,000 years before present until about 10,000 years ago (Colhoun, 1985).

The Central Plateau forms the core of the island and is the result of an extensive dolerite intrusion dating to the Jurassic Period (Davies, 1974). The plateau is mostly above 1,000 metres, with several peaks exceeding 1,500 metres. It is bordered to the north and east by a steep scarp, which ranges from 500 to 1,000 metres in height, known as the Great Western Tiers. The Midlands are situated between the Central Plateau and the Eastern Highlands and is the only region of extensive inland plains on the island. The Eastern Highlands consist of low mountains and dissected, hilly terrain up to nearly 400 metres in elevation. The northeast and the extreme northwestern parts of Tasmania are typified by extensive coastal plains.

3.2 Geology

Tasmania's present landscape is dominated by extensive sheets of Jurassic dolerites and Tertiary basalts. These have been further modified by extensive Tertiary faulting which produced horst and graben topography, and repeated glaciations (Colhoun *et al.*, 1988). Predominant rock types in Tasmania are dolerite, sandstone, quartzite, conglomerate and granite. The pre-Carboniferous rocks of the island can be divided into two tectonostratigraphic terranes; the NE Tasmania Terrane and the Western Tasmania Terrane (Berry *et al.*, 1990). The NE Tasmania Terrane is characterised by Ordovician to Devonian turbiditic shales and sandstones (the Mathinna Beds) which have been folded and intruded by upper Palaeozoic granitoids. There are no exposures of Pre Cambrian rocks. The Western Tasmania Terrane is lithologically more complex, consisting of numerous Pre Cambrian blocks or massifs, separated or overlain by belts of lower to middle Palaeozoic rocks of highly variable

composition. The boundary between the two terranes is thought to be located within the broad Tertiary graben occupied by the River Tamar.

3.3 Soils

Soils in Tasmania are generally infertile, owing to strong leaching due to high rainfall totals, or to great age. The main soil types are podzolic soils, podzols, krasnozems, black earths, brown earths and prairie soils (Wilson, 1990) (Figure 3.2). The most common soil type is the Podzolic soil, typified by a heavily leached A horizon, and high accumulation of clay in the B horizon instead of organic material or iron. Soils of this general type dominate much of the western half of the island including most of the field locations from this study. Many of the mountain soils are classified as skeletal soils, particularly those on steep slopes overlying quartzite or granite, which are shallow, sandy and heavily leached, with many rock fragments and some humus (Wilson, 1990). Soils in the Frenchmans Cap area are typically of this sort.

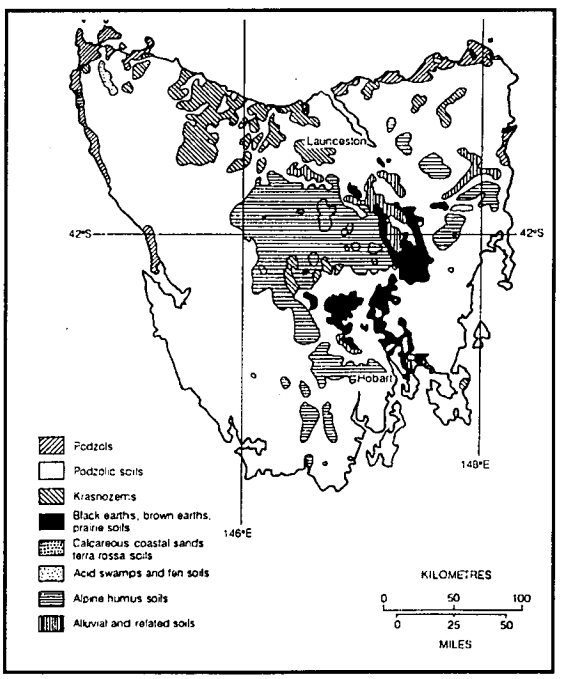

Figure 3.2. Soil Types of Tasmania. Much of the island consists of rock types rich in silica, resulting in abundant podzols and podzolic soils. Most Tasmanian soils are thin and nutrient poor in areas of high rainfall, particularly in the mountains where shallow, skeletal soils are common. (From Wilson, 1990).

3.4 Climate

Tasmania's temperate-maritime climate is influenced by its position in the latitudinal belt of the "Roaring Forties", a zone of intense westerly wind flow dominated by Southern Ocean air masses (Tchernia, 1980). The island is situated along the Subtropical Front, adjacent to the Subantarctic Zone of Nowlin and Klinck (1986), and is heavily influenced by the circulation of the Southern Ocean (Figure 1.1). Zonal circulation is greatest during winter months due to an equatorward expansion of the circumpolar vortex, while during summer months there is a slackening of zonal circulation, and a correspondingly greater influence from mainland Australia and the subtropical high pressure system over the Tasman Sea (Coughlan, 1983; Lough, 1991). Consequently, most precipitation falls during winter along the west coast of the island.

The Western Highlands and the Central Plateau form an orographic barrier which intercepts much of the westerly, moisture-bearing low pressure systems, resulting in a distinct gradient of both rainfall and temperature on the island (Langford, 1965) (Figure 3.3). Prevailing winds over most of Tasmania are from northwest to southeast and strongest during late winter. The greatest wind speeds are associated with low pressure troughs over the ocean areas to the south of Tasmania. The summer winds are generally weaker and tend to be northerly and northwesterly, bringing warmer continental air across Bass Strait.

Rainfall over much of Tasmania is copious, and heaviest in the winter months. Precipitation in this latitude belt is controlled by one of two general climatic patterns observed for Australia, where the latitude of the surface high pressure belt over eastern Australia dictates the penetration of westerly rainfall along the southern coasts of the mainland and Tasmania (Pittock, 1975; 1978). Annual precipitation ranges from around 1,200 to 1,400 mm on the west coast at low elevation, and 1,500 to

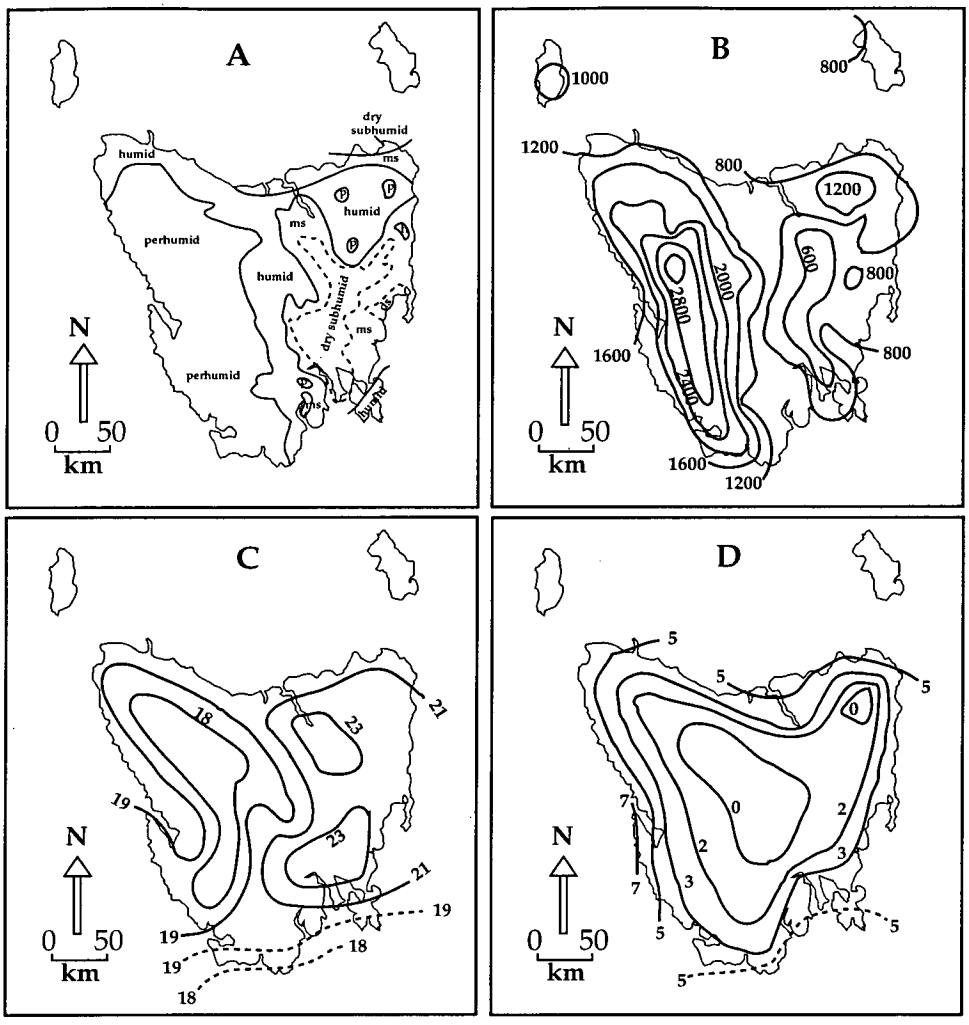

Figure 3.3. Climate regions and gradients over Tasmania. A; the climate regions of Tasmania (adapted from Gentilli, 1972), B; the annual precipitation gradient (mm), C; the mean maximum temperature for January (°C), D; mean minimum temperature for July (°C) (adapted from Bureau of Meteorology, 1983).

3,600 mm in the Western Highlands. Much of the winter precipitation in the high elevations of the Western Highlands and Central Plateau is in the form of snow. There is a general decrease in precipitation totals as one moves east across the island, with less than 600 mm in the Midlands. Rainfall increases again towards the east due to orographic lifting from the Eastern Highlands, and coastal precipitation from occasional cyclonic systems over the Tasman Sea. Drought is not uncommon in eastern and southeastern Tasmania where evapotranspiration losses may exceed summer precipitation (Gentilli, 1972).

Annual average temperature in Tasmania also has a gradient dependant upon the topography of the island. This gradient, illustrated in Figure 3.3c-d, reflects the contrast between the maritime climate along the west coast and the more continental climate of the interior and east coast. While Tasmania generally experiences a mild maritime climate, extremes of temperature are not uncommon. Summer maxima may reach 40° C during excursions of hot continental air masses from mainland Australia, while frosts are common in the winter months, and the high interior of the state receives much of its winter precipitation in the form of snow.

3.5 Vegetation

The present-day vegetation of the Australasian region can be attributed to three basic influences (Dietz and Holden, 1970; Weissel *et al.*, 1977). First is an ancient element derived from continental Gondwanaland. Vegetation from this source can be found in all of the southern continents and generally requires moist, temperate, oceanic conditions, characterised by the genera *Nothofagus*, *Phyllocladus*, *Podocarpus*, *Lagarostrobos*, and *Dacrydium*. The second influence is a tropical element coming from the Malaysian region as the distances from Australia and New Zealand decreased, while the third is an endemic element, including some of the large genera like *Eucalyptus* in Australia and *Hebe* in New Zealand. These genera were able to evolve *in situ* due to their isolation and in response to oscillating climatic conditions and extensive topographic changes throughout the Quaternary (Ogden, 1982).

Tasmanian vegetation assemblages are largely the expression of the first and third elements outlined above. There is a high degree of endemicity in the flora of Tasmania (Jackson, 1965; Williams, 1974), with about 200 of the nearly 1250 species, along with 10 genera, of angiosperms being endemic, while most of Tasmania's conifers are also endemic. The

species density in Tasmania is the greatest in Australia; twice as great as that for nearby Victoria and nearly ten times greater than Australia as a whole (Williams, 1974).

Tasmanian vegetation may be broadly classified into five categories (Davies, 1964); rainforest, sclerophyll forest, moorland, sedgeland, and coastal heath. These categories are influenced by local conditions such as elevation, aspect, and soil type, but many intermediate assemblages can be found. Based on an analysis of several pollen assemblages from throughout the state (Macphail, 1979), the island's vegetation composition has undergone considerable structural change over the past 10,000 years. Towards the end of the Pleistocene Tasmania was nearly devoid of trees, as climates were colder and drier than at present (Davies, 1967). Temperatures rose between 11,500 and 9,500 years B.P, accompanied by a rise in effective precipitation which allowed for the expansion of forest vegetation throughout the island (Macphail, 1979). During the early post-glacial, there was a possible reversion to colder and drier conditions, which delayed the development of forests in inland eastern Tasmania until after 9,500 years B.P. The pollen records indicate no major changes in climate since that time, but two broad phases of development in Tasmania's forests are noted. First was an early Holocene phase of development of *Nothofagus cunninghamii* cool-temperate rainforest in western, central, and southeastern Tasmania. *Eucalyptus* sclerophyll forests established their dominance in eastern Tasmania at this time. The second phase, during the mid to late Holocene, saw a re-expansion of *Eucalyptus* and shade-intolerant species into more open forests and alpine communities. This was attributed by Macphail (1979) to a mid-Holocene "optimum" from about 8,000 to 5,000 years B.P., when climate was wetter and possibly warmer than at present, though the effects of human burning cannot be discounted. After this phase, climate became cooler and drier, leading to an increase in both fires

and frost. The structural changes in the vegetation of post-glacial Tasmania are generally similar to those at similar latitudes in New Zealand and South America, suggesting a response to a similar forcing.

Much of the present-day vegetation in Tasmania has been burned, and combined with the rugged terrain and the associated wide range of microhabitats, this serves to diffuse the boundaries between plant communities (Macphail, 1979). Generally, the distribution of major plant communities closely follows the climatic provinces constructed by Gentilli (1972) (Figure 3.3d). A climatic timberline ranges from 750 to 915 m on the mountains of the west and southwest, to around 1220 m on the eastern plateaux. In the former, the treeline is typically dominated by *Nothofagus cunninghamii*, while the latter primarily consists of *Eucalyptus* spp. with *Nothofagus cunninghamii* scattered throughout a shrub understory.

3.6 Site Descriptions

3.6.1 Mt. Read

Mt. Read is a 1,124 metre high mountain located in western Tasmania, 10 kilometres southeast of the town of Rosebery (Figure 3.4). Huon pine grow in two disjunct stands on the southern side of the mountain between 950 and 1,000 metres. The Lake Johnston site (Plate 3.1) consists of two discrete, adjacent units around 950 metres in elevation. The lower unit (LJH) is made up of approximately 300 living trees, while the uppermost portion (JDA) is comprised of standing, dead trees killed by a 1961 fire. A separate, disjunct stand (KDH) is located about 1.5 kilometres to the northwest, and at an elevation of 1,000 metres it is the highest known occurrence of Huon pine.

The Mt. Read Huon pine stands occur within the subalpine zone, between 850 and 1,030 metres (Kirkpatrick, 1977a). Treeline is located at ca. 940 metres, with occasional krummholz occurrences of *Athrotaxis*

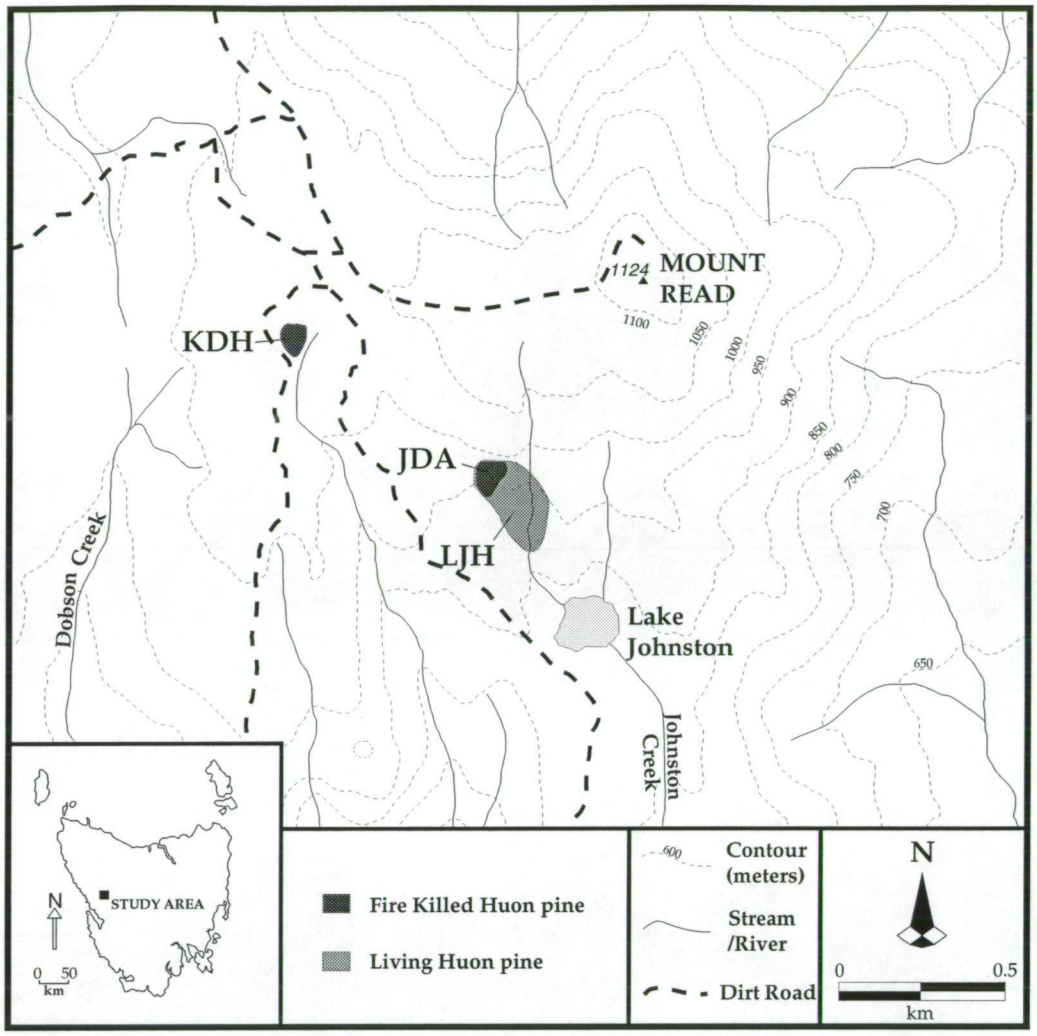

Figure 3.4. Mt. Read site map.

selaginoides, *Diselma archeri*, *Podocarpus lawrencii*, and *Lagarostrobos franklinii* amongst alpine heath (Bacon, 1992). These are relict rainforest assemblages whose presence indicates the exclusion of fire for thousands of years (Kirkpatrick and Dickinson, 1984b; Peterson, pers. comm.).

Mt. Read is formed of Ordovician volcanic rock which is thinly overlain by glacial till and weathers rapidly when exposed, resulting in a soil with sufficient nutrient content to sustain endemic rainforest species. In contrast, much of the West Coast Range is typified by low nutrient, skeletal soils derived from Ordovician conglomerates, and supporting primarily *Eucalyptus* and heath vegetation communities (Anker *et al.*, 1996). The poor nutrient status of these soils is likely related to repeated

Plate 3.1. The Lake Johnston Huon pine site. The dashed line marks the boundary of the living (LJH) stand, while the standing dead trees (foreground) were killed by fire in 1961, and comprise the JDA stand where much of the subfossil wood recovered from Mt. Read has come from. Lake Johnston is visible in the background to the southeast.

burning which, when combined with high rainfall, results in the rapid leaching of nutrients (Kirkpatrick and Dickinson, 1984b).

Sampling of Mt. Read's subalpine Huon pine began in 1990, with cores taken from 20 living trees at the LJH stand. Over successive years, samples of subfossil logs from the JDA and KDH sites have enabled the extension of the chronology to nearly 4,000 years B.P. The inclusion of subfossil wood has also resulted in a marked improvement of the sample depth in the earliest part of the chronology (Chapter 5.1), making the Mount Read Huon pine chronology the most well-replicated long chronology in the Southern Hemisphere.

There are only 3 living stems at the KDH site, as the remainder of this krummholz, tree-line stand was killed by fire in 1894. The bulk of the subfossil material obtained at Mt. Read has come from this site, and the fire-killed JDA site. In total, 88 subfossil samples have been taken from JDA and LJH combined, and 115 from KDH. Not all of the subfossil logs have been included in the final chronology, however, due to severe circuit-uniformity problems, or other growth anomalies in some samples.

Sample	No. of Rings	Measured Time Span	Pith	Bark
JDA01*	1000+	BC 1300 - BC 440	Y	N
JDA04	1500+	BC 1210 - AD 299	Y	N
JDA08	660+	BC 1004 - BC 354	Y	N
JDA15	500+	BC 950 - BC 590	Y	Y
JDA39	600+	BC 1240 - BC 651	Y	Y
KDH23*	1000+	BC 1723 - BC 827	N	N
KDH27	800+	BC 781 - BC 19	Y	N
KDH56	500+	BC 1059 - BC 589	N	Y
KDH79	560+	BC 866 - AD 551	N	N
KDH115	400+	BC 1300 - BC 959	Y	Y

Table 3.1. Details of 10 of the more than 200 subfossil samples included in the Mt. Read chronology. The number of rings is most often approximate, as portions of the samples may be too suppressed to count accurately. One sample not included in this table (JDA37) has more than 2,000 rings, the most of any sample from Mt. Read so far. The oldest sample listed (KDH23) dates to BC 1723, though one recent sample (JDA70) appears to predate this, though by how much is uncertain. The measured time-span refers to the time period included in the chronology, and may exclude periods which have anomalous growth due to injury or compression of rings. The presence or absence of pith and bark is also noted. The * denotes the oldest documented sample from each site.

The Lake Johnston cirque basin was occupied by ice during Tasmania's most recent glaciation (the Margaret Glaciation) which attained its maximum about 18,000 years BP (Colhoun and Fitzsimons, 1990). The small cirque glacier is thought to have occupied the valley between Mt. Read and Mt. Hamilton, and possibly separated the two Huon pine sites (Anker *et al.*, 1996), which may have previously been one contiguous unit, given that both populations appear to be comprised of all male trees that are genetically identical (Shapcott, 1991). The mechanism for their separation would then be suppression by névé or glacial ice during the last glacial episode, implying the existence of the stand throughout the last glaciation maximum.

It is also possible that the entire stand was established subsequent to glaciation during the early Holocene, and that separation was the result of fire. This would require that vegetative reproduction alone could account for the spread of more than a kilometre between the two stands over the past 10,000 years, and while pollen records from Lake Johnston indicate the presence of Huon pine in the basin for at least the past 10,000 years (Anker *et al.*, 1996), the slow growth rates from Mt. Read make this an unlikely scenario. The two sites may have always been disjunct from each other, as it is plausible that wind, birds, or some other mechanism could have initiated the transportation of vegetatively-reproductive material from one location to the other.

Mt. Read is in one of the wettest areas of Tasmania, as part of the first major orographic barrier on the island's west coast. Snow is common on the mountain throughout the winter months, occasionally falling in summer as well. Figure 3.5 shows daily temperature, rainfall, and radiation values obtained from an Automatic Weather Station (AWS) positioned in the JDA stand on Mt. Read. The data encompass most of two summers and one complete winter. The general statistics for the Mt. Read temperature data are listed in Table 3.2.

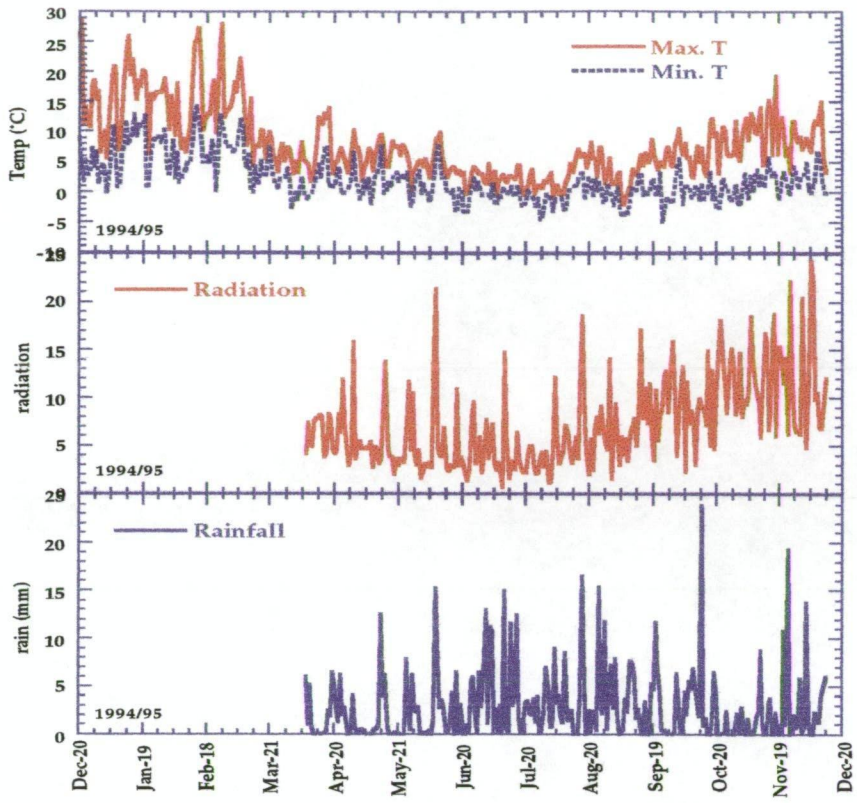

Figure 3.5. Mt. Read meteorological data for nearly one year. The top plot shows maximum and minimum temperature; the middle plot shows radiation, measured at wavelengths between 400 and 1000 nm, and plotted as µmol quanta/m^2/s^{-1}; and the bottom plot is total rainfall in millimetres.

	Max S 1	Max W 1	Max S 2	Min S 1	Min W 1	Min S 2
Min.	3.30	-0.70	3.20	-2.90	-4.50	-1.10
Max.	28.90	10.00	19.40	14.30	8.20	6.90
N	102.00	123.00	42.00	102.00	123.00	42.00
Mean	14.13	3.98	10.09	5.89	0.36	2.13
Median	14.15	3.80	10.25	5.80	0.00	2.30
Std. Dev.	6.08	2.53	3.48	3.76	2.19	1.93
Var.	36.95	6.40	12.18	14.17	4.80	3.74
St. Error	0.60	0.23	0.54	0.37	0.20	0.30

Table 3.2. Statistics of Mt. Read daily temperature records from Dec. 20, 1994 to Dec. 12, 1995, the date the AWS stopped recording. S 1 is the summer period from Dec 20, 1994 to March 31, 1995, W 1 is the Winter from May 1 to August 31, 1995, S 2 is only from Nov. 1 to Dec. 12, 1995. "Max" columns show the statistics for the daily maximum temperatures for that season, while "Min" columns refer to daily minimum temperature. The two summers contrast one of the warmer summers on record, with the coldest summer on record for Tasmania in 1995/1996. Data supplied by David Pepper, University of Sydney.

3.6.2 Frenchmans Cap

The Frenchmans Cap is a 1,443 metre high quartzite mountain in Tasmania's interior southwest (Plate 3.2). Several Huon pine sites were noted in the region by Hickey and Felton (1988), and Figure 3.6 shows the locations and extent of known Huon pine stands and the areas that were sampled for this study. The highest stand (BCH) is located above Lake Gertrude, between 800 and 900 metres in elevation. Huon pine in the Lake Marilyn catchment were divided into two sampling populations known as Lake Marilyn High (LMH) and Lake Marilyn Low (LML) at around 800 and 700 metres, respectively. The final sampling location was at the 560 metre high Lake Vera (LVH) where both living trees and subfossil logs were sampled.

The first BCH samples (Feb, 1993) were taken from a gully accessed via Artichoke Valley, while the second, higher location (March, 1993) was approached from the upper limit of the stand (Plate 3.2b). In total, 45 living trees were sampled from these two parts of the BCH stand; 35 from the upper portion and 10 from the lower portion. No subfossil trees were sampled, though the presence of several logs of undetermined age was noted, particularly in the lower portion of the stand.

The plant community in the interior of the BCH stand can be described as implicate rainforest using the nomenclature of Jarman *et al.* (1984). Co-dominant with *Lagarostrobos franklinii* are old-growth *Athrotaxis selaginoides*, both species attaining heights up to 10m, with diameters of some of the largest trees up to 80cm. Other canopy species include *Eucryphia lucida, Nothofagus cunninghamii* and *Phyllocladus asplenifolius*. Dense tangles of *Anodopetalum biglandulosum* are found throughout the interior of the stand, particularly in the gully below Artichoke Valley. *Diselma archeri* is found throughout the highest part of the stand, often in tree form with stems upwards of 30cm in diameter. Hickey and Felton (1988) described a shrub layer consisting

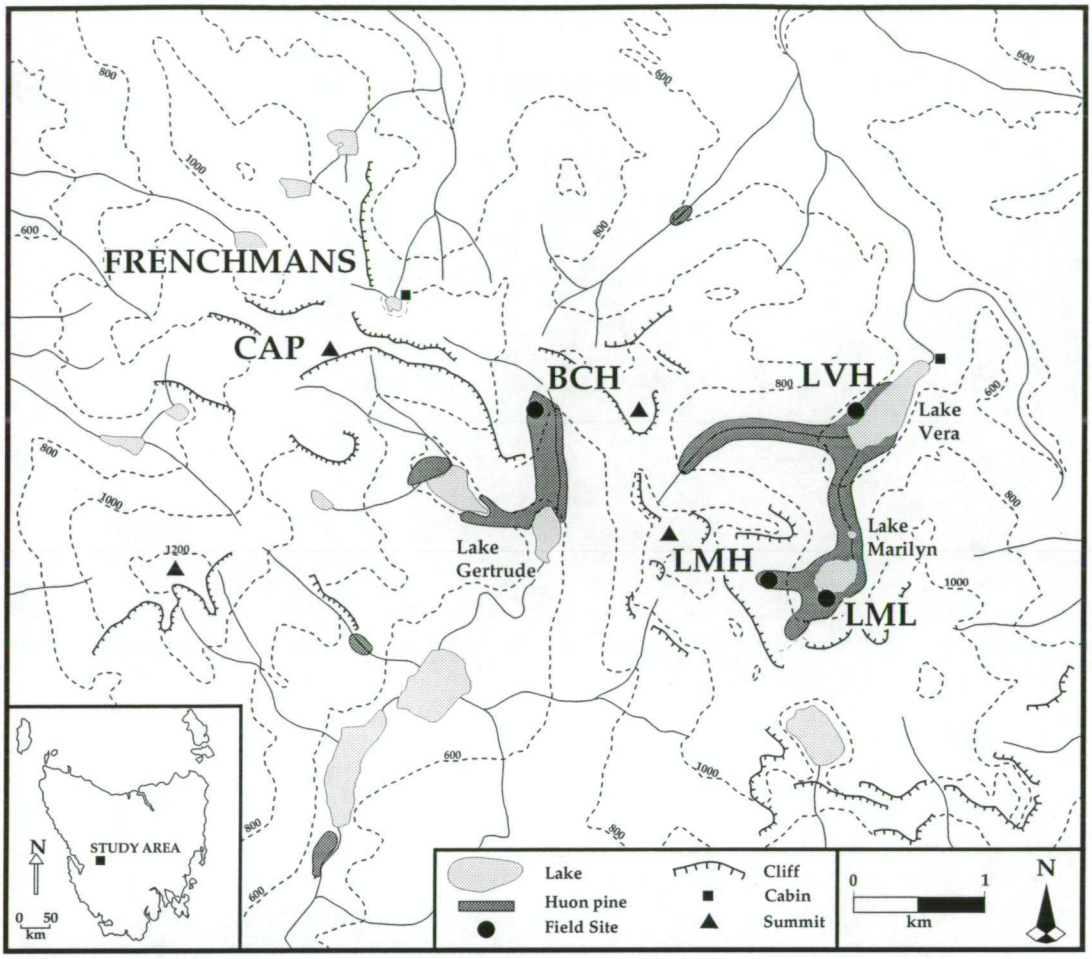

Figure 3.6. Frenchmans Cap chronologies site map. (Contours in metres).

of *Archeria serpyllifolia*, *Nothofagus gunnii*, *Trochocarpa cunninghamii* and *Trochocarpa gunnii*. They also noted the common shrubs *Coprosma nitida*, *Lomatia polymorpha*, *Orites diversifolia*, *Podocarpus lawrencii*, *Richea pandanifolia*, *Richea scoparia*, *Tasmannia lanceolata*, and *Telopea truncata*.

Hickey and Felton (1988) remarked on the unusual association of Huon pine with *Nothofagus gunnii*, *Diselma archeri* and *Podocarpus lawrencii*, a co-existence that had not previously been reported. Since then, these same associations were found within the 950 metre LJH stand on Mt. Read (Bacon, 1992; Peterson, pers. comm.). The 800 metre LMH site, however, does not display such associations, exhibiting a more abrupt ecotone to wet sclerophyll forest at the upper limits of the stand.

A

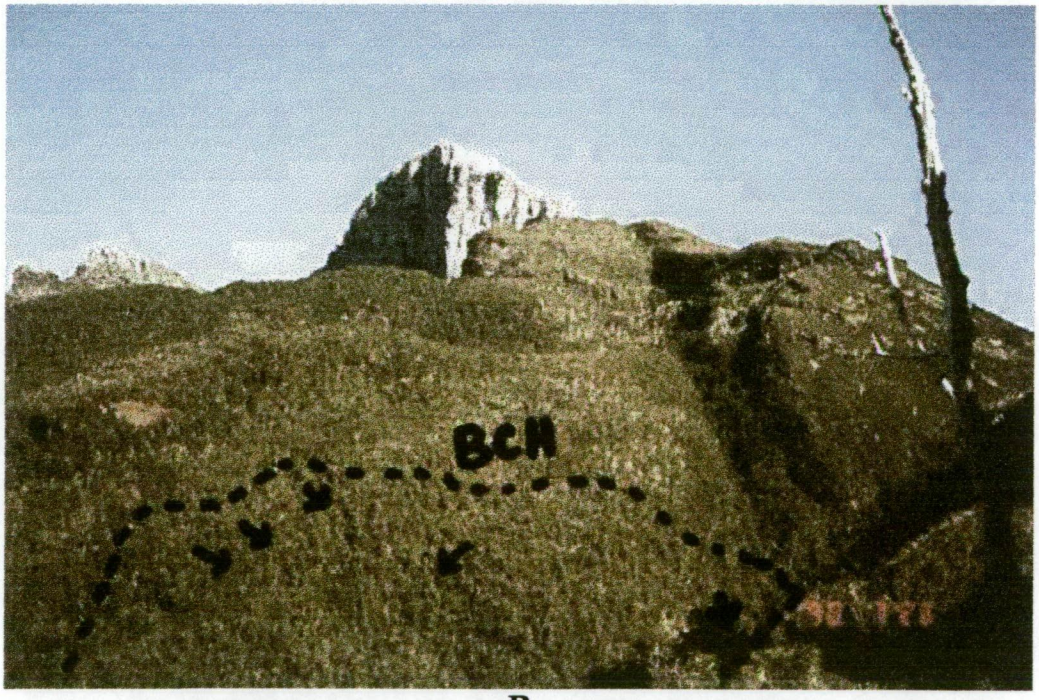

B

Plate 3.2. Field sampling sites in the Frenchmans Cap area. Photo **A** was taken from the summit of the Frenchmans Cap looking southeast toward Barron Pass with the locations of Lake Marilyn (M), Lake Vera (V), and Buckley's Chance (B) indicated. Lakes Cecily and Gertrude are visible in the foreground. Photo **B** was taken from Barron Pass loooking into the southeast face of the Cap, with the approximate outline of the BCH site indicated by the dashed line. The arrows mark the primary locations of sampling within the stand.

A

B

Plate 3.3. Sampling of subfossil logs in Lake Vera. **A** shows the removal of LVS54 with the use of a tirfer and cable, one of 49 subfossil logs sampled from the lake in 1994. **B** shows a close-up of the same log with charcoal visible from a fire in the late AD 1480s.

The two collections from the Lake Marilyn cirque consist of core samples from living trees only; 14 from the LMH site, and 15 from the LML site in March, 1994, and no subfossil trees were sampled in either stand. Downed logs were found on the steep slopes of LMH but they did not appear to be of great age, while even the oldest of the living trees dates back only to AD 1541. The upper boundary of the stand formed a ragged ecotone with wet sclerophyll forest, dominated by widely scattered *Eucalyptus* spp. The ages of the Huon pine decrease with increasing elevation on the slope, suggesting a possible re-establishment following burning. It is possible that the above-mentioned ecotone marks the edge of a 1400s burn, possibly coincident with the 1480s Lake Vera burn discussed below. A bushfire in 1965 is reported to have reached this ecotone as well, and would have contributed to the maintenance of the wet sclerophyll vegetation above the LMH stand (Corbett, 1992).

The LML site consists of mature Huon pine trees growing in dense rainforest along the southern and western shores of Lake Marilyn. The oldest tree from this site germinated before AD 620, with several others extending before AD 1300. A dense understory, dominated by *Anodopetalum biglandulosum*, is overtopped by occasional old-growth *Nothofagus cunninghamii*, *Phyllocladus aspleniifolius* and *Atherosperma moschatum*. Many downed and half-buried logs were found on the forest floor, and several logs were detected by probing the deep sediments of the near-shore margins of the lake. Given the abundance of subfossil material, there seems to be scope for extending the Lake Marilyn chronology for at least the past few millennia.

Lake Vera is nearly 1 km in length, and occupies a steep-sided glacial valley at 560 metres elevation (Figure 3.6). Vegetation around the lake is highly dependant upon aspect, with Huon pine-dominated, implicate rainforest found along the northwestern shore of the lake where fire has been largely excluded. The west facing slopes are fire-

prone, with young, apparently even-aged stands of *Eucalyptus nitida* growing in open forest from the lake shore to the timberline at ca. 860 metres (Macphail, 1979). The understory in this wet sclerophyll forest contains remnant stands of *Nothofagus cunninghamii* and *Phyllocladus asplenifolius*. A wide till plain, extending out to the Rumney Creek Plain some 30 metres above the lake, is covered by *Gymnoschoenus* sedge lands (buttongrass plains). Several preserved Huon pine logs were found buried under the Rumney Creek Plain, and a preliminary radiocarbon date from the sample RCS1 indicates death at *ca.* 3,100 years ago. A substantial burn would have been required to initially penetrate and destroy the existing rainforest, followed by repeated burning to prevent its re establishment.

Fires in modern times have altered much of the vegetation in the Frenchmans Cap area. For example, a bushfire in 1966 burned a large tract of vegetation in the Lake Tahune area and destroyed a walker's hut at the lake, while an escaped bushwalker's fire burned nearly 6,450 hectares near Lake Vera in 1980. However, fire promoting and fire requiring species, in particular *Eucalyptus* and *Gymnoschoenus*, offer abundant evidence for a lengthy history of fire throughout the region, as high fire frequencies are required to produce and maintain *Gymnoschoenus* sedge lands such as those found at Rumney Creek and throughout the Frenchmans Cap area (Macphail, 1979). Given low fire frequencies, rainforest vegetation will suppress and then eliminate sclerophyll species, as it is difficult for fire to reach the centre of these moist forests. It therefore requires repeated burning to result in and maintain *Gymnoschoenus* sedge lands (Cunningham and Cremer, 1965; Ellis, 1971). The ignition source for these fires is a subject for debate, yet it seems almost certain that humans were the primary cause, with only occasional fires started by lightning (Horton, 1982).

Macphail (1975a; 1979) sampled the sediments from the *Restio* sedge mat at the northern end of the lake for pollen analysis (Table 3.3). He noted the abundant evidence for fire-related species in the catchment throughout the Holocene, but did not detect charcoal lenses from the fires noted above. It is likely that charcoal production from these fires was low enough to be either absent from the record, or easily missed at the resolution of his palynological study. The presence of Huon pine pollen was noted for most of the past 12,000 years, though it only becomes prominent for the past 6,000 to 7,000 years (Macphail, 1979).

Depth (cm)	Material
0-15	Rhizomes
15-75	Well-humified sedge peat
75-160	Coarse detritus mud
160-208	Bluish-grey clay mud (weathered erosion products)
208-280	Dark-brown clay detritus mud
280-285	Oblique contact b/t lacustrine mud and pebbly outwash clay
285-300	Bluish-grey clay (unweathered erosion products)

Table 3.3. Listing of stratigraphic material by depth in centimetres from a core taken on the northern sedge mat on Lake Vera. Three radiocarbon dates were as follows; 150-159cm = 4590 +/- 175 ybp; 208-213cm = 6950 +/- 175 ybp; 270-280cm = 11,530 +/- 240 ybp. All data from Macphail (1979).

The presence of subfossil logs at the southwestern end of Lake Vera was noted in February of 1993 during a reconnaissance to the area. An expedition to Lake Vera the following summer resulted in the recovery of 43 subfossil logs from the lake bottom along the western shore. Many of these logs exhibited significant amounts of charcoal, and two of the samples retained the outer cambial zone and bark along one radius. Analyses of these samples suggest a synchronous death resulting from a fire in the late AD 1480s (estimated at AD 1488 $\pm$ 2 years), though the exact year was difficult to determine due to the compressed nature of the growth rings in the zone of bark preservation. None of the submerged

logs recovered from Lake Vera post-date the time of this fire. It appears that the majority of these trees had been killed by the burn and were subsequently deposited into the lake in various states of decay (Plate 3.3). The possible effects of this and other fires on the chronology indices is discussed in Chapter 5.1.

Along with recovery of the logs from the lake, 29 living Huon pine were sampled from the western shore, immediately adjacent to the lake sampling location. The oldest tree germinated before AD 620, with several more dating back before AD 1000. A chronology from these samples reveals three highly anomalous growth periods, with the most prominent one immediately following the AD 1480s burn. The other two were in the early AD 1000s, and the AD 1630s, respectively. These growth features are synchronous across the entire stand, and are visible with the naked eye in all of the samples from this site. It is unclear whether these extreme growth departures are related to major fires in the region, though that is one plausible explanation. This question requires further research, and for purposes of this study these features are being treated as growth anomalies unrelated to climate.

3.6.3 Stanley and Harman Rivers

Two of the field sites used in this study are from the Pieman River catchment in western Tasmania; the 450 metre high Harman River site (HAR) and the 225 metre Stanley River site (SRT) (Figure 3.7). The HAR site was visited in 1991 and 1992, and sampling was limited to the coring of 32 living trees and 3 non-living, downed logs. The SRT site has been the focus of an interdisciplinary research project for more than a decade (e.g., Francey *et al.*, 1984; Barbetti *et al.*, 1992; 1995; Nanson *et al.*, 1995). A modern chronology from living and subfossil trees, combined with

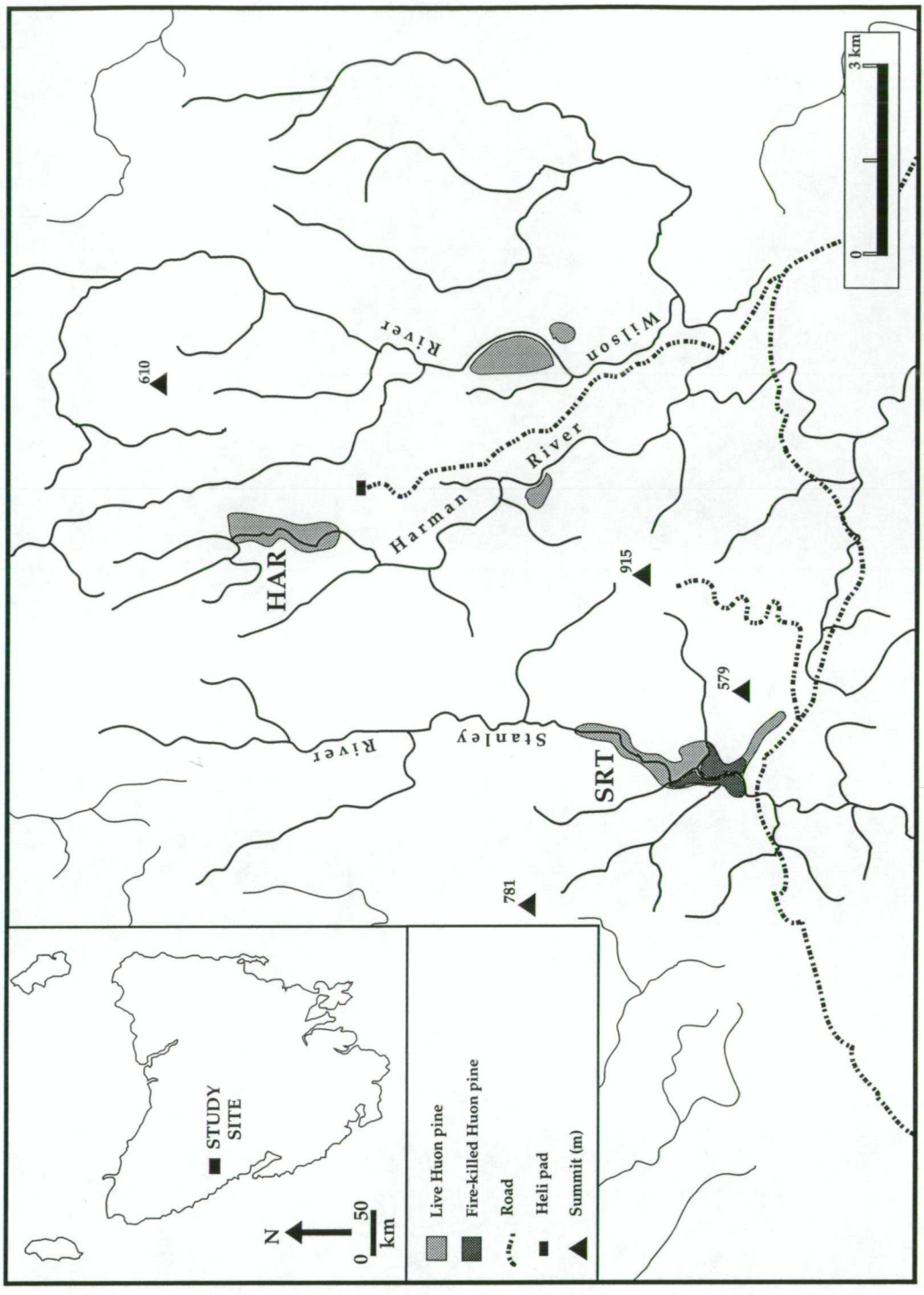

Figure 3.7. Site map for Pieman River chronologies. Two sites were sampled in this catchment, at the Stanley River (SRT) and at the Harman River (HAR), respectively.

two floating chronologies from subfossil logs, create a nearly-continuous coverage of the past 7,000 years (Figure 3.8). Logs from throughout the Holocene have been excavated from the SRT site, affording an opportunity for a continuous chronology for the past 10,000 years.

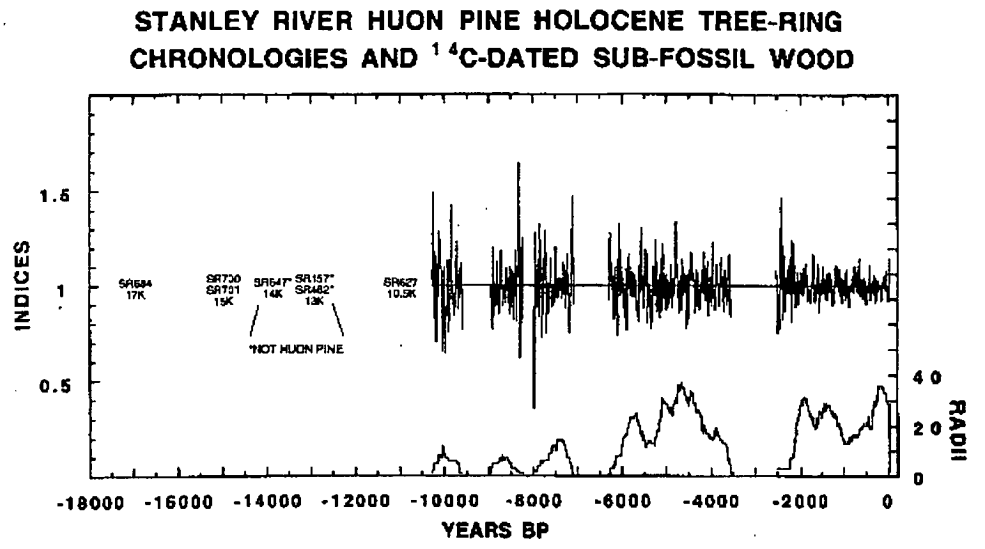

Figure 3.8. Huon pine tree-ring chronologies from Stanley River, and the radiocarbon-dated logs in the late glacial period. The chronologies have been smoothed with a 20-year low-pass filter for plotting purposes. The annual sample size (N) of each chronology is provided at the bottom of the plot.

The climate of the region is temperate maritime, with an average annual rainfall of around 2000 mm. The elevation is low enough in the SRT site (225 metres) that precipitation in the form of snow seldom occurs. The HAR site, at 450 metres, would be correspondingly colder and may experience winter snowfalls. Mean daily maximum temperatures from nearby Queenstown and Strahan suggest a range from around 20° C in January to 9° C in July, with mean daily minima from around 9° C to 3° C in January and July, respectively. Hot and dry summer conditions are not uncommon, and fires have burned much of the surrounding area. Both Huon pine stands exist in isolated, relict rainforest patches surrounded by sclerophyll forest and *Gymnoschoenus sphaerocphalus*-dominated sedgeland.

The Stanley River is a right-bank tributary of the Pieman River, draining a catchment of 67 km^2, and ranging in elevation from 50 metres where it enters the Pieman to 900 metres at its headwaters. The SRT site lies at approximately 225 metres above mean sea level. Preserved Huon

pine logs, excavated from the river channel and floodplain range from greater than 38,000 RCYBP to modern (Barbetti *et al.*, 1992; 1995).

Vegetation in the SRT site is primarily cool-temperate rainforest, while the surrounding area consists of *Gymnoschoenus sphaerocphalus*-dominated sedgeland where repeated fires have removed and inhibited the re establishment of rainforest assemblages (Macphail and Colhoun, 1985). The region has experienced substantial disturbance in recent decades due to logging, alluvial tin mining and fire, though the study site itself has been largely undisturbed (Nanson *et al.*, 1995). The rainforest is dominated by *Nothofagus cunninghamii, Lagarostrobos franklinii,* and *Phyllocladus aspleniifolius* with *Anopterus glandulosus, Atherosperma moschatum* and *Eucryphia lucida.* Rainforest vegetation is most protected near the river, where seedlings of Huon pine and *Nothofagus* co-exist with mature trees along the river bank. Huon pine logs are found in abundance and form several log jams across the river channel, which Nanson *et al.* (1995) interpreted as evidence of reduced stream discharge around 3.5 ka YBP in response to ameliorating climatic conditions. The build-up of log jams serves to further reduce stream power, thereby increasing channel stability over the past 2 millennia.

The modern SRT chronology is primarily comprised of a subset of some 46 Huon pine trees sampled in 1982 (Francey *et al.*, 1984). A total of 62 modern trees were sampled, including 16 celery top pine. Most of these were core-sampled, however 13 cross-sections of Huon pine, and 4 of celery top pine were cut from fallen and logged trees. Excavation and retrieval of logs from the river channel and floodplain since 1981 has yielded more than 358 subfossil sections, mostly of Huon pine (Barbetti, pers. comm.). There were 68 logs sampled between 1981 and 1984, 104 logs during the 1992 excavation, and a further 186 sampled in 1994 (Plate 3.4). In an attempt to update the modern chronology 40 additional living trees were cored in 1994 but these have yet to be processed.

Plate 3.4. Excavation of subfossil logs from the Stanley River. Perhaps the greatest potential for a Holocene-length Tasmanian chronology comes from the ongoing research at this site (e.g., Francey *et al.*, 1984; Barbetti *et al.*, 1992; 1995; Nanson *et al.*, 1995). More than 300 subfossil conifer logs have been excavated since 1982, in three separate excavations. Logs collected so far have dated as far back as 38,000 years ago, with several subsets comprising "floating chronologies" that cover much of the past 10,000 years (see Figure 3.8). The logs from the Stanley River have been a critical part of an international study on the inter-hemispheric comparison of ^{14}C production over the past few millennia, and also give important information about key climatic periods such as the Northern Hemisphere's Younger Dryas between 10 and 12 ka B.P., or the time of deglaciation in Tasmania around 14-12 ka B.P.

Of the 358 subfossil conifer logs sampled from the Stanley River, nearly 150 have known ages, while the remainder have yet to be studied (Barbetti, pers. comm.). Nearly 90% of the dated logs are younger than 9ka RCYBP, while four are older than 30ka RCYBP. Five logs fall between 10 and 9 ka RCYBP, four of which are discussed by Barbetti *et al.* (1995), while nine are known to be between 18ka and 10ka RCYBP. Several appear to fall either in, or nearby, the time of the Northern Hemisphere's post-glacial cool period known as the Younger Dryas. Only the modern SRT chronology, covering the past 2,554 years, is used for this study.

The Harman River is a main tributary of the Wilson River, entering just north of the Pieman River Road (Figure 3.7). Elevation ranges from 110 metres where it joins the Wilson, to more than 600

metres at its headwaters. The HAR site is about 8 km north of the Pieman River Road, located in a protected patch of rainforest at 450 to 550 metres in elevation. Huon pine are found along a 1.5 km stretch of the river, primarily within 20 metres of the river banks in a steep sided, north-south trending valley through which the Harman River flows. They grow primarily on nutrient poor, granite-derived soils which are thin and sandy, above a contact zone with serpentine. Several patches of Huon pine extend upslope on both sides of the river, particularly at the upper end of the stand. Vegetation within the stand is implicate rainforest with dense tangles of *Anodopetalum biglandulosum* in the understory. Co-dominant with Huon pine are *Phyllocladus aspleniifolius, Nothofagus cunninghamii* and *Atherosperma moschatum*. Huon pine seedlings are common, particularly along the banks of the river where they are often found growing in shallow pockets of soil and on downed logs. Wet sclerophyll forest completely surrounds the rainforest enclave, testimony to extensive burning of the region.

The average diameter of the Huon pine sampled at the HAR site is 80cm, with the smallest being 40cm. The largest tree is HAR09 (Plate 3.5), which has a diameter of 187cm, longer than our longest increment corer. At more than 2,500 years in age this is the oldest known living specimen of Huon pine, and the absolute age of the tree could only be estimated at around 3,000 years. Subfossil logs were found in significant numbers at the HAR site, but none were sampled. It is unclear what time-span would be covered by the logs found in the river channel and bed, as the soil depth does not appear to be deep enough to contain logs of early Holocene age. It is likely that the conditions leading to channel stabilisation at the Stanley River (Nanson *et al.*, 1995) may have had a similar effect at the Harman, implying that logs greater than 3 to 4 ka BP in age are unlikely to be found. Many of the trees sampled from the HAR site were riverbank trees, and exhibited poor circuit uniformity due to

channel undercutting and flood damage. Crossdating was therefore difficult in many samples, and a total of 34 cores from 18 of the 35 sampled trees was used in the final chronology. The details and statistics of the finalised chronology are discussed in Chapter 5.1.

Plate 3.5. The oldest-documented living Huon pine. The tree, known as HAR09, is growing in the Harman River in western Tasmania, and is more than 2,500 years old with a diameter of nearly 2 metres. Its actual germination date has not been determined due to insufficient length of the corers used, but it is estimated to have germinated more than 3,000 years ago. A mature celery top pine, estimated at more than 200 years in age, grows from the crown of the old tree.

CHAPTER 4: MATERIALS AND METHODS

4.1 Phenology of *Lagarostrobos Franklinii*

Lagarostrobos franklinii (Huon pine) is a member of the family Podocarpaceae and is endemic to Tasmania. Previously classified in the genus *Dacrydium*, it was reclassified by Quinn (1982). It is a relict Gondwanan species, with its closest relative (and the only other member of the genus *Lagarostrobos*) being *L. colensoi* of New Zealand.

Huon pine (Plate 4.1) is a long-lived, slow-growing species that is prized by craftsmen and boat builders for its highly rot-resistant, fragrant timber. Its resistance to decay is attributed to the production of the extractive oil *methyl eugenol*, which inhibits the activities of wood-consuming micro-organisms (Millington *et al.*, 1979), and is responsible for the preservation of logs for many thousands of years. Due to its long time to maturity (*ca.* 500 years) Huon pine has not been a viable plantation species, and exploitation of natural stands for commercial use has led to a significant reduction in old-growth over the past 180 years. Individuals greater than 1,000 years are not uncommon in most of the sites presented for this study, with the exception of LMH where an apparent upslope migration since the late 1400's is possibly the result of post-fire regeneration (Chapter 3.6.2).

Huon pine are presently found only in Tasmania. However, the fossil record suggests a more widespread distribution during the late Cretaceous/early Tertiary as far as 100 million years ago (Playford and Dettman, 1979). The oldest known Huon pine macro fossils, in the form of well preserved twigs, were found at Regatta Point, Tasmania and are believed to be 1-3 million years old (Hill and Macphail, 1985). Previous palynological evidence for high-elevation occurrences of Huon pine during the late Pleistocene were largely discounted, due to the perception of Huon pine as a lowland species (Colhoun, 1985; Macphail and Colhoun, 1985; Colhoun and van de Geer, 1986; 1988). However, recent

Plate 4.1. A millennia-old Huon pine tree from the BCH stand (**A.**), and a close-up of foliage from a tree on Mt. Read (**B.**).

confirmation of stands at altitudes up to 1,000 metres, combined with research demonstrating a greater frost resistance than expected (Read and Hill, 1988), lends credibility to these prior findings.

SPECIES	LAT. RANGE (deg.)	ALT. RANGE (m a.s.l.)	% RECORDS (800 m a.s.l.)
Nothofagus cunninghamii	7*	0-1260	27
Nothofagus gunnii	3	550-1260	88
Atherosperma moschatum	12*	0-1120	12
Eucryphia lucida	3	0-1000	3
Athrotaxis selaginoides	3	20-1300	56
Phyllocladus aspleniifolius	3	0-1160	25
Lagarostrobos franklinii	3	0-1000	<1

Table 4.1. Distribution of major Tasmanian rainforest canopy species with respect to altitude and latitude. Data from Read and Hill (1988) and Read (1989). Percentages refer to recorded occurrences from survey and herbarium records from Tasmania, and are not necessarily a measure of stem frequency. (Adapted from Read and Busby, 1990).
* indicates that species range extends onto mainland Australia.

Gibson *et al.* (1991) recognised four major community types for Huon pine, mostly restricted to west coast river systems. They found that the floristic variability of these communities correlated with temperature, rainfall, and geological gradients, and concluded that the present restricted nature of the species distribution is probably related to slow dispersal rates and the effects of fire, rather than a narrow ecological niche. Gibson and Brown (1991) noted that Huon pine's present distribution is far less than its potential (Figure 4.1), and suggest that this could be the result of slow terrestrial dispersal away from the glacial refugia of the species. Dispersal into canopy gaps away from river systems is also slow, yet Huon pine's propensity for vegetative resprouting from fallen trees assures that once it is established at a site, competitive exclusion is unlikely (Read and Hill, 1988; Gibson and Brown, 1991). Down-river dispersal is far more rapid due to the movement of vegetative material by high energy river systems (Gibson *et al.*, 1991).

The role of fire as a factor in controlling the present distribution of Huon pine is poorly understood (Gibson *et al.*, 1991). They appear

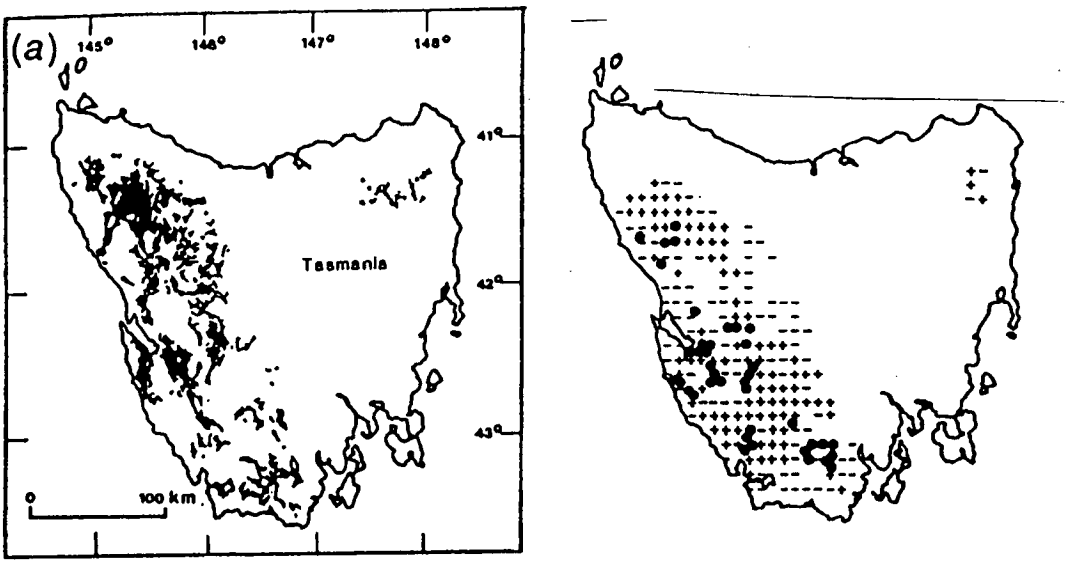

Figure 4.1. The actual and potential distribution of Huon pine in Tasmania. The map on the left (a) shows the present distribution of Tasmanian rainforest (from Kirkpatrick and Dickinson, 1984a). The map on the right shows the actual (black circle) and potential (+ = strong prediction, - = marginal prediction) distribution for *L. franklinii* derived from the program BIOCLIM. The actual coverage of Huon pine is far less than might be expected, and is likely related to the slow dispersal away from species refugia, as well as its general intolerance of fire. Similar patterns can be seen for other Tasmanian rainforest species. (From Read and Busby, 1990.)

to be very intolerant of fire, and even radiant heat from low-intensity burns has been reported to result in mortality (M. Peterson, pers. comm.). There is evidence, however, to support regeneration of Huon pine into areas previously burned, such as in the Denison River (Gibson and Brown, 1991), the Stanley River (Barbetti, pers. comm.), and at Lake Vera (Chapter 3.6.2). In areas where buttongrass plains now cover subfossil Huon pine logs, such as at Rumney Creek near Lake Vera and the Governor River (M. Barbetti, pers. comm.), it is likely that repeated fires are responsible for the ultimate removal of rainforest assemblages. Such fires were most likely the result of Aboriginal burning or lightning.

Given the importance of Huon pine as an economic resource and as a rare endemic species, there has been a relative dearth of ecophysiological research. Notable studies include a series of reports concerned with establishing the distribution of Huon pine in the state, along with some basic information concerning stand structure and

management issues (e.g., Millington *et al.*, 1979; Pedley *et al.*, 1980; Davies, 1983; Gibson, 1986; and Peterson, 1990). Francey *et al.* (1984; 1985) analysed physiological influences on carbon isotope discrimination in Huon pine, towards the goal of reconstructing past changes in atmospheric ^{13}C. Shapcott (1991) analysed the population biology and genetic variation in a number of stands across the species' range. Read and Busby (1988) and Read and Hill (1990) studied frost resistance and photosynthetic rates in a number of Tasmanian species, including Huon pine, while more detailed discussions regarding its ecology can be found in Gibson *et al.* (1991) and Gibson and Brown (1991).

Huon pine are mostly dioecious, though bisexual individuals have been noted (Quinn, 1982). They are capable of both sexual and vegetative reproduction. Sexual reproductive activity is thought to be episodic with years of synchronised, high seed production (or mast years) occurring every 5-7 years (Shapcott, 1991). Seeds are not widely laterally-dispersed, yet can be transported significant distances in flowing water, and possibly by Green Rosellas which have been reported to feed on both female and male mature cones (Shapcott, 1991). In a controlled experiment on the viability of seed following continued submergence in water, Shapcott (1991) determined that up to 50% of seeds remained afloat for one month, while 5% remained floating for at least 2 months. There was virtually no embryonic deterioration even after 2 months in water, illustrating the potential for distant transport of viable seeds.

Low germination rates for Huon pine seeds may also be a factor in limiting the distribution of the species. Shapcott (1991) noted an overall germination of only 20% in seeds undergoing a variety of treatments in glasshouse experiments, and even lower germination rates in the field. Germination of seeds in the field commenced between weeks 29 and 36, only slightly later than those in the glasshouse experiments. Of those seedlings found in the field at several sites (Table 4.2), 77% were

Site	# on logs	# on soil	Total #
Newall Creek	9	12	21
Stanley River (SRT)	**14**	**65**	**79**
Greystone Bluff	20	29	49
Pine Creek	0	13	13
Riveaux Creek	185	2	187
Denison River	10	4	14
Gordon River	40	0	40
Teepookana Reserve	1	5	6
Frenchmans Cap (BCH)	**22**	**0**	**22**
Picton River	88	0	88
Pieman River	20	4	24
Gilbert Leitch	5	12	17
Anne River	8	0	8
Tahune Reserve	71	41	112
Condominium Creek	71	1	72
Huon River	138	4	142
King River	12	0	12
Junction Creek	25	23	58
Eagle Creek (Gordon)	85	27	112
Total	824	242	1066
Total % of Seedlings	77.30%	22.70%	

Table 4.2. Seedling establishment at 19 Huon pine stands, for two surface types; on logs and on soil. The two sites listed in boldface were also used in this research project. Note the difference in the percentages for these two sites. The Mt. Read site (not listed here) is comprised of only male trees and relies entirely on vegetative reproduction. Adapted from Shapcott (1991).

established on logs or on living trunks, while 23% were established on soil (Shapcott, 1991). This percentage varied significantly by site and illustrates the importance of downed logs as a medium for the establishment of seedlings.

Annual growth rates for Huon pine are low, and Francey *et al.* (1984) estimated that they range from 0.3 - 2.0 mm across the species distribution. In general, annual radial growth appears to decrease with elevation (Table 4.3), though soil type and site characteristics may play as important a role in restricting or enhancing growth in a general sense (Gibson *et al.*, 1991). Larger than expected growth rings for the LMH site (900 m) largely reflect the stand's composition of entirely "young" (<500 years) trees growing in an open environment, while many of the time-series included in the Mt. Read series come from below-ground sections

of subfossil logs, with often exaggerated ring widths due to a slight "buttressing" effect in the trees. The large standard deviation for the LVH chronology reflects the influence of several stand-wide, anomalous growth departures which are discussed in Chapters 3.6.2 and 5.1 and shown in Figure 5.5.

Site	Mn RW	Mx RW	Std Dev	Tot.#	Elev.	Soil
KDH	0.28	1.53	0.146	38,151	1000	Volc.
LJH	0.27	2.46	0.111	112,972	950	Volc.
BCH	0.36	1.58	0.138	35,149	900	Quar.
LMH	0.52	1.80	0.189	7,811	850	Quar.
LML	0.42	1.55	0.149	10,602	700	Alluv.
LVH	0.35	2.18	1.482	52,717	600	Alluv.
HAR	0.38	1.44	0.149	23,784	450	Gran.
SRT	0.49	3.18	0.200	48,601	200	Alluv.

Table 4.3. Mean and maximum annual radial growth rates (in mm) for several Huon pine sites at a number of elevations in Tasmania. Ring measurements may reflect a bias away from exceptionally large or narrow ring sequences, where anomalous growth from buttressing, reaction wood or injury are often avoided. KDH = Mt. Read krummholz; LJH = Mt. Read Lake Johnston; BCH = Frenchman's Cap High; LMH = Lake Marilyn High; LML = Lake Marilyn Low; LVH = Lake Vera; HAR = Harman River; SRT = Stanley River.

4.2 Sample Collection and Preparation

The tree-ring samples used for this study were collected via one of two methods: core sampling using a Swedish increment borer, or sectioning using a chainsaw or handsaw. Living trees were always sampled by coring, while non-living trees were mostly sectioned. A standard minimum of ten trees per site was sampled with at least two cores taken from each tree, parallel to the slope and avoiding all bole injuries and branches to minimise distortion of rings (Stokes and Smiley, 1968; and Fritts, 1976). While it is desirable to take cores from opposite sides of each tree, this was not always possible due to the distorted nature of many Huon pine stems and the congested nature of the stands. Cross-sections from subfossil logs were retrieved from a number of different situations: exposed on the surface, buried in river

deposits, lying on lake bottoms, and exposed from the erosional action of rivers.

Standard procedures were followed in the preparation of all samples (Stokes and Smiley, 1968; Fritts, 1976; Swetnam *et al*, 1985). After slow air drying, sanding films were used to polish the transverse surfaces of both cores and sections. Mechanical belt and orbital sanders were used to produce a surface up to 400 grit, and the final polishing was done by hand using sanding films up to 1500 grit. Given the generally microscopic nature of Huon pine growth rings, most samples required a polished surface to 600 grit or higher. This degree of surface preparation was necessary for visually inspecting ring sequences during the crossdating procedure.

4.3 Development of the Tree-Ring Chronologies

4.3.1 Crossdating: assuring accuracy of temporal control

Crossdating refers to the matching of naturally-occurring patterns in annual growth around the circumference of a single tree, and more importantly between different trees across a site (Figure 4.2). The science of dendrochronology is built upon the concept of crossdating ring sequences between trees within a stand, and when possible across broader regions (Douglass, 1914; Stokes and Smiley, 1968; Fritts, 1976; Hughes *et al.*, 1982; Cook and Kairiukstis, 1990). If sufficient covariance can be demonstrated among ring widths from different trees, and sample size is large enough, the exact year in which each ring was formed can be determined.

Crossdating is made possible because tree growth is frequently affected by variability in climate (Fritts, 1976). The annual sequence of favourable and unfavourable climate (e.g., years of ample rainfall and years of drought, or years of optimum temperature for growth and those when temperature inhibits growth) is faithfully recorded by the sequence

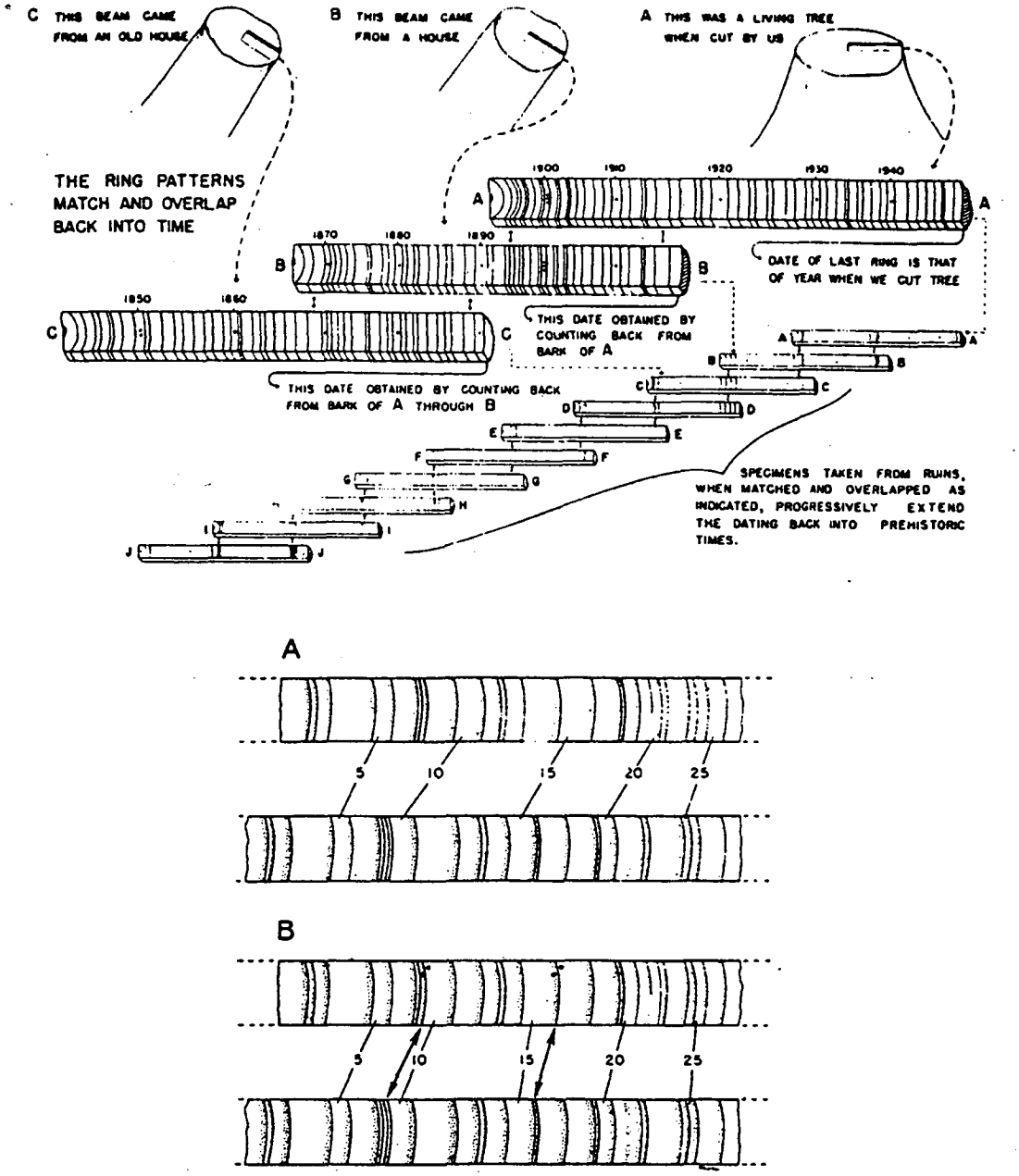

Figure 4.2. The principle of crossdating. Dendrochronology makes use of ring sequences from living trees and from overlapping sequences of non-living wood, as shown at the top of the diagram. Crossdating of ring sequences makes it possible to identify areas where rings are either locally absent, or where an intra-annual growth band appears to be a true annual band, as in the bottom half of the diagram; every fifth ring is numbered and in **A** the patterns of wide and narrow rings match until ring number 9 is reached, after which the pattern is offset. In the lower segment from **A**, rings 9 and 16 are very narrow and do not appear at all in the upper segment. Rings 21 (lower **A**) and 20 (upper **A**) exhibit intra-annual bands. In the upper segment of **B** the locations of the absent rings are designated by two dots, while the intra-annual band in ring 20 is recognised, and the patterns in all ring widths are synchronously matched. (From Fritts, 1976, drawings by M. Huggins).

of wide and narrow, or dense and less dense, rings in large numbers of trees. These patterns are sometimes observable in living and non-living trees over broad regions, making regional inferences about climate possible (Fritts, 1976; 1991).

If crossdating cannot be established, any ensuing research based on ring counting of the undated material cannot be regarded as dendrochronology, as there may be errors in dating. This is due to the possibility of non-detection of false ring boundaries and locally-absent rings in some species under certain environmental conditions (Stokes and Smiley, 1968; Fritts, 1976). Even if the ring-width patterns of two samples can be matched, it is only considered acceptable when comparison with other samples confirms the dating. An error of even a single year destroys the integrity of the crossdating and invalidates any subsequent interpretation of results (Douglass, 1934; 1935; Pilcher, 1990).

Crossdating procedures for this study followed standard methods during the initial construction of the chronologies (e.g., Stokes and Smiley, 1968; Swetnam *et al.*, 1985), including visually inspecting samples and using skeleton plots or key-year lists to match up patterns in the individual time-series. These procedures incorporated the width of individual rings, along with visually-detected variations in latewood density, frost-damaged tracheid cells, and cracking along latewood boundaries at specific years (Plates 4.2a-c).

Computer-assisted crossdating was employed for dating subfossil samples of unknown age. Crossdating was first established between separate paths along the sample, accounting for each ring around the circuit and detecting possible locally-absent rings or false ring boundaries. The best radii were selected and measured before being compared against the existing chronology using the program COFECHA, a quality control program that uses correlation statistics to test the crossdating of measured tree-ring time-series (Holmes, 1983; Holmes *et al.*, 1986). When the

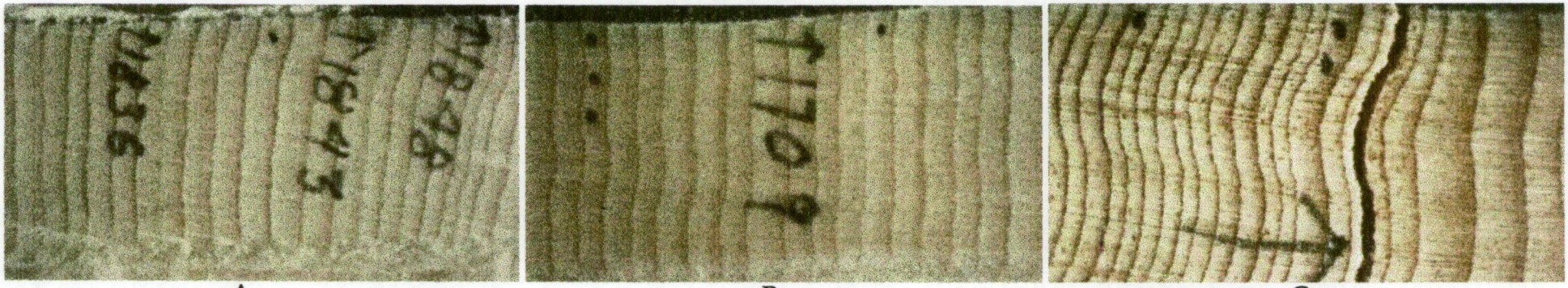

A. B. C.

Plate 4.2. Details of Huon pine rings from 3 subalpine trees. Other features were used for crossdating ring sequences in addition to ring width. For example the 1830s-1840s light-ring sequence (**A.**) where consistent light-density latewood boundaries were formed in 1836, 1843, and 1848 in trees from above 800 metres; and the highly reliable 1709 light ring (**B.**) also found only in trees from above 800 metres. Latewood boundary cracks, such as that shown in (**C.**) from a subfossil log from Lake Vera, also served as reliable markers for crossdating. One of the most reliable latewood boundary cracks was between the AD 1662/63 rings on Mt. Read, a boundary of severely reduced latewood density, and ruptured tracheid cell walls was common.

undated sample sufficiently overlaps the dated chronology a suggested date and correlation statistics are supplied. The researcher must then visually inspect the sample to corroborate the suggested date. COFECHA was used to assess the crossdating of each of the chronologies used in this study and the output from these tests are summarised in Chapter 5.1.

4.3.2 Standardisation: the removal of non-climatic signals

Arguably the most important procedure in the development of tree-ring chronologies for dendroclimatic research involves the removal of the growth trend, or *standardisation* of the tree-ring time-series. Consequently, much attention has been given to the subject and detailed discussions can be found in Fritts (1976), Fritts and Swetnam (1986), Hughes *et al.* (1982), and Cook and Kairiukstis (1990). Standardisation is necessary because ring-width time-series are non-stationary processes; bounded by zero at their lower limit, with a highly variable upper limit that is dependent upon several limiting factors (Douglass, 1914; Fritts, 1976; Cook, 1990). Standardisation therefore seeks to minimise growth trends which are unique to individual trees, while maximising the variance or "signal" common to all trees from a site (Graybill, 1982). Each tree has its own potential growth "corridor", and the absolute width for a given year t is dependant upon factors such as the age of the tree at year t, and its unique microsite characteristics which may have influenced its overall corridor of potential ring width values for that year (Fritts, 1976). As a result it may be inappropriate to compare the measurements of individual series without accounting for these differences and standardising the ring-width series to dimensionless, stationary time-series with a similar mean and standard deviation (Douglass, 1914; 1919; Fritts, 1976; Hughes *et al.*, 1982; Cook *et al.*, 1990a).

The objective of standardisation is, therefore, to reduce the large average growth of youth so that it may be compared with the slower

growth of maturity and old age in individual trees (Schulman, 1945). In essence this process amounts to the extraction of the desired "signal" from the remaining "noise" associated with tree growth for each tree in a given stand (Fritts, 1976). In this case *signal* may be defined as the information contained within the tree ring series that is relevant to a particular study, while *noise* may be defined as the information that is not directly relevant (Cook, 1990). For purposes of dendroclimatological studies a linear aggregate model of tree growth may be considered, as outlined by Cook (1990) and expressed as:

$$R_t = A_t + C_t + \delta D1_t + \delta D2_t + E_t, \qquad (4.1)$$

where:

R_t = the observed ring-width series;

A_t = the age-size-related trend in ring width;

C_t = the climatically-related environmental signal;

$D1_t$ = the disturbance pulse caused by a local endogenous disturbance;

$D2_t$ = the disturbance pulse caused by a stand wide exogenous disturbance;

E_t = the largely unexplained year-to-year variability not related to the other signals.

The model is expressed in linear form for purposes of simplification, in spite of known non-linear relationships associated with ring-width, such as that between the mean and standard deviation (Fritts, 1976). However, such relationships can be linearised by log transformation, indicating the intrinsically linear nature of the process (Cook, 1990). The δ associated with $D1_t$ and $D2_t$ is a binary indicator of the presence or absence of either class of disturbance at some time t in the ring widths: when $\delta = 1$ the disturbance is present, when $\delta = 0$ it is absent. Therefore A_t, C_t, and E_t are

all assumed to be continuously present in R_t, and depending on whether the intervention of some disturbance has occurred at some time t, $D1_t$ and $D2_t$ may not be present (Cook, 1990).

The age-size-trend (A_t) is a non-stationary process that partially reflects the geometrical constraint of adding a volume of wood to a stem of increasing radius (Fritts, 1969). If this constraint is the primary source of the trend then A_t will exhibit an exponential decay as a function of time, subsequent to the juvenile period of increasing radial growth (Fritts, 1976; Cook, 1990). This type of growth trend is typified by trees growing in very open environments where the effects of competition and disturbance are minimised (Stokes and Smiley, 1968; Fritts, 1976). In closed canopy stands where the effects of competition and endogenous disturbances are more frequent, the behaviour of A_t may be strongly influenced in ways that may not be synchronous in all trees in the stand (Fritts, 1976; Cook, 1985; 1990). Figure 4.3 illustrates some typical growth trends found in ring width data. There is no predictable shape for A_t, in that it does not necessarily arise from any family of deterministic growth curve models such as the negative exponential curve. It should instead be thought of as a nonstationary, stochastic process that may, in special circumstances, be treated as a deterministic process (Cook, 1990; Cook *et al.*, 1990a).

C_t is representative of the aggregate influence of all climate variables on tree growth. The typical variables which comprise C_t include precipitation, temperature and solar radiation. These variables combine to influence tree growth by controlling photosynthesis and the amount of available moisture for physiological activity within the constraints of the phenology of a given species (Fritts, 1976; Salisbury and Ross, 1992). It is the broad scale quality of these climate variables that is typically of interest to the dendroclimatologist, as all trees in a stand will be affected in a similar manner, thereby maximising the common signal

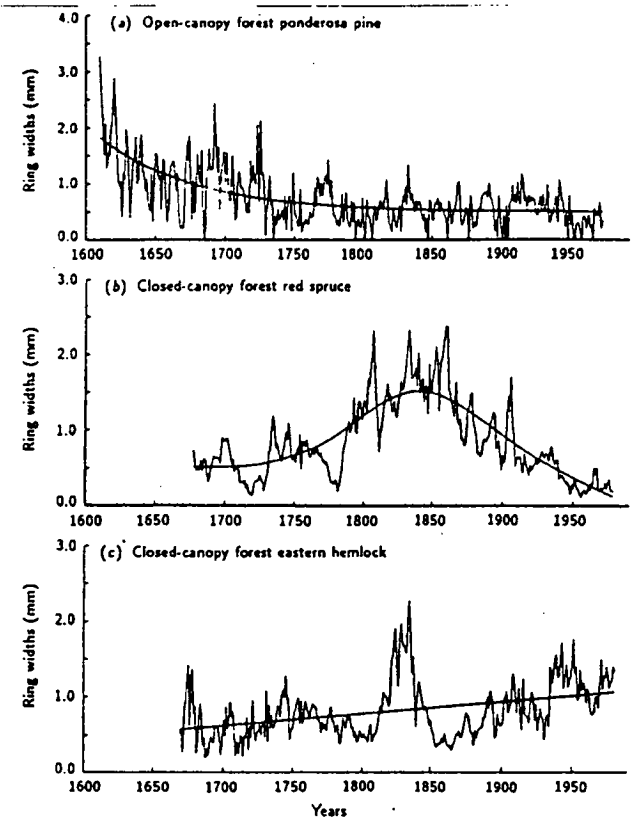

Figure 4.3. Three common growth trends associated with tree-ring time series. Series (a) is from a *Pinus ponderosa* (Ponderosa pine) growing on a semi-arid site, in an undisturbed, open-canopy situation. The classic negative exponential decay of ring width, based on the argument of the geometric constraint of adding a given volume of wood to a tree of expanding radius, is clearly shown in this series. This type of growth trend is expected when the effects of competition and disturbances are kept to a minimum. The series in (b) and (c) are both from closed-canopy stands of *Picea rubens* (red spruce) and *Tsuga canadensis* (eastern hemlock), respectively. These two series illustrate the effects that competition and disturbance pulses can have on the expected negative exponential decay as shown in the first example. Standardisation techniques have been developed to attempt to remove these disturbance effects from the individual time series, while maximising the common signal amongst all trees in the stand. (From Cook, 1990.)

(Fritts, 1976). These climate variables may usually be thought of as stationary, stochastic processes, though there may be some persistence in an autoregressive sense (Cook, 1985; 1990; Guiot, 1987).

The endogenous disturbance pulses represented by $D1_t$ vary from tree to tree. They are typified by gap-phase stand development in which trees are removed from the canopy by localised processes effecting only those trees adjacent to the gap (White, 1979). They usually create patterns of suppression and release in the ring widths of affected trees. Truly endogenous disturbances are random events in space and time, and the

corresponding effect in a ring width series will be largely uncorrelated with similar pulses in other trees, even from the same stand (Cook, 1990). Exogenous disturbances, denoted by $D2_t$, are characterised by stand wide disturbances attributed to such phenomena as fire, insect damage, disease, logging effects and pollution, though they may also result from episodic climate-related events like frost, wind, or ice damage. The key factor which may distinguish $D2_t$ from $D1t$ is the synchrony in time of the former across the stand, unlike the latter which will exhibit non-synchronous, random behaviour in individual trees (Fritts, 1976).

The final term in the equation is E_t which represents the variance in the ring widths that remains unexplained after accounting for A_t, C_t, $D1_t$, and $D2_t$ (Cook, 1990). Sources for this unexplained variance include microsite characteristics such as variability in soil quality or type across the stand, hydrological gradients across the site, or measurement error. It is assumed that E_t is serially uncorrelated within, and spatially uncorrelated between, trees in the stand.

This linear aggregate model for ring-width series assumes that there is no covariance between any of the components outlined above. This assumption will not always hold, however, as in the case where the transient response time of the disturbance pulses of $D1_t$ or $D2_t$ exceed the length of the ring-width series and its corresponding growth trend A_t. In this instance the trend component may consist largely of the trend in either of the two types of disturbance pulse, and will be difficult to decompose. To account for this potential problem in identifying the growth trend, Cook (1990) offers the alternative notation:

$$G_t = f(A_t, \delta D1_t, \delta D2_t)\,, \tag{4.2}$$

where the growth trend (G_t) is a function of the pure age trend component (A_t) and the stochastic perturbers of that pure age trend ($\delta D1_t$

and $\delta D2_t$) which may or may not be present in the ring width series. This definition suggests that C_t is the signal of interest, as all other components are considered collectively as non-climatic variance or noise.

Standardisation must therefore aim to convert the non-stationary ring-width series into a new stationary series, known as *indices*, which have a mean of 1.0 and nearly constant variance (Fritts, 1976; Fritts and Swetnam, 1986). This is usually accomplished by dividing each measured ring width value by the expected value estimated from G_t, as follows:

$$I_t = R_t / G_t \tag{4.3}$$

where I_t is the relative tree-ring index. Due to the heteroscedastic nature of ring-width series, the indices are usually produced by division instead of differencing, reflecting the relationship between the local mean and variance; a relationship that is usually positive and linear (Fritts, 1976). While the ratio method (division as outlined above) is still the most common way of generating indices, Eriksson (1989) demonstrated that regression models developed within this conceptual framework were theoretically biased. The source of the bias was shown to be in the division process used to generate the tree-ring indices, and calculating simple residuals from the growth curve, instead of ratios or indices, produced regressions which were unbiased.

Eriksson (1989) did not describe the actual source of the bias in the tree-ring indexing procedure. However, Cook *et al.* (1992) suggested that one source might be related to the inherent asymmetry of radial growth in trees; a defined lower boundary of zero and a poorly-defined, highly-variable maximum. This asymmetry fosters a dependence between the local mean and standard deviation by roughly defining the overall corridor within which a tree can respond to environmental inputs such as climate (Cook *et al.*, 1992). Trees growing at faster rates have a wider

corridor within which to respond to climatic effects than do slower-growing trees. Thus, the variance increases in proportion to the mean and the effect of division on the resultant index can be highly nonlinear, especially where the estimated growth curve approaches zero (Cook *et al.*, 1992). Figure 4.4 illustrates this relationship and the way it effects both a constant, hypothetical ring-width value of 1mm, and the standardised indices of the Mount Read (LJH) Huon pine chronology. Note that in the former case even ratios below 2, a range which includes most tree-ring indices, exhibit a distinct nonlinear effect. By first stabilising the variance and then using residuals instead of ratios, this nonlinear effect can be completely removed.

Cook *et al.*, (1992) used this approach for the standardisation of the Mount Read chronology, employing a data-adaptive power transformation prior to detrending as a one-step procedure, using the relationship between the local spread and level (the standard deviation S, and mean M, respectively) for the estimation of the best power transformation (Emerson and Strenio, 1983). The model is as follows:

$$\log S = k + b \log M , \tag{4.4}$$

which is a simple linear regression in logarithmic space, where $S = cM^b$, and $k = \log c$, and b is the slope of the spread-versus-level relationship (Cook *et al.*, 1992). This being the case, then $p = 1 - b$ is the appropriate value for the exponent used for the power transformation (Emerson and Strenio, 1983).

For this study the raw ring-width chronologies (no detrending) were analysed prior to deciding on the appropriate models for standardisation. The inclusion of subfossil logs with living-trees in the chronology development procedure may actually serve to filter some of the trend associated with G_t , as can be seen from a perusal of Figures 5.1 - 5.7. A variety of single and double detrending options were tested, based

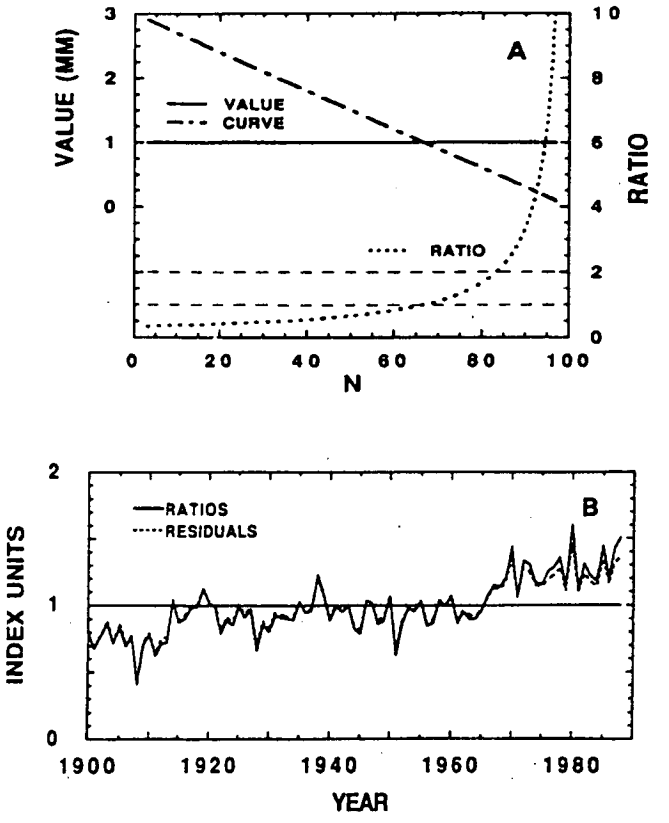

Figure 4.4. Illustrating the potential bias in the indexing procedure used in chronology building. **A** shows the potential nonlinear effect of division on the resultant tree-ring index (RATIO) when the estimated growth curve approaches zero. This plot shows the change in the ratio for a hypothetical ring width value of 1mm, as the curve-fit value varies from 3 mm to 0.1 mm. Even for ratios below 2, a range which includes most tree ring indices, there is a decidedly nonlinear effect. **B** shows the outer 89 years of the Mt. Read Huon pine chronology, estimated using the traditional indexing procedure (RATIO) and the two stage procedure (RESIDUAL) used by Cook *et al.* (1992) where the variance was stabilised by power transformation before detrending. All other standardisation parameters were kept constant (i.e., a 500-year spline and a biweight robust mean used for the creation of the mean value function). In order to keep the comparison simple, however, no autoregressive modelling was applied to either series. A systematic deviation between the two methods is apparent from the plot in **B**, with the RATIO method overpredicting the end values estimated from the RESIDUAL method. This disparity probably reflects a bias in the traditional indexing procedure. (From Cook *et al.*, 1992.)

on both *a priori* and *a posteriori* criteria. The standardisation options used for all seven Huon pine chronologies followed the methods of Cook *et al.* (1992) for the Mt. Read chronology, with a one-step power transformation used for stabilising the variance, prior to detrending with a cubic smoothing spline with a 50% frequency response cutoff of 500 years. The residuals method, as described above, was used for the generation of the ring-width indices. Complete chronology details are disclosed in Chapter 5.1.

4.3.3 Estimation of the mean value function

Three general methods have been used for estimating the mean value function, subsequent to detrending of ring-width series: the arithmetic mean, a mean based on testing for a mixture of normal distributions in the sample, and the biweight robust mean that discounts outliers (Cook *et al.* 1990b).. For this study the biweight robust mean was used for the computation of the mean value function for all chronologies. This method automatically discounts the influence of outlier values in the computation of the mean, thereby reducing variance and bias likely to be caused by these outliers (Mosteller and Tukey, 1977; Cook, 1985). Outlier values may result from endogenous disturbances which behave as random events in space and time, particularly in ring-width series from closed-canopy, mesic forests like those used for this study (Cook *et al.*, 1990b). The biweight mean for a given year t is computed through iteration as:

$$\bar{I}_t^* = \sum_{j=1}^{m} w_t I_t \ , \tag{4.5}$$

where

$$w_t = [1 - [\frac{I_t - \bar{I}_t^*}{cS_t^*}]^2]^2 \ , \tag{4.6}$$

when

$$[\frac{I_t - \bar{I}_t^*}{cS_t^*}]^2 < 1 \ . \tag{4.7}$$

The weight function is denoted by w_t and is symmetric and therefore unbiased in its estimation of central tendency, provided that the data are symmetrically distributed (Cook, 1985). S_t^* is a robust measure of the

standard deviation of the frequency distribution, that is defined here by the median absolute deviation, or MAD, calculated as follows:

$$S_t^* = \text{median} \{ | I_t - I_t | \} , \quad (4.8)$$

and c is a constant, often given as six or nine (Mosteller and Tukey, 1977). This constant, c, determines the point at which an outlying value is given a weight of zero, at which point the outlier is discounted and has no influence on the estimation of the mean index (Cook *et al.*, 1990b). When c is set to nine, for example, any value exceeding $\pm$ 6 standard deviations from the mean is rejected (Mosteller and Tukey, 1977). A potential drawback of using the biweight robust mean is its lower statistical efficiency compared to the arithmetic mean when the sample population is devoid of outliers and approximates a Gaussian distribution (Cook, 1985). However, given the nature of closed-canopy, cool-temperate rainforest sites, like those used for this study, the biweight robust mean is justified as insurance against outliers in the estimation of the mean value function.

Autoregressive modelling, based on ARMA time-series modelling (Box and Jenkins, 1970), has also been shown to be an effective way of generating a more statistically-efficient estimate of the mean value function (Cook, 1985; Guiot, 1987). This is particularly true where autocorrelation within individual time-series is high and out-of-phase between series. Tree ring indices can be expressed as an ARMA process of order p and q, in difference equation form as:

$$I_t = \varnothing_p I_{t-p} + \ldots + \varnothing_1 I_{t-1} + e_t - \theta_1 e_{t-1} \ldots - \theta_q e_{t-q} , \quad (4.9)$$

where e_t values are serially-random inputs or shocks driving tree growth as reflected in the ring widths, and the $\varnothing_i$ values are the p autoregressive (AR) coefficients, and the θ_i values are the q moving average (MA) coefficients. These two coefficients combine to produce the characteristic

persistence or "memory" exhibited in the I_t (Fritts, 1976; Cook 1985). For each ring-width series, the values for e_t are assumed to be a combination of inputs related to the factors C_t, $D1_t$ and E_t as outlined in equation (4.1). The age-size trend, A_t, is considered to be either nonexistent in the raw ring width series (in other words $I_t = R_t$) or sufficiently removed by the detrending process (Guiot, 1987).

Tree-ring indices can be modelled and prewhitened as AR(p) or ARMA (p,q) processes in order to remove the effects of unwanted, disturbance-related transience on the common signal (Cook, 1985; Guiot, 1987). The Akaike Information Criterion, or AIC (Akaike, 1974), can be used to effectively determine the order of the process (Cook, 1985). Prewhitening is carried out following the estimation of the ARMA (p,q) coefficients, and converts the tree-ring series to *white noise* (Cook, 1985), calculated in difference equation form as:

$$e_t = I_t - \varnothing_1 I_{t-1} - \ldots - \varnothing_p I_{t-p} + \theta_1 e_{t-1} + \ldots + \theta_q e_{t-q} \qquad (4.10)$$

The result is an e_t which represents the contributions of C_t, $D1_t$, and E_t, while $D2_t$ is assumed to be absent (Cook *et al.*, 1990b). The transient effects of the endogenous disturbance pulses are also reduced, and thus foster an increase in fractional common variance in the mean-value function of e_t (Cook, 1985). Combined with the biweight robust mean for the computation of e_t, an improved estimate of C_t is derived. However this estimate of C_t, in the form of e_t, is lacking the natural persistence which is related to climate and tree physiology (Fritts, 1976; Hughes *et al.*, 1982; Cook and Kairiukstis, 1990), and during climatic reconstruction the persistence from the original climate calibration variable must be added back to the reconstructed series (Chapter 4.4).

In order to completely model the common signal within an ensemble, it is necessary to estimate the common persistence structure among all detrended tree-ring series. A pooled estimate of autoregression

is computed directly from lag-product sum matrices of the ensemble, including information on persistence both within and among series (Cook, 1985). This pooling procedure is quite robust for dealing with high levels of out-of-phase fluctuations among series that are the result of endogenous disturbances, and is easy to apply for pure AR models. However it is not easily applied to the ARMA modelling procedure due to the highly nonlinear MA coefficients (Cook, 1985; Cook *et al.*, 1990b).

A final tree-ring chronology ($\mathbf{I_t}$) can be created, following the estimation of the common signal components as outlined above, by convolving the pooled AR coefficients with the $\mathbf{e_t}$ upon the selection of appropriate starting values (Cook, 1985). All chronologies used for this project were pre-whitened using AR modelling as outlined above, combined with the biweight robust mean. Plots of each chronology, both prewhitened and containing the pooled autoregression, are presented in Chapter 5.1.

4.4 Reconstructing Climate from Tree Rings

4.4.1 Introduction

As outlined in Chapter 2, the response of tree growth to climatic forcing involves the interaction of many complex factors, and due to this complexity there are no suitable theoretical models to allow for the extraction of a climatic signal from tree-rings based on ecophysiological or mechanistic studies alone (Fritts, 1976; Hughes *et al.*, 1982; Cook and Kairiukstis, 1990). Dendroclimatologists therefore rely upon semi-empirical relationships between tree growth and climate for calibrating the climate response of a given chronology (Fritts, 1976; Guiot *et al.*, 1982). The multivariate statistical analyses used include principal component or eigenvector analysis, and canonical correlation and regression (Fritts *et al.*, 1971; Fritts, 1976; 1991; Guiot *et al.*, 1982).

The procedure that estimates the statistical growth-environment relationship is called *calibration*. The tree-growth/climate relationships revealed in this manner, called *response functions*, may not necessarily reflect a directly-coupled response. Rather, they may involve long chains of interacting cause and effect linkages that ultimately effect growth in the tree, resulting in enhanced or suppressed growth for a particular year (Figure 4.5). The climate response is evident because the elements of weather and climate affect the microclimates for individual trees, and thereby the physiological processes which in turn control growth (Gates, 1968a; 1968b; Fritts *et al.*, 1971; Fritts, 1976; Salisbury and Ross, 1992). When a sufficiently strong relationship has been established between tree growth and some parameter of climate (e.g., temperature or precipitation), the statistically-calibrated relationship can be used to generate a *transfer function* for the reconstruction of climate from tree-growth for the period prior to the available climatic data set (Lofgren and Hunt, 1982).

For calibration, standardised tree-ring indices are compared with the longest available instrumental records of climate, from meteorological stations that most closely represent conditions at the site. Long climatic time-series are required for a proper and robust statistical comparison (Fritts, 1976; Hughes *et al.*, 1982; Cook and Kairiukstis, 1990). However, baseline weather data for a given tree site are usually lacking, and the nearest meteorological stations may be many kilometres from the location of the trees. This problem is compounded by the search for the oldest and least disturbed trees available, which are likely to be in areas remote from most weather stations, and at substantially higher elevations. Hughes *et al.* (1978) illustrated how the percentage of chronology variance explained by climate and prior growth, respectively, could change from 34% and 31% to 45% and 28%, respectively, when rainfall data from sites 60km and 6km distant were

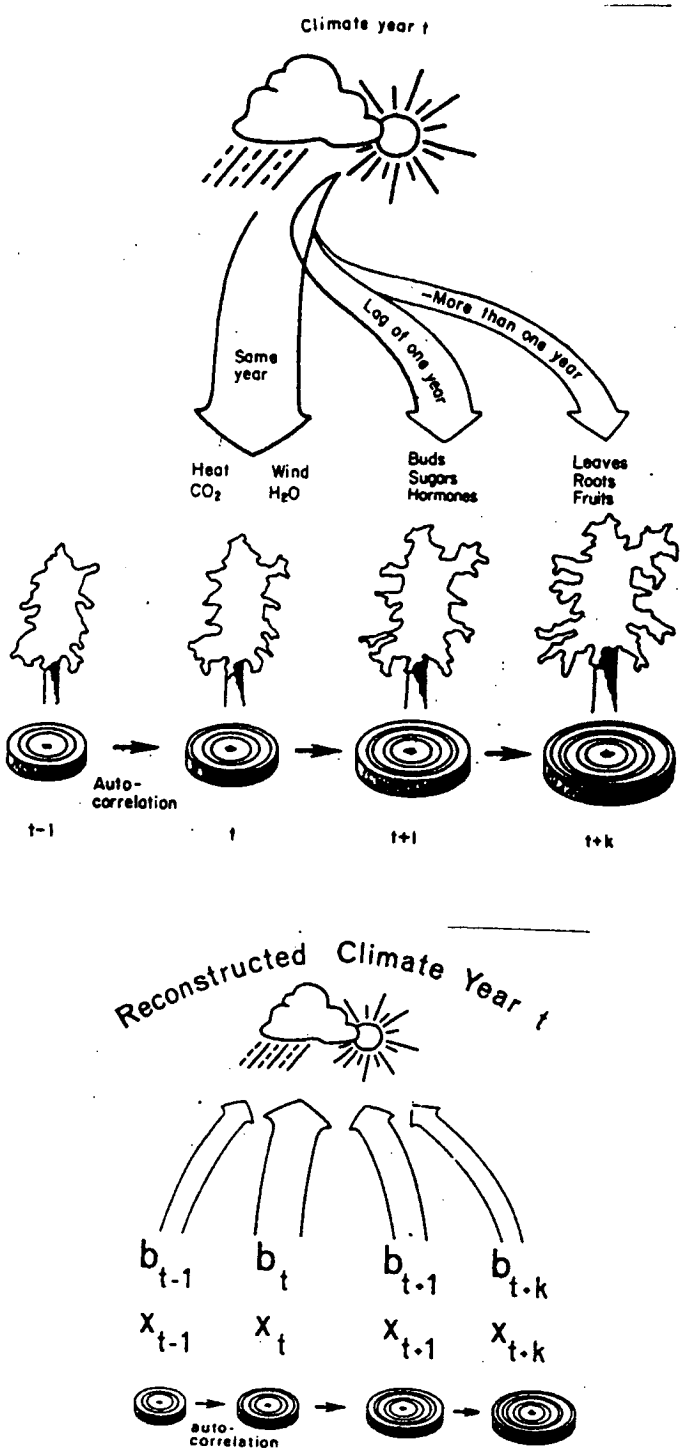

Figure 4.5. Schematic diagram showing the relationship of tree-growth with climate (top) followed by a transfer function reconstructing climate from tree growth (bottom) based upon the relationship determined by a calibration of tree-ring and climate data. Climate of a given year *t* has an impact on the ring width for that year through the effects on the operating environment for the tree. Heat, wind, water and Carbon dioxide can all affect the tree in year *t* as well in subsequent years up to year *t* +*k*. The calibrated relationship is then used to reconstruct climate for the period before the existing climatic data. (Drawing by M. Huggins, from Fritts, 1976.)

used. To some extent, this problem may be ameliorated by analysing broad scale parameters such as sea level pressure (SLP) and sea surface temperature (SST) anomaly patterns, which may in turn influence local conditions at the site (e.g., Douglas, 1973; Buckley *et al.*, 1992). In most instances temperature exhibits far less spatial variability than precipitation, and may therefore be more accurately represented by relatively distant instrumental records.

It is desirable to monitor radial growth in conjunction with daily or even sub-daily environmental conditions over successive seasons at important dendroclimatic sites. This allows for a more mechanistically-based climate/growth model. Such models are actively being pursued, though at present they are limited to open-canopy, arid-site conifers with wide rings and uncomplicated growth structure (e.g., Fritts and Shaskin, 1994). Application of such mechanistic models to more mesic, closed-canopy forest environments, such as those sampled for the present study, is not yet viable (Fritts and Shaskin, pers. comm.).

In traditional dendroclimatological studies, tree growth for an entire season, as determined from the mean value function for each annual ring, is usually compared against monthly or seasonal climate parameters for the determination of the most significant factors affecting growth at the site (Fritts, 1982). In reality, climatic conditions on daily or even shorter time-scales may have a significant impact on the annual growth ring. Transient climate features such as severe frosts, very high temperatures, heavy snowfall, or wind storms may impact on growth for a given year *t*. In most instances, however, such short-term factors can only be modelled where they leave obvious features in growth rings (e.g., traumatic resin ducts, frost-rings, false-rings), and monthly and seasonal data are more reliably modelled.

Some important assumptions and limitations exist for dendroclimatic reconstructions, which must be carefully considered:

1) It must be assumed that the Uniformitarian Principle applies; i.e., the physical and biological processes that link the present environment with present variations in tree growth are the same processes that will have been in operation throughout any segment of the pre-calibration period (Fritts, 1976).

2) The climatic conditions, which produced past anomalies in tree growth, are assumed to be analogous to the same processes enacting upon tree growth during the calibration period.

3) It is usually assumed that the systematic relationship between the limiting climatic parameter and the biological responder (tree growth) can be approximated by a linear mathematical expression. Lofgren and Hunt (1982) note, however, that in the case of transfer functions the predictand set need not be a linear function of climate; e.g., the logarithm of a precipitation record could be used and therefore the linearity constraint is not so severe a restriction as it might first appear.

4) The data are assumed to be normally distributed when parametric statistics are tested for significance, as the effects of outliers and any other non-normal data may distort the testing of significance (Fritts, 1990). Non-normal data can be normalised prior to regression through several techniques outlined in Fritts (1976) and Cook and Kairiukstis (1990).

5) The observations must also be assumed to be independent of each other for most statistical testing procedures. A serial-dependence or autocorrelation among successive observations, or among observations in space, may seriously reduce the number of degrees of freedom used for statistical significance testing. The effects of autocorrelation may be removed by prewhitening the data through autoregressive modelling (e.g., Cook *et al.*, 1992). Alternatively, prior growth can be included in the regression as a predictor variable, lagged up to m prior years.

It is clear that the assumptions listed above are not completely met by the climate/growth relationship used for calibration and climate reconstruction procedures. They may instead be regarded as comprising the limitations of the system (Fritts *et al.*, 1971; Lofgren and Hunt, 1982), and within these limitations some percentage of the variability of climate will be explained by a dendroclimatic reconstruction. The quality and the length of both the tree-ring and climatic data play a crucial role in the validity of the resulting models, and results derived from their calibrations and climate reconstructions should be verified, as discussed in Chapter 4.4.4.

4.4.2 Calibration of the climate response

The word *calibration* in dendroclimatology refers to the fitting of statistical models which can be applied to one or more *predictor* variables in order to estimate or reconstruct one or more *predictand* (Fritts, 1990). The term *response functions* refers to the weights or coefficients of the statistical model that describes the manner in which trees respond to climate (Fritts *et al.*, 1971; Fritts, 1976). The response function does not measure the climate-growth response directly but rather the effectiveness of a particular statistical model at predicting the element of tree-ring variation forced by external factors (Hughes *et al.*, 1982).

Climate parameters are often highly intercorrelated, making classical multiple regression difficult to directly apply for response functions analysis. Instead, the principal components of climate are often used in order to provide orthogonalised data sets for use in regression (Fritts *et al.*, 1971; Fritts, 1976; Guiot *et al.*, 1982; Briffa and Cook, 1990). Additional complications may arise from the autoregressive properties of the tree-ring series, where the growth in a particular year is not only dependant upon conditions in the season of growth but also in one or more previous seasons (Fritts *et al.*, 1971; Fritts, 1976). Some form of prior

growth parameter is often employed through lagging the tree-ring series up to *m* prior years. Alternatively, both the tree-ring time-series and the climate data can be prewhitened through autoregressive modelling to remove the effects of autocorrelation prior to response functions analysis (e.g., Cook *et al.*, 1992).

There are several response functions procedures in use at present. The primary differences relate to the manner in which relatively unimportant predictor PCs are removed from consideration during regression screening (Briffa and Cook, 1990). Blasing *et al.* (1984) noted that this is not always a straightforward procedure. Decisions regarding the number of climatic variables to include, confidence limits, and the number of eigenvectors to allow as candidate predictors in the regression, can affect the response function in unpredictable ways, leading to errors in interpretation. Blasing *et al.* (1984) recommended using the correlation function as an initial, interpretive guide prior to response function analysis, since the correlation functions are easier to understand, easier to replicate, and more difficult to subjectively alter. They also demonstrated how prior tree growth variables used in the regression can mask true climatic effects, and noted the usefulness of the correlation function for detecting such masking. The effect of prior growth variables can lead to mistakenly attributing real climatic effects to prior growth and should be considered separately from the response functions.

For this study, the simple correlation functions between the tree-ring chronologies and the climate variables are used to interpret the climate response. Both the tree rings and the climate variables (where warranted) are first prewhitened as an order-p autoregressive (AR) process of the form:

$$X_t = \sum_{i=1}^{p} \phi_i X_{t-i} + e_t \qquad (4.11)$$

where X_t is the time series being modelled, the ϕ_i are the p autoregressive coefficients, and e_t is the series of random shocks or white noise residuals unexplained by the AR(p) model (Box and Jenkins, 1970). The e_t of the tree rings and climate variable are used to develop the regression model and subsequent climate reconstructions, with persistence due to climate added back (where warranted).

4.4.3 Climate reconstruction

Transfer functions are statistically-derived equations which relate two sets of variables for which a causal relationship can be described, but for which the derivation of an analytical expression cannot be achieved (Fritts *et al.*, 1971; Lofgren and Hunt, 1982). In the case of dendroclimatology, one set of variables consists of the tree-ring indices, and the other the climatic parameter of interest (e.g., temperature or precipitation). The calibrated function of tree growth with the appropriate climate parameter can then be used to transfer the annual patterns of tree growth into yearly estimations of the climate variable, for periods of time prior to the recording of that variable (Fritts, 1976; Lofgren and Hunt, 1982).

For this study, PC regression analysis is used to transform tree-ring indices into estimates of a single climate variable (i.e., temperature). Prior to regression, the tree ring chronologies and climate variables are pre-whitened as order-p AR processes, as per equation 4.11. The reconstruction of climate (Y) is therefore accomplished by estimating the regression equation over the calibration period as:

$$Y = X\beta + E \qquad (4.12)$$

where matrix X is the tree-ring predictor set, β is the column vector of standardised regression coefficients used to estimate climate from tree rings, and E is the column vector of errors due to unexplained variance

in the regression model. β can be estimated by ordinary least-squares (OLS) as:

$$\beta = (X^TX)^{-1} X^TY \tag{4.13}$$

where the superscript T denotes the transpose of matrix X and $(X^TX)^{-1}$ denotes the inverse of X^TX. In the form of normalised departures, the estimates of climate from tree rings ($\hat{Y}$) can be obtained by multiplying X by β as follows:

$$\hat{Y} = X\beta \tag{4.14}$$

When PCA is performed on the tree-ring chronologies, values of X are multiplied by the eigenvector loadings (E), producing a new set of predictors:

$$U = XE \tag{4.15}$$

which are the PC amplitudes or scores. Prior to regression each amplitude is normalised by the square-root of its respective eigenvalue. The yearly variations in each amplitude reflect the relative importance of its eigenvector in describing the overall pattern of variance seen in the original data.

At this stage, a subset of amplitudes that explain most of the original variance in each data set is selected for regression analysis, after deleting the higher order eigenvectors. The eigenvalue-1 criterion (e.g., Guttman, 1954) is used here for screening predictors, deleting those eigenvectors with eigenvalues less than 1.0. This selection criterion is conservative in that it only retains around 20-40 per cent of the eigenvectors, which may explain 60-70 per cent of the total variance in the original data (Cook *et al.*, 1994). In this way the number of candidate predictors is reduced and, therefore, so is the potential for artificial

predictability which might arise from the inclusion of too many predictors in the model (Davis, 1976; Lofgren and Hunt, 1982).

Once a subset of the predictor eigenvectors is selected, the predictand is regressed on selected predictor PCs, and the standardised regression coefficients are nothing more than the simple correlations between the two. The best-order regression model is selected by the minimum AIC criterion (Akaike, 1974), and the regression model is then:

$$Y = U'B' + E \tag{4.16}$$

where the prime denotes the reduced-order model of PC amplitudes and regression coefficients selected by the AIC. The matrix B' of regression coefficients can then be expressed in terms of the original predictors as

$$\beta = E'B' \tag{4.17}$$

This back-transformation to coefficients on the original predictors eliminates the interpretational disadvantage of working with regression weights of the PC amplitudes (Cook *et al.*, 1994).

4.4.4 Verification of results

The statistical verification of climatic reconstructions is an integral part of dendroclimatology (Fritts, 1976; Hughes *et al.*, 1982; Cook and Kairiukstis, 1990). Both response function and transfer function procedures can be verified through statistical analyses. The climate response equations generated in this study are verified by comparing estimated values of tree growth with the actual values over an independent period (Briffa, 1984; Briffa and Cook, 1990). For this purpose the climatic data are split into two equal segments. Identical predictor-selection criteria are used for both time periods to enable a more direct

comparison of results, as recommended by Briffa and Cook (1990). Standardised periods of analysis, each of sufficient length to minimise sample to sample variability in the PC loading patterns (i.e., usually greater than 25 - 30 years) are also used. The problem of determining the confidence limits, both on R^2 and on the original climate predictors, is due to the fact that the selection of final PC predictors is an *a posteriori* decision, with an unclear definition of what the correct degrees of freedom are (Briffa and Cook, 1990).

The reliability of a particular model is assessed directly by calculating a number of verification statistics that measure the degree of similarity between independent estimates of climate from the model, and the corresponding instrumental data from independent time periods (Gordon, 1982; Fritts *et al.*, 1990). Verification procedures may employ several statistics: parametric statistics which involve assumptions of the underlying probability distributions of the data, and are therefore sensitive to violations of these assumptions, and nonparametric statistics which are insensitive to such violations.

The following verification statistics are used for this study: the Pearson product-moment correlation (R_P), the sign test (ST), the reduction of error test (RE), the product means test (PM), and the coefficient of efficiency (CE). Full descriptions of these tests can be found in the following: Fritts *et al.*, 1990; Cook *et al.*, 1992; 1994; Salinger *et al.*, 1994.

The R_P statistic is one of the simplest and most commonly used verification statistics. It measures the relative variation (covariance) between two data sets, and is totally insensitive to differences in the mean and variance between the two (Fritts *et al.*, 1990). Since it reflects the entire spectrum of variation (both high and low frequencies) its value can be affected by trends in the two data sets. This is resolved by calculating a new correlation coefficient from the first differences of the two data sets,

thereby measuring only the high-frequency variance in common. The data sets are assumed to be normally distributed, and the variance is assumed to be linearly related (Fritts, 1976; Fritts *et al.*, 1990).

The ST is a nonparametric measurement of reliability which counts the number of times the signs of the departures from the sample means agree or disagree, and offers the advantage of measuring the associations at all frequencies. Results are based on two possible outcomes: (+1) when the estimate and observations agree (i.e., are on the same side of the dependent data mean) and (-1) when they disagree (Fritts *et al.*, 1990). A successful ST is indicated by the sign of the estimates being correct more often than would be expected from random numbers.

The RE statistic offers a highly-sensitive measure of reliability. It is similar to the explained variance statistic obtained with the calibration of the dependent data, and values range from negative infinity to a maximum of 1.0, which indicates a perfect estimation (Fritts *et al.*, 1990). The RE is calculated by dividing the sum of the squared differences between actual and estimated values by the sum of the squared differences between actual values and the mean of the calibration period, and subtracting that value from 1.0. The significance of RE cannot be tested, though positive values indicate some degree of model skill. Errors are unbounded, so that even one extreme error in an otherwise nearly-correct set of estimates may result in a negative RE and unfounded rejection of the model. While RE does estimate the explained variance with considerable accuracy (Gordon and LeDuc, 1981) the size of the sample being analysed (n') may markedly affect its significance. For example, with $n' = 20$, an RE of zero was roughly equivalent to the 0.95 confidence limit, but for $n' = 10$ or 15 an RE statistic significantly different from zero would have to be greater than 0.25 and 0.12, respectively (Fritts *et al.*, 1990).

The CE was introduced into dendroclimatology by Briffa *et al.* (1988) and is very similar to the RE, with values ranging from negative infinity to a maximum value of 1.0. The only difference is that the CE statistic uses the mean of the verification period in the denominator, instead of the mean of the calibration period. Consequently, if the verification and calibration means are identical, then CE = RE. However, when the means are not equal RE will be greater than CE by a factor related to that difference (Cook *et al.*, 1994). Since the value of the CE statistic will usually be less than for RE, it is an even more difficult test to pass. Although there is no significance test for CE, any value greater than zero indicates some degree of model skill (Cook *et al.*, 1994).

The PM test takes into account both the sign and magnitude of the departure from the calibration average, and is computed from the product of the actual and estimated annual departures from the mean, with positive and negative means summed separately (Fritts, 1976). The product is positive when the departure sign is estimated correctly, and negative when incorrectly estimated. If randomly guessed the means of the positive and negative products are approximately the same (ignoring their signs), while for a correct reconstruction the mean is larger for the positive products (Fritts, 1976). The difference between positive and negative products is tested with the *t* statistic, and is considered statistically significant when the value of *t* is higher than the expected value at the appropriate confidence level. A mean positive product that is significantly larger indicates a tendency for both actual and estimated departures from the average value to be large when the sign is correctly estimated, and small when the sign is incorrectly estimated. The latter case indicates that approximately average conditions both occurred and were estimated, thereby indicating the correctness of the reconstruction in spite of its incorrect sign (Fritts, 1976).

CHAPTER 5: THE DATA

5.1 Chronologies

The seven Huon pine chronologies, standardised as described in Chapter 4.3.2, are presented in Figures 5.1 - 5.7. They are presented first as mean ring-width chronologies with no detrending, followed by plots of the sample depth through time, the ARSTAN chronology (pooled autocorrelation included) and the RESIDUAL chronology (pre-whitened through autoregressive modelling). Some common chronology statistics are summarised in Table 5.1 for the entire chronology periods, and in Table 5.2 for a common period analysis from AD 1700 - 1990. This common period was chosen in order to compare the chronologies with each other, as overlapping segments related to the inclusion of subfossil logs in several of the chronologies prevented a proper common period of all included series.

Mean sensitivity is a commonly used statistic in dendrochronology to evaluate the year to year variability in a tree-ring chronology (Fritts, 1976). It is a measure of the mean percentage change from each measured yearly value to the next. Values range from 0.0 where no change occurs, to 2.0, where there is a change from a zero to a non-zero measurement in the time sequence. The mean sensitivity values are quite low for all seven chronologies (i.e., less than 0.3) due to the generally complacent nature of Huon pine ring sequences. However, this statistic is not an adequate measure of the crossdating of these chronologies which are from mesic, closed-canopy forest environments. The mean R-bar value is a much better measure of overall crossdating, as it expresses the mean of all possible correlations in the entire chronology through time, for 100 year periods lagged by 50 years. There is a general tendency for an improvement in the R-bar with an increase in elevation, with the highest values for the BCH and LMH chronologies, and the lowest values from HAR and SRT.

Site	No. Series	Total Timespan	Mean sens.	Std. Dev.	AC 1	R-Bar All	AR Model
LJH	284	-1723 to 1990	0.108	0.176	0.669	0.243	3 (47.9%)
BCH	84	910 to 1991	0.110	0.158	0.595	0.301	6 (40.1%)
LMH	23	1542 to 1992	0.091	0.105	0.419	0.250	2 (23.9%)
LML	24	1058 to 1992	0.107	0.145	0.532	0.301	4 (36.6%)
LVH	127	69 to 1993	0.097	0.173	0.708	0.247	3 (54.6%)
HAR	34	-2 to 1990	0.103	0.138	0.529	0.181	3 (30.5%)
SRT	110	-571 to 1992	0.106	0.143	0.496	0.210	2 (28.1%)

Table 5.1. Summary statistics for the seven chronologies. No. Series = total number of samples included in the chronology; Mean sens. = the mean sensitivity; AC 1 = the serial correlation; R-Bar All = the mean r-bar statistic for the prewhitened indices for all possible correlations through time; AR Model = the order of the autoregressive model followed in parentheses by the r-squared due to pooled autoregression.

Site	No. Series	No. Years	Mean sens.	Std. Dev.	AC 1	R-Bar All	AR Model
LJH	46	291	0.211	0.190	0.552	0.420	1
BCH	68	291	0.176	0.158	0.571	0.319	6
LMH	18	291	0.192	0.171	0.390	0.264	1
LML	17	291	0.185	0.164	0.362	0.318	3
LVH	45	291	0.173	0.152	0.411	0.335	3
HAR	32	291	0.201	0.180	0.371	0.234	1
SRT	39	291	0.213	0.189	0.208	0.201	4

Table 5.2. Summary statistics for the seven chronologies over a common period from AD 1700-1990.

The LJH chronology as presented here (Figure 5.1) includes at least 20 radii since 1200 BC, making it one of the best-replicated chronologies of its length from the Southern Hemisphere. Much of the robust sample depth in the earliest period results from this study, with the inclusion of more than 50 subfossil samples collected in 1994 (Chapter 3.6.1). Before 1400 BC, where the sample depth drops to five series or less, the plots clearly show the increased variance associated with the estimation of the mean. Therefore, this early segment was regarded as less reliable for any

interpretation of past environmental conditions, and was not included in the ensuing climatic analyses.

The LJH mean ring-width plot shows the apparent effect of a marked increase in samples around 500 BC, due to the inclusion of several subfossil logs which germinated at around this time. The effect of this sample increase is to introduce an apparent juvenile growth trend into the mean ring-width chronology that is largely removed through standardisation, as can be seen in the ARSTAN and RESIDUAL chronologies. It is possible that this apparent increase in germination is indicative of some real ecological change at the site, manifested as a synchronous increase in population through regeneration. However, Cook *et al.* (1995b, p. 233-34) demonstrate the potential for random variation in sample-size distribution through time, and caution against interpreting such variation as a proxy for past environmental change. Interestingly, a very similar feature commences around 500 BC in the SRT chronology (Figure 5.7), following a gap in the subfossil wood record from *ca.* 500 BC to *ca.* 1500 BC (Chapter 3.6.3, Figure 3.9). The lack of wood samples on either side of this gap accounts for the low sample depth in the earliest part of the SRT chronology, which is evident in the increased variance associated with the mean. While it is likely that the earliest part of the SRT chronology merely represents juvenile growth, the similarity to LJH is intriguing.

There is evidence suggesting that the *ca.* 1,000 year Stanley River gap may result from extensive fires in the region (Barbetti, pers. comm.), roughly coincident with evidence for several other probable burning episodes such as at the Governor River, and at Rumney Creek Plains (Chapter 3.6.2). This may be indicative of increased, wide-scale burning throughout western Tasmania at that time, and it must therefore be considered that the *ca.* 500 BC growth increase at LJH may not be artefactual. It may instead be related to broad-scale factors such as

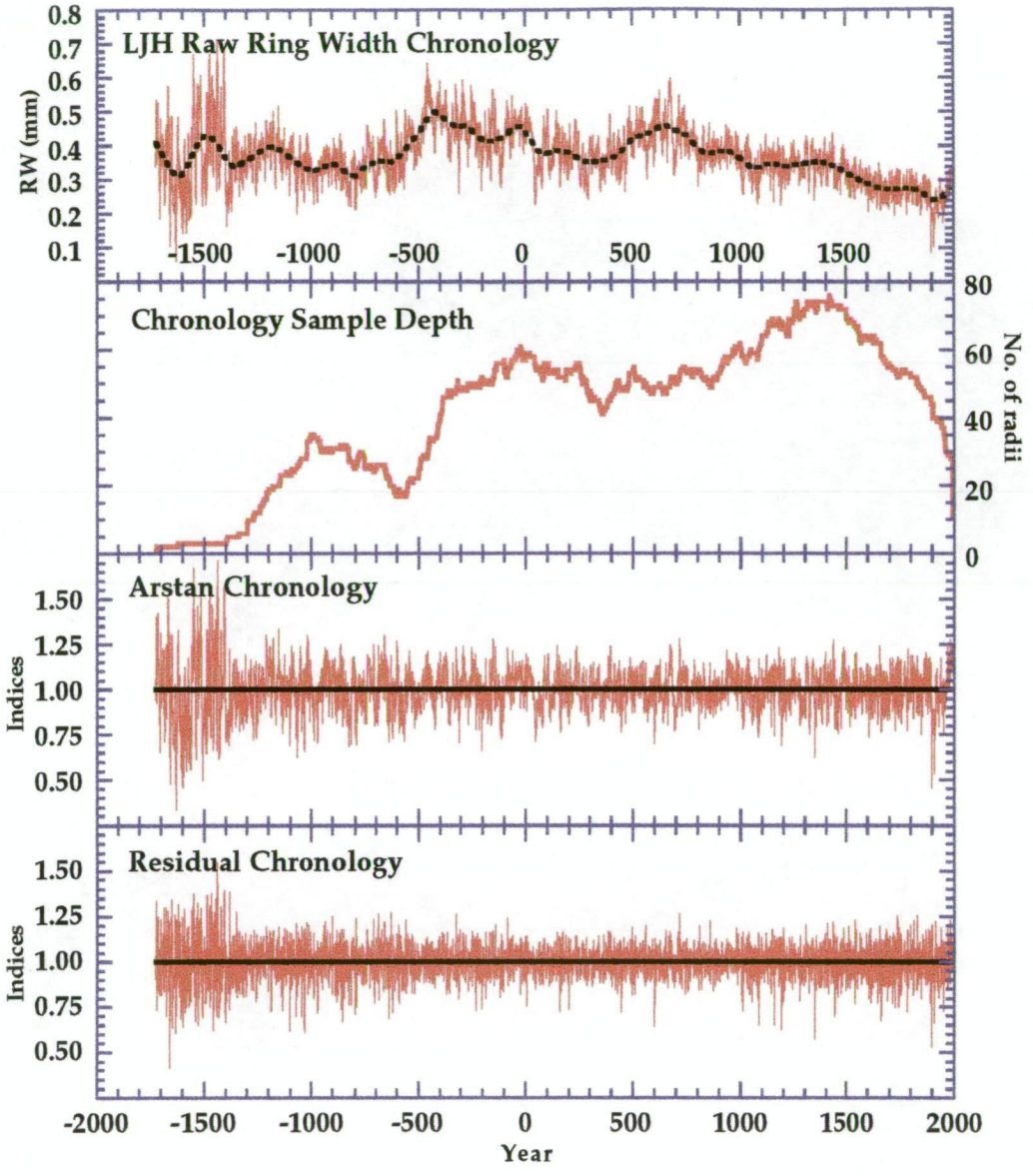

Figure 5.1. Mt. Read chronology plots. From top to bottom: the raw ring-width chronology (no detrending); the chronology sample depth through time; the Arstan (ARS) chronology (containing pooled persistence); and the Residual (RES) chronology which has been pre-whitened through autoregressive modelling. All plots show the effects of sample depth on the data prior to BC 1400 where the chronology is based on less than five series, while only the raw ring-width chronology is significantly effected just after BC 500 where there is a marked increase in subfossil logs being introduced. The general decrease in mean ring width after AD 700 reflects the growth trend of primarily living trees from that point on. Aside from the pre-BC 1400 problem, these effects are largely resolved through standardisation.

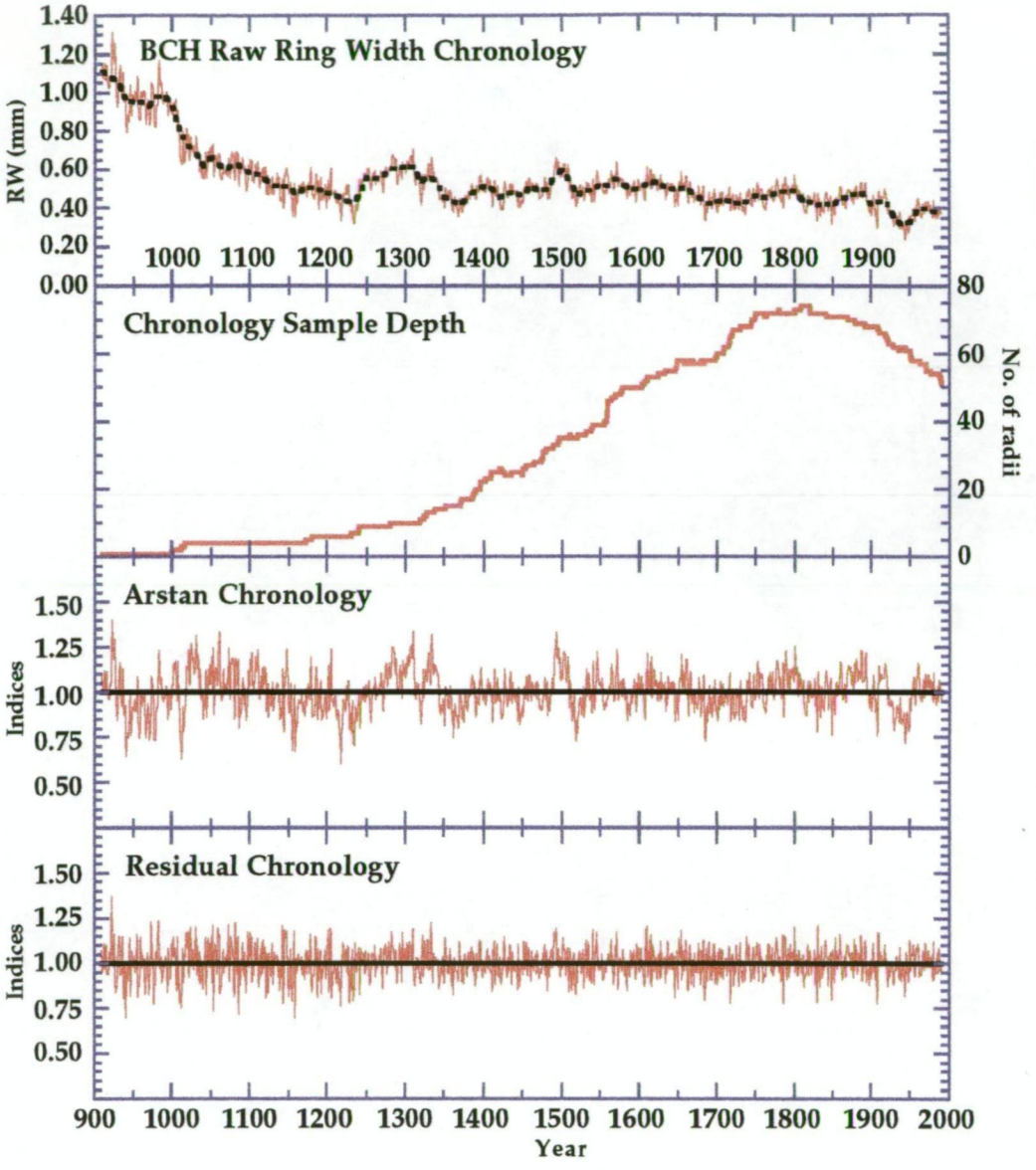

Figure 5.2. Buckley's Chance chronology plots. The BCH chronology consists entirely of living trees, with sample depth tapering off to less than 10 series before AD 1300. A general exponential decay can be seen for about the first 400 years, followed by a reduced influence from G_t acting upon mostly mature trees with a very robust sample depth of more than 40 time series for much of the past 500 years. Some noteworthy features in the chronology include an anomalous growth increase, followed by a sharp decrease, around AD 1500, and a similar feature around AD 1630, both of which are present in other chronologies from the Frenchmans Cap area.

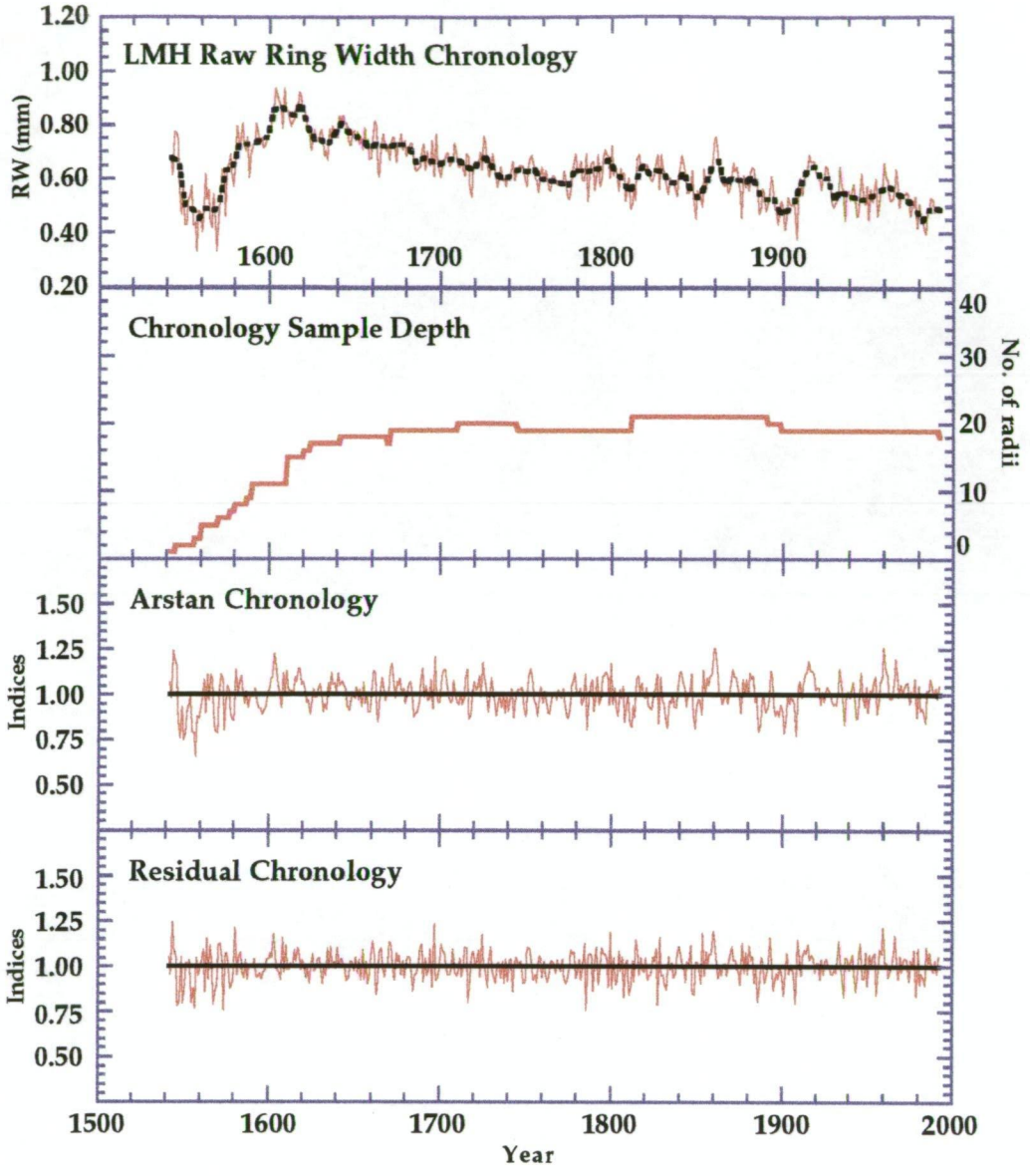

Figure 5.3. Lake Marilyn High chronology plots. The LMH chronology consists of all living trees, with a sample depth of less than 20 series for its entire length. A general exponential trend is evident from about AD 1600, preceded by suppressed juvenile growth typical of sub-canopy, rainforest environments.

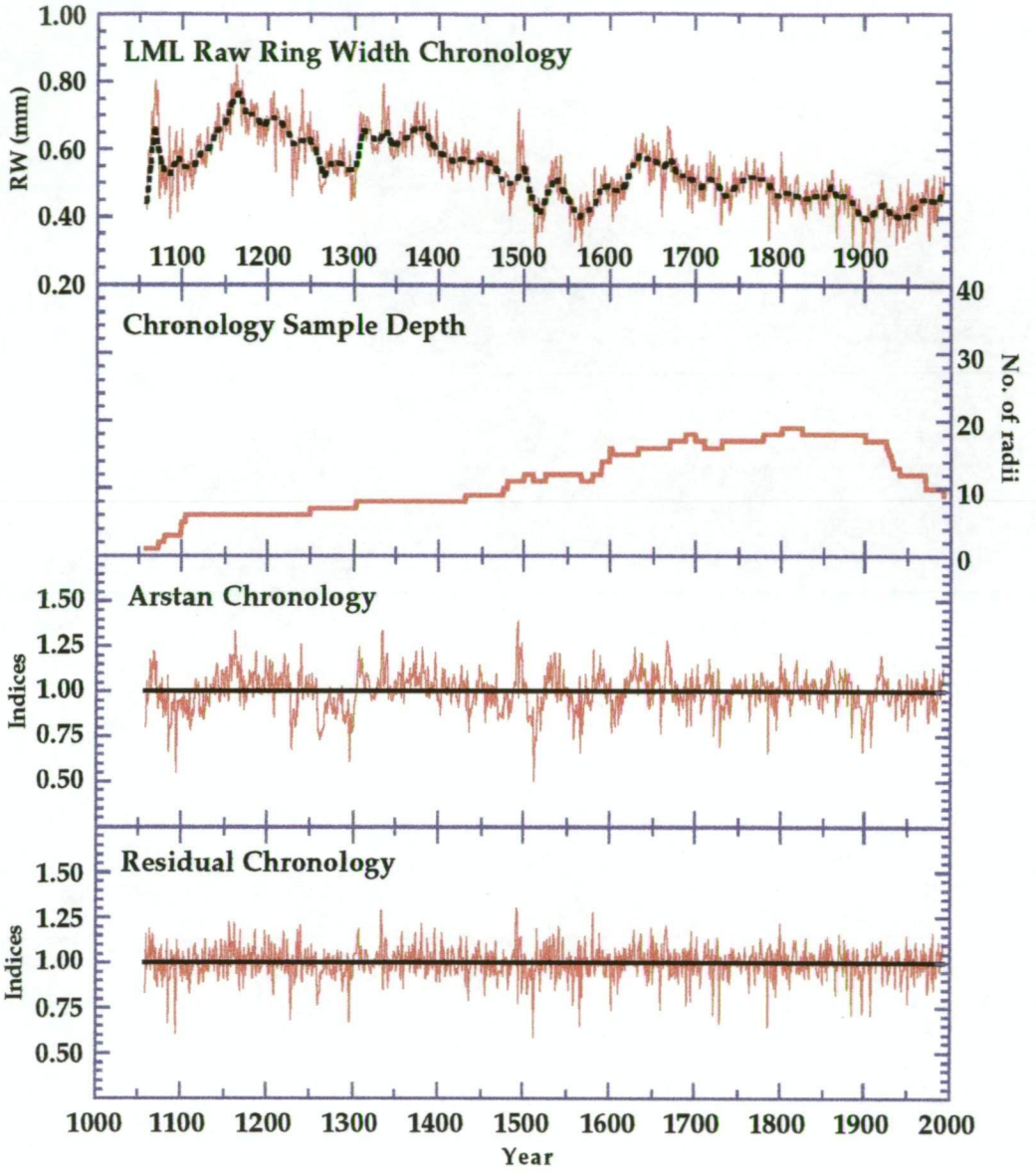

Figure 5.4. Lake Marilyn Low chronology plots. Like BCH and LMH, the LML chronology consists of only living trees, with a sample depth of less than 20 series for most of its length. A general decrease in growth with age is evident, though there are several departures from this trend which are preserved in the ARSTAN chronology, and mostly removed through autoregressive pre-whitening as seen in the RESIDUAL chronology. These departures are similar for all of the chronologies in the Frenchmans Cap region (Figure 5.8), and are possibly related to fire or other non-climatic effects.

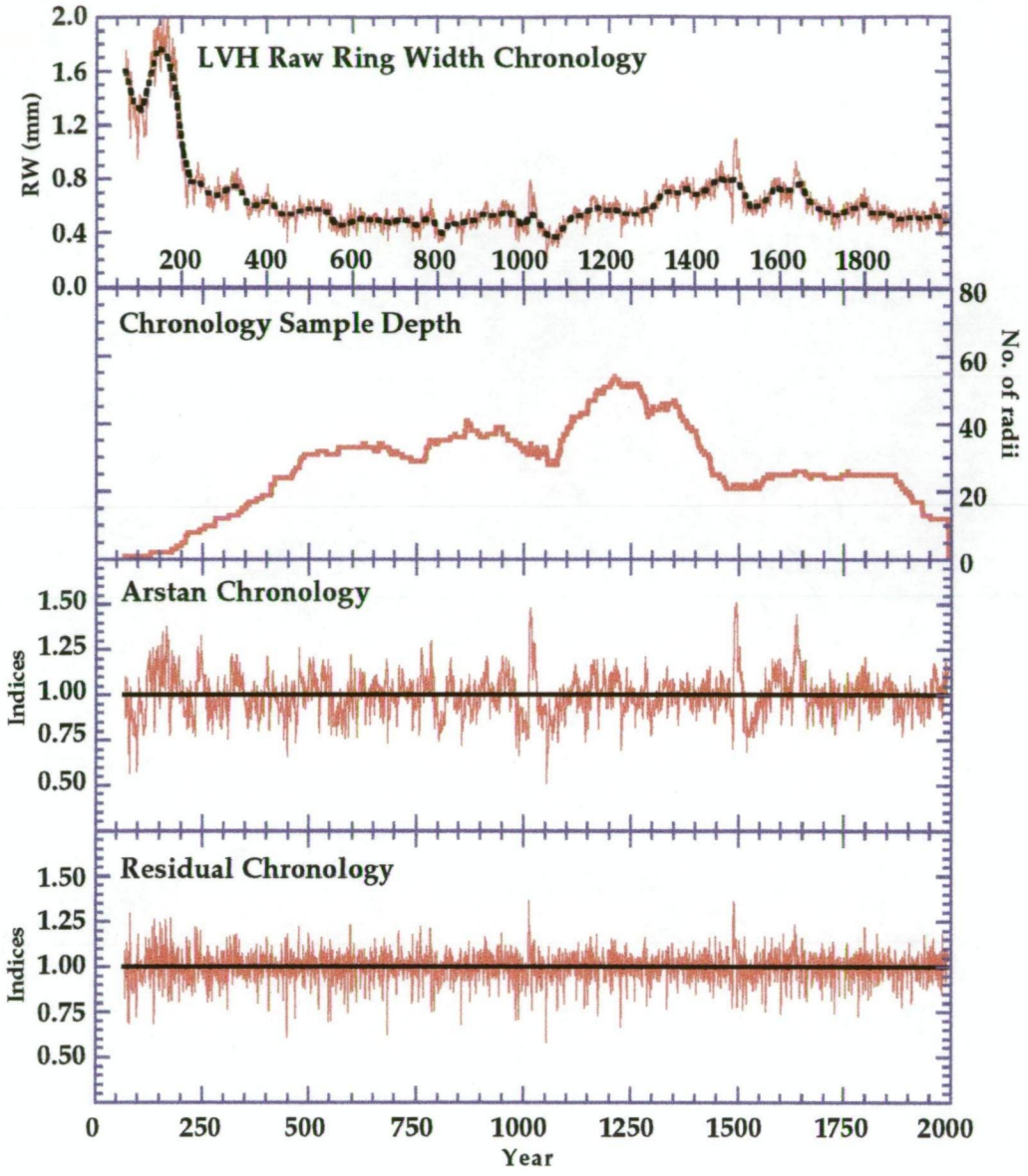

Figure 5.5. Lake Vera chronology plots. The LVH chronology is largely based upon subfossil logs which were removed from the bottom of Lake Vera, in combination with living trees from the slope adjacent to the lake. The earliest portion of the chronology shows greatly exaggerated mean ring width, due to the distorted growth rings from one sample. The most striking features of this chronology are the three major growth departures with telltale "spikes" immediately followed by growth "crashes" around AD 1000, 1490, and 1630, respectively. These departures are synchronous across the site, and are very likely related to wide-scale disturbance such as fire, as discussed in Chapter 3.6.2. The LVH chronology correlates most strongly with the chronologies from below 700 m AMSL (Table 5.9), however shows a fairly strong regional agreement with the other Frenchmans Cap chronologies as well.

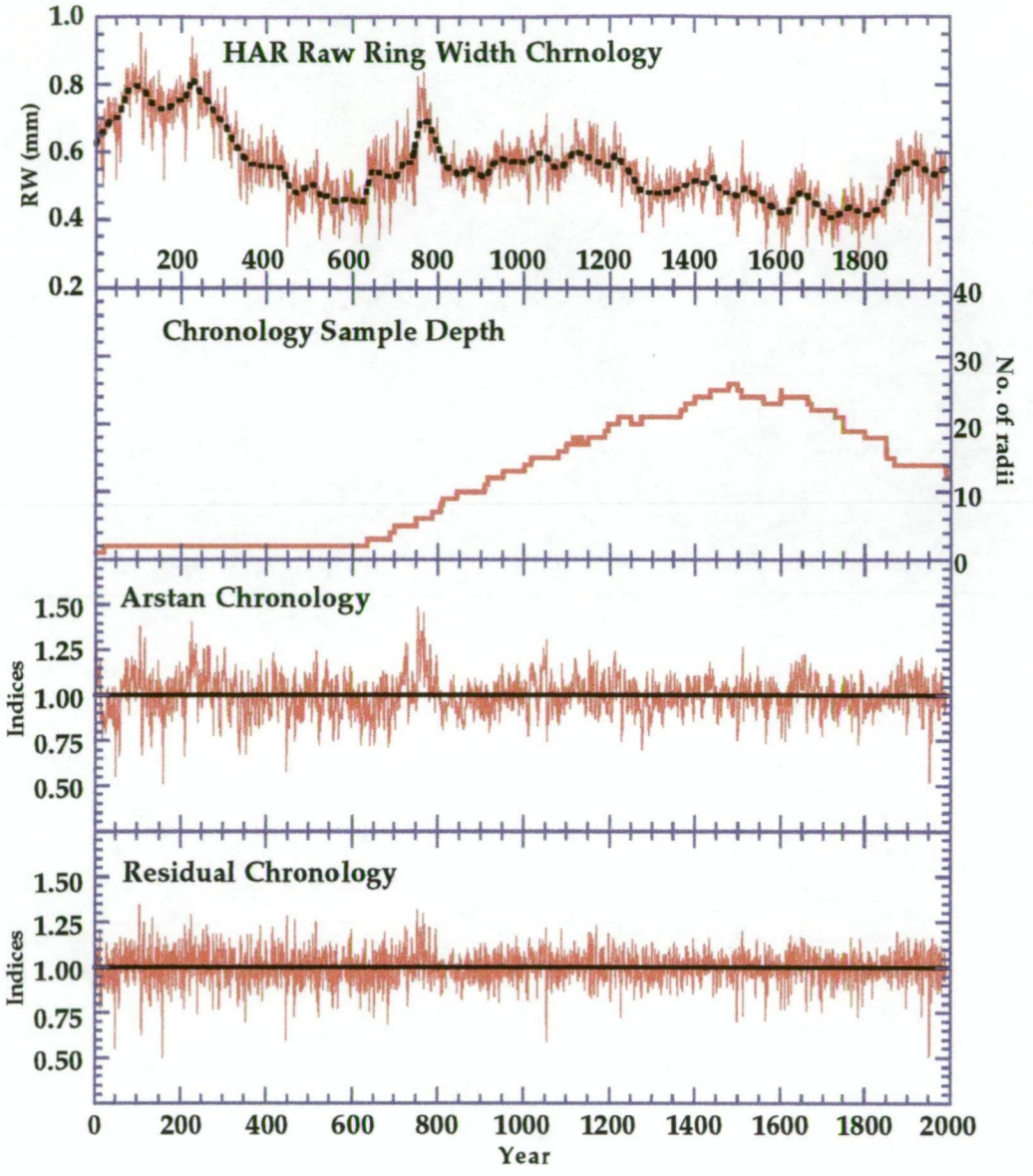

Figure 5.6. Harman River chronology plots. The HAR chronology is built from living trees only. The sample depth is greater than 10 series after AD 800, however consists of only one sample from BC 2 to just after AD 600. The effect of this can be seen in the reduction in variance after AD 800, along with a generally negative trend in mean. The HAR chronology exhibits the poorest crossdating of any of the seven chronologies (Table 5.1), owing to its riparian environment with disturbances from both flooding events and channel undercutting (Chapter 3.6.3). Poor circuit uniformity and ring "wedging" problems contributed to the difficulties in crossdating, and only a subset of the samples collected were included in the final chronology.

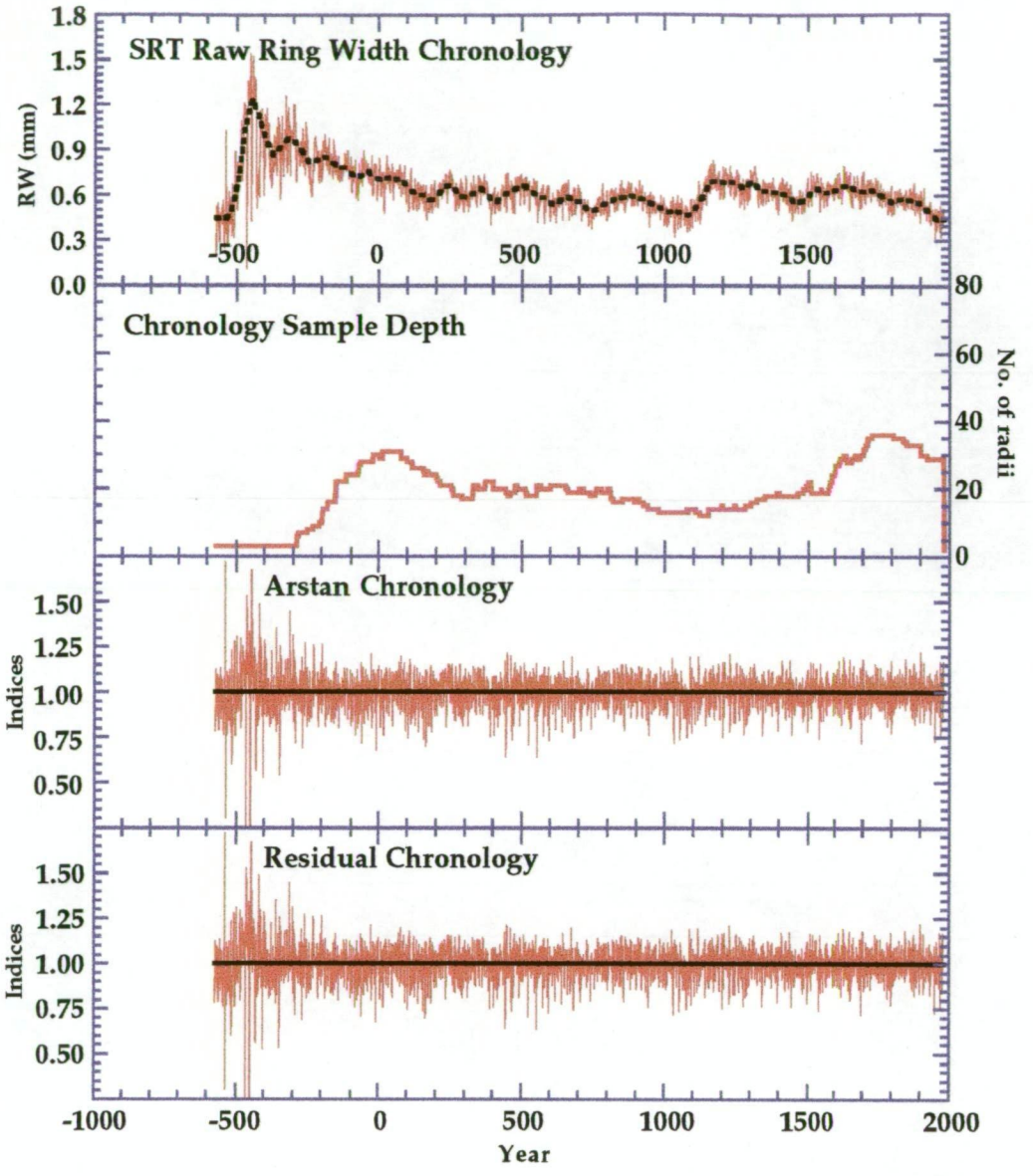

Figure 5.7. Stanley River chronology plots. The SRT chronology is mostly composed of subfossil samples cut from logs exposed along the river channel and from excavations in the alluvium adjacent to the river. The subfossil logs are combined with a smaller subset of living trees extending out to AD 1992. Before about 300 BC there is a notable increase in variance around the mean owing to low sample depth. Like HAR, the SRT chronology exhibits generally poor crossdating compared with the chronologies from higher elevations, owing in large part to poor circuit-uniformity and anomalous growth patterns related to endogenous disturbances, such as stand dynamics, river channel undercutting, flooding, and other non-climatic effects.

anthropogenic burning in conjunction with climatic conditions favourable to burning. Given the fact that both the LJH and SRT features are associated with juvenile growth trend, however, the nature of this *ca.* 500 BC growth feature will remain largely unresolved until samples from several sites are analysed through this period. Therefore, for purposes of this study it will be treated as artefactual. The other main features of the LJH chronology are consistent with the findings of previous research (TTRP); i.e., the growth decrease in the late nineteenth/early twentieth century, and the marked growth increase since about AD 1960, which correspond to regionally anomalous cold and warm periods, respectively.

All of the Frenchmans Cap chronologies are built entirely from core samples from living trees, with the exception of LVH which includes several subfossil logs dating from AD 67 to *ca.* 1488 (Chapter 3.6.2). The highest of these, BCH (Figure 5.2), exhibits a nearly classic, negative exponential decay for its first 400 years, from AD 900 to *ca.* AD 1300 where the sample depth approaches 10 series. Several striking departures from the mean occur, with growth increases at around 1300, 1500 and in the early 1600s, as well as a growth decrease in the first half of the 20th century. The post-1960's growth increase is neither as pronounced nor as prolonged as in the LJH chronology, though a recovery from below average growth since the 1950s can still be seen.

The LMH chronology (Figure 5.3) is the shortest of the seven chronologies, dating back only to AD 1542, and is based entirely on core samples from 18 living trees. A suppression of growth prior to 1600, followed by a growth release and then systematically decreasing growth for the remainder of the series, is suggestive of a classic juvenile growth trend for sub-canopy rainforest trees (e.g., Fritts, 1976). However, the other Frenchmans Cap chronologies (BCH, LML, and LVH) exhibit similar structure through the 1500s and 1600s (Figure 5.8), suggesting that the early portion of the LMH series is indeed reflecting the actual,

regional growth related to climate, and is not an artefact of small sample size and juvenile growth. A similar feature is also weakly evident at the 950 metre LJH site, and at the more distant and lower elevation HAR and SRT sites, though its greatest expression is seen in the Lake Marilyn/Lake Vera catchment chronologies.

The above-mentioned growth structure in the Frenchmans Cap chronologies may in part reflect an extensive, regional burn during a period of climatic conditions conducive to burning. For example, a 1490s growth increase at LVH was immediately preceded by a fire in 1488 $\pm$ 2 (Chapter 3.6.2), though it is unclear if the highly-anomalous growth increase and subsequent decline (Figure 5.5) are directly related to the fire or to some other factor such as climate, or related hydrological conditions of the lakeshore environment. There is evidence to support fairly widespread burning in the Frenchmans Cap region at this time (Chapter 3.6.2), and it is possible that this growth signature reflects the effects of this fire. The results are thus far inconclusive. A similar feature just after AD 1000 also appears to immediately follow burning, though the evidence for fire is less compelling in this instance. It is noteworthy that these features, while greatly enhanced at LVH where the evidence for fire is strongest, have some degree of expression in nearly all of the chronologies, suggestive of broad-scale forcing that is not necessarily related to fire. Determining the causes of such striking growth anomalies remains a challenge, particularly where the anomaly has apparent regional expression.

The two remaining Frenchmans Cap chronologies, LML and LVH, are from similar lakeshore sites in the same catchment, though the former is nearly 150 m higher in elevation with a northerly aspect, while the latter site faces southeast. The LML chronology (Figure 5.4), extends from AD 1058 to 1992, and is the only Frenchmans Cap chronology to exhibit a pronounced, recent growth increase comparable to that for LJH,

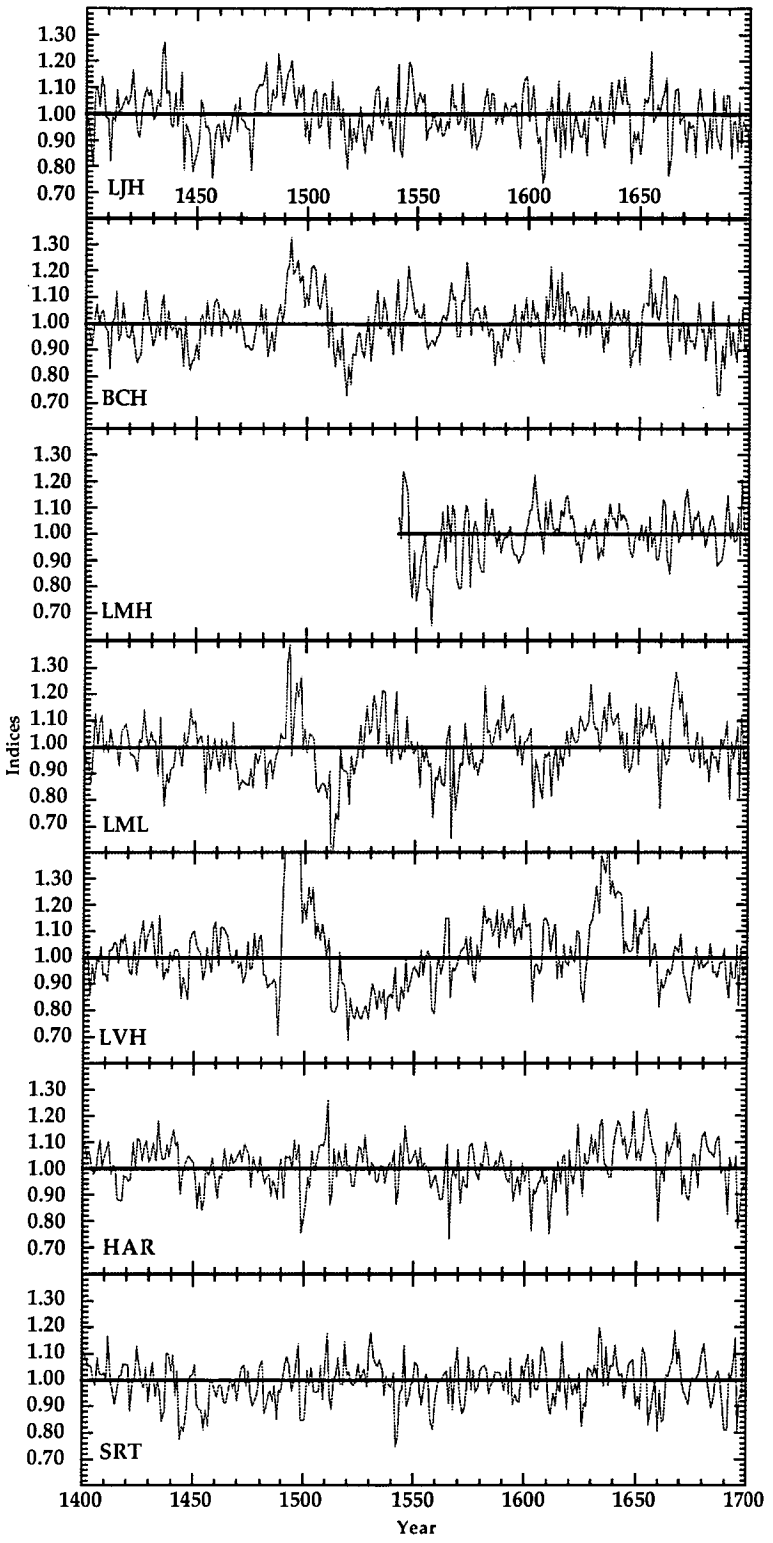

Figure 5.8. Growth indices from AD 1400 to 1700. The indices are from the seven ARSTAN chronologies which have been re-whitened by returning the pooled autocorrelation to the RESIDUAL series. Anomalous growth departures from the late 1400s to the mid 1600s are evident in all of the Frenchmans Cap area chronologies, and more weakly evident in the other chronologies as well. The LVH chronology shows the most extreme departures from the mean, with a large growth surge in the late 1400s followed immediately by a major growth decline in the early half of the 1500s, from which it is the slowest site to recover.

though all can be seen to exhibit a general recovery from below-average growth before 1950. This disparity will be discussed further in Chapter 6.2.3, as there are important implications regarding the interpretation of recent changes in temperature based on the tree-ring reconstructions.

The LVH chronology dates back to AD 67 (Figure 5.5). The mean ring-width plot shows the effects of highly-inflated growth for the earliest portion which is based entirely on measurements from one sample. The most striking features of the LVH chronology are the anomalous growth surges and declines, already noted above, in the AD 1000s, 1490s, and 1630s. While crossdating of the LVH chronology was excellent overall (e.g., a mean R-bar statistic for all possible correlations of 0.247), several samples were unworkable in the decline periods immediately following the three above-mentioned growth surges, particularly in the early 1500s. The ensuing gaps resulted in several discontinuous, shortened time series in the final chronology, which thereby reduced the mean segment length, and consequently the resolvable low-frequency variability for the final chronology (e.g., Cook *et al.*, 1995b).

HAR and SRT are generally the two poorest quality chronologies, in a dendrochronological sense. This in large part reflects their lower elevations (where growing season temperature is less likely to be growth limiting) and riparian site conditions (which encourage endogenous disturbance factors such as riverbank undercutting and channel flooding, that result in mechanical damage to tree roots and stems). Samples from these two sites exhibit more problems with circuit uniformity and ring wedging than any of the other five sites, and many samples from both locations were found to be unworkable. The HAR chronology exhibits the weakest crossdating of all sites, with a mean R-bar statistic of 0.181 (Table 5.1), while SRT has the second-lowest value at 0.210. Even for the common period analysis (Table 5.2), the two lowest R-bar statistics are accounted for by HAR and SRT, at 0.234 and 0.204, respectively.

A general indication of the regional crossdating between sites can be gleaned from Table 5.3, which shows the correlation matrix for the seven pre-whitened RESIDUAL chronologies over their common periods. A general clustering of sites by elevation is evident, with the strongest agreement between the highest chronologies (LJH, BCH, LMH, and LML) which are of notably better quality than the lower sites, and correlate with r values ranging from 0.596 - 0.771. In contrast the lower chronologies (SRT, HAR, and LVH) also correlate highest with each other, with values of r ranging from 0.46 to 0.54. LVH also exhibits fairly high correlations with nearby LML (r = 0.640) and LMH (r = 0.612), indicative of the regional signal in addition to that of elevation.

	LJH	BCH	LMH	LML	LVH	HAR	SRT
LJH	**1.000**	0.729	0.631	0.611	0.543	0.466	0.439
BCH	0.729	**1.000**	0.771	0.596	0.473	0.260	0.360
LMH	0.631	0.771	**1.000**	0.638	0.612	0.308	0.338
LML	0.611	0.596	0.638	**1.000**	0.640	0.466	0.431
LVH	0.543	0.473	0.612	0.640	**1.000**	0.540	0.462
HAR	0.466	0.260	0.308	0.466	0.540	**1.000**	0.514
SRT	0.439	0.360	0.338	0.431	0.462	0.514	**1.000**

Table 5.3. Correlation matrix for the seven pre-whitened Residual chronologies over their common periods. The strongest agreement is between the chronologies from greater than 700 metres AMSL.

5.2 Meteorological data

5.2.1 Temperature

Instrumental temperature records from Tasmania date back into the late 19th century at the earliest, with most stations recording temperature only since 1910 or later (Bureau of Meteorology, 1993). Homogeneity testing for Tasmania's longest temperature records has been hampered by a lack of other long records of known homogeneity with which to compare them, particularly for the earliest period

(Shepherd, 1991). A review of Tasmanian station records by Torok (1996) revealed several problems in the temperature data, ranging from single-year inaccuracies due to measurement or other errors, to systematic errors resulting from equipment changes and station moves.

Tasmania initiated a change to standardised Stevenson screens for all thermometer housings in the mid-1890s; however the network was only properly maintained after 1908 when the Federal BOM was established (Torok, 1996). Therefore, prior to about 1910 Tasmanian temperature data are systematically less reliable, and in many cases incomparable due to a lack of standardised, quality data for comparisons on which to base adjustments (Shepherd, 1991; Torok, 1996). The problem is manifested as a consistent, but unpredictable, overestimation of maximum temperature for many stations, and an equally unpredictable underestimation of minimum temperature (Torok, pers. comm.). The effect on the diurnal temperature ranges, prior to about 1910, poses a problem which may be difficult to completely resolve. This is because the max/min bias is not symmetrical, and is therefore not cancelled out by averaging together for the means which are generally too warm by an amount that is difficult to determine (Nicholls and Torok, pers. comm.). While adjustments have been made for the pre-1910 temperature data, they are viewed with less confidence than subsequent data (Torok, pers. comm.). Accordingly, the implications for tree-ring calibration and verification statistics, based on these data for one or other process, must be considered.

The development of an appropriate temperature time-series for the calibration of the chronologies involved several trade-offs with regard to the length of record and proximity to the field site locations. For example, Cook *et al.* (1991; 1992) calibrated the Mt. Read chronology using a composite series of the three longest Tasmanian records available; Low Head Lighthouse, Launceston and Hobart. This composite (referred to

henceforth as the "Cook Series") spans the period from 1885 to 1989. The three stations comprising the Cook Series were confirmed as being some of the highest quality records in the state, following several important corrections as noted above (Torok pers. comm.). All three stations are located in the eastern half of the island at elevations from 5 to 166 metres AMSL (Figure 5.9 and Table 5.4), and are consequently from a different climatic zone than the west-coast mountain region where Mt. Read is located (Bureau of Meteorology, 1993). However, Tasmanian temperature is far more spatially coherent than precipitation, being mostly controlled by elevation and distance from the coastline (Bureau of Meteorology, 1993). Cook *et al.* (1992) demonstrated this spatial coherence by correlating the Cook Series with two of the highest stations in western Tasmania: Butler's Gorge and Lake St. Clair (666 m and 730 m AMSL, respectively). The Cook Series mean monthly temperatures correlate strongly with both stations (i.e., r = 0.9 or greater for 10 of the 12 months, including all warm-season months).

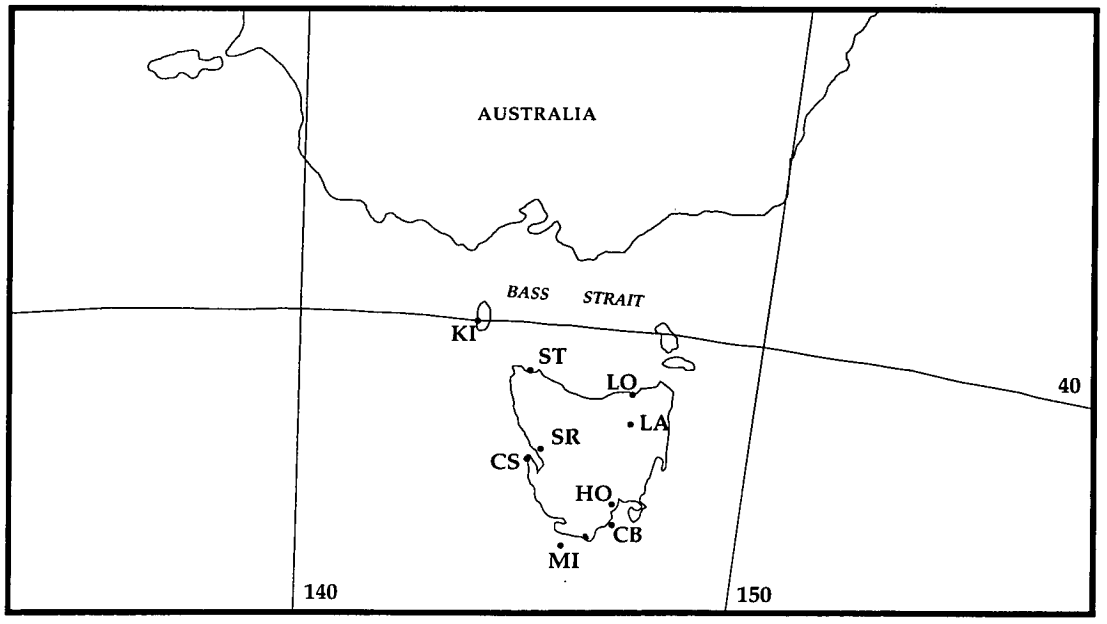

Figure 5.9. Location of the meteorological stations used for the development of the Cook and Buckley Series records of mean monthly and warm season (Nov - Apr) temperature. KI = King Island, ST = Stanley, LO = Low Head Lighthouse, LA = Launceston, HO = Hobart, CB = Cape Bruny Lighthouse, MI = Maatsuyker Island Lighthouse, CS = Cape Sorrel, SR = Strahan. The Buckley Series incorporates the data from all nine of these stations, while the Cook Series is based upon LO, LA, and HO.

The Cook Series has also been compared with a temperature time-series developed by P.D. Jones (Climatic Research Unit, University of East Anglia in the U.K.), known henceforth as the "Jones Series" (Cook *et al.*, 1996b). The Jones Series, originally expressed in anomaly units, was based on Hobart air temperature and sea surface temperature (SST) measurements from within a 5° x 5° grid square that completely encompasses Tasmania. The original anomaly units were transformed into absolute temperatures by regressing them on the Cook Series (Cook *et al.*, 1996b). While the two time-series are not completely independent of each other (i.e., both include the Hobart record) the methods used for regionalisation of the data were different, and the Jones Series was corrected for inhomogeneity problems in the SST data. In spite of these differences, the Cook and Jones Series are very similar (r = 0.86) for the entire common period of 1885 - 1994 (Figure 5.10d). One difference is in the autocorrelation of each time-series, with the Cook Series being modelled as an AR1 process, and the Jones Series as an AR3 process. The stronger autocorrelation of the Jones Series is likely related to ocean circulation influences due to the inclusion of the SST data.

In order to generate a more geographically-representative temperature record than the Cook Series, a new data set (referred to henceforth as the "Buckley Series") was derived from nine coastal or near-coastal stations from throughout Tasmania, including the three used for the Cook Series (Figure 5.9 and Table 5.4). Mean minimum, maximum, and mean monthly temperature series from all nine stations were standardised to a common mean, following several corrections made to individual station records based on the findings of Torok (1996; pers. comm.). A warm-season (Nov. - Apr.) time series was developed, that reveals a latitudinal temperature gradient of about 2.38° C (1.78° for min, 2.99° for max) for the common period (1937-1970), based on the

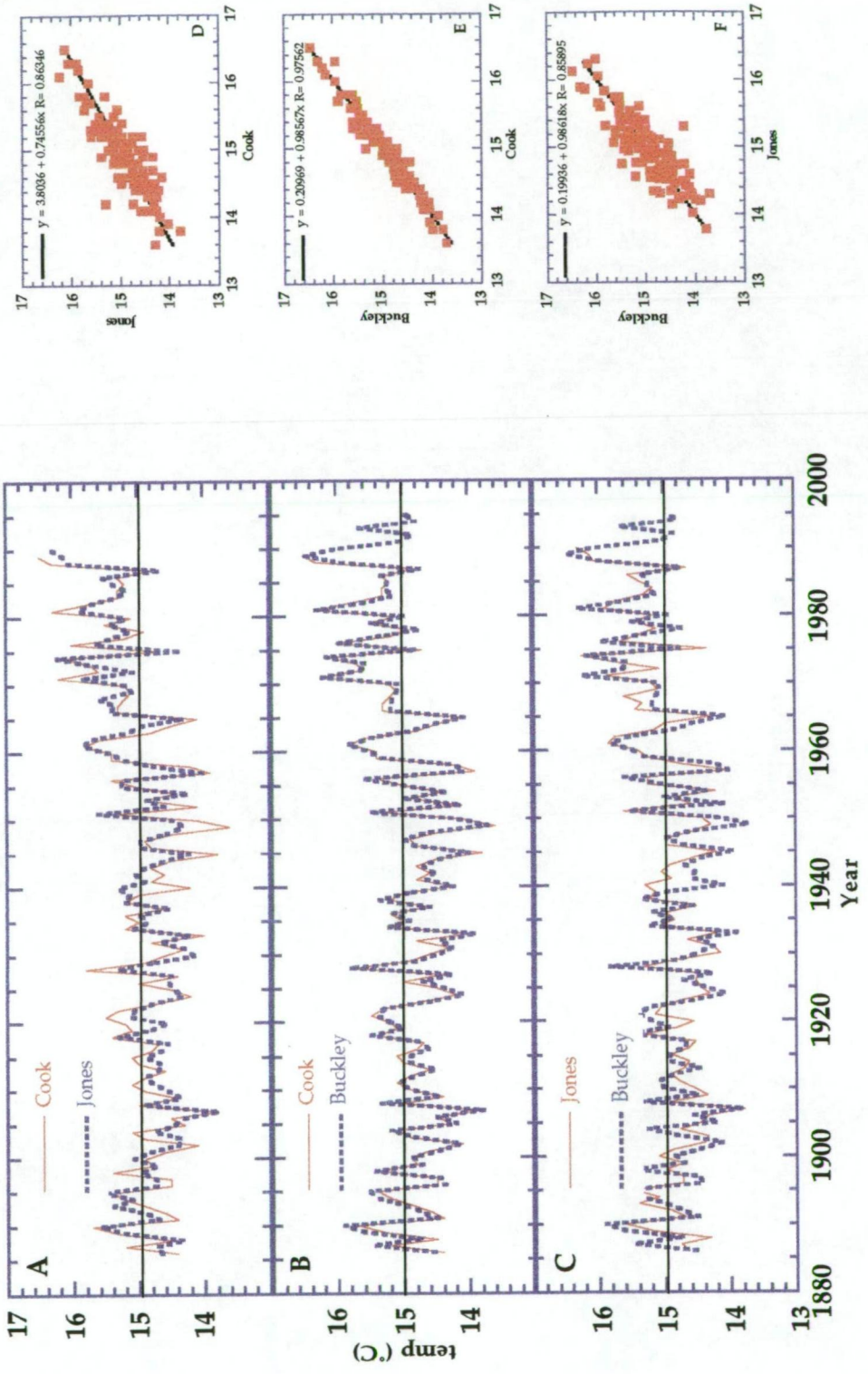

Figure 5.10. Plots of the Cook, Jones, and Buckley temperature series. The three warm season (Nov-Apr) series are plotted against each other in A, B, and C. Plots D - F show the scatter plots for each pair. The Cook and Buckley composite series share three stations and are very similar (r = 0.975), in spite of the addition of six widely-spaced stations to the Buckley Series, the locations of which are shown in Figure 5.9.

difference between King Island in Bass Strait and Maatsuyker Island off the southern coast of Tasmania. The sea-level temperature equivalent for Mt. Read is estimated from Strahan and Cape Sorrel, both of which have a mean for the common period of 14° C. Based on a mean lapse rate of around 0.6° C/100m, the mean warm-season temperature on Mt. Read for the same period is estimated at around 8° C.

Station	Elev.(m)	First yr.	Last yr.	Min	Max	Mean
King Island	24	1919	1993	11.45	18.77	15.11
Stanley	10	1896	1975	11.13	18.60	14.86
Low Head LH	28	1896	1993	11.61	18.51	15.06
Launceston	166	1886	1993	8.69	20.63	14.66
Hobart	5	1883	1993	10.18	19.68	14.93
Cape Bruny LH	5	1925	1995	10.16	16.72	13.44
Maatsuyker Is. LH	147	1937	1995	9.67	15.78	12.73
Strahan	7	1901	1991	11.05	16.96	14.00
Cape Sorrel	19.3	1901	1970	11.05	16.96	14.00

Table 5. 4. The nine temperature records comprising the Buckley Series. The station elevation and their timespans are shown, along with the mean warm-season (November to April) values for minimum, maximum, and mean temperatures for the common period of 1937 to 1970. The stations in bold-face were also used for development of the Cook Series.

To further evaluate the validity of using the Cook Series for the calibration of west coast, high-elevation tree-ring chronologies, daily temperature records for several Tasmanian stations are compared, including data recorded from an AWS installed on Mt. Read within the fire-killed part of the LJH stand at 950 metres (Chapter 3.6.1; Figure 3.6 and Table 3.2). The Mt. Read data were recorded from December 20, 1994 to December 12, 1995. The daily temperatures correlate strongly with several widely-spaced stations for a common 182 day period (Table 5.5). For example, high correlations are found with Hobart minimum, maximum, and mean daily temperature (r = 0.795, 0.704, and 0.824, respectively), in spite of a distance of nearly 150 kms and nearly 1,000 metres in elevation. A mean lapse rate of around 0.6° C per 100 metres is extrapolated for Mt.

Read, as noted above, with a greater rate for maximum (0.7° C/100m) than minimum (0.45° C/100 m) temperature. It is notable that the correlation for daily temperature from stations many kilometres apart and at varying elevation should be so strong, given the incumbent "noise" expected due to local topography, cloudiness, and other parameters unique to a given site. It must be pointed out, however, that much of the period analysed was a time of predominantly high pressure and stable weather conditions over most of Tasmania, and this might account for some of the agreement. Nevertheless, these findings support the use of the longest-available temperature records from throughout Tasmania for calibration of the tree-ring chronologies.

	Mt. Read min.	Mt. Read max.	Mt. Read mean
Hobart	0.795	0.704	0.824
Launceston	0.797	0.803	0.872
Low Head	0.803	0.709	0.830
Queenstown	0.693	0.731	0.864
Strathgordon	0.883	0.705	0.866
Strahan	0.679	0.759	0.812

Table 5.5. Mt. Read daily temperature correlations with six other stations. Listed are the values for *r* based on simple linear regression for the minimum, maximum, and mean daily values from each station with the same parameter from the AWS on Mt. Read.

In order to examine Huon pine's response to temperature in greater detail, additional comparisons were made with maximum and minimum temperature. These series were based upon the average normal standard deviates of monthly minimum and maximum temperatures from the western Tasmanian stations of King Island (Currie), Erriba and Stanley (data supplied by K. Allen, University of Tasmania). The time period covered by both of these data sets is 1910 to 1993, offering 83 years of independently-derived data for comparison with results from the Cook and Buckley Series mean temperature data. The utilisation of maximum and minimum temperature data enables an

evaluation of the seasonal importance of these two parameters as they relate to a dynamic regime of light, moisture availability, and temperature. For example, the relationship between maximum summer temperature and precipitation may be important as it relates to the amount of available light for photosynthesis during the season of growth.

5.2.2 Precipitation Data

Tasmanian rainfall is highly spatially variable, and several distinct climate zones are recognised largely based upon this variability (Bureau of Meteorology, 1993). A particular challenge for this study was to obtain an appropriate rainfall time series for comparison with the seven Huon pine chronologies. As is the case for temperature, most long precipitation records are from stations at elevations lower than 200 metres AMSL and far from the study sites. Also, precipitation exhibits far less spatial coherence than temperature with regard to elevation and topography, making the use of single station records less reliable.

It was important to test the expectation that rainfall would prove to be a less significant factor for Huon pine growth than temperature, particularly at higher elevations, except for as the two are intercorrelated. To this end, several of the longer individual station records from western Tasmania (e.g., Queenstown and Maatsuyker Island) were compared against the tree-ring chronologies. Although the calibration results were similar, the individual stations reflected a large degree of localised signal that was undesirable. Therefore, a composite time series representing west coast monthly rainfall was used for the calibration of Huon pine growth with precipitation (Table 5.6). The data are expressed as average normal standard deviates from 1915 - 1990, based on monthly rainfall records from seven west-coast stations (data supplied by K. Allen, University of Tasmania). Three of these stations (Yolla, Queenstown, and Irishtown) are among the highest quality rainfall records from western

Tasmania, as determined by a survey of Tasmanian station records by B. Lavery (pers. comm.). It was felt that this composite record was adequately representative of west coast rainfall to be useful for calibration purposes, and the results of these tests are described in the next chapter.

Station	Elevation (m)	First Year	Last Year
Yolla	*ca.* 300	1905	1990
Cape Grim	*ca.* 90	1888	1990
Stanley	*ca.* 10	1868	1990
Lake Margaret	*ca.* 600	1912	1990
Queenstown	*ca.* 130	1906	1990
Waratah	*ca.* 550	1882	1973
Irishtown	*ca.* 100	1906	1990

Table 5.6. The seven rainfall stations used for the west coast precipitation record. The final time series is expressed as the average normal standard deviates of the original data from 1915 - 1990. (data supplied by K. Allen, University of Tasmania).

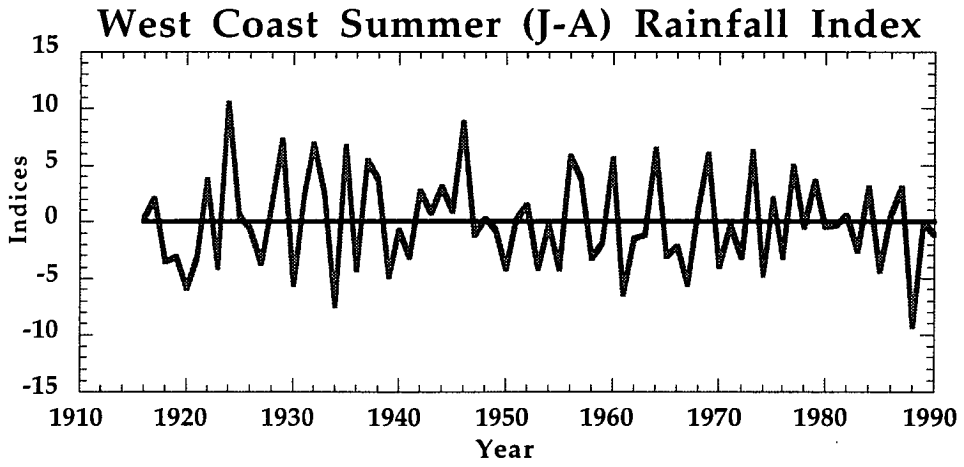

Figure 5.11. West coast summer rainfall indices (January - April season), expressed as the average normal standard deviates from the seven rainfall stations listed in Table 5.6.

CHAPTER 6: RESULTS AND DISCUSSION

6.1 Climate Response of *Lagarostrobos franklinii*

6.1.1 Response functions

The climate response plots for the seven chronologies are shown in Figures 6.1 - 6.4. These correlation functions were based on calibrations of the prewhitened Residual chronology indices with the entire common period for: A) mean monthly temperature from 1883 - 1995; B) western Tasmanian mean-minimum and mean-maximum temperature, expressed as average normal standard deviates, from 1910 - 1993; and C) western Tasmanian precipitation, also expressed as average normal standard deviates, from 1915 - 1990 (all climate series are described in Chapter 5.2).

A 21 month dendroclimatic window was used, from May of the season of growth (year *t*) back 21 months to September prior to year *t*-1. Prewhitening of the mean temperature data prior to regression accounts for the loss of 3 years of data (due to the AR(3) model for the months of April and May, whereas most months were modelled as AR(1) processes). The 21 month window accounts for the loss of an additional 2 years and, following the shift of the data backwards by one year (in order to account for the Southern Hemisphere growth season), the final predictor-predictand common period is 1887 - 1989. Autoregressive modelling of the other three climatic time series indicated that prewhitening was unnecessary, and was therefore not employed prior to analyses. Thus, the final timespans are from 1912 - 1993 for both maximum and minimum temperature, and from 1917 - 1990 for the precipitation series.

There are similarities in the suggested climate response for all seven chronologies. However, the three sites from elevations higher than 700 metres (HIGH) exhibit a far stronger response to warm season climate in year *t*, while the three lower sites (LOW) respond more vigorously to the previous growth season. Cook *et al.* (1992) identified

the season of strongest temperature response for LJH as November to April, which is the "warm-season" period of their temperature reconstruction. It is only LJH, however, that shows significance ($p < 0.05$) for November (with minimum and mean temperature), while BCH is the only site to show significance for December (maximum temperature only). The strongest response "window" for all of the HIGH sites is clearly from January through April, with much of the correlation in January apparently related to the influence of maximum temperature, and much of April's correlation related to the influence of minimum temperature.

The temperature responses for January and April are accompanied by significant responses with precipitation for these same months (i.e., an inverse correlation with January, and a direct response to April rainfall for all of the HIGH chronologies). It is difficult to envisage that the availability of moisture in this high rainfall region (*ca.* 3,000 mm annually) could be directly limiting to growth, and this apparent response most likely stems from the intercorrelation between precipitation and temperature (Buckley *et al.*, 1997). For example, low precipitation in January corresponds to higher maximum temperatures and increased photosynthetically-active radiation during the early growing season. High April rainfall might be expected to result in lower maximum, yet higher minimum, temperature due to inhibited radiational cooling toward the end of the growing season.

The consistently strongest correlations for all of the significant year t months are with BCH, while the only significant t - 1 correlations for the HIGH chronologies are positive with April mean temperature (LJH, BCH, LMH), May mean temperature (LJH), and April maximum temperature (BCH). There are no significant correlations with precipitation for any months in year t - 1 for any of the HIGH

chronologies, and indeed little to indicate a strong prior season response of any kind for these subalpine sites.

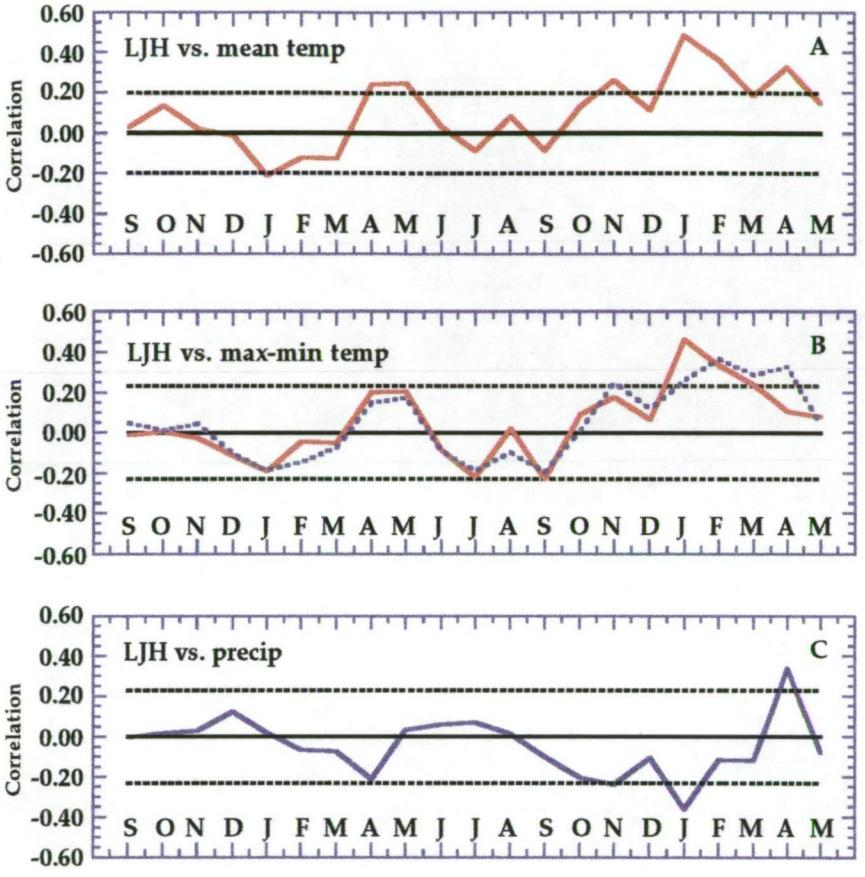

Figure 6.1. Climate response plots for LJH. Correlations are based on analyses of a 21-month dendroclimatic window beginning with May (M) of the current year on the extreme right hand side, back to September (S) 21 months prior. The three plots show the correlations of the prewhitened LJH chronology with; **A**) mean monthly temperature; **B**) mean monthly minimum (dashed line) and maximum (solid line) temperature; and **C**) total monthly precipitation. The horizontal dashed lines represent the 0.05 confidence levels, and values extending beyond these lines are significant at the 95% level.

The three LOW chronologies exhibit a direct response to warm season temperature in year t which is considerably weaker than that of the three HIGH sites. They also reveal a significant ($p < 0.05$), negative response to temperature in the previous warm season, that is strongest in the HAR chronology. The strongest temperature response window for the LOW sites is from December - March of year t - 1, with the highest correlations associated with minimum temperature for January, February

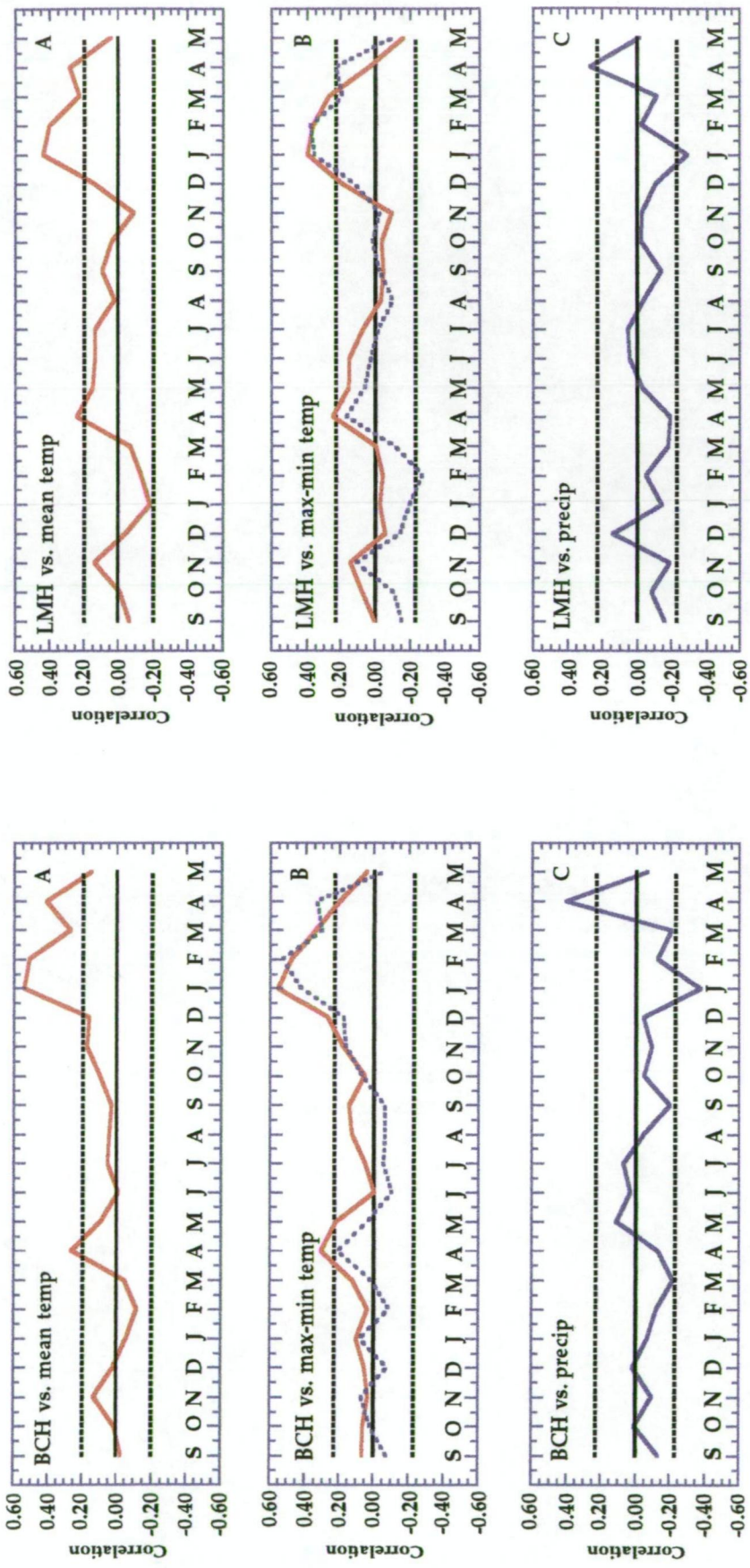

Figure 6.2. Climate response plots for BCH and LMH. (Same as for Figure 6.1).

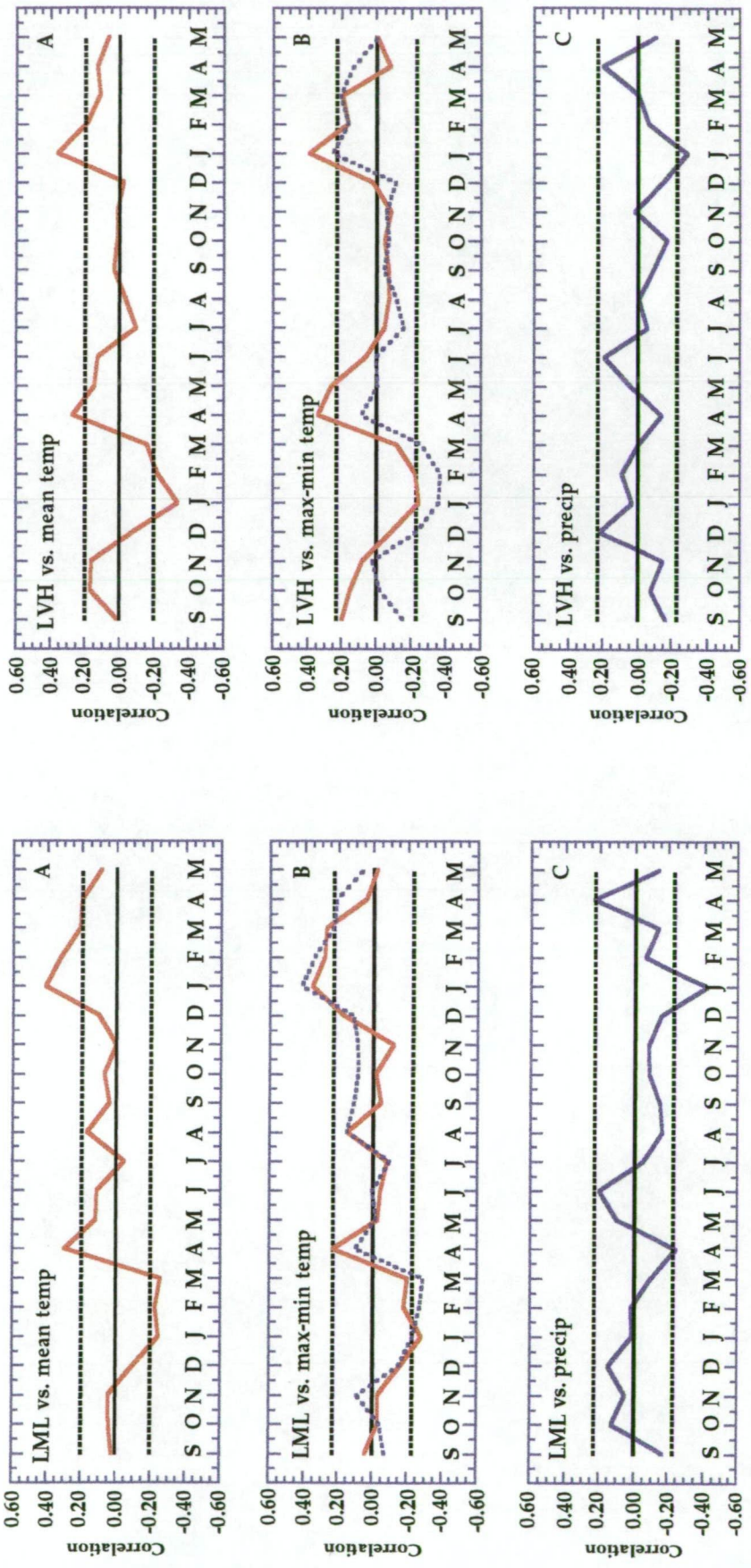

Figure 6.3. Climate response plots for LML and LVH.

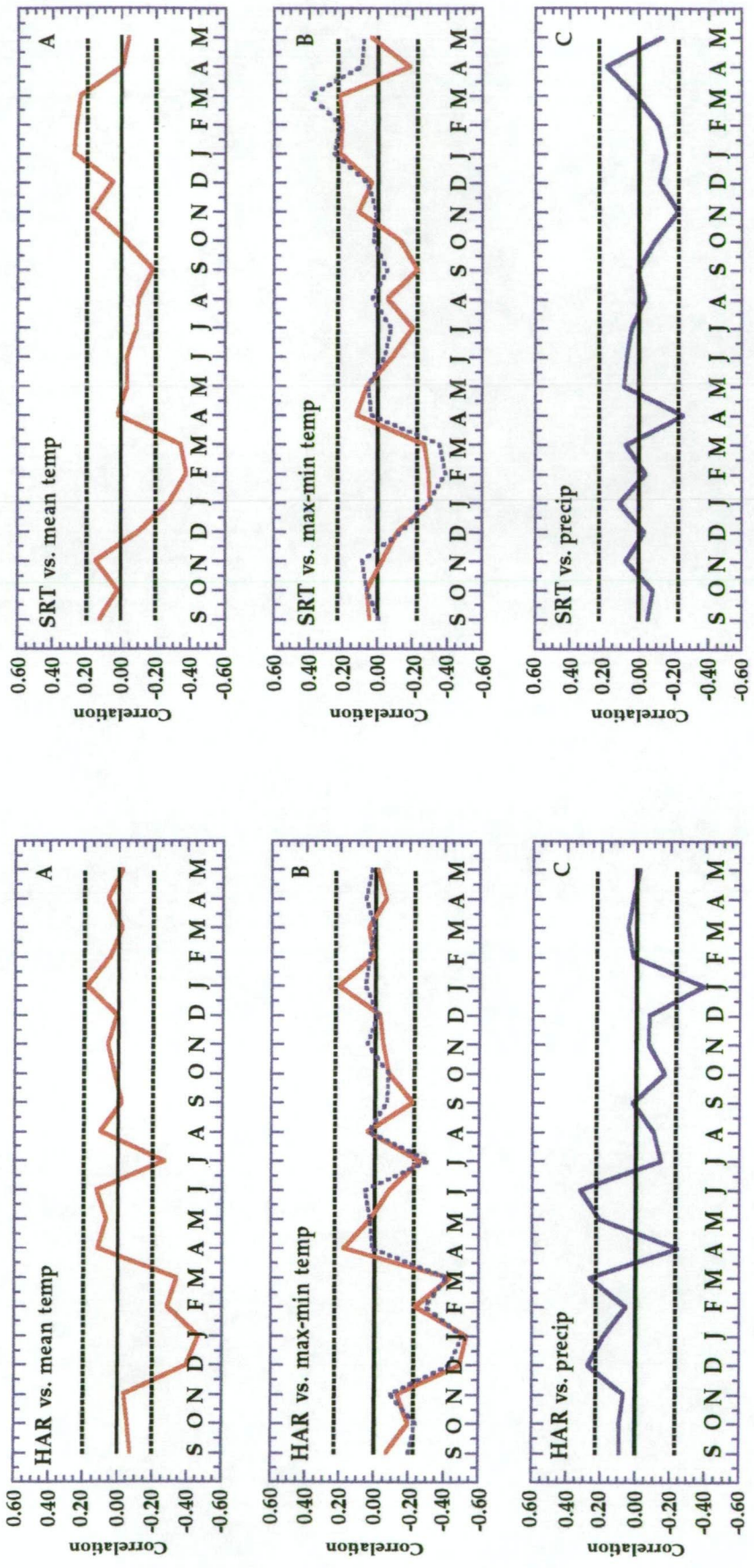

Figure 6.4. Climate response plots for HAR and SRT.

and March. This same response is weakly apparent in the HIGH sites but is not statistically significant for any of them. The 700-metre LML site falls almost directly between the two groupings, with both the inverse year *t*-1 and the direct year *t* response to temperature showing significance at the 0.05 level. Precipitation exhibits weaker correlations and greater variation between sites with the LOW rather than with the HIGH chronologies. Only HAR exhibits a significant, direct response with December, March, and June of year *t* - 1, and negative with April (*t* - 1) and January of year *t*. The only other significant correlations with precipitation are for LVH and SRT, both with an inverse response (January of year *t* for the former, and April of year *t* - 1 for the latter).

The strong, inverse prior-season response to temperature for the LOW sites is not presently well understood. It is plausible that, given the nutrient-poor conditions of the soils, coupled with extremely slow growth rates for Huon pine, warm growing season conditions that result in optimum growth rates may actually serve to deplete stores of carbohydrate and nutrients (Schulze and Caldwell, 1994). This might in turn result in a negative feedback in the form of reduced growth the following season. This is because the use of stored carbohydrates leads to the uncoupling of growth and carbon assimilation rates, and storage of carbohydrates in the following season may actually compete with growth for current photosynthate availability (Peirera, 1994). Such an effect might not be evident in the subalpine sites where temperature seldom exceeds optimum levels for photosynthesis, and cold winter conditions ensure dormancy (Salisbury and Ross, 1992; Schulze and Caldwell, 1994).

The weak correlation with precipitation for all LOW sites argues against drought stress (as related to high temperature and dry conditions) as the source of the year *t* - 1 temperature response. The effects of photoinhibition (where cloud-free conditions result in high light intensity and overexcitation of the trees' light harvesting system,

resulting in photochemical damage) must also be considered (Björkman and Demmig-Adams, 1994). However, Francey *et al.* (1985) demonstrated a stomatal insensitivity to light for Huon pine at the Stanley River, even under very high light intensities, which suggests that photoinhibition is not likely to be a factor.

In order to assess the temporal integrity of these climate signals, split calibration-verification periods were created by dividing the long temperature time series into two nearly equal parts, and using each half to calibrate and verify against the other (results shown in Table 6.1a-b).

Site	Early Calibration Period						(1887-1939)	
	R_p	R_S	R_R	ST	PM	R^2	AR^2	DW
LJH	0.579	0.599	0.544	39+ 14-	3.89	0.336	0.323	1.71
BCH	0.623	0.654	0.628	41+ 12-	4.42	0.388	0.376	1.84
LMH	0.500	0.495	0.511	37+ 16-	2.57	0.250	0.235	1.90
LML	0.517	0.508	0.496	37+ 16-	2.63	0.267	0.253	1.43
LVH	0.462	0.486	0.458	38+ 15-	2.15	0.214	0.198	2.03
HAR	0.549	0.513	0.529	39+ 14-	2.82	0.302	0.274	1.74
SRT	0.598	0.492	0.544	35+ 18-	2.98	0.357	0.346	1.64
Site	Verification Period					(1940-1990)		
	R_p	R_S	R_R	ST	PM	RE	CE	
LJH	0.508	0.417	0.473	33+ 18-	2.53	0.155	0.095	
BCH	0.579	0.532	0.578	35+ 16	2.61	-0.042	-0.044	
LMH	0.357	0.291	0.341	31+ 20-	1.62	-0.053	-0.053	
LML	0.402	0.284	0.321	28+ 23-	2.30	0.094	0.094	
LVH	0.351	0.341	0.362	31+ 20-	1.83	0.096	0.086	
HAR	0.529	0.504	0.496	33+ 18-	2.93	0.239	0.238	
SRT	0.338	0.327	0.326	31+ 22-	2.09	0.007	0.007	

Table 6.1a. Calibration - verification statistics for temperature response models for the seven chronologies for the early calibration period (1887-1939). The verification tests used include R_P, which is the Pearson product-moment correlation coefficient; R_S the Spearman rank correlation coefficient; R_R a robust correlation coefficient; the sign test ST; the product means test PM; the reduction of error test RE; and CE, the coefficient of Efficiency. R^2 is the usual coefficient of determination; AR^2 is the R^2 adjusted for degrees of freedom; and DW (Durbin-Watson) is a statistical test for autocorrelation in the residuals. No significance tests exist for AR^2, RE, or CE, but an RE or CE > 0 indicates some degree of model fidelity.

Site	Late Calibration Period						(1940-1990)	
	R_p	R_s	R_R	ST	PM	R^2	AR^2	DW
LJH	0.579	0.533	0.603	35+ 16-	2.73	0.335	0.322	2.55
BCH	0.673	0.657	0.703	41+ 10-	2.21	0.453	0.442	1.73
LMH	0.492	0.510	0.488	35+ 16-	3.40	0.242	0.226	1.87
LML	****	****	****	****	****	****	****	****
LVH	****	****	****	****	****	****	****	****
HAR	0.631	0.634	0.598	32+ 19-	3.97	0.398	0.372	1.72
SRT	0.452	0.457	0.415	37+ 16-	2.52	0.205	0.189	2.06
Site	Verification Period					(1887-1939)		
	R_p	R_s	R_R	ST	PM	RE	CE	
LJH	0.319	0.374	0.370	32+ 21-	2.34	0.148	0.100	
BCH	0.447	0.433	0.422	34+ 19-	2.53	0.158	0.157	
LMH	0.369	0.404	0.380	34+ 19-	1.53	0.098	0.098	
LML	****	****	****	****	****	****	****	
LVH	****	****	****	****	****	****	****	
HAR	0.483	0.384	0.440	36+ 17-	2.33	0.233	0.233	
SRT	0.558	0.476	0.526	36+ 17-	2.899	0.281	0.281	

Table 6.1b. Calibration - verification statistics for temperature response models for the seven chronologies for the late calibration period (1940 - 1990). Columns the same as for Table 6.2a. Note that for SRT the calibration period extends to 1992. **** indicates no model selected based on minimum AIC criterion (Akaike, 1974).

A PCA regression was employed, using the PCs of the significant predictor variables with eigenvalues greater than 1.0. The best order model was selected based on the minimum AIC criterion (Akaike, 1974). In general, calibration with the 1940-1990 period resulted in an increase in the percent variance of the tree rings explained by climate, compared with the 1887-1939 period. Although there are some differences between the two periods of the calibration-verification analyses, relative to the total period (Figures 6.1 - 6.4), the overall signal is essentially the same. In nearly all instances the verification statistics indicate good model fidelity, and the correlation functions presented here are considered to be accurate reflections of the true climate signal for Huon pine.

As noted in Chapter 5, the meteorological data are of generally higher quality in the latter half of the record, particularly after 1910, and

this might partially explain the differences between the two calibration periods. It is also true, however, that the general climatic conditions over both periods are different, with increased influence from the Subtropical High over the Tasman Sea for the latter period (e.g. Lough, 1991), and intensified zonal westerlies during the early period. The relative strength of these two influences is demonstrated by Figure 6.5 which shows the spatial correlations between the Mt. Read temperature reconstruction with SST for each period, revealing a greater influence from the Tasman Sea over the later period, and from the southwest of Tasmania during the earlier period of anomalously cool temperature (Cook *et al.*, 1996b).

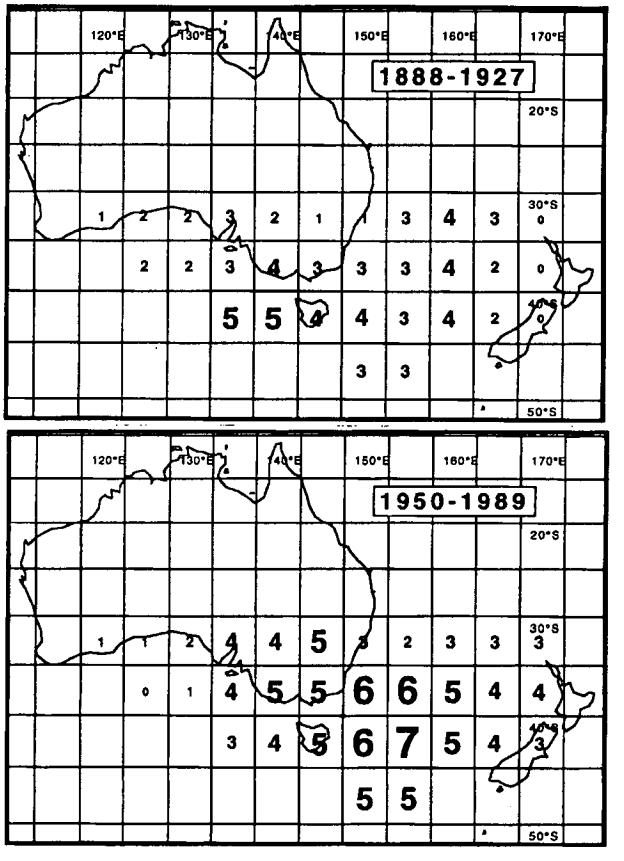

Figure 6.5. Spatial correlations between reconstructed Tasmanian summer temperature and 5° x 5° gridded land/marine temperature surrounding Tasmania. The numbers in the grid boxes are correlations rounded up or down to the nearest tenth and multiplied by 10 (e.g., if $r = 0.44$ the grid box value is 4, while if $r = 0.46$ then the value is 5). The correlations were computed on pre-whitened temperature to remove the effects of autocorrelation and trend on the estimation of r. For 38 degrees of freedom, grid box values greater than or equal to 4 (and most values of 3) are statistically significant at the 0.05 level of confidence, assuming a 1-tailed hypothesis test (i.e., H_0: $r = 0$; H_a: $r > 0$). (From Cook *et al.*, 1996b).

The effects of such changes in large-scale circulation are also evident in Figure 6.6, which shows warm season Hobart SLP anomalies, the L-Index of Pittock (1973) (a measure of the mean latitude of the STHPB off the east coast of Australia), and zonal circulation indices derived from the difference in SLP between Hobart with Brisbane, Sydney, Melbourne, and Adelaide. All three indicate the change from a predominantly westerly airstream during the Austral summer in the early part of the record (accompanied by lower SLP over Hobart and generally colder conditions) to an increasing L-Index, and a systematic decrease in the difference between warm season SLP in Hobart and the other stations for the latter part of the record (Cook *et al.*, 1996b). Slight changes in the apparent climate relationship from one half of the record to the other might be expected under different climate regimes, yet the general physiological factors underlying this response would be the same.

It is clear that the empirical relationships between climate and Huon pine ring widths, as presented in this thesis and elsewhere, have their basis in very complex physiological interactions that are broadly correlated with temperature. With increasing elevation, reduced temperature (energy) becomes increasingly limiting to overall growth, with a corresponding increase in explained variance for ring width over the entire season of growth. Nevertheless, a large percentage of the variance in annual growth will remain unexplained until careful physiological studies are employed to reveal the underlying mechanisms being controlled by the temperature of their operating environment. It is possible that subtle changes in these complex relationships through time may be responsible for the corresponding change in the climatic response presented here.

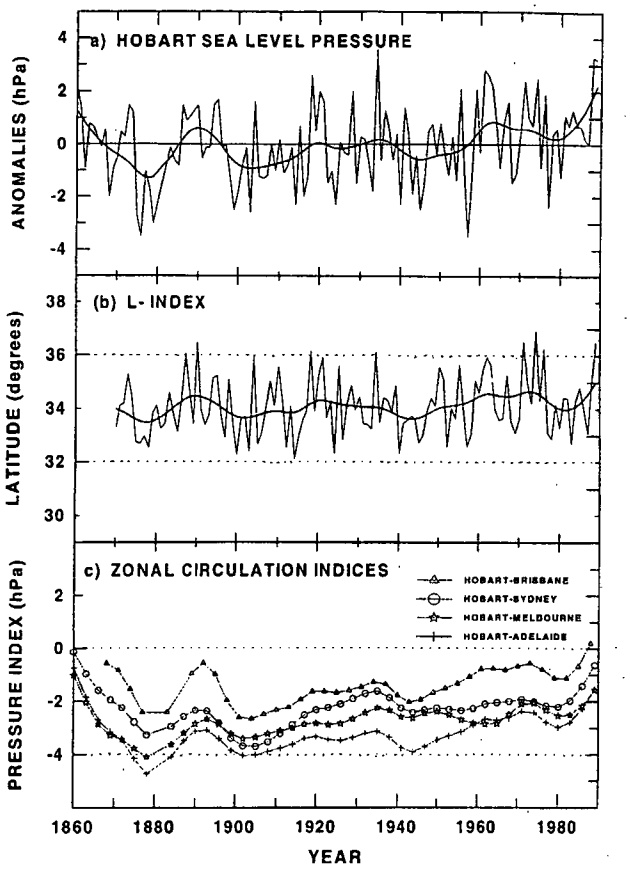

Figure 6.6. Three measures of general circulation over Tasmania: a) Hobart warm-season (November to April) SLP anomalies; b) the L-index of Pittock (1973) which plots the latitude of the STHPB off eastern Australia; and c) zonal circulation indices, calculated as the pressure difference between Hobart and Brisbane, Sydney, Melbourne and Adelaide. The yearly values have been smoothed to accentuate fluctuations of greater than 20 years. Note the anomalously high pressure over Tasmania since 1960, associated with the poleward migration of the STHPB and the corresponding weakening of the zonal circulation in the recent decades. All appear to be associated with the recent warming trend over Tasmania. (From Cook *et al.*, 1996b).

6.1.2 Climate response with elevation

As noted in Chapter 1.3, the objectives of this thesis include evaluating the LJH climate signal with regard to its representativeness of the broader regional climate, and not just the microclimate of Mt. Read. It was also intended to assess Huon pine's response to climate with respect to an elevational gradient. Toward that end, a rotated Principal Component Analysis (PCA) (Richman, 1986) was performed on the seven Residual chronologies (Table 6.2, Figure 6.7). The period of analysis is from 1560 - 1990, which accounts for the maximum period of

No.	Eigenvalue	% Variance	Cumulative%	Mean	95% Limit
1	**3.935	56.212	56.212	1.189	1.267
2	**1.201	17.162	73.373	1.110	1.154
3	0.543	7.763	81.136	1.050	1.088
4	0.471	6.734	87.870	0.997	1.031
5	0.398	5.681	93.551	0.940	0.975
6	0.282	4.032	97.583	0.888	0.922
7	0.169	2.417	100.000	0.826	0.879

** First two eigenvectors with eigenvalues > 1 are rotated

Unrotated Eigenvector Loadings

Eigenv.	LJH	BCH	LMH	LML	LVH	HAR	SRT
1	0.388	0.397	0.361	0.417	0.403	0.336	0.335
2	-0.323	-0.467	-0.378	0.050	0.251	0.480	0.489

Rotated Varimax Loadings

1	**0.805	**0.926	**0.808	0.572	0.402	0.135	0.126
2	0.260	0.157	0.180	0.601	**0.744	**0.839	**0.844

** Chronologies that load similarly and significant at 0.05 level

Table 6.2. Results from a rotated PCA, with an analysis period from 1560 to 1990. This method of analysis does not presume any relationships between the chronologies. For the first two components (the only ones significant at the 95% level) there is a clear separation of the high and low chronologies, both before and after varimax rotation. Together the first two eigenvalues account for more than 73% of the total variance of all seven time-series. The rotated varimax loadings clearly illustrate the separation of the chronologies by elevation into two groups, from above and below 700 metres, respectively.

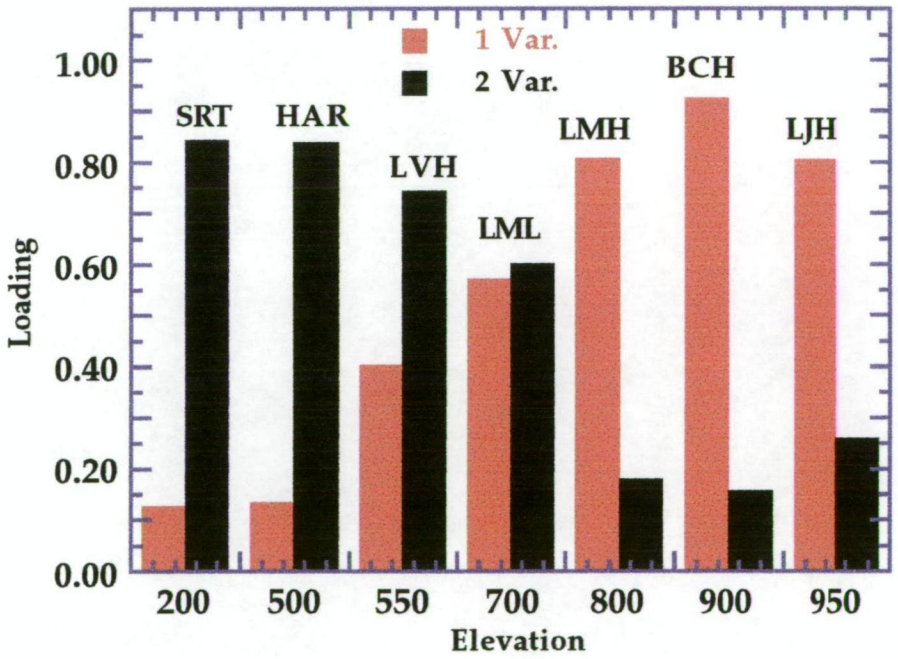

Figure 6.7. Varimax loadings for the first and second rotated eigenvectors from the seven Huon pine chronologies. A clear elevational dependence is revealed from this rotated PCA, with the first eigenvector accounting for the variance in the high elevation sites, and the second eigenvector relating to the low elevation sites. The 700 metre LML site is interpreted to represent an important climatic ecotone in Tasmania, above which growing season temperature is the factor most directly limiting to growth of the current year.

overlap with adequate replication in all seven chronologies. Only the first two PCs are significant at the 0.05 level, a result based on a rigorous Monte Carlo significance test (Preisendorfer *et al.*, 1981), which validates the rotation of the first two eigenvectors. These two eigenvectors are the only two that have eigenvalues greater than 1.0, and together they explain 73.3% of the total variance among all seven series.

Both before and after varimax rotation the grouping of the chronologies into two distinct clusters by elevation is evident, with the first varimax factor representing the high-elevation sites, and the second eigenvector relating to those sites below 700 metres. The LML chronology apparently represents a transitional site between the two groupings with about equal loadings for both factors, suggesting a critical elevation for Huon pine growth with regard to its response to growing season temperature (Buckley *et al.*, 1997). This is certainly the case for at least the period of calibration over the past nearly 100 years, and since the rotated PCA includes data from all seven chronologies well before the calibration period (i.e., from 1560 - 1888), this same elevational response to temperature can be inferred to have remained relatively stable throughout this period.

The above results support the expected increase in the fidelity of the year *t* response to temperature with elevation, based on the principle of limiting factors as discussed in Chapter 2.1.4. An additional test of this elevation-dependence of Huon pine's temperature response strengthens this assertion. Response functions were generated using the scores from the two varimax factors as predictand variables with mean monthly temperature as the predictor variables (Figure 6.8). The monthly correlation functions exactly mirror the responses denoted for the chronologies as presented in Figures 6.1 - 6.4: the first varimax scores reflect the year *t* response of the HIGH chronologies, and the second varimax scores reflect the year *t*-1 response of the LOW sites. Although

these factor scores are derived from the original tree-ring chronologies, they represent an orthogonalised data set that is not constrained to produce similar results. Therefore, these results represent a strong measure of the robustness of the correlation functions presented in this thesis, and strongly support the elevation dependence of the temperature response for Tasmanian Huon pine.

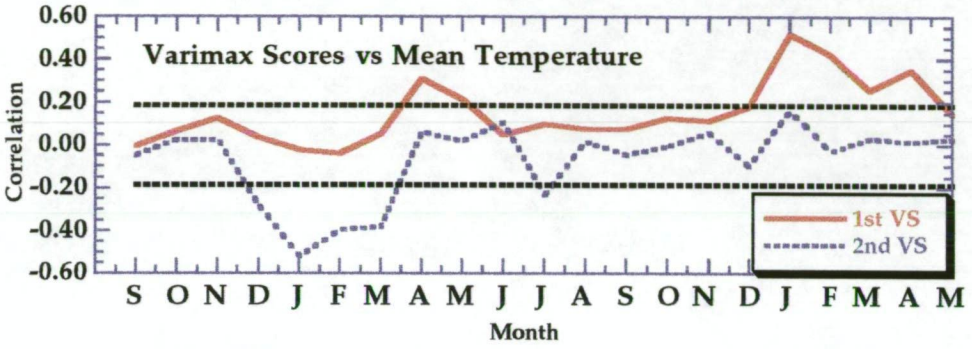

Figure 6.8. Correlation functions for the varimax scores from a rotated PCA with mean monthly temperature. The solid line plots the correlations for the first varimax score, while the dashed line represents the correlations for the second varimax score for the same 21-month window used in Figures 6.1-6.4.

The results of both the climate response modelling and the rotated PCA support the existence of an important environmental zone near the 700 metre contour in western Tasmania, where a physiological threshold is reached with regard to Huon pine's climatic response. Above this zone, temperature drops below optimum levels and becomes increasingly more directly limiting to growth. As noted earlier, Mt. Read's sea level equivalent, mean warm-season temperature is around 14° C. Using adiabatic lapse rates for dry and saturated air of 1.0° C/100 m and 0.56° C/100 m, respectively (for air at *ca.* 10° C and 1000 hPa pressure), the mean warm-season temperature for elevations of 700 metres over the same period is calculated to range from about 7° to 10° C, respectively. For elevations of 1,000 metres the range is from 5° to around 8.5° C.

Read and Busby (1990) determined that the optimal temperature for photosynthesis in Huon pine is 20° C, based on studies using specimens from 80 metres AMSL. The response of photosynthesis to temperature is curvilinear, with a reduction to 80% of maximum photosynthesis at a low temperature of 14° C, and at a high temperature of 27° C for plants acclimatised to 20° C (Figure 6.9). In addition, the percentage of maximum photosynthesis drops to only 30% when plants are acclimatised to 8° C and remains low at 49% when plants are acclimatised to 32° C (Read and Busby, 1990). The authors noted that specimens from sites at higher elevation are likely to have lower optimum temperatures and even greater resistance to frost than the low elevation samples used in their study. The interannual variability of temperature might therefore be expected to account for a large percentage of the variability of annual growth, as is the case for LJH where nearly 37% of the variance in annual growth can be explained by temperature (Cook *et al.*, 1992).

Based on the adiabatic lapse rates alone, it seems plausible that the 700 metre contour corresponds to a critical environmental zone with regard to photosynthetic activity in Huon pine, as mean warm season temperature drops to near or below 10° C. Above this zone, warm season temperature becomes increasingly more limiting to growth through the inhibition of net photosynthesis during prolonged periods of low temperature and increased cloudiness. Extended periods of temperature above 25° C at subalpine locations would be very rare. For example, daily temperatures recorded from within the 950-metre LJH site for the Austral summer of 1994 (one of Tasmania's warmest summers on record) reveals a mean maximum of 14.1°, an absolute maximum of 28.9°, and a minimum maximum of 3.3° C (see Table 3.2). Minimum temperature for that same summer had a mean of 5.9°, a maximum of 14.3°, and a minimum of -2.9° C.

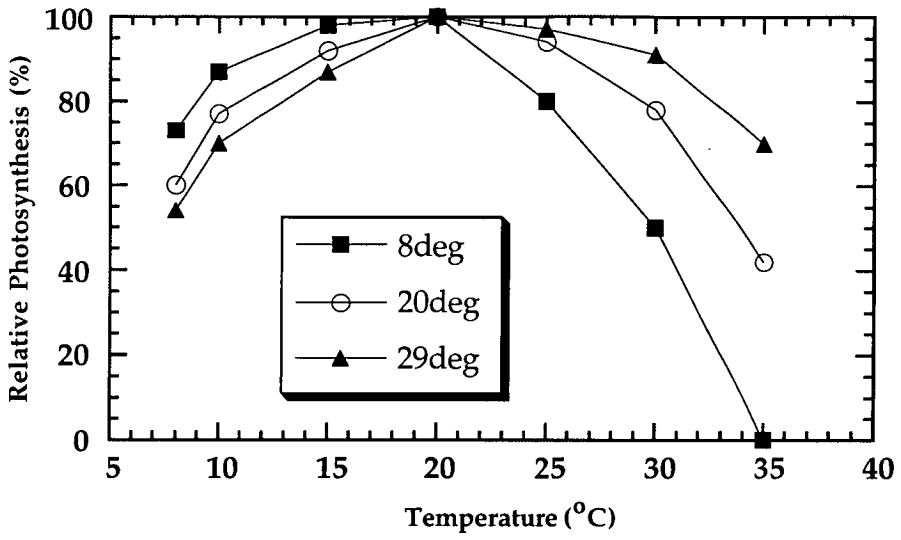

Figure 6.9. The response of net photosynthesis in Huon pine to instantaneous temperatures in foliage acclimatised to three temperatures; 8°, 20°, and 29° C, respectively. The rates of net photosynthesis are expressed as a percentage of the maximum rate of photosynthesis recorded for that acclimation temperature. Each value represents the mean of five replicates from samples taken from the Picton River in southern Tasmania at an elevation of 80 metres. The optimum temperature for photosynthesis is 20° C for all acclimation temperatures. The lowest acclimation temperature produced the highest rates of net photosynthesis at cooler temperatures, and the lowest rates when instantaneous temperature exceeds 20° C. Conversely, a higher acclimation temperature resulted in reduced net photosynthesis at lower temperature, and enhanced rates at higher temperatures. (Adapted from Read and Busby, 1990.)

6.1.3. Photosynthesis, climate, and tree growth

The above interpretations necessarily assume that growth is more or less directly correlated with photosynthesis; in this case growth refers specifically to annual radial growth in the tree stem, resulting from cambial cell production. This seems a reasonable assumption since the production of cell wall material is dependent on the photosynthetic apparatus, which affects both the availability of carbohydrates and the content of growth regulators (Schulze and Caldwell, 1994). In general, however, the correlation between photosynthesis and plant growth is poor, with growth exhibiting far greater overall variability (Peirera, 1994). A stronger correlation emerges when nitrogen is limiting; i.e., when N is in ample supply the relative growth rate is directly proportional to

photosynthetic rate, and when N is low photosynthesis has little effect on growth (Fichtner *et al.*, 1994). While soils in western Tasmania are typically nutrient poor and heavily leached (Wilson, 1990), it is unclear how this relationship effects growth at the sites used for this study, particularly with regard to the different temperature regimes under which they exist and the possibility of transient nutrient influx due to the burning of adjacent vegetation. Furthermore, the partitioning of carbon and nitrogen between root and shoot has a long lasting effect on whole-plant carbon relations and on photosynthesis, which overrides in feedback the actual effect of carbon gain. Storage of carbohydrates, as starch and nitrates, are intermediate accumulatory processes that essentially exclude each other. Maximum growth rates occur when both of these accumulatory processes reach a minimum (Schulze and Caldwell, 1994). Vegetative growth is generally assumed to reach maximum rates when plants invest as much carbohydrate as possible in the growth of new leaves, for it is only with new leaves that additional production organs are established, that then contribute to further growth (Harper, 1989). However, the operating conditions (i.e., climate, and particularly temperature) in which these processes take place are critically important, and since different processes are optimised at varying temperatures and light intensities, detailed physiological studies are needed to resolve these relationships. To date no such studies have been undertaken for Huon pine.

Along with temperature, the effects of cloudiness and moisture availability combine to further influence net photosynthesis in Huon pine. Moisture availability alone is not problematic for subalpine stands in western Tasmania where, as noted earlier, the median annual rainfall totals in the mountainous areas exceed 3,000 mm. Indeed, the role of precipitation is likely to be a minor one, except as it correlates with temperature and light-availability. Drought does occur in the rainforest

areas of western Tasmania, and it is possible for trees to experience moisture deficit under conditions of high temperature and low water availability. However, these conditions would not be expected to persist for more than a matter of days at subalpine sites (Buckley et al., 1997). For example, the warm summer of 1994, noted above, experienced only 16 days when the maximum temperature on Mt. Read exceeded 20° C, and only 6 of those days exceeded 25°. Mean daily temperature throughout the summer never exceeded 20° C.

Perhaps more important in the subalpine zone is the role of cloudiness and its effects on temperature, light availability and, therefore, photosynthesis. For example, the annual mean-maximum temperature for stations such as Strathgordon (elevation 320 m) and Savage River (365 m) is 14.0° and 14.2° C, respectively, and the mean 3:00 PM relative humidity is around 70% (Bureau of Meteorology, 1993). This implies a dewpoint of about 7° C, which gives an average cloud base of approximately 800 metres above terrain at the warmest time of the day, translating into a mean cloud base of approximately 1,100 m AMSL. For the bulk of the time, however, the cloud base is less than 500 m above the terrain and probably 500 m AMSL or less early in the morning (M. Pook, pers. comm.). The net effect is a dynamic cycle of light, temperature and moisture below 1,000 metres, with an alpine zone regularly in cloud. This is interrupted during times of slackened zonal circulation and easterly conditions, such as during atmospheric blocking events (Pook, 1996). Trees on windward slopes at higher elevations likely experience even lower temperature and less light, as they would spend much of their time in dense, orographically-generated cloud, resulting in reduced photosynthesis and suppressed growth.

6.1.4 Tasmania's vertical climate structure

Vertical zonation of climate in western Tasmania was proposed by Kirkpatrick and Brown (1987) to explain the existence of a sharp vegetation boundary between sedgeland and alpine flora above 700 metres in southwestern Tasmania, from four different mountains ranging nearly 60 kms in a northwest - southeast transect. The boundary could not be attributed to species interactions, and persisted on all four mountains despite an apparent climatic, geologic, edaphic and topographic continuity of the environment. The authors hypothesised the most likely cause of this boundary to be climatic, in the form of a persistent cloud ceiling with a mean position somewhere above 700 metres, though they lacked the data to properly test this hypothesis. Kirkpatrick *et al.* (1997) later confirmed this model, following two years of climate monitoring on Mt. Sprent in southwestern Tasmania. They documented a frequent subsidence-inversion layer between 850 and 930 metres, along with a sharp change in vegetation which was coincident with a rapid decrease in temperature and increase in relative humidity (see Figure 6.10). Air and soil temperature decreased most steeply in this zone, while humidity was at its highest levels. Both above and below this layer were zones of more gradual change, between 930 and 1,050 metres, and 510 and 820 metres, respectively.

The regional-scale inversion is related to atmospheric subsidence associated with the passage of high pressure systems over Tasmania. Kirkpatrick *et al.* (1997) noted that the height of the inversion base in the free air can be observed by examining the daily radiosonde soundings from Hobart Airport, which indicates the median height to be around 1,138 m AMSL. This is higher than that noted for Mt. Sprent due to the effect of radiative cooling of the earth's surface which lowers the height of the inversion in the west coast mountains. A gradual west to east

increase in the inversion height is also expected as air flows over successive orographic obstacles.

This vertical climate zonation model adequately accounts for the different mean climatic regimes for lowland and subalpine sites in western Tasmania, and is consistent with the results from the climate response modelling and the rotated PCA presented in this paper. Periods of common variance between the HIGH and LOW chronologies may be explained by extended periods of uniform conditions of cloudiness, or persistent periods of clear skies and increased solar radiation. Past changes in this vertical structure might be analysed through the use of an elevational chronology network such as that presented here. The past 100 year period, which exhibits changes in the relative climatic influence from the STHPB and Southern Ocean circulation (noted above), affords a modern analogue for such changes in the past which might be analysed through this approach.

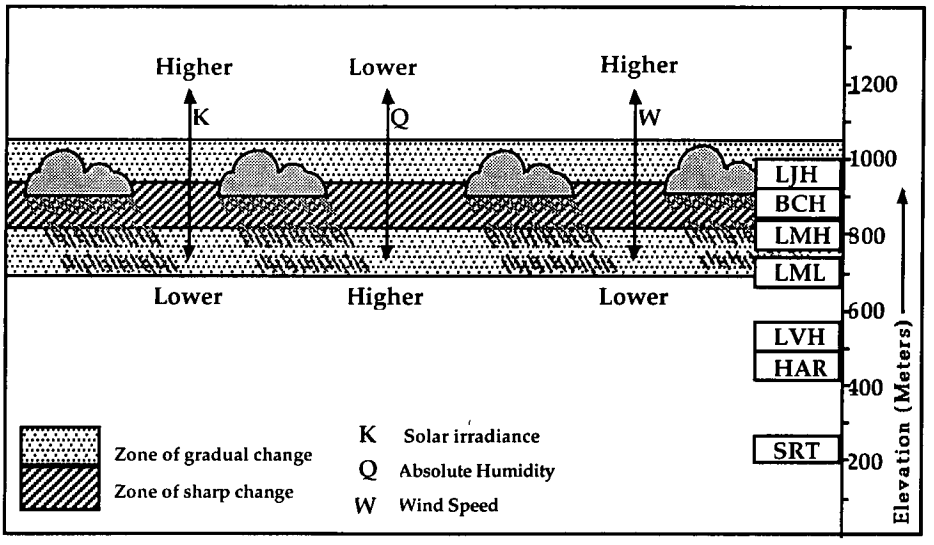

Figure 6.10. Schematic illustration of the vertical climate structure over Tasmania's west coast mountains. Note the location of the LJH site along the top of the zone of greatest change. (Adapted from Kirkpatrick *et al.*, 1997).

6.2 Climate Reconstructions

6.2.1 Mt. Read temperature reconstruction

The Mt. Read warm season temperature reconstruction (Figure 6.11) is based on a correlation analysis first described by Cook *et al.* (1991), and first presented by Cook *et al.* (1992). A six month warm season average (from November through April) was created from the Cook Series for calibration and verification purposes, and simple linear regression was employed to transform the LJH ring-width chronology into estimates of the November to April seasonal temperatures. Both the tree-ring chronology and the climate data were prewhitened as autoregressive (AR) processes prior to regression, with the persistence due to climate subsequently added back into the reconstruction.

A split calibration-verification scheme was used to develop and validate the regression model for the Mt. Read temperature reconstruction, splitting the temperature data into two nearly equal periods: the early period from 1887-1937 was used for model verification, while the 1938-1989 period was used for the calibration of the model. The calibration and verification statistics are summarised in Table 6.3. The model passed all of the verification tests except for the coefficient of efficiency (CE), which is the most difficult verification statistic to pass on a routine basis, and a slightly negative value was considered insufficient grounds to reject the regression model (Cook *et al.*, 1992). Cross-spectral analysis (Jenkins and Watts, 1968) also revealed good fidelity in the frequency domain for bandwidths greater than 12 years and less than 5 years (Cook *et al.*, 1992).

The length of the Mt. Read reconstruction enabled Cook *et al.* (1995; 1996a; 1996b) to assess the recent 100 years of climate within the context of the natural variability of the past 3 millennia. Of particular interest was the recent temperature increase, in evidence since the mid-1960s, and

which appeared as one of the warmest episodes of the entire reconstruction. While this warming period is more than 4.5 standard

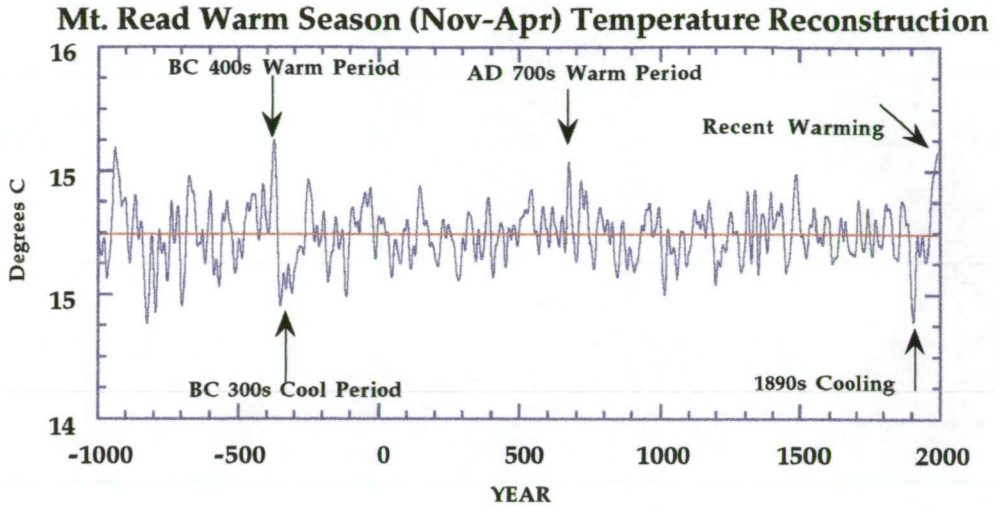

Figure 6.11. The Mt. Read warm season temperature reconstruction from Tasmania (Cook *et al.*, 1996b), shown back to BC 1000. The LJH chronology now extends back to nearly BC 2000, partly as a result of work completed for this study. The reconstructed temperatures, based on a warm-season mean of 14.99°C, have been smoothed with a 25-year low-pass filter to accentuate lower frequency variance in the time series. The last 100 years exhibit one of the coldest, as well as one of the warmest, periods of the entire record. The recent warming trend, though unusual, is within the range of natural variability for this site, and is not statistically unprecedented.

Calibration period: 1938 - 1989

R_p	R_S	R_R	ST	PM	R^2	AR^2	DW	RUNS
0.607	0.515	0.569	31+ 21-	3.60	0.369	0.356	2.09	-0.410
(<0.001)	(<0.001)	(<0.001)	(0.106)	(<0.001)	(<0.001)		ns	(0.341)

Verification period: 1887 - 1937

R_p	R_S	R_R	ST	PM	RE	CE
0.471	0.553	0.592	39+ 12-	2.57	0.101	-0.038
(<0.001)	(<0.001)	(<0.001)	(<0.001)	(0.006)		

Table 6.3. Calibration and verification results for the Mt. Read temperature reconstruction. Column labels are the same as for Table 6.1, except for RUNS which is a second test for autocorrelation in the residuals. Probability levels for the statistics are shown in parentheses where available. No tests exist for AR^2, RE, or CE, but an RE or CE > 0 indicates some degree of model fidelity. The "ns" under the DW column stands for "not significant" ($\alpha = 0.05$). With the exception of the CE the verification period tests indicate a valid regression model. The R_P, R_S, R_R, ST, and PM statistics all passed with significance well below the 5% confidence limits and RE was positive. The validity of the regression model is indicated by the agreement in results from both periods. (From Cook *et al.*, 1992)

errors from the long term mean it is not statistically unprecedented, and is within the range of natural variability of climate over the past three millennium (Cook *et al.*, 1996a; 1996b). Other periods of anomalously cool and warm temperature were noted from the reconstruction as shown in Figure 6.11, in particular the BC 400s warm period which is followed by an apparently severe BC 300s cold period, both among the most anomalous such periods of the entire record.

6.2.2 A new warm season temperature reconstruction

Based on the climate response modelling presented earlier in this chapter, the climatic window of January - April was selected as the most appropriate season for the reconstruction of mean temperature. Reconstructions using single and multiple sites were developed and compared against each other and the Mt. Read reconstruction. The most robust temperature reconstruction (the "Buckley" reconstruction shown in Figures 6.12 - 6.13) was obtained using the two highest chronologies (LJH and BCH), and explains 46.88% of the variance in mean warm season temperature. This is an increase of nearly 10% explained variance over the Mt. Read reconstruction, which explained 36.9% of the variance in November to April temperature data. Calibration and verification statistics are summarised in Table 6.4, based on the same procedures as outlined above for the Mt. Read reconstruction. The mean temperature over the entire period of reconstruction (AD 914-1991) is 15.4°C (Table 6.5), nearly half a degree warmer than the November to April season mean of 14.9° C.

Much of the increase in explained variance for the Buckley reconstruction owes to the year-to-year agreement of BCH with the temperature data over the calibration period, as demonstrated by the improvement in the correlations with temperature when the data are first-differenced; i.e., when the later calibration period is used, 45% of the

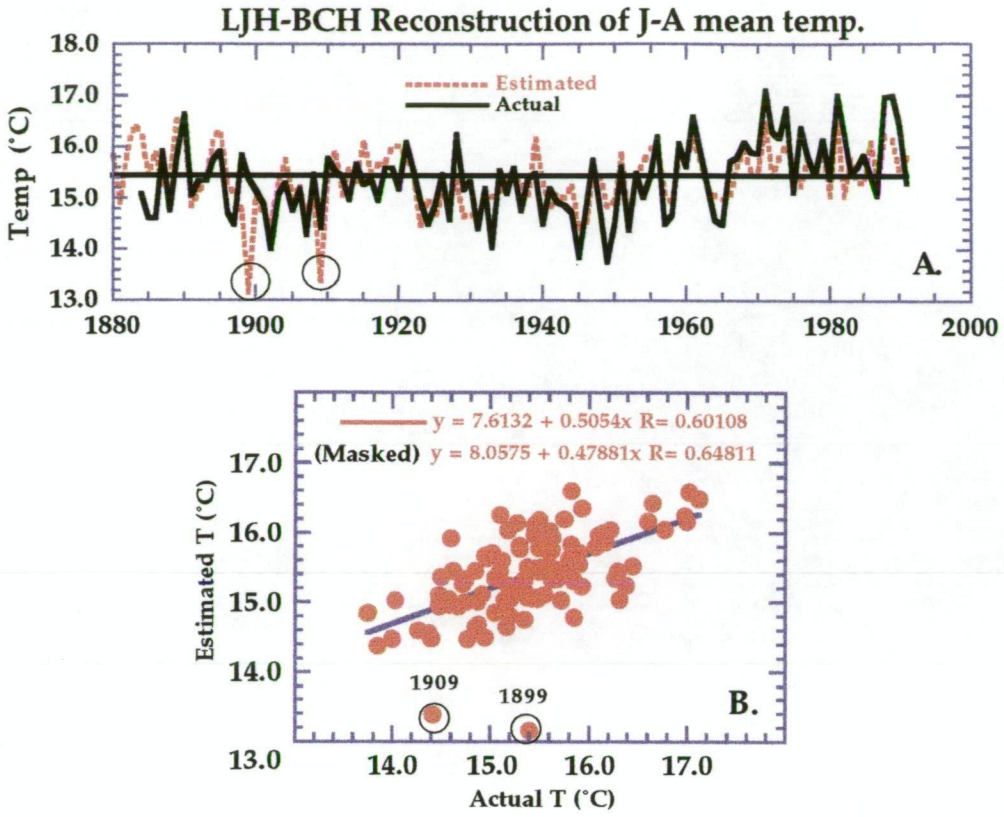

Figure 6.12. The Buckley temperature reconstruction versus actual temperature over the full 1885-1991 period. (**A.**) plots the actual temperature against the estimated temperature based on the regression model, while (**B.**) shows the linear relationship between the two. Note that masking the two circled outliers (1899 and 1909) improves the correlation from 0.601 to 0.648.

Calibration period: 1938 - 1991

R_P	R_S	R_R	ST	PM	R^2	AR^2	DW	%EXV
0.685	0.644	0.685	40+ 14-	0.258	0.469	0.459	2.08	46.88
(<0.001)	(<0.001)	(<0.001)	(<0.001)	(<0.001)	(<0.001)		ns	(<0.001)

Verification period: 1885 - 1937

R_P	R_S	R_R	ST	PM	RE	CE
0.463	0.534	0.522	38+ 15-	0.166	0.016	-0.118
(<0.001)	(<0.001)	(<0.001)	(0.001)	(0.002)		

Table 6.4. Calibration and verification statistics for the Buckley temperature reconstruction. All columns are the same as for Table 6.3 except for %EXV which is the percent of variance explained by the model (46.88% of the variance of January-April warm-season temperature). With the exception of the CE the verification period tests indicate a valid regression model and, as for the Cook reconstruction, a slightly negative value for CE does not warrant rejection of the model, particularly as the R_P, R_S, R_R, ST, and PM statistics all passed with significance well below the 0.05 confidence limit and RE was positive. The validity of the regression model is indicated by the agreement in results from both periods, in nearly all cases stronger than that for the Mt. Read temperature reconstruction. Full statistics are shown in Appendix 2.

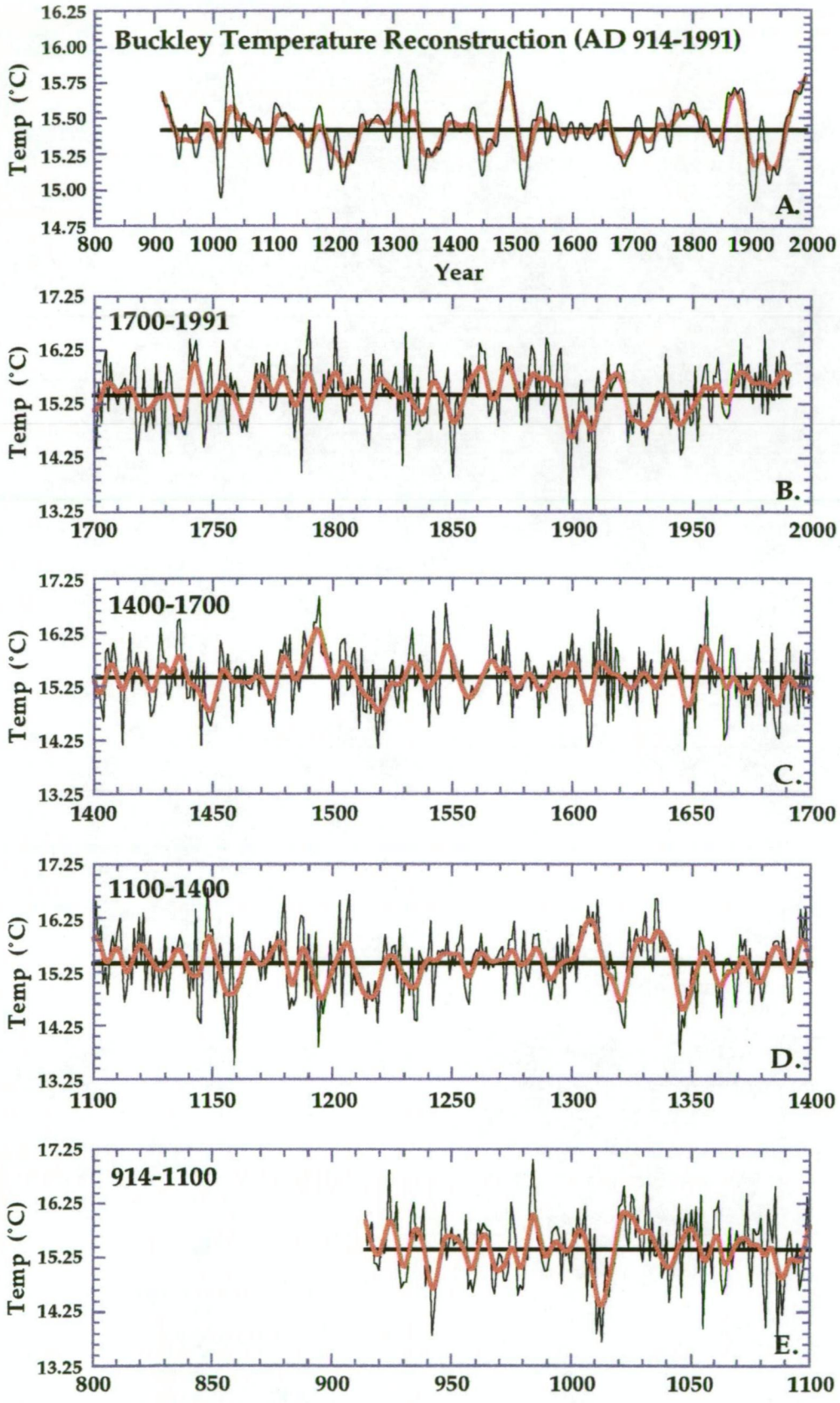

Figure 6.13. The Buckley temperature reconstruction. (**A.**) plots the entire period from AD 914 to 1991, showing the 50 year low-pass filtered series (heavy line) superimposed on the 25 year filtered series to emphasise variance with wavelengths greater than 50 and 25 years, respectively. (**B. - E.**) plot the entire reconstruction in 300 year segments with the 10 year low-pass filtered data (heavy line) superimposed on the yearly values.

	Reconstructed	Actual
Minimum	13.31	13.75
Maximum	17.07	17.12
N	1078	111
Mean	15.42	15.38
Median	15.44	15.38
Standard Deviation	0.566	0.704
Variance	0.321	0.495
Standard Error	0.017	0.067
Skewness	-0.223	0.209
Kurtosis	0.183	-0.102

Table 6.5. Statistics from the Buckley reconstructed and actual warm season temperature data. The Reconstructed column lists the statistics from the full reconstruction period (AD 914-1991), and the Actual column shows statistics from the climate data (AD 1885-1995).

variance is explained by the undifferenced data, increasing to 55% when the data are first differenced. There are similar improvements for R_P (0.673 - 0.770), R_R (0.703 - 0.810), and R_S (0.657 - 0.741). Since BCH does not exhibit the pronounced, systematic increase in growth since the mid-1960s apparent for LJH (see Chapter 5.1), there is a somewhat reduced warming trend indicated for the recent decades compared with the Mt. Read reconstruction. In fact, it can be seen in Figure 6.12A that the tree rings underestimate temperature for this period, which was also noted by Cook *et al.* (1996b) for the Mt. Read reconstruction. This important disparity will be discussed in Chapter 6.2.3.

In addition to underpredicting the trend in mean of the outer 30 years of the calibration period, the tree rings also slightly overpredict temperature in the coldest years of 1945 and 1949 (Figure 6.12). In two instances the tree rings grossly underpredict the actual temperature; in 1899 and 1909 (Figure 6.12). This was also the case for the Mt. Read reconstruction, and Cook *et al.* (1992) concluded that these two years were responsible for the slightly negative value of CE and a reduced R_P, in the verification period results. If these two years are considered as outliers and censored, the Pearson correlation between actual and estimated

temperature improves from 0.601 to 0.648 (Figure 6.12B). While the instrumental data used here do not indicate extreme cold events for these years, anecdotal evidence from newspaper accounts indicates very cold temperature and snowfalls throughout the summers for both years at a mining settlement on Mt. Read (T. Bird, pers. comm.). As already noted, the quality of the instrumental data in the early period is less reliable, and this might account for the discrepancy. However, it is equally likely that local conditions in the West Coast Ranges differed significantly from the lower elevation coastal stations, due to the strong zonal circulation in this period as discussed earlier (see Figure 6.5), and its corresponding influence on the vertical gradient of the climate over western Tasmania.

The most striking features of the Buckley reconstruction are visible in Figure 6.13A, which plots the reconstruction after smoothing with both a 25 and 50 year low-pass filter, in order to accentuate longer term fluctuations from the mean. Table 6.6 lists the twelve warmest and coldest 25-year periods of the entire reconstruction. The warmest periods include the striking anomaly in the 1490s, as well as the recent warming since the mid-1960s, already noted. A long warm period extends from the mid 13th century to the late 1330s, though this is less pronounced in the higher frequency (Figure 6.13D). Conditions were generally above the overall mean from the mid 1700s through to the late 1890s, interrupted by a short period of below average temperature in the 1840s. The most anomalous cold period is in the early half of the 20th century, with the lowest temperatures experienced from the late 1890s to 1910. This is interrupted by warmer temperatures from 1915-1922 before a reversion to cold temperatures in the 1940s. This is wholly consistent with the instrumental data for the region, as can be seen in Figure 6.12, with the recent 100 years apparently exhibiting one of the coldest and one of the warmest periods of the past 1000 years.

Warm Period Interval	Mean	Std Dev	Std Err	DEP1	DEP2
(3) 1476-1500	15.76	0.516	0.103	+0.27**	+0.34**
(5) 1855-1879	15.69	0.459	0.092	+0.20*	+0.27**
(1) 1965-1989	15.68	0.438	0.088	+0.19*	+0.26**
1020-1044	15.66	0.574	0.113	+0.17*	+0.24**
1873-1898	15.65	0.500	0.100	+0.16*	+0.23**
1320-1345	15.60	0.598	0.119	+0.11	+0.18**
1296-1320	15.58	0.570	0.114	+0.09	+0.16**
(7) 1115-1139	15.53	0.427	0.085	+0.04	+0.11**
(2) 975-999	15.51	0.585	0.117	+0.02	+0.09**
1405-1429	15.50	0.492	0.096	+0.01	+0.08**
(4) 1169-1193	15.49	0.598	0.120	0.00	+0.07**
(8) 1808-1832	15.49	0.539	0.108	0.00	+0.07**
Cold Period Interval	**Mean**	**Std. Dev**	**Std Err**	**DEP1**	**DEP2**
1925-1949	15.08	0.410	0.082	-0.41**	-0.34**
1345-1369	15.11	0.574	0.115	-0.38**	-0.31**
1210-1237	15.12	0.495	0.092	-0.37**	-0.30**
(1) 1890-1914	15.14	0.729	0.146	-0.35**	-0.28**
(2) 1194-1218	15.14	0.660	0.132	-0.35**	-0.28**
(8) 1664-1688	15.17	0.595	0.119	-0.32**	-0.25**
995-1020	15.22	0.692	0.138	-0.27**	-0.20**
1505-1530	15.22	0.530	0.106	-0.27**	-0.20**
(6) 1445-1469	15.23	0.488	0.098	-0.26*	-0.19**
1829-1854	15.25	0.626	0.123	-0.24*	-0.17**
(5) 1604-1628	15.34	0.637	0.127	-0.15*	-0.08**
(3) 1278-1302	15.39	0.421	0.084	-0.10	-0.03

Table 6.6. The twelve warmest and coldest 25-year periods of the Buckley reconstruction. Intervals are ranked in descending order of magnitude, and the numbers in parentheses rank the intervals in descending order for the Mt. Read reconstruction as noted by Cook *et al.* (1992). DEP1 are departures from the 1938-1991 calibration period mean of 15.49° C, and DEP2 are departures from the AD 914-1991 reconstructed mean of 15.42° C. * indicates departure is greater than 2 standard errors from the mean; ** greater than 4 standard errors from the mean.

6.2.3 Post 1960s warming trend

At this point it is important to discuss the disparity between the actual data and the temperature reconstructions discussed in this thesis for the post-1960s period. Figure 6.14 plots the actual warm season temperatures against the values estimated from reconstructions using the LJH and BCH chronologies, respectively. All three time series are smoothed with a 10-year weighted average to accent the decadal-scale

fluctuations. Both reconstructions underpredict the increasing trend-in-mean for the actual temperature since the mid 1960s, moreso for the BCH rather than the LJH reconstruction. However, much of this underprediction can be attributed to the loss of explained variance due to regression. Since BCH explains greater than 10% more of the variance in the warm season temperature than does LJH, the actual degree of disparity between the two reconstructions is probably even greater than that suggested by Figure 6.14.

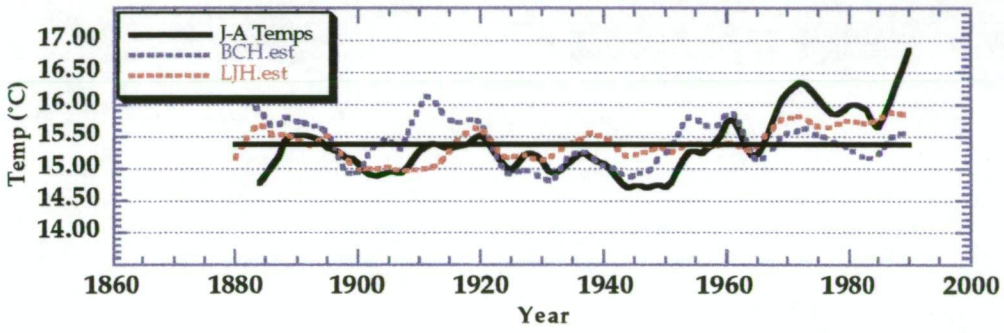

Figure 6.14. Comparison of decadal trends in warm season temperature for actual data with estimates from LJH and BCH reconstructions.

Aside from the loss of variance due to regression, another possible reason for both chronologies to underpredict temperature relates to the narrow "response window" of these slow growing, high-elevation trees, which may reduce their ability to respond to positive temperature anomalies beyond a certain point. For example, under optimum conditions growth might be expected to increase until other factors become limiting (Fritts, 1976). In this case, the general lack of available nutrients might strongly limit growth beyond optimum levels. The resolution of cold anomalies would also be limited by the fact that ring width is bounded by an absolute minimum value of zero. This would be particularly important at LJH where annual growth is often limited to fewer than 5 cells in a radial direction in poor growth years, leaving very little room to respond further.

The reasons for BCH not exhibiting the recent increasing trend that is evident in both the instrumental temperature record and in LJH, are even less clear. The most plausible explanation is related to the vertical climate zonation model of Kirkpatrick *et al.* (1997), discussed earlier in this chapter and shown in Figure 6.10. According to the model, the location of LJH at *ca.* 950 metres puts it just at the top of the zone of greatest change, near the mean height of the bottom of the subsidence-inversion layer. The trees sampled at the BCH site range from about 850 - 900 metres, with the bulk of trees coming from the lower half of this range. BCH is, therefore, located entirely within the zone of frequent orographically-generated cloud with its corresponding decline in temperature and increase in humidity. While the year-to-year changes in temperature would still be recorded, it is likely that the recent warming trend would not be as evident within the frequent cloud zone, and would consequently not be expressed well in the tree-rings from BCH. Since this climatic zone of rapid change between 820 and 930 metres is the result of orography, the instrumental data (which are from near-coastal stations at low elevation) would fall outside of this zone and would therefore reflect the warming temperatures. Kirkpatrick *et al.* (1997) noted that daily minimum air and soil temperature actually increased slightly with elevation above 930 metres on Mt. Sprent, while maximum daily air and soil temperatures declined most gently between 930 and 1050 metres. Therefore, such a systematic warming should be evident above 930 metres and could explain the increasing growth trend for trees at LJH.

It is not presently possible to test the above hypothesis. It is necessary to find at least one other Huon pine stand above the 930 metre threshold for comparison with LJH over the recent period, and as of this writing no such stands are known. It may be possible to use other species, in conjunction with carefully implemented meteorological monitoring, for comparison. For example, the 1,200 metre *Athrotaxis cuppressoides*

chronologies used by LaMarche and Pittock (1982), discussed earlier, exhibit a very similar systematic growth increase after 1960 to that for Mt. Read. However, these chronologies end in the 1970s and need to be updated to the present for a proper comparison. There are occurrences of *A. cuppressoides*, and the closely related *A. selaginoides*, on Mt. Read in close proximity to LJH, with the latter species ranging to tree-line at nearly 1,200 metres. Both species also occur in the Frenchmans Cap area near BCH, affording an appropriate comparison. Until such studies are completed, however, this question will remain largely unresolved.

6.3 Regional Extent of the Climate Signal

In order to determine the representativeness of the Buckley temperature reconstruction for the Tasmanian region, comparisons are made with other proxy records. First, four versions of the January-April temperature reconstruction are analysed back to AD 1000 (Figure 6.15), using various combinations of the four highest chronologies: A.) LJH only; B.) the Buckley reconstruction (LJH and BCH); C.) LJH, BCH and LML; and D.) LJH, BCH, LMH and LML. The reconstructions explain 34.76%, 46.88%, 39.76%, and 37.76%, respectively, of the variance for January-April mean temperature. As expected, all of the reconstructions are quite similar, however some notable differences emerge as the additional chronologies are introduced.

The primary influences of adding the three Frenchmans Cap chronologies to LJH are a reduction of the magnitude of the anomalous warming over the past three decades, a strengthening of the magnitude of the 1930s - 40s cold period, and a general increase in the low frequency variance as expressed in reconstructions B - D. As discussed in the previous section, only the LJH chronology exhibits the strong increase in ring width since 1965 that accounts for the majority of the warming trend (Figure 5.9). The 1490s warm period and the late 1600s cold period become

far more prominent, owing to their stronger expression in the Frenchmans Cap sites as shown in Figure 5.8. The prominence of the generally warm period from the mid 1700s to the late 1800s is also enhanced, as is the unusual period in the early 14th Century, where two very warm 25-year departures (centered on AD 1310 and 1340) are followed by two strong cold periods (centered on AD 1320 and 1345, respectively).

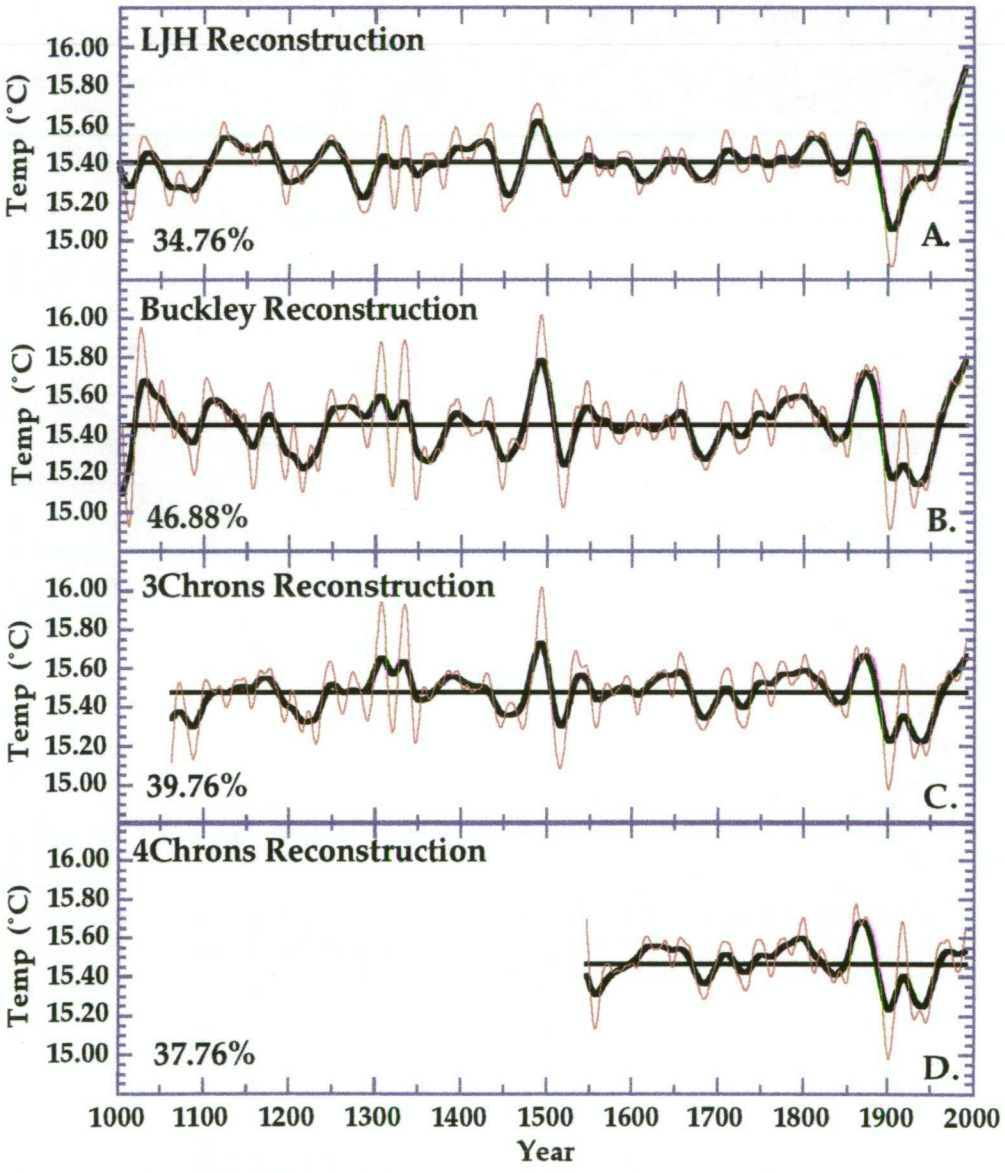

Figure 6.15. Comparison of 4 warm-season temperature reconstructions from Huon pine. The plots show Jan-Apr reconstructions derived from: (**A.**) only LJH; (**B.**) the Buckley Reconstruction from LJH and BCH; (**C.**) from LJH, BCH, and LML; (**D.**) all four chronologies from ≥ 700 metres, LJH, BCH, LML and LMH (limited to the early 1500s due to the short length of the LMH site).

Two previous temperature reconstructions from Tasmania are compared with the Buckley reconstruction; the Mt. Read reconstruction (Figure 6.11) and the LaMarche and Pittock (1982) reconstruction discussed in Chapter 2.2.2. Because the LJH chronology is used for both the Mt. Read and Buckley reconstructions, there are obvious similarities between them. However, there are some important differences, due in part to the different climatic season used, the influence of the BCH chronology on the regression model, and the increase in sample depth for the LJH chronology resulting in large part from this research project.

Perhaps the most important difference is in the reduction of the relative importance of the recent warming period in the context of the past millennium. Cook *et al.* (1992) show the 25-year period of 1965-1989 to be the warmest of the past thousand years, about 0.1° C warmer than the next warmest period of AD 975-999. For the Buckley reconstruction this period is far less pronounced due to a dampening of the growth increase over that period at the BCH site when compared with LJH. The warmest 25-year period for the Buckley reconstruction is 1476-1500, which is the second-warmest period over the same time scale in the Mt. Read reconstruction (Table 6.6), and is noted as an anomalously rapid growth period in all of the Frenchmans Cap chronologies (Figure 5.8). The most prolonged warm period in the Buckley reconstruction is in the latter half of the 1800s (Figure 6.13). This period is also evident in the Cook reconstruction, though far less prominent.

In order to more appropriately compare the Buckley and Mt. Read reconstructions, the January - April season was reconstructed using only LJH (Figure 6.16). With the added sample depth in the earliest portion of the LJH chronology (Chapter 3.6.1) some important changes occur over the earlier reconstruction. The 300s BC cold anomaly shown in Figure 6.11, along with the highly anomalous warm episode preceding it in the 400s BC, have both been substantially reduced, though still in evidence

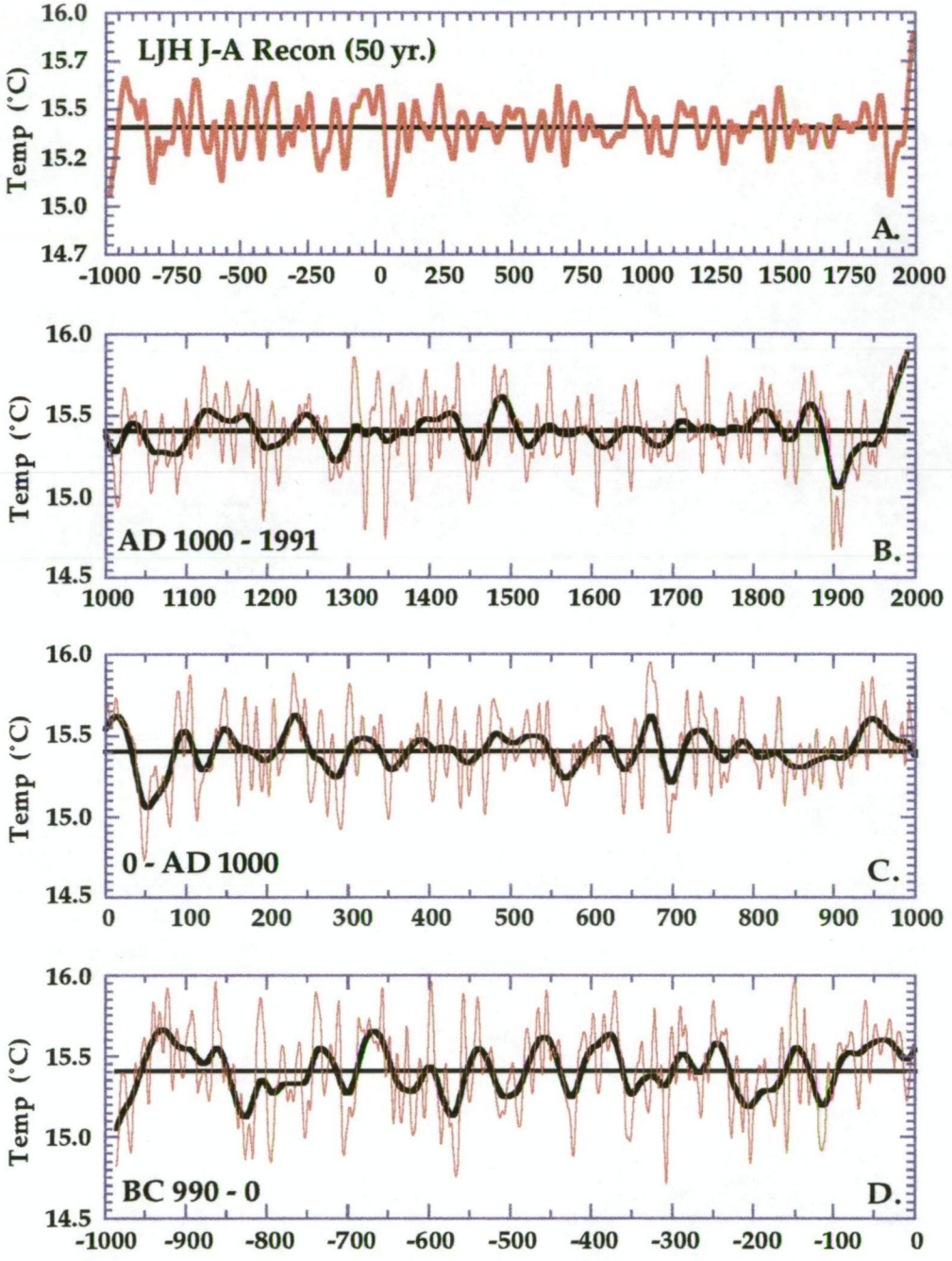

Figure 6.16. LJH Reconstruction of January-April temperature from 990 BC - AD 1991. (**A.**) the reconstruction back to BC 1000, smoothed with a 50 year low-pass filter; (**B.**) AD 1000-1991; (**C.**) 0-AD 1000; and (**D.**) 990 BC-0, all plotted as the 50 year smoothed data (heavy line) superimposed on the 25 year smoothed data.

(Figure 6.16D). This can be attributed to increased sample depth as discussed in Chapter 5.1, resulting in a more robust estimate of growth through this period. A prominent cool phase is suggested for the period centered on AD 50, preceded by a very warm period from 90 BC to AD 20,

both of which are features of the earlier Mt. Read reconstruction. In general, the reconstruction is nearly identical to the Mt. Read reconstruction from the BC/AD transition outward, where the sample depth was already quite substantial. Major differences with the Buckley reconstruction over the past millennium have already been noted.

LaMarche and Pittock (1982) reconstructed Tasmanian warm season (October - May) temperature from AD 1776 - 1973, based on a canonical regression with 11 tree-ring chronologies from four different species; each with varying climate response functions, and from sites at a range of elevations. Their reconstruction (Figure 6.17) shows some notable differences with both the Mt. Read and Buckley reconstructions that can be directly attributed to the variable growth characteristics of the chronologies used, related to species, elevational and habitat differences. The most striking example is the transition from the nineteenth to twentieth century, where the most anomalously warm temperatures of their reconstruction are suggested from about 1880 to 1920, in direct contrast to both Huon pine reconstructions, as well as the actual temperature data for Tasmania (see Figure 5.10).

The positive anomaly for the 1880 - 1920 period appears to be mostly attributed to the influence of the 7 *Phyllocladus aspleniifolius* chronologies on the regression model. Two high-elevation chronologies of *Athrotaxis cupressoides* , both from elevations greater than 1,200 metres, nearly duplicate the growth indices for the highest Huon pine chronologies. The response functions derived for these two species revealed opposite responses to temperature; i.e., the high-elevation *A. cupressoides* exhibited a significant, positive response for both the current and prior growing season, similar to that seen for Huon pine, while the *P. aspleniifolius* chronologies exhibited a significant, inverse response for both the current and prior season (LaMarche and Pittock, 1982). The growth signature of the *A. cupressoides* is essentially

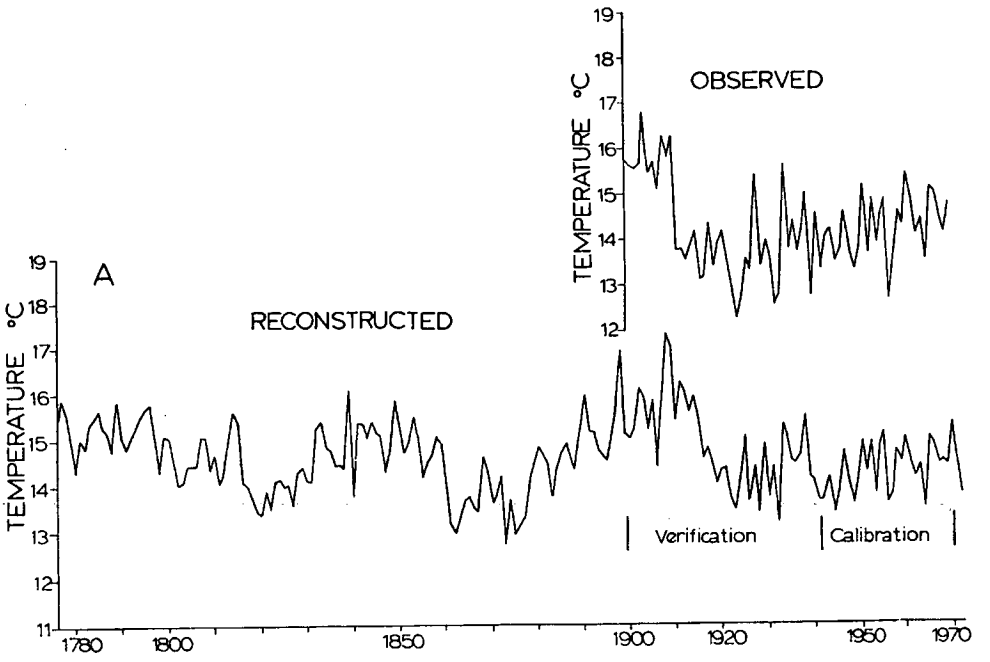

Figure 6.17. LaMarche and Pittock reconstruction of Tasmanian warm season temperature. The reconstruction is based on a canonical regression using eleven tree-ring chronologies from four species from three genera. The "observed" temperature data is the series from Waratah which was not corrected for a serious anomaly in the early part of the record. (From LaMarche and Pittock, 1982).

eliminated by the opposite sign of the *Phyllocladus* chronologies in the regression analyses, resulting in the suggestion of warming through this period of anomalously cold temperature. A similar discrepancy is also noted for the recent warm period where their reconstruction failed to track the post-1950s temperature increase, although the *Athrotaxis* chronologies again seem to reflect this with a marked increase in growth.

Another possible source of error comes from the 15-station, gridded temperature data set used for the regression, which contained at least one station record (Waratah) that was not corrected for a serious problem in the early portion of the record, raising the possibility that other, similar problems remained uncorrected as well. As demonstrated in this study, however, the climatic signal even within a single species can change dramatically with site changes related to elevation alone, and great care must be taken in attempting to "blend" such variable signals.

The broad-scale climatic features which influence Tasmania's climate are also evident in New Zealand over the period of common record since about the middle of the nineteenth century. For example, the two most striking anomalies of the past *ca.* 100 years in the Tasmanian records (i.e., the cool period around the turn of the century and the warming since about 1950) both have expression in the New Zealand regional records (Salinger, 1979; 1980a; 1980b; 1982b; Salinger and Gunn, 1975; Trenberth, 1976). Figure 6.18 plots a composite temperature series for New Zealand from the 1850s to the 1990s showing a steady increase in mean temperature since the turn of the last century. The recent warming has been attributed to the weakening of mean zonal circulation from the west and south, with more frequent airflow from east to north bringing warmer temperature. The anomalous cold period, from 1897 - 1906 in New Zealand, has also been linked to general circulation during a time of increased strength in zonal circulation and a corresponding increase in the influence of cold, westerly airflow (Salinger, 1980a; 1980b). These same features, evident in Tasmania, have already been discussed and define broad-scale, regional agreement on both sides of the Tasman Sea.

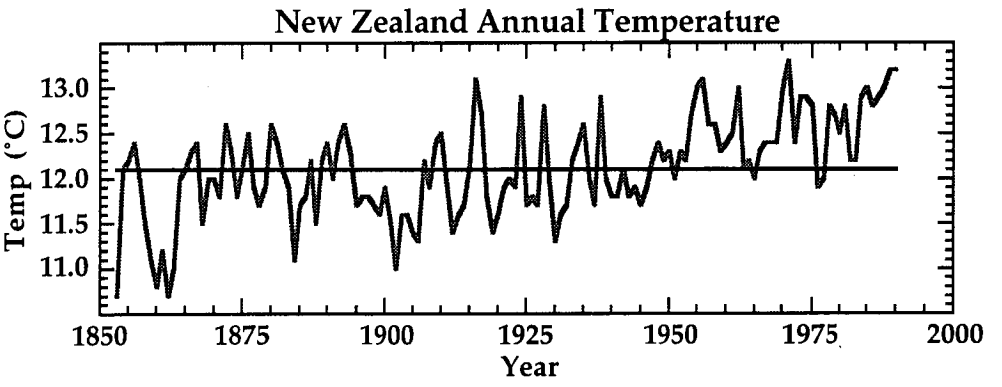

Figure 6.18. New Zealand annual temperature since 1850. The time series is a composite of several records from New Zealand's North and South Islands (time series constructed by Salinger and supplied courtesy of A. Ruddell, University of Tasmania).

New Zealand's topography plays a more important role in controlling local climates than is the case for Tasmania. In particular the presence of higher, glaciated mountains and the greater latitudinal and meridional expanse of land mass of the three major islands serve to intercept moisture-bearing air masses. The result is often a reversal in sign of precipitation and temperature anomalies from one side of the islands to the other (Salinger, 1980a; 1980b). Nevertheless, the general climate features on both sides of the Tasman Sea appear to be broadly correlated with regard to temperature.

Dendroclimatic reconstructions of warm season temperature have been developed from New Zealand using different approaches. Norton *et al.* (1989) used ten subalpine chronologies from two species of the same genus (*Nothofagus*) from the South Island to reconstruct warm season (December-March) temperature. Salinger *et al.* (1994) incorporated five species from three genera, from widely-spaced sites on the North and South Islands, in their warm season (November-March) reconstructions of temperature, and zonal and meridional flow anomalies. Dendroclimatic investigations of pink pine (*Halocarpus biformis* [Hook.] C.J. Quinn) by D'Arrigo *et al.* (1995) on Stewart Island also suggest very similar climatic features over the Tasmanian/New Zealand region since the mid 1600s. Both reconstructions, and the pink pine research from Stewart Island, are in general agreement with the Tasmanian reconstructions presented here, reflecting a basic stability of the regional climate over at least the last four centuries. It seems clear that a reasonable degree of confidence can be placed in the palaeoclimatic history which is emerging from the Tasmanian/New Zealand sector of the Southern Ocean. Further dendroclimatic studies from both Tasmania and New Zealand can begin to test for broad-scale climate changes related to changes in Southern Ocean circulation, over the past millennium and beyond.

CHAPTER 7: CONCLUSIONS AND FUTURE RESEARCH

7.1 Conclusions

The climate response modelling presented in this thesis demonstrates an elevation dependence for Huon pine's response to temperature. This is supported by the results of a rotated PCA which clearly separates high and low elevation chronologies, and suggests that a critical threshold is reached at around 700 metres. There is an increasingly robust response to growing season temperature with elevation above this zone, and an increasing importance of prior year temperature with decreasing elevation below 700 metres. This elevation dependence appears to be controlled by a distinct stratification of Tasmania's west coast climate. This vertical zonation is related to orography and the passage of high pressure systems across this latitude band from a predominantly westerly/southwesterly airstream, with strong connections to Southern Ocean circulation and Antarctic climate.

This study confirms the usefulness of Huon pine as a species for the reconstruction of temperature. The empirical approach used in this thesis for dendroclimatic reconstruction accounts for almost half of the overall variance in annual warm season temperature, and offers a simplified view of the complex physiological interactions between tree growth and environment. As a result, there is some degree of uncertainty that is difficult to gauge, and which can best be resolved through careful mechanistic studies of overall growth and the response to climatic conditions. The complexities can be minimised, in the case of Huon pine, by sampling from subalpine locations where tree growth/climate relationships are simplified. Above 700 metres, low temperatures become increasingly limiting to growth processes in a general sense, and correspond to a more or less causal input-output relationship with a reduced prior-year influence. Single species

regression models assure that species-specific response functions are not competing with each other and possibly negating real climate signals.

A substantial discrepancy in the post-1960 warming trend is revealed for two temperature reconstructions based on the two highest chronologies. The 950 metre LJH chronology indicates a systematic growth increase that is not evident in the 900 metre BCH chronology, yet is clearly evident in the instrumental data. Due to strong year-to-year agreement with the instrumental data, however, the inclusion of BCH improves the explained variance in warm season temperature by 10% over the period of calibration for the Buckley reconstruction. The reasons for the disparity in decadal-scale trend over the past few decades are not clear. The most likely cause seems to be related to a frequent cloud zone that extends from about 830 to 920 metres. The LJH chronology is located above this zone where it appears that a systematic warming, clearly evident in the instrumental record since the mid-1960s, has had a corresponding influence on tree growth. The BCH chronology sits entirely within the frequent cloud zone, and consequently seems to have not been influenced by systematically rising temperatures.

A new warm season temperature reconstruction improves our understanding of the regional climate over the past millennium, surpassing a previous reconstruction by an increase of nearly 10% explained variance. However, the relative importance of the recent warming has been substantially reduced and is the third warmest period of the past thousand years, rather than the first as previously reported. This is largely due to the disparity in growth trend between the BCH and LJH chronologies, as discussed above. Nevertheless, caution must be exercised in interpreting the recent warming as evidence for an hypothesised Greenhouse Effect, since several other pre-industrial periods appear to be as warm or warmer, placing the recent period well within the natural variability of the climate system. However, further

analyses of the temporal dynamics of climatic stratification in western Tasmania must be undertaken to more accurately interpret the disparity in decadal-scale trend between the LJH and BCH chronologies over the past few decades.

The Buckley reconstruction largely reinforces the findings of the previous warm season reconstruction over the past millennium, changing only the magnitudes of some of the warmest and coldest periods. The increased sample depth in the earliest portion of LJH allows for a more robust estimate of temperature for the period from 1000 BC - AD 100. Two previously reported anomalous periods of warm and cold temperature (in the 400s BC and 300s BC, respectively) have been substantially reduced in severity, though both are still apparent. A very cold period around AD 50 - 100 more clearly emerges as one of the coldest periods of the past 3,000 years. This follows an extended period of warm temperatures from about 100 BC until about AD 40. The Buckley reconstruction's warmest 25-year period of the past millennium, from AD 1476 - 1500, corresponds to a period of apparently extensive burning in the Frenchmans Cap region. The coldest 25-year period, from AD 1925 - 1949, was more than 4 standard errors below the long-term mean and comes only one decade after the 4th coldest period of 1890 - 1914.

Expressions of a Medieval Warm Period or Little Ice Age signal in the Tasmanian temperature reconstructions are ambiguous at present. There is a general reduction in the amplitude of departures from the mean from the early 16th through the late 19th centuries. This could be indicative of more vigorous zonal circulation throughout this period that roughly coincides with the Northern Hemisphere's Little Ice Age as defined by Lamb (1977). Cold periods centered around the AD 1340s and AD 1510s are consistent with classic Little Ice Age episodes that are also exhibited in the South American dendroclimatic and glacial records presented by Villalba (1994). However, it is difficult to make a strong

claim for a Little Ice Age in Tasmania based on the evidence presented here. There is even less clear evidence for a Medieval Warm Period in the Tasmanian reconstructed temperature records.

While the higher elevation Huon pine chronologies exhibit a more robust response to temperature, the very long time periods afforded by lower elevation sites may yield important palaeo-environmental information from key climatic periods, such as the Younger Dryas (*ca.* 10,000 - 12,000 YBP), or the Hypsithermal (*ca.* 7,000 - 9,000 YBP). These low elevation sites also play a crucial role for the inter-hemispheric comparison of ^{14}C production (Barbetti *et al.*, 1995). The remarkable preservation qualities of Huon pine offer the chance to develop chronologies spanning all of the past 10,000 years, and possibly beyond the *ca.* 40,000 year range of ^{14}C dating, from low-elevation sites in western Tasmania (Barbetti, pers. comm.). Preservation in the harsher, subalpine environment on Mt. Read appears to be less effective, possibly due to mechanical erosion through ice-abrasion, combined with less rapid rates of deposition and burial of downed logs. The oldest material so far recovered from Mt. Read dates back nearly 5,000 years, in spite of pollen evidence that the Lake Johnston Huon pine stand has existed for at least the past 10,000 years (Anker *et al.*, 1996.). It is not clear if logs older than 5,000 years will be recoverable from Mt. Read and other subalpine locations, or if the conditions of exposure at these sites inhibit preservation for longer periods of time.

7.2 Future Research

It is clear that the physiological processes related to tree growth and their response to climatic controls are not well understood. Empirical studies are useful as an overall guide, and can offer valuable information about past climate. However, mechanistic studies are critical due to the natural variability of the climate system, which might cause marked

changes in the overall climate regime. Such changes could result in an altered response to climate that may be misinterpreted when simplified linear transfer functions are employed. For example, periods of accelerated growth might result from the optimisation of one of several environmental conditions, each with different seasonal expression. While it presently seems that moisture plays little role in controlling annual growth in Huon pine, it is not inconceivable that periods of extended drought stress (that could have resulted in suppressed growth) would be interpreted as prolonged cold periods based on the analyses presented in this thesis. Other proxy records might help resolve such discrepancies but should be augmented by carefully designed experiments to more accurately identify the underlying processes related to whole plant growth and climate.

Other dendrochronological techniques should be incorporated into future research efforts, using the vast archive of Huon pine samples already collected and dated. For example, the high-elevation chronologies exhibit clear variations in latewood density and anatomical features (e.g., light rings and frost rings) which are likely related to growing season temperature characteristics. The development of a light-ring chronology would be of great value in conjunction with the temperature reconstructions presented here. Measurements of latewood density might increase the explained variance for growing season temperature when combined with ring-width measurements (e.g., Briffa *et al.*, 1990; 1992). The methods of cambial growth modelling developed by Fritts and Shaskin (1994) and Shaskin and Fritts (1994) could be employed over successive seasons at important sites. Combined with the other approaches just mentioned, this could supply the baseline data for a more accurate, mechanistically-derived transfer function for the reconstruction of past climate in Tasmania.

Analyses of the deuterium to hydrogen (D/H) ratios of the non-exchangeable hydrogen of Huon pine cellulose might afford even greater detail of past climatic conditions in Tasmania. The D/H ratios of tree cellulose, expressed in δD values, are known to respond to basic climatic parameters such as changes in temperature and the amount of precipitation (Dansgaard, 1964). White *et al.* (1994) determined that the D/H ratios in tree rings from North American white pine (*Pinus strobos*) were responding primarily to changes in the D/H ratios of the source water. Feng and Epstein (1995) found good correlations between δD and temperature for several North American trees, particularly with regard to low-frequency variations. They also determined that trees from locations with simple climate regimes and flat topography are potentially the best temperature recorders. Since the source-region climatology controlling the water that goes into the D/H ratio appears to be relatively simple in western Tasmania, interpretations may be less complicated than in more continental regions. The vast Huon pine resource at sites like SRT offer the unique opportunity for a statistically robust calibration with the instrumental data, which can then be transferred to periods throughout the past 10,000 years of the Holocene.

Future efforts should focus on finding additional subalpine sites, and on the search for subfossil wood at these sites. The spatial and temporal characteristics of climatic stratification in Tasmania's West Coast Range should also be explored. The use of elevational transects, like the one presented in this thesis, might enable a reconstruction of climate on a more detailed level not normally afforded by dendroclimatic analyses. Transient changes in circulation, and associated changes in SST and air temperature, might lead to changes in the mean height of the orographically-generated cloud zone in western Tasmania and in New Zealand. A more complete chronology network, both latitudinally and altitudinally, might allow for the analysis of such changes through time.

REFERENCES

Ahmed, M., & Ogden, J. (1985). Modern New Zealand tree-ring chronologies 3. *Agathis Australis* (Salib.) - kauri. *Tree-Ring Bulletin*, **45**, 11-24.

Akaike, H. (1974). A new look at the statistical model identification. IEEE Transactions on Automatic Control, AC-19, 716-723.

Anker, S. A., Colhoun, E. A., Barton, C. E., Peterson, M. J., & Barbetti, M. (1996). Holocene vegetation, palaeoclimatic and palaeomagnetic history from Lake Johnston, Tasmania. (unpublished manuscript), 15 pp.

Ash, J. (1983a). Growth rings in *Agathis robusta* and *Auracaria cunninghamii* from Tropical Australia. *Australian Journal of Botany*, **31**, 269-275.

Ash, J. (1983b). Tree-rings in tropical *Callitris macleayana* F. Muell. *Australian Journal of Botany*, **33**, 81-88.

Bacon, C. A. (1992). Management of the flora of the Mt. Read RAP (Report No. 30). Tasmania Department of Mines.

Barbetti, M., Bird, T., Dolezal, G., Taylor, G., Francey, R. J., Cook, E. R., & Peterson, M. J. (1992). Radiocarbon variations from Tasmanian conifers: first results from late Pleistocene and Holocene logs. *Radiocarbon*, **34**(3), 806-817.

Barbetti, M., Bird, T., Dolezal, G., Taylor, G., Francey, R., Cook, E., & Peterson, M. (1995). Radiocarbon variations from Tasmanian conifers: results from three early Holocene logs. In G. T. Cook, D. D. Harkness, B. F. Miller, & E. M. Scott (Eds.), proceedings of the 15th International ^{14}C Conference, Tucson, Arizona: *Radiocarbon*, **37**(2), 361-369.

Barry, R. G. (1978). Climatic fluctuations during periods of historical and instrumental record. In A.B. Pittock, L.A. Frakes, D. Jenssen, J.A. Peterson, & J.W. Zillman (Eds.), Climatic change and variability: a Southern Hemisphere perspective (pp. 150-166). London: Cambridge University Press.

Bell, R. E. (1958). Dendrochronology. *New Zealand Science Review*, **16**, 13-17.

Berry, R. F., Elliott, C. G., & Grey, D. R. (1990). Structure and tectonics of western and northern Tasmania (Excursion Guide No. E3). 10th Australian Geological Convention.

Bindoff, N. L., & Church, J. A. (1992). Warming of the water column in the southwest Pacific Ocean. *Nature*, **357**, 59-62.

Björkman, O., & Demmig-Adams, B. (1994). Regulation of photosynthetic light energy capture, conversion, and dissipation in leaves of higher plants. In E. D. Schulze & M. M. Caldwell (Eds.), Ecophysiology of Photosynthesis (pp. 17-48). Berlin Heidelberg: Springer-Verlag.

Blasing, T. J., Solomon, A. M., & Duvick, D. N. (1984). Response functions revisited. *Tree-Ring Bulletin*, **44**, 1-15.

Boninsegna, J. A. (1992). South American dendroclimatological records. In R. S. Bradley & P. D. Jones (Eds.), Climate since A.D. 1500 (pp. 446-442). London: Routledge.

Boninsegna, J., & Villalba, R. (1996). Dendroclimatology in the Southern Hemisphere: review and prospects. In J.S. Dean, D.M. Meko, & T.W. Swetnam, Eds., Tree Rings, Environment, and Humanity. *Radiocarbon*, Department of Geosciences, The University of Arizona, Tucson (pp. 127-141).

Bottomley, M., Folland, C. K., Hsiung, J., Newell, R. E., & Parker, D. E. (1990). Global Ocean Surface Temperature Atlas (GOSTA). London: HMSO.

Box, G. E. P., & Jenkins, G. M. (1970). Time Series Analysis: Forecasting and Control. San Francisco: Holden-Day.

Bradley, R. S., & Jones, P. D. (1992). (Eds.) Climate since A.D. 1500. London: Routledge.

Bridge, M. C., & Ogden, J. (1986). A sub-fossil kauri (*Agathis australis*) tree-ring chronology. *Journal of the Royal Society of New Zealand*, **16**, 17-23.

Briffa, K. R. (1984). Tree-climate relationships and dendroclimatological reconstruction in the British Isles. PhD thesis, University of East Anglia, Norwich, England.

Briffa, K. R., & Cook, E. R. (1990). Methods of response function analysis. In E. R. Cook & L. A. Kairiukstis (Eds.), Methods of Dendrochronology: applications in the environmental sciences (pp. 240-247). Dordrecht: Kluwer Academic Publishers.

Briffa, K. R., Jones, P. D., Pilcher, J. R., & Hughes, M. K. (1988). Reconstructing summer temperatures in northern Fennoscandinavia back to A.D. 1700 using tree-ring data from Scots pine. *Arctic and Alpine Research*, **20**, 385-394.

Briffa, K. R., Bartholin, T. S., Eckstein, D., Jones, P.D., Karlen,W., Schweingruber, F.H. & Zetterberg, P. (1990). A 1,400-year tree-ring record of summer temperatures in Fennoscandia. *Nature* **346**: 434-439.

Briffa, K. R., P. D. Jones, Bartholin, T.S., Eckstein, D., Schweingruber, F.H., Karlen, W., Zetterberg, P. & Eronen, M. (1992). Fennoscandian summers from A.D. 500: temperature changes on short and long timescales. *Climate Dynamics* **7**: 111-119.

Buckley, B. M., D'Arrigo, R. D., & Jacoby, G. C. (1992). Tree-ring records as indicators of air-sea interaction in the northeast Pacific sector. In K. T. Redmond (Ed.), Proceedings of the Eighth Annual Pacific Climate (PACLIM) Workshop, (pp. 35-45). Asilomar, California: California Department of Water Resources, Interagency Ecological Studies Program Technical Report 31.

Buckley, B. M., Peterson, M. J., & Cook, E. R. (1993). Changes in the climatic response of Huon pine with elevation in western Tasmania, Australia. In R. S. Hill (Ed.), Abstracts, Southern Temperate Ecosystems: Origin and Diversification., (pp. 28). Hobart, Tasmania: The Australian Systematic Botany Society, and the Ecological Society of Australia.

Buckley, B. M., Barbetti, M., Watanasak, M., D'Arrigo, R. D., Boonchirdchoo, S., & Sarutanon, S. (1995). Dendrochronological investigations in Thailand. *IAWA Journal*, **16**(4), 393-409.

Buckley, B. M., Cook, E. R., Peterson, M. J., & Barbetti, M. (1997). A changing temperature response with elevation for *Lagarostrobos franklinii* in Tasmania, Australia. *Climatic Change*, (in press).

Bureau of Meteorology (1983). Climate of Tasmania. Canberra: Australian Government Publishing Service.

Bureau of Meteorology (1993). Climate of Tasmania. Canberra: Australian Government Publishing Service, 30 pp.

Campbell, D. A. (1982). Preliminary estimates of summer streamflow for Tasmania. In M. K. Hughes, P. M. Kelly, J. R. Pilcher, & V. C. LaMarche Jr. (Eds.), Climate From Tree Rings (pp. 170-177). Cambridge, UK: Cambridge University Press.

Chouard, P. (1960). Vernalization and its relations to dormancy. *Annual Review of Plant Physiology*, **11**, 191-238.

Colhoun, E.A. (1985). Glaciations of the West Coast Range, Tasmania. *Quaternary Research*, **24**, 39-59.

Colhoun, E. A., & Fitzsimons, S. J. (1990). Late Cainozoic glaciation in western Tasmania, Australia. *Quaternary Science Reviews*, **9**, 199-216.

Colhoun, E. A., & Van de Geer, G. (1986). Vegetation history and past climate before the maximum of the last glaciation at Crotty, western Tasmania. *Papers and Proceedings of the Royal Society of Tasmania*, **121**, 69-74.

Colhoun, E. A., Gibson, N., & Van de Geer, G. (1988). Tasmania: environmental synopsis, in Cainozoic vegetation of Tasmania. In E. A. Colhoun (Ed.), 7 International Palynological Congress, (pp. 1-13). Brisbane, Qld., Australia: the University of Newcastle, Dept. of Geography.

Cook, E. R. (1985). A time series analysis approach to tree-ring standardization. PhD thesis, University of Arizona.

Cook, E. R. (1987). The decompostion of tree-ring series for environmental studies. *Tree-Ring Bulletin*, **47**, 37-59.

Cook, E. R. (1990). A conceptual linear aggregate model for tree rings. In E. R. Cook & L. A. Kairiukstis (Ed.), Methods of Dendrochronology: applications in the environmental sciences (pp. 98-104). Dordrecht: Kluwer Academic Publishers.

Cook, E. R. (1995). Temperature histories from tree rings and corals. The 1995 IPCC Assessment.

Cook, E. R., & Kairiukstis, L. A. (Eds.). (1990). Methods of Dendrochronology: applications in the environmental sciences (1 ed.). Dordrecht: Kluwer Academic Publishers, 394 pp.

Cook, E. R., Briffa, K., Shiyatov, S., & Mazepa, V. (1990a). Tree-Ring Standardization and Growth-Trend Estimation. In E. R. Cook & L. A. Kairiukstis (Eds.), Methods of Dendrochronology: Applications in the Environmental Sciences (pp. 104-123). Dordrecht: Kluwer Academic Publishers.

Cook, E. R., Shiyatov, S., & Mazepa, V. (1990b). Estimation of the mean chronology. In E. R. Cook & L. A. Kairiukstis (Eds.), Methods of Dendrochronology; applications in the environmental sciences (pp. 123-133). Dordrecht: Kluwer Academic Publishers.

Cook, E. R., Bird, T., Peterson, M., Barbetti, M., Buckley, B., D'Arrigo, R., Francey, R., & Tans, P. (1991). Climatic change in Tasmania inferred from a 1089-year tree-ring chronology of Huon pine. *Science*, **253**, 1266-1268.

Cook, E. R., Bird, T., Peterson, M., Barbetti, M., Buckley, B., D'Arrigo, R., & Francey, R. (1992). Climatic change over the last millennium in Tasmania reconstructed from tree rings. *The Holocene*, **2**, 205-217.

Cook, E. R., Briffa, K. R., & Jones, P. D. (1994). Spatial regression methods in dendroclimatology: a review and comparison of two techniques. *International Journal of Climatology*, **14**, 379-402.

Cook, E. R., Buckley, B. M., & D'Arrigo, R. D. (1995a). Decadal-scale oscillatory modes in a millennia-long temperature reconstruction from Tasmania. In D.G. Martinson, K. Bryan M. Ghil, M.M. Hall, T.R. Karl, E.S. Sarachik, S. Sorooshian & L.D. Talley, Natural Climate Variability on Decade-to-Century Time Scales (pp. 523-532). Washington, D.C: National Academy Press.

Cook, E. R., Briffa, K. R., Meko, D. M., Graybill, D. A., & Funkhouser, G. (1995b). The 'segment length curse' in long tree-ring chronology development for palaeoclimatic studies. *The Holocene*, **5**(2), 229-237.

Cook, E. R., Buckley, B. M., & D'Arrigo, R. D. (1996a). Inter-decadal climate oscillations in the Tasmanian sector of the Southern Hemisphere: Evidence from tree rings over the past three millennia. In P. D. Jones & R. S. Bradley (Eds.), Climatic Variations and Forcing Mechanisms of the Last 2000 Years (pp. 141-160). Berlin Heidelberg: Springer-Verlag.

Cook, E. R., Francey, R. J., Buckley, B. M., & D'Arrigo, R. D. (1996b). Recent increases in Tasmanian Huon pine ring widths from a subalpine site: natural climate variability, CO_2 fertilisation, or greenhouse warming? *Papers and Proceedings of the Royal Society of Tasmania*, **130**(2) 65-72.

Corbett, S. (1992). Fires in the Frenchmans Cap Area. Map, Hobart: Department of Parks, Wildlife & Heritage.

Coughlan, M. J. (1979). Recent variations in annual-mean maximum temperatures over Australia. *Quarterly Journal of the Royal Meteorological Society*, **105**, 707-719.

Coughlan, M. J. (1983). A comparative climatology of blocking action in the two hemispheres. *Australian Meteorological Magazine*, **31**, 3-13.

Cunningham, T.M. & Cremer, K.W. (1965). Control of understory in wet eucalypt forests. *Australian Forestry*, **29**, 4-14.

D'Arrigo, R. D., Buckley, B. M., Cook, E. R., & Wagner, W. S. (1995). Temperature-sensitive tree-ring width chronologies of pink pine (*Halocarpus biformis*) from Stewart Island, New Zealand. *Palaeogeography, Palaeoclimatology, Palaeoecology*, **119**, 293-300.

Dansgaard, W. (1964). Stable isotopes in precipitation. *Tellus*, **16**, 436-468.

Davies, J. L. (1964). A vegetation map of Tasmania. Geographical Review, **54**, 249-253.

Davies, J. L. (1965). High level erosion surfaces and landscape development in Tasmania. In J. L. Davies (Ed.), Atlas of Tasmania (pp. 19-25). Hobart.

Davies, J. L. (1967). Tasmanian landforms and Quaternary climates. In J. N. Jennings & J. A. Mabbut (Eds.), Landform Studies from Australia and New Guinea (pp. 1-25). Canberra: Australian National University Press.

Davies, J. L. (1974). Geomorphology and Quaternary environments. In W. D. Williams (Ed.), Biogeography and Ecology in Tasmania (pp. 17-27). Hague: W. Junk.

Davies, J. (1983). Huon pine survey 1983. Technical Report 83/2, Hobart: National Parks and Wildlife Service.

Davis, R. E. (1976). Predictability of sea surface temperature and sea level pressure anomalies over the North Pacific Ocean. *Journal of Physical Oceanography*, **6**(3), 249-266.

Dietz, R., & Holden, J. C. (1970). The breakup of Pangaea. *Scientific American*, **223**, 30-41.

Digby, J., & Wareing, P. F. (1966). The relationship between endogenous hormone levels in the plant and seasonal aspects of cambial activity. *Annals of Botany*, **30**, 608-622.

Douglas, A. V. (1973). Past air-sea interactions off southern California as revealed by coastal tree-ring chronologies. M.S. thesis, University of Arizona.

Douglass, A. E. (1914). A method of estimating rainfall by the growth of trees. In E. Huntington (Ed.), The Climatic Factor (pp. 101-122). Washington: Carnegie Institute of Washington Publications.

Douglass, A. E. (1919). Climatic Cycles and Tree Growth (Publication 289). Washington, D.C.: Carnegie Institution of Washington.

Douglass, A. E. (1934). Accuracy in dating. *Tree-Ring Bulletin*, **1**(2), 10-11.

Douglass, A. E. (1935). Accuracy in dating - II. The presentation of evidence. *Tree-Ring Bulletin*, **1**(2), 19-21.

Dunwiddie, P. D. (1979). Dendrochronological studies of indigenous New Zealand trees. *New Zealand Journal of Botany*, **17**, 251-266.

Dunwiddie, P. W., & LaMarche V. C. Jr. (1980a). Dendrochronological characteristics of some native Australian trees. *Australian Forestry*, **43**, 124-135.

Dunwiddie, P. W., & LaMarche V. C. Jr. (1980b). A climatically responsive tree-ring record for Widdringtonia cedarbergensis, Cape province South Africa. *Nature*, **286**, 796-797.

Dyer, T. G. J. (1982). South Africa. In M. K. Hughes, P. M. Kelly, J. R. Pilcher, & V. C. LaMarche Jr. (Eds.), Climate From Tree Rings Cambridge, UK: Cambridge University Press.

Ellis, R. C. (1971). Dieback of alpine ash as related to changes in soil temperature. *Australian Forestry*, **35**, 152-163.

Emerson, J. D., & Strenio, J. (1983). Boxplots and batch comparisons. In D.C. Hoaglin, F. Mosteller & J.W. Tukey (Ed.), Understanding robust and exploratory data anlaysis (pp. 58-96). New York: John Wiley & Sons.

Eriksson, M. (1989). Integrating forest growth and dendrochronological methodologies. PhD thesis, University of Minnesota.

Esau, K. (1977). Anatomy of Seed Plants (2nd ed.). New York: John Wiley & Sons, Inc. 550 pp.

Feng, X., & Epstein, S. (1995). Climatic temperature records in δD data from tree rings. *Geochimica et Cosmochimica Acta*, **59**(14), 3029-3037.

Fichtner, K., Koch, G. W., & Mooney, H. A. (1994). Photosynthesis, storage, and allocation. In E. D. Schulze & M. M. Caldwell (Eds.), Ecophysiology of Photosynthesis (pp. 133-146). Berlin Heidelberg: Springer-Verlag.

Francey, R. J., Barbetti, M., Bird, T., Beardsmore, D., Coupland, W., Dolezal, J.E., Farquhar, G.D., Flynn, R.G., Fraser, P.J., Gifford, R.M., Goodman, H.S., Kunda, B., McPhail, S., Nanson, G., Pearman, G.I., Richards, N.G., Sharkey, T.D., Temple, R.B. & Weir, B. (1984). Isotopes in tree rings (Technical Paper No. 4). Melbourne: CSIRO Division of Atmospheric Research.

Francey, R. J., Gifford, R. M., Sharkey, T. D., & Weir, B. (1985). Physiological influences on carbon isotope discrimination in huon pine (*Lagarostrobos franklinii*). *Oecologia*, **66**, 211-218.

Fritts, H. C. (1966). Growth-rings of trees: their correlation with climate. *Science*, **154**(3752), 973-979.

Fritts, H. C. (1969). Bristlecone pine in the White Mountains of California: growth and ring-width characteristics (Papers of the Laboratory of Tree-Ring Research No. 4). University of Arizona Press, Tucson, AZ, USA.

Fritts, H. C. (1976). Tree Rings and Climate. London: Academic Press. 567 pp.

Fritts, H. C. (1982). The climate-growth response. In M. K. Hughes, P. M. Kelly, J. R. Pilcher, & V. C. LaMarche Jr. (Eds.), Climate From Tree Rings Cambridge, UK: Cambridge University Press.

Fritts, H. C. (1990). Methods of calibration, verification, and reconstruction: introduction. In E. R. Cook & L. A. Kairiukstis (Eds.), Methods of Dendrochronology: Applications in the Environmental Sciences (pp. 163-165). Dordrecht: Kluwer Academic Publishers.

Fritts, H. C. (1991). Reconstructing large-scale climatic patterns from tree-ring data: a diagnostic analysis. Tucson, AZ, USA: University of Arizona Press.

Fritts, H. C., & Shaskin, A. V. (1994). Modeling tree-ring structure as related to temperature, precipitation, and day length. In T. E. Lewis (Ed.), Tree rings as indicators of ecosystem health (pp. 17-57). Boca Raton: CRC Press.

Fritts, H. C., & Swetnam, T. W. (1986). Dendroecology: a tool for evaluating variations in past and present forest environments (Technical Report). Laboratory of Tree-Ring Research, University of Arizona, Tucson, AZ, USA.

Fritts, H. C., & Wu, X. (1986). A comparison between response function analysis and other regression techniques. *Tree-Ring Bulletin*, **46**, 31-46.

Fritts, H. C., Mosimann, J. E., & Bottorff, C. P. (1969). A revised computer program for standardizing tree-ring series. *Tree-Ring Bulletin*, **29**, 15-20.

Fritts, H. C., Blasing, T. J., Hayden, B. P., & Kutzbach, J. E. (1971). Multivariate techniques for specifying tree-growth and climate relationships and for reconstructing anomalies in paleoclimate. *Journal of Applied Meteorology*, **10**(5), 845-864.

Fritts, H. C., Guiot, J., & Gordon, G. A. (1990). Verification. In E. R. Cook & L. A. Kairiukstis (Eds.), Methods of Dendrochronology: Applications in the Environmental Sciences (pp. 178-185). Dordrecht: Kluwer Academic Publishers.

Gates, D. M. (1968a). Transpiration and leaf temperature. *Annual Review of Plant Physiology*, **19**, 211-238.

Gates, D. M. (1968b). Energy exchange between organisms and environment. *Australian Journal of Science*, **31**(2), 67-74.

Gentilli, J. (1972). Australian Climate Patterns. Melbourne, Australia: Nelson.

Gibson, N. (1986). Huon pine conservation and management (Wildlife Division Technical Report No. 86/3). National Parks & Wildlife Service, Tasmania.

Gibson, N., & Brown, M. J. (1991). The ecology of *Lagarostrobos franklinii* (Hook.f.) Quinn (Podocarpaceae) in Tasmania. 2. Population structure and spatial pattern. *Australian Journal of Ecology*, **6**, 223-229.

Gibson, N., Davies, J., & Brown, M. J. (1991). The ecology of *Lagarostrobos franklinii* (Hook.f.) Quinn (Podocarpaceae) in Tasmania. 1. Distribution, floristics and environmental correlates. *Australian Journal of Ecology*, **16**, 215-222.

Gordon, G. A. (1982). Verification of dendroclimatic reconstructions. In M. K. Hughes, P. M. Kelly, J. R. Pilcher, & V. C. LaMarche Jr. (Eds.), Climate From Tree Rings (pp. 58-61). Cambridge, UK: Cambridge University Press.

Gordon, G. A., & LeDuc, S. K. (1981). Verification statistics for regression models. In, proceedings of the Seventh Conference on Probability and Statistics in Atmospheric Sciences. Monterey, California, USA.

Graybill, D. A. (1982). Chronology development and analysis. In M. K. Hughes, P. M. Kelly, J. R. Pilcher, & V. C. LaMarche Jr. (Eds.), Climate From Tree Rings (pp. 21-31). Cambridge, UK: Cambridge University Press.

Graybill, D. A., & Shiyatov, S. G. (1992). Dendroclimatic evidence from the northern Soviet Union. In R. S. Bradley & P. D. Jones (Eds.), Climate since A.D. 1500 (pp. 393-414). London: Routledge.

Guiot, J. (1987). Standardization and selecton of the chronologies by the ARMA analysis. In L. Kairiukstis, Z. Bednarz, & E. Feliksik (Eds.), Methods of Dendrochronology - 1 (pp. 97-105). Laxenburg, Warsaw: International Institute for Applied Systems Analysis, and the Polish Academy of Sciences-Systems Research Institute.

Guiot, J. (1990). Methods of calibration, verification, and reconstruction: methods of calibration. In E. R. Cook & L. A. Kairiukstis (Eds.), Methods of Dendrochronology: applications in the environmental sciences (pp. 165-178). Dordrecht: Kluwer Academic Publishers.

Guiot, J., Berger, A. L., & Munaut, A. V. (1982). Response functions. In M. K. Hughes, P. M. Kelly, J. R. Pilcher, & V. C. LaMarche Jr. (Eds.), Climate From Tree Rings (pp. 38-47). Cambridge, UK: Cambridge University Press.

Guttman, L. (1954). Some necessary conditions for common-factor analysis. *Psychometrika*, **19**, 149-161.

Harper, J. L. (1989). The value of a leaf. *Oecologia*, **80**, 53-58.

Hickey, J.E. & Felton, K.C. (1988). Subalpine Huon pine near Frenchmans Cap. *The Tasmanian Naturalist*, **93**, 1-4.

Hill, R. S., & MacPhail, M. K. (1985). A fossil flora from rafted Pio-Pleistocene mudstones at Regatta Point, Tasmania. *Australian Journal of Botany*, **33**, 497-517.

Holmes, R. L. (1983). Computer-assisted quality control in tree-ring dating and measurement. *Tree-Ring Bulletin*, **44**, 69-75.

Holmes, R. L., Adams, R. K., & Fritts, H. C. (1986). Tree-ring chronologies of western North America: California, Eastern Oregon and Northern Great Basin with procedures used in the chronology development work including users manuals for computer programs COFECHA and ARSTAN. Tucson, AZ, USA: Laboratory of Tree-Ring Research, University of Arizona.

Horton, D. R. (1982). The burning question: Aborigines, Fire and Australian Ecosystems. *Mankind*, **13**(3), 237-251.

Hughes, M. K., Kelly, P. M., Pilcher, J. R., & V. C. LaMarche Jr. (Eds.). (1982). Climate From Tree Rings. Cambridge, UK: Cambridge University Press. 223 pp.

Jackson, W. D. (1965). Vegetation. In J. L. Davies (Ed.), Atlas of Tasmania Hobart: Hobart Lands and Surveys Department.

Jacoby, G. C. (1989). Overview of tree-ring analysis in tropical regions. In P. Baas & R. E. Vetter (Eds.), Growth Rings in Tropical Woods (pp. 99-108). *IAWA Bulletin* n.s.

Jarman, S. J., & Brown, M. J. (1983). A definition of cool temperate rainforest in Tasmania. *Search*, **14**(3-4), 81-87.

Jarman, S. J., Brown, M. J., & Kantvilas, G. (1984). Rainforest in Tasmania. Department of Parks, Wildlife & Heritage Report, Hobart, Tasmania.

Jones, P. D., & Briffa, K. R. (1992). Global surface air temperature variations over the twentieth century: Part 1, Spatial, temporal and seasonal details. *The Holocene*, **2**, 165-179.

Jones, P. D., Raper, S. C. B., & Wigley, T. M. L. (1986). Southern Hemisphere surface air temperature variations: 1851-1984. *Journal of Climate and Applied Meteorology*, **25**, 1213-1230.

Kirkpatrick, J. B. (1977a). Native vegetation of the West Coast Region of Tasmania. In Landscape & Man (pp. 55-80). Hobart: Royal Society of Tasmania.

Kirkpatrick, J. B. (1977b). The impact of man on the vegetation of the West Coast Region. In Landscape & Man (pp. 151-156). Hobart: Royal Society of Tasmania.

Kirkpatrick, J. B. (1982). Phytogeographical analysis of Tasmanian alpine floras. *Journal of Biogeography*, **9**, 255-271.

Kirkpatrick, J. B., & Dickinson, K. J. M. (1984a). Vegetation Map of Tasmania. 1:500 000. Hobart: Tasmanian Forestry Commission.

Kirkpatrick, J. B., & Dickinson, K. J. M. (1984b). The impact of fire on Tasmanian alpine vegetation and soils. *Australian Journal of Botany*, **32**, 613-629.

Kirkpatrick, J.B., & Brown, M.J. (1987). The nature of the transition from sedgeland to alpine vegetation in south-west Tasmania. I. Altitudinal vegetation change on four mountains. *Journal of Biogeography*, **14**, 539-549.

Kirkpatrick, J.B., Nunez, M., Bridle, K., & Chladil, M.A. (1997). Explaining a sharp transition from sedgeland to alpine vegetation on Mount Sprent, south-west Tasmania. *Journal of Vegetation Science*, (in press).

LaMarche, V. C., Jr (1974). Paleoclimatic inferences from long tree-ring records. *Science*, **183**, 1043-48.

LaMarche, V. C. Jr. (1975). Potential of tree-rings for reconstruction of past climatic variations in the Southern Hemisphere. In proceedings from the Symposium on Long-Term Climatic Fluctuations, No. 421 (pp. 21-30). Norwich, England: World Meteorological Organisation, Geneva.

LaMarche, V. C. Jr., & Pittock, B. (1982). Preliminary temperature reconstruction for Tasmania. In M. K. Hughes, P. M. Kelley, J. R. Pilcher, & V. C. LaMarche Jr. (Eds.), Climate from Tree Rings (pp. 177-185). Cambridge: Cambridge University Press.

LaMarche, V. C. Jr., Holmes, R. L., Dunwiddie, P. W., & Drew, L. G. (1979a). Tree-ring chronologies of the Southern Hemisphere 1. Argentina (Chronology Series V), Laboratory of Tree-Ring Research, University of Arizona.

LaMarche, V. C. Jr., Holmes, R. L., Dunwiddie, P. W., & Drew, L. G. (1979b). Tree-ring chronologies of the Southern Hemisphere 2. Chile (Chronology Series V), Laboratory of Tree-Ring Research, University of Arizona.

LaMarche, V. C. Jr., Holmes, R. L., Dunwiddie, P. W., & Drew, L. G. (1979c). Tree-ring chronologies of the Southern Hemisphere 3. New Zealand (Chronology Series V), Laboratory of Tree-Ring Research, University of Arizona.

LaMarche, V. C. Jr., Holmes, R. L., Dunwiddie, P. W., & Drew, L. G. (1979d). Tree-ring chronologies of the Southern Hemisphere 4. Australia (Chronology Series V), Laboratory of Tree-Ring Research, University of Arizona.

LaMarche, V. C. Jr., Holmes, R. L., Dunwiddie, P. W., & Drew, L. G. (1979e). Tree-ring chronologies of the Southern Hemisphere 5. South Africa (Chronology Series V), Laboratory of Tree-Ring Research, University of Arizona.

Lamb, H. H. (1977). Climate: Present, Past and Future. London: Methuen.

Langford, J. (1965). Weather and climate. In J. L. Davies (Ed.), Atlas of Tasmania (pp. 2-11). Hobart, Australia: Department of Lands and Surveys.

Lara, A., & Villalba, R. (1993). A 3620-year temperature record from *Fitzroya cuppressoides* tree rings in southern South America. *Science*, **260**, 1104-1106.

Lilly, M. A. (1977). An assessment of the dendrochronological potential of indigenous tree species in South Africa (Occasional paper No. 18). Dept. of Geography and Environmental Studies, University of Witwatersrand, South Africa.

Lofgren, G. R., & Hunt, J. H. (1982). Transfer Functions. In M. K. Hughes, P. M. Kelly, J. R. Pilcher, & V. C. LaMarche Jr. (Eds.), Climate From Tree Rings (pp. 50-56). Cambridge, UK: Cambridge University Press.

Lough, J. M. (1991). Rainfall variations in Queensland, Australia: 1891-1986. *International Journal of Climatology*, **11**, 745-768.

Lough, J. M. (1992). Variations of sea-surface temperatures off North-Eastern Australia and associations with rainfall in Queensland. *International Journal of Climatology*, **12**, 765-782.

Macphail, M. (1975a). The history of the vegetation and climate in southern Tasmania since the late Pleistocene (ca. 13,000 - 0 BP). PhD thesis, Dept. of Botany, the University of Tasmania.

Macphail, M. K. (1975b). Late Pleistocene environments in Tasmania. *Search*, **6**, 295-300.

Macphail, M. K. (1979). Vegetation and climates in southern Tasmania since the last glaciation. *Quaternary Research*, **11**, 306-341.

Macphail, M. K., & Colhoun, E. A. (1985). Late last glacial vegetation, climates and fire activity in southwest Tasmania. *Search*, **16**, 43-45.

Macphail, M. K., & Hill, R. S. (1983). Cool temperate rainforest in Tasmania: a reply. *Search*, **14**(7-8), 186-187.

Mariaux, A. (1981). Past efforts in measuring age and annual growth in tropical trees. In F. H. Bormann & G. Berlyn (Eds.), Age and Growth Rate of Tropical Trees: New Directions for Research. New Haven, CT, USA: School of Forestry and Environmental Studies, Yale University.

McPhail, S., Barbetti, M., Francey, R. J., Bird, T., & Dolezal, J. (1983). ^{14}C Variations from Tasmanian trees-preliminary results. *Radiocarbon*, **25**(3), 797-802.

Millington, R. J., Jones, R., Brown, D., & Vernon, B. (1979). Huon pine - endangered? (Environmental Studies Occassional Paper No. 9). Hobart: University of Tasmania.

Mosteller, F., & Tukey, J. W. (1977). Data Analysis and Regression. Reading, MA, USA: Addison-Wesley.

Nanson, G. C., Barbetti, M., & Taylor, G. (1995). River stabilisation due to changing climate and vegetation during the late Quaternary in western Tasmania, Australia. *Geomorphology*, 13, 145-158.

Nobel, P. S. (1974). Introduction to biophysical plant physiology. San Francisco: W.H. Freeman and Company.

Norton, D. A. (1983a). Modern New Zealand tree-ring chronologies. I. *Nothofagus solandri*. *Tree-Ring Bulletin*, **43**, 1-17.

Norton, D. A. (1983b). Modern New Zealand Chronologies. II. *Nothofagus menziesii*. *Tree-Ring Bulletin*, **43**, 39-49.

Norton, D. A., Briffa, K. R., & Salinger, M. J. (1989). Reconstruction of New Zealand summer temperatures to 1730 AD using dendroclimatic techniques. *International Journal of Climatology*, **9**, 633-644.

Nowlin, W. D., & Klinck, J. M. (1986). The physics of the Antarctic circumpolar current. *Reviews of Geophysics*, **24**, 469-491.

Ogden, J. (1978). On the dendrochronological potential of Australian trees. *Australian Journal of Ecology*, **3**, 339-356.

Ogden, J. (1981). Dendrochronological studies and determination of tree ages in the Australaian tropics. *Journal of Biogeography*, **8**, 405-420.

Ogden, J. (1982). Australasia. In M. K. Hughes, P. M. Kelly, J. R. Pilcher, & V. C. LaMarche Jr. (Eds.), Climate From Tree Rings Cambridge, UK: Cambridge University Press.

Palmer, E., & Pitman, N. (1972). Trees of South Africa. Cape Town: A.A. Balkema.

Palmer, J. G. (1982). A dendrochronological study of kauri (*Agathis australis*). M.Sc. thesis, University of Auckland.

Palmer, J. G. (1989). A dendroclimatic study of *Phyllocladus trichromanoides* D.Don (tanekaha). Ph.D. thesis, University of Auckland.

Pedley, J., Brown, M. J., & Jarman, S. J. (1980). A survey of Huon pine in the Pieman River State Reserve and environs (Wildlife Division Technical Report No. 80/2). National Parks and Wildlife Service, Tasmania.

Peirera, J. S. (1994). Gas exchange and growth. In E. D. Schulze & M. M. Caldwell (Eds.), Ecophysiology of Photosynthesis (pp. 147-175). Berlin Heidelberg: Springer-Verlag.

Peterson, M. J. (1990). Distribution and conservation of Huon pine. Hobart: Forestry Commission of Tasmania.

Pilcher, J. R. (1990). Sample preparation, cross-dating, and measurement. In E. R. Cook & L. A. Kairiukstis (Eds.), Methods of Dendrochronology: Applications in the Environmental Sciences (pp. 40-51). Dordrecht: Kluwer Academic Publishers.

Pittock, A. B. (1973). Global meridional interactions in stratosphere and troposphere. *Quarterly Journal of the Royal Meteorological Society*, **99**, 424-437.

Pittock, A. B. (1975). Climatic change and patterns of variation in Australian rainfall. *Search*, **6**, 498-504.

Pittock, A. B. (1978). A critical look at long-term sun-weather relationships. *Reviews of Geophysics and Space Physics*, **16**, 400-420.

Playford, G., & Dettmann, M. E. (1979). Pollen of *Dacrydium franklinii* Hook.f. and comparable early Tertiary microfossils. *Pollen et Spores*, **20**(4), 513-534.

Pook, M. J. (1994). Atmospheric blocking in the Australasian region in the Southern Hemisphere winter. PhD thesis, University of Tasmania.

Preisendorfer, R.W., Zwiers, F.W., Barnett T.P. (1981). Foundations of Principal Components Selection Rules. SIO Reference Series, 81-4, Scripps Institution of Oceanography, La Jolla, USA.

Quinn, C. J. (1982). Taxonomy of *Dacrydium* Sol. ex Lamb. emend. de Laub. (Podocarpaceae). *Australian Journal of Botany*, **30**, 311-320.

Read, J. (1989). Phenology and germination in some rainforest canopy species at Mt. Field National Park. *Proceedings of the Royal Society of Tasmania*, **123**, 211-221.

Read, J., & Busby, J. R. (1990). Comparative responses to temperature of the major canopy species of Tasmanian cool temperate rainforest and their ecological significance. II. Net photosynthesis and climate analysis. *Australian Journal of Botany*, **38**, 185-205.

Read, J., & Hill, R. S. (1988). Comparative responses to temperature of the major canopy species of Tasmanian cool temperate rainforest and their ecological significance. I. Foliar frost resistance. *Australian Journal of Botany*, **36**, 131-143.

Richman, M. B. (1986). Rotation of principal components. *Journal of Climatology*, **6**, 293-335.

Robinson, E. A., & Treital, S. (1980). Geophysical Signal Analysis. Englewood Cliffs, NJ, USA: Prentice Hall.

Ruddell, A. R. (1995). Recent glacier change and climate change in the New Zealand Alps. PhD thesis, University of Melbourne.

Salinger, M. J. (1979). New Zealand climate: the temperature record, historical data and some agricultural implications. *Climatic Change*, **2**, 109-126.

Salinger, M. J. (1980a). New Zealand climate: 1 precipitation patterns. *Monthly Weather Review*, **108**, 1892-1904.

Salinger, M. J. (1980b). New Zealand climate: 2 temperature patterns. *Monthly Weather Review*, **108**, 1905-1912.

Salinger, M. J. (1982a). New Zealand climate: scenarios for a warm high-CO_2 world. *Weather and Climate*, **2**, 9-15.

Salinger, M. J. (1982b). On the suggestion of post-1950 warming over New Zealand. *New Zealand Journal of Science*, **25**, 77-86.

Salinger, M. J., & Gunn, J. M. (1975). Recent climatic warming around New Zealand. *Nature*, **256**, 396-398.

Salinger, M. J., Fitzharris, B. B., Hay, J.E., Jones, P.D., J.P. Macveigh, & I. Schmidely-Leleu (1995). Climate trends in the southwest Pacific. *International Journal of Climatology*, **15**: 285-302.

Salinger, M. J., Palmer, J. G., Jones, P. D., & Briffa, K. R. (1994). Reconstructions of New Zealand climate indices back to AD 1731 using dendroclimatic techniques: some preliminary results. *International Journal of Climatology*, **14**, 1135-1149.

Salisbury, F. B., & Ross, C. W. (1992). Plant Physiology (4th ed.). Belmont, California: Wadsworth Publishing Co. 682 pp.

Samish, R. M. (1954). Dormancy in woody plants. *Annual Review of Plant Physiology*, **5**, 183-204.

Schulman, E. (1945). Tree rings and runoff in the South Platte River basin. *Tree-Ring Bulletin*, **11**, 18-24.

Schulman, E. (1956). Dendroclimatic Change in Semiarid America. Tucson: University of Arizona Press.

Schulze, E. D., & Caldwell, M. M. (Eds.). (1994). Ecophysiology of Photosynthesis (1 ed.). Berlin Heidelberg: Springer-Verlag.

Schulze, W., & Schulze, E. D. (1994). The significance of assimilatory starch for growth in Arabidopsis thaliana wild-type and starchless mutants. In E. D. Schulze & M. M. Caldwell (Eds.), Ecophysiology of Photosynthesis (pp. 123-132). Berlin Heidelberg: Springer-Verlag.

Shapcott, A. (1991). Studies in the population biology and genetic variation of Huon pine (Lagarostrobos franklinii) (NRCP Technical Report No. 4). The National Rainforest Conservation Program and Department of Parks, Wildlife and Heritage, Hobart.

Shaskin, A., & Fritts, H. C. (1994). TREERING 2.0: A process model simulating cambial activity and ring structure in conifers using daily climatic data. (unpublished) 43 pp.

Sheldrake, A. R. (1968). The production of auxin by tobacco internode tissues. *New Phytologist*, **67**, 1-13.

Sheldrake, A. R. (1971). Auxin in the cambium and its differentiating derivatives. *Journal of Experimental Botany*, **22**, 735-740.

Shepherd, D. J. (1991). The effect of site changes on climatic records - A Tasmanian example (Met Note No. 194). Australian Bureau of Meteorology.

Shigo, A. L. (1984). Compartmentalization: a conceptual framework for understanding how trees grow and defend themselves. *Annual Review of Phytopathology*, **22**, 189-214.

Stokes, M. A., & Smiley, T. L. (1968). An Introduction to Tree-Ring Dating. Chicago: University of Chicago Press.

Swetnam, T.W., Thompson, M.A. & Sutherland, E.K. (1985). Using dendrochronology to measure radial growth of defoliated trees. Agricultural Handbook No. 639, Washington, D.C.: US Department of Agriculture.

Tchernia, P. (1980). Descriptive Regional Oceanography (1 ed.). Oxford: Pergamon Press.

Thompson, H. C. (1953). Vernalization of growing plants. In W. E. Loomis (Ed.), Growth and Differentiation in Plants (pp. 179-196). Ames: The Iowa State College Press.

Torok, S. J. (1996). The development of a high quality historical data base for Australia. PhD thesis, School of Earth Sciences, Faculty of Science, The University of Melbourne.

Trenberth, K. E. (1976). Fluctuations and trends in indices of the southern hemispheric circulation. *Quaterly Journal of the Royal Meteorological Society,* **102,** 65-75.

Villalba, R. (1990). Climatic fluctuations in northern Patagonia during the last 1000 years as inferred from tree-ring records. *Quaternary Research,* **34,** 346-360.

Villalba, R. (1994). Tree-ring and glacial evidence for the Medieval Warm Epoch and the Little Ice Age in southern South America. *Climatic Change,* **26,** 183-197.

Weissel, J. K., Hayes, D. E., & Herron, E. M. (1977). Plate tectonics synthesis. The displacements between Australia, New Zealand and Antarctica since the Late Cretaceous. *Marine Geology,* **25,** 231-277.

White, J. W. C., Lawrence, J. R., & Broecker, W. S. (1994). Modeling and interpreting D/H ratios in tree rings: a test case of white pine in the northeastern United States. *Geochimica et Cosmochimica Acta,* 58(2), 851-862.

White, P. S. (1979). Pattern, process, and natural disturbance in vegetation. *Botanical Review,* **45,** 229-299.

Williams, W. D. (1974). Introduction. In W. D. Williams (Ed.), Biogeography and Ecology in Tasmania (pp. 3-15). The Hague: Dr. W.Junk b.v., Publishers.

Wilson, R. (1990). Soils and soil erosion. In A. P. Scanlon, G. J. Fish, & M. L. Yaxley (Eds.), Behind the Scenery: Tasmania's landforms and geology (pp. 23-36). Hobart: Department of Education and the Arts, Tasmania.

Worbes, M. (1985). Structural and other adaptations to long-term flooding by trees in central Amazonia. *Amazonia,* 9(3), 459-484.

APPENDIX 1: ACTUAL AND ESTIMATED WARM SEASON TEMPERATURE

TASMANIAN WARM-SEASON ACTUAL TEMPERATURE

YEAR	ACTUAL
1884	15.100
1885	14.620
1886	14.600
1887	15.930
1888	14.750
1889	15.820
1890	16.650
1891	15.050
1892	15.350
1893	15.350
1894	15.750
1895	15.930
1896	14.720
1897	14.480
1898	15.850
1899	15.400
1900	15.150
1901	14.880
1902	14.000
1903	15.080
1904	15.300
1905	14.750
1906	15.180
1907	14.270
1908	15.480
1909	14.420
1910	15.780
1911	15.520
1912	15.430
1913	14.970
1914	15.680
1915	15.270
1916	15.380
1917	14.950
1918	15.600
1919	15.600
1920	15.180
1921	16.100
1922	15.520
1923	14.950
1924	14.500
1925	14.850
1926	15.480
1927	14.580
1928	16.270
1929	15.170
1930	15.350
1931	14.400
1932	15.200
1933	14.030
1934	15.550
1935	15.100
1936	15.600
1937	14.750
1938	15.380
1939	15.500
1940	14.500
1941	15.200
1942	14.920
1943	14.870
1944	14.730
1945	13.850
1946	14.770
1947	15.750
1948	14.850
1949	13.750
1950	14.480
1951	15.630
1952	14.380
1953	15.500
1954	15.020
1955	15.450
1956	16.220
1957	14.500
1958	14.680
1959	16.070
1960	15.620
1961	16.600
1962	15.900
1963	15.200
1964	14.580
1965	14.480
1966	15.720
1967	15.800
1968	16.100
1969	15.900
1970	15.880
1971	17.120
1972	16.300
1973	16.170
1974	16.770
1975	15.120
1976	16.380
1977	15.820
1978	15.450
1979	16.150
1980	15.380
1981	17.020
1982	16.320
1983	15.500
1984	15.620
1985	15.850
1986	15.450
1987	15.050
1988	16.980
1989	17.000
1990	16.450
1991	15.300
1992	15.620
1993	16.420
1994	15.570

Buckley and LJH Reconstructions of Warm Season Temperature

YEAR	BCK.RECON	LJH.RECON
1000	14.990	15.240
1001	15.799	15.532
1002	15.529	15.328
1003	16.156	15.555
1004	15.606	15.175
1005	15.806	15.370
1006	16.211	15.892
1007	14.464	14.636
1008	15.790	15.248
1009	14.705	15.137
1010	15.688	15.983
1011	13.851	14.427
1012	14.397	15.211
1013	13.703	14.776
1014	14.656	15.117
1015	15.247	15.111
1016	14.530	14.765
1017	15.205	14.964
1018	15.106	14.884
1019	15.576	15.153
1020	16.203	15.469
1021	16.248	15.809
1022	16.589	15.757
1023	15.653	15.752
1024	15.456	15.328
1025	16.427	15.776
1026	16.339	15.793
1027	15.635	15.355
1028	16.039	15.695
1029	15.405	15.411
1030	15.182	14.966
1031	15.814	15.733
1032	16.664	16.042
1033	15.200	15.068
1034	15.982	15.540
1035	15.299	15.232
1036	15.274	15.710
1037	15.825	15.744
1038	14.889	15.262
1039	15.062	15.408
1040	15.719	16.057
1041	14.437	14.876
1042	14.936	15.074
1043	15.196	15.365
1044	15.508	15.425
1045	16.246	15.806
1046	14.527	14.811
1047	15.838	15.714
1048	16.065	15.634
1049	15.448	15.321
1050	16.135	15.653
1051	15.563	15.539
1052	16.196	15.614
1053	14.987	15.114
1054	16.416	15.691
1055	13.955	14.499
1056	15.182	14.980
1057	15.543	15.184
1058	15.361	15.029
1059	14.879	14.758
1060	16.128	15.411
1061	16.149	15.394
1062	16.312	15.399
1063	14.968	15.199
1064	14.586	14.884
1065	14.746	15.103
1066	15.246	15.339
1067	15.811	15.663
1068	15.050	15.049
1069	15.498	15.552
1070	15.758	15.765
1071	15.446	15.498
1072	15.597	15.352
1073	15.441	15.338
1074	16.453	15.679
1075	15.193	15.142
1076	14.730	14.816
1077	15.785	15.285
1078	15.686	15.186
1079	15.706	15.307
1080	15.980	15.609
1081	14.765	15.102
1082	13.979	14.429
1083	16.149	15.672
1084	15.814	15.652
1085	15.537	15.667
1086	16.569	16.178
1087	13.693	14.247
1088	14.933	14.889
1089	14.197	14.612
1090	14.941	15.204
1091	15.557	15.532
1092	15.733	15.263
1093	15.327	15.176
1094	14.976	15.051
1095	15.517	15.342
1096	14.672	15.259
1097	14.920	14.964
1098	15.336	15.554
1099	16.382	15.956
1100	15.556	15.466
1101	16.567	15.928
1102	15.791	15.425
1103	16.106	15.353
1104	15.031	15.085
1105	15.329	15.225
1106	14.837	14.984
1107	15.620	15.289
1108	15.915	15.474
1109	15.632	15.466
1110	15.976	15.678
1111	16.239	15.676
1112	15.329	15.346
1113	14.685	14.952
1114	14.906	15.215
1115	15.572	15.457
1116	15.010	15.196
1117	16.057	15.726
1118	15.322	15.441

YEAR	BCK.RECON	LJH.RECON	YEAR	BCK.RECON	LJH.RECON
1119	16.264	15.899	1183	14.761	15.151
1120	15.469	15.444	1184	14.619	15.004
1121	16.346	16.167	1185	14.750	14.825
1122	14.916	15.545	1186	16.019	15.646
1123	15.653	15.873	1187	16.295	15.818
1124	15.921	16.008	1188	16.244	16.183
1125	14.893	15.511	1189	14.809	15.266
1126	15.552	15.417	1190	15.946	15.917
1127	15.392	15.413	1191	14.755	15.039
1128	14.903	15.047	1192	15.360	15.275
1129	15.356	15.564	1193	15.968	15.853
1130	15.905	15.662	1194	13.854	13.945
1131	14.765	15.002	1195	14.826	14.943
1132	15.280	15.440	1196	14.465	14.714
1133	15.717	15.667	1197	14.748	14.941
1134	15.650	15.671	1198	15.188	15.152
1135	15.679	15.453	1199	15.823	15.688
1136	15.931	15.807	1200	15.135	15.358
1137	15.772	15.716	1201	14.850	15.050
1138	15.227	15.439	1202	15.586	15.434
1139	15.566	15.608	1203	16.573	16.118
1140	14.761	15.340	1204	14.594	14.744
1141	15.334	15.608	1205	15.538	15.566
1142	14.909	15.286	1206	16.362	15.820
1143	16.416	15.877	1207	16.680	16.074
1144	14.411	14.945	1208	14.819	15.054
1145	14.292	14.579	1209	15.228	15.403
1146	15.789	15.344	1210	14.988	15.336
1147	15.828	15.240	1211	15.223	15.328
1148	16.808	16.114	1212	15.099	15.137
1149	15.993	15.755	1213	14.893	14.949
1150	16.035	15.880	1214	14.468	14.767
1151	14.772	15.316	1215	15.058	15.231
1152	15.156	15.673	1216	14.796	15.127
1153	15.775	15.767	1217	14.695	15.422
1154	15.408	15.789	1218	15.077	15.727
1155	14.620	15.286	1219	14.296	15.426
1156	14.029	14.871	1220	15.126	15.386
1157	15.061	15.611	1221	15.337	15.531
1158	16.242	15.984	1222	15.930	15.616
1159	13.532	14.177	1223	15.490	15.305
1160	15.065	15.412	1224	15.268	15.143
1161	15.159	15.295	1225	15.704	15.408
1162	15.033	15.353	1226	15.734	15.373
1163	15.443	15.359	1227	15.037	14.952
1164	15.783	15.705	1228	16.041	15.794
1165	15.996	16.000	1229	14.480	15.163
1166	15.464	15.374	1230	15.226	15.675
1167	15.482	15.377	1231	15.133	15.398
1168	15.496	15.320	1232	14.809	15.538
1169	15.353	15.548	1233	15.685	15.606
1170	15.078	15.305	1234	14.355	15.093
1171	15.724	15.944	1235	14.339	14.832
1172	15.096	15.470	1236	15.641	15.565
1173	15.594	15.649	1237	15.492	15.565
1174	15.808	15.612	1238	15.410	15.579
1175	15.391	15.577	1239	15.259	15.450
1176	15.667	15.514	1240	15.642	15.661
1177	15.994	15.863	1241	16.191	16.069
1178	15.351	15.464	1242	14.625	15.031
1179	16.262	15.988	1243	15.297	15.237
1180	16.655	16.166	1244	15.642	15.427
1181	15.118	15.199	1245	15.611	15.673
1182	14.549	14.936	1246	15.653	15.597

YEAR	BCK.RECON	LJH.RECON	YEAR	BCK.RECON	LJH.RECON
1247	15.547	15.602	1311	16.581	15.883
1248	15.979	15.896	1312	15.599	15.550
1249	15.187	15.282	1313	15.167	15.409
1250	15.563	15.256	1314	14.835	15.353
1251	15.361	15.487	1315	15.003	15.489
1252	15.722	15.773	1316	15.635	15.821
1253	15.784	15.823	1317	15.309	15.471
1254	16.114	16.035	1318	15.342	15.146
1255	15.022	15.325	1319	14.689	14.583
1256	14.758	14.993	1320	14.627	14.686
1257	14.644	15.122	1321	14.295	14.605
1258	15.373	15.481	1322	14.199	14.578
1259	15.547	15.393	1323	15.435	15.267
1260	15.661	15.448	1324	16.072	15.589
1261	15.585	15.421	1325	15.152	15.157
1262	15.953	15.573	1326	15.864	15.589
1263	15.305	15.502	1327	16.040	15.580
1264	15.707	15.644	1328	15.760	15.371
1265	15.281	15.362	1329	15.548	15.483
1266	15.438	15.418	1330	16.103	15.601
1267	15.333	15.258	1331	16.364	15.958
1268	15.462	15.235	1332	15.389	15.195
1269	15.533	15.487	1333	15.538	15.362
1270	15.641	15.220	1334	15.258	15.357
1271	15.714	15.715	1335	16.593	15.924
1272	14.738	15.108	1336	16.617	16.015
1273	15.469	15.587	1337	15.625	15.793
1274	15.837	15.635	1338	15.838	15.550
1275	15.864	15.664	1339	15.631	15.685
1276	16.181	15.724	1340	15.834	15.827
1277	15.363	14.637	1341	15.636	15.457
1278	14.819	14.668	1342	15.647	15.578
1279	15.180	15.077	1343	15.319	15.222
1280	16.001	15.750	1344	15.679	15.689
1281	15.265	15.030	1345	13.705	13.646
1282	15.073	14.806	1346	14.427	14.827
1283	15.415	15.097	1347	14.208	14.529
1284	15.936	15.181	1348	14.932	15.209
1285	15.908	15.332	1349	14.871	15.134
1286	15.950	15.440	1350	15.345	15.284
1287	15.509	15.295	1351	15.118	15.396
1288	15.051	14.868	1352	14.469	14.713
1289	15.590	15.288	1353	16.007	15.759
1290	15.098	15.084	1354	15.900	15.925
1291	14.729	15.015	1355	15.651	15.666
1292	15.092	15.127	1356	15.477	15.714
1293	15.042	15.066	1357	15.573	15.604
1294	15.799	15.443	1358	15.236	15.505
1295	15.219	15.026	1359	15.809	15.594
1296	15.867	15.672	1360	15.303	15.435
1297	14.745	14.883	1361	14.592	14.911
1298	16.124	15.609	1362	15.001	15.134
1299	15.252	15.066	1363	14.396	15.142
1300	15.357	15.006	1364	15.347	15.553
1301	15.719	15.320	1365	15.478	15.525
1302	15.063	14.825	1366	15.491	15.731
1303	15.818	15.315	1367	15.412	15.660
1304	16.096	16.140	1368	15.273	15.531
1305	16.035	15.571	1369	14.608	14.892
1306	15.970	15.896	1370	15.079	15.306
1307	16.469	16.084	1371	15.936	15.704
1308	16.100	15.607	1372	15.646	15.503
1309	16.355	15.994	1373	15.856	15.938
1310	15.778	15.572	1374	15.133	15.457

YEAR	BCK.RECON	LJH.RECON	YEAR	BCK.RECON	LJH.RECON
1375	15.687	15.889	1439	15.022	14.980
1376	14.651	14.972	1440	15.042	15.107
1377	15.021	14.804	1441	15.545	15.659
1378	15.408	15.238	1442	14.981	15.087
1379	15.106	14.900	1443	15.451	15.514
1380	14.698	14.757	1444	15.793	16.024
1381	14.921	14.835	1445	14.153	14.363
1382	15.617	15.532	1446	15.681	15.459
1383	15.550	15.509	1447	14.851	15.053
1384	15.507	15.522	1448	14.642	15.112
1385	15.794	15.640	1449	14.518	14.589
1386	15.827	15.424	1450	14.717	14.860
1387	15.822	15.700	1451	15.034	15.002
1388	15.392	15.458	1452	14.977	15.235
1389	16.017	15.990	1453	16.097	15.859
1390	15.449	15.636	1454	15.857	15.602
1391	14.674	14.993	1455	15.369	15.316
1392	14.737	15.142	1456	15.838	15.311
1393	15.706	15.863	1457	15.293	15.129
1394	15.469	15.813	1458	14.568	14.459
1395	15.415	15.557	1459	15.552	15.236
1396	16.415	16.208	1460	15.617	15.337
1397	15.826	15.644	1461	15.577	15.424
1398	16.444	16.046	1462	14.869	15.008
1399	15.363	15.093	1463	15.658	15.499
1400	15.064	15.224	1464	15.245	15.136
1401	15.080	15.141	1465	15.193	15.132
1402	15.187	15.270	1466	15.195	15.332
1403	14.889	14.976	1467	15.415	15.480
1404	14.603	14.635	1468	15.740	15.664
1405	15.879	15.950	1469	15.071	15.173
1406	15.960	15.763	1470	15.907	15.798
1407	15.537	15.579	1471	15.315	15.272
1408	16.057	16.014	1472	15.239	15.358
1409	15.825	15.710	1473	14.903	15.169
1410	15.235	15.266	1474	15.024	15.220
1411	15.178	15.262	1475	14.498	14.550
1412	14.164	14.559	1476	15.136	15.418
1413	15.515	15.470	1477	15.652	15.794
1414	15.393	15.249	1478	15.919	15.880
1415	16.244	15.901	1479	15.851	15.899
1416	15.165	15.410	1480	16.154	15.804
1417	15.456	15.533	1481	15.595	15.831
1418	15.863	15.561	1482	16.201	16.085
1419	15.541	15.657	1483	14.722	15.133
1420	15.257	15.482	1484	15.182	15.379
1421	15.441	15.663	1485	15.521	15.644
1422	15.883	16.010	1486	15.139	15.515
1423	15.215	15.465	1487	15.582	15.602
1424	14.690	15.026	1488	16.265	16.278
1425	14.793	14.982	1489	16.035	15.723
1426	15.107	15.392	1490	15.483	15.401
1427	15.797	15.625	1491	15.833	15.620
1428	16.320	15.826	1492	16.440	15.854
1429	15.771	15.636	1493	16.423	15.895
1430	15.767	15.741	1494	16.913	16.073
1431	15.001	15.184	1495	15.872	15.528
1432	15.205	15.378	1496	15.809	15.304
1433	15.558	15.561	1497	16.025	15.649
1434	15.262	15.439	1498	15.509	15.448
1435	16.447	16.382	1499	15.866	15.749
1436	16.495	16.326	1500	14.822	14.852
1437	15.259	15.514	1501	15.407	15.307
1438	15.840	15.623	1502	14.908	14.848

YEAR	BCK.RECON	LJH.RECON	YEAR	BCK.RECON	LJH.RECON
1503	16.025	15.596	1567	15.683	15.454
1504	16.092	15.730	1568	15.837	15.603
1505	16.118	15.797	1569	14.912	15.166
1506	15.170	15.125	1570	15.099	15.359
1507	15.233	15.266	1571	15.978	15.894
1508	15.812	15.702	1572	15.360	15.048
1509	15.957	15.673	1573	16.277	15.535
1510	15.328	15.359	1574	15.740	15.313
1511	14.468	14.839	1575	14.665	14.881
1512	15.939	16.016	1576	15.429	15.443
1513	14.792	15.300	1577	15.021	14.818
1514	14.755	15.436	1578	15.195	15.116
1515	15.439	15.657	1579	15.157	15.137
1516	14.749	15.073	1580	15.319	15.580
1517	15.635	15.565	1581	15.861	15.738
1518	14.601	14.901	1582	15.709	15.874
1519	14.098	14.627	1583	15.165	15.346
1520	15.217	15.531	1584	15.614	15.778
1521	14.433	14.849	1585	15.456	15.607
1522	15.346	15.423	1586	14.661	15.186
1523	15.065	15.035	1587	15.285	15.378
1524	15.637	15.433	1588	15.163	15.373
1525	15.735	15.638	1589	14.931	15.222
1526	15.070	15.089	1590	15.712	15.612
1527	14.844	14.930	1591	15.456	15.446
1528	15.397	15.316	1592	15.329	15.388
1529	15.625	15.355	1593	15.713	15.534
1530	14.764	15.114	1594	15.609	15.485
1531	15.588	15.644	1595	15.870	15.569
1532	15.991	15.815	1596	15.021	15.127
1533	16.317	15.881	1597	14.700	14.884
1534	15.258	15.274	1598	15.924	15.814
1535	15.347	15.258	1599	15.728	15.874
1536	15.825	15.430	1600	16.215	15.979
1537	15.634	15.656	1601	15.238	15.169
1538	14.960	15.119	1602	15.500	15.544
1539	15.342	15.355	1603	15.943	15.727
1540	14.501	14.783	1604	15.164	15.093
1541	15.370	15.363	1605	15.196	14.937
1542	16.633	16.256	1606	15.043	15.061
1543	14.880	14.722	1607	14.125	14.318
1544	14.731	14.927	1608	14.329	14.685
1545	15.640	15.438	1609	16.060	15.697
1546	15.781	15.714	1610	15.434	15.418
1547	16.788	16.297	1611	16.662	15.920
1548	16.333	16.069	1612	15.270	15.223
1549	15.854	15.657	1613	15.346	15.086
1550	15.337	15.308	1614	16.330	16.028
1551	15.482	15.484	1615	14.576	14.606
1552	15.402	15.611	1616	16.213	15.702
1553	15.366	15.472	1617	14.599	14.758
1554	15.734	15.642	1618	15.954	15.731
1555	14.740	14.856	1619	15.868	15.714
1556	14.857	15.208	1620	14.937	14.801
1557	14.977	15.164	1621	15.403	15.283
1558	15.250	15.494	1622	15.505	15.427
1559	15.091	15.311	1623	15.287	15.307
1560	15.223	15.184	1624	14.897	15.130
1561	15.401	15.412	1625	15.180	15.135
1562	15.380	15.083	1626	15.547	15.442
1563	15.457	15.186	1627	14.694	14.776
1564	15.488	15.386	1628	15.969	15.647
1565	15.546	15.248	1629	15.259	15.549
1566	16.386	16.021	1630	15.887	15.795

YEAR	BCK.RECON	LJH.RECON	YEAR	BCK.RECON	LJH.RECON
1631	15.304	15.323	1695	14.646	14.883
1632	15.431	15.345	1696	15.909	15.759
1633	15.739	15.693	1697	14.887	14.845
1634	15.038	15.010	1698	15.863	15.497
1635	14.658	14.944	1699	14.943	15.212
1636	15.319	15.288	1700	15.204	15.308
1637	15.195	15.537	1701	14.454	14.774
1638	16.201	15.963	1702	15.638	15.674
1639	15.265	15.203	1703	14.901	15.082
1640	15.753	15.679	1704	15.971	15.867
1641	15.954	15.878	1705	16.257	16.121
1642	15.652	15.621	1706	15.115	15.200
1643	15.425	15.494	1707	16.016	15.827
1644	15.971	15.912	1708	15.461	15.884
1645	15.306	15.366	1709	15.387	15.516
1646	15.629	15.501	1710	15.249	15.387
1647	14.074	14.458	1711	15.542	15.539
1648	14.966	15.224	1712	15.607	15.585
1649	14.732	14.925	1713	15.732	15.679
1650	15.436	15.269	1714	15.042	15.160
1651	14.481	14.823	1715	15.505	15.486
1652	15.727	15.295	1716	16.116	15.949
1653	16.015	15.770	1717	16.210	15.997
1654	15.941	15.648	1718	14.307	14.744
1655	15.949	15.783	1719	14.796	15.161
1656	16.906	16.410	1720	15.154	15.171
1657	15.121	15.084	1721	15.873	15.962
1658	15.753	15.395	1722	14.750	15.014
1659	15.310	15.428	1723	15.122	15.488
1660	15.236	15.336	1724	15.210	15.381
1661	15.764	15.630	1725	14.805	14.950
1662	16.111	15.677	1726	15.998	15.862
1663	16.201	15.914	1727	15.448	15.404
1664	14.255	14.251	1728	15.674	15.600
1665	14.394	14.865	1729	14.295	14.392
1666	15.338	15.433	1730	15.475	15.612
1667	15.950	15.832	1731	16.010	15.779
1668	15.948	15.836	1732	15.806	16.021
1669	15.019	15.237	1733	15.175	15.207
1670	15.408	15.392	1734	14.689	14.995
1671	15.352	15.325	1735	15.092	15.154
1672	14.486	14.790	1736	15.053	15.208
1673	15.504	15.436	1737	14.766	15.110
1674	15.008	15.180	1738	14.679	14.931
1675	15.215	15.360	1739	14.970	14.979
1676	14.731	14.778	1740	16.456	16.259
1677	15.598	15.666	1741	16.024	16.019
1678	16.105	15.837	1742	16.232	15.954
1679	15.320	15.383	1743	16.422	16.077
1680	15.421	15.340	1744	15.822	15.645
1681	14.520	14.772	1745	15.696	15.797
1682	15.577	15.485	1746	14.455	14.487
1683	14.822	14.862	1747	14.780	15.051
1684	16.232	15.996	1748	15.801	15.878
1685	14.683	15.013	1749	16.092	15.923
1686	14.357	15.135	1750	14.934	14.936
1687	14.291	14.907	1751	15.198	15.212
1688	15.675	15.872	1752	15.476	15.284
1689	14.923	15.323	1753	15.913	15.518
1690	15.939	15.858	1754	16.429	16.100
1691	16.065	15.655	1755	15.316	14.915
1692	14.718	14.662	1756	14.678	14.705
1693	15.553	15.413	1757	15.814	15.570
1694	15.117	15.261	1758	15.494	15.460

YEAR	BCK.RECON	LJH.RECON	YEAR	BCK.RECON	LJH.RECON
1759	15.682	15.544	1823	15.480	15.619
1760	15.412	15.196	1824	15.350	15.286
1761	14.926	15.227	1825	15.649	15.700
1762	14.722	14.991	1826	15.929	15.708
1763	14.929	15.283	1827	15.026	15.343
1764	14.735	15.082	1828	15.570	15.474
1765	15.281	15.427	1829	14.106	14.745
1766	15.466	15.355	1830	16.568	16.263
1767	15.671	15.650	1831	15.291	15.414
1768	15.998	15.596	1832	15.995	15.875
1769	15.403	15.271	1833	14.780	15.055
1770	16.021	15.654	1834	14.906	15.226
1771	15.967	15.872	1835	15.738	15.597
1772	15.396	15.494	1836	14.927	15.151
1773	16.194	16.027	1837	14.825	14.831
1774	15.133	15.175	1838	14.905	14.923
1775	15.142	15.377	1839	14.880	15.006
1776	15.246	15.290	1840	15.803	15.563
1777	15.605	15.629	1841	16.239	15.852
1778	15.971	15.387	1842	15.688	15.225
1779	16.143	15.701	1843	15.701	15.540
1780	15.748	15.320	1844	15.498	15.419
1781	15.761	15.676	1845	14.788	15.165
1782	15.198	15.257	1846	15.497	15.488
1783	15.517	15.411	1847	15.585	15.620
1784	14.637	14.828	1848	15.918	15.750
1785	15.042	15.121	1849	14.703	14.910
1786	16.263	15.934	1850	13.900	14.424
1787	13.985	14.373	1851	15.238	15.206
1788	16.134	15.799	1852	15.392	15.440
1789	16.179	15.824	1853	14.784	15.045
1790	16.793	16.379	1854	14.872	14.973
1791	15.367	15.327	1855	16.094	15.822
1792	15.096	14.930	1856	15.455	15.457
1793	15.497	15.142	1857	16.048	15.835
1794	14.952	15.138	1858	15.478	15.500
1795	15.080	15.154	1859	15.711	15.521
1796	15.796	15.508	1860	15.377	15.283
1797	15.378	15.141	1861	16.372	15.884
1798	15.883	15.613	1862	16.226	15.945
1799	15.548	15.408	1863	16.226	16.023
1800	15.434	15.378	1864	15.647	15.764
1801	16.780	16.245	1865	15.025	15.255
1802	15.488	15.467	1866	15.132	15.347
1803	16.014	15.822	1867	15.493	15.477
1804	15.228	15.379	1868	15.469	15.580
1805	14.897	15.057	1869	14.826	14.937
1806	15.740	15.634	1870	15.711	15.637
1807	15.221	15.237	1871	16.295	16.144
1808	15.758	15.745	1872	16.285	15.969
1809	15.531	15.842	1873	15.802	15.430
1810	15.612	15.685	1874	16.120	15.903
1811	16.059	16.101	1875	16.081	15.885
1812	15.105	15.576	1876	15.506	15.475
1813	15.245	15.646	1877	15.304	15.347
1814	14.912	15.249	1878	15.646	15.443
1815	14.478	14.596	1879	14.859	15.001
1816	15.152	14.911	1880	15.816	15.322
1817	16.163	16.042	1881	14.905	14.766
1818	15.345	15.511	1882	15.888	15.531
1819	15.979	15.853	1883	16.317	16.102
1820	16.058	15.863	1884	16.169	15.988
1821	15.434	15.591	1885	15.416	15.431
1822	15.559	15.556	1886	15.850	15.679

YEAR	BCK.RECON	LJH.RECON
1887	15.233	15.042
1888	15.393	15.379
1889	16.473	16.069
1890	16.331	15.919
1891	14.889	14.769
1892	15.158	15.036
1893	15.318	15.251
1894	16.139	15.816
1895	16.275	15.972
1896	15.289	15.472
1897	15.122	15.209
1898	14.814	14.830
1899	13.312	13.146
1900	15.141	15.332
1901	14.745	14.844
1902	14.524	14.753
1903	15.315	15.105
1904	15.686	15.252
1905	14.982	14.880
1906	15.216	15.199
1907	14.554	14.723
1908	15.030	14.997
1909	13.310	13.709
1910	15.508	15.057
1911	15.856	15.247
1912	15.107	14.639
1913	15.587	15.091
1914	15.322	14.943
1915	16.102	16.140
1916	15.481	15.302
1917	15.644	15.538
1918	15.695	15.619
1919	15.978	15.603
1920	16.005	15.917
1921	15.813	15.618
1922	15.470	15.499
1923	14.536	14.806
1924	15.037	15.132
1925	14.694	14.959
1926	15.134	15.538
1927	15.014	15.190
1928	15.377	15.499
1929	14.676	14.568
1930	14.780	15.201
1931	14.485	14.928
1932	15.061	15.513
1933	15.054	15.279
1934	15.118	15.320
1935	15.447	15.339
1936	15.498	15.619
1937	15.301	15.428
1938	15.041	15.382
1939	16.178	16.197
1940	15.340	15.661
1941	14.800	15.038
1942	15.083	15.379
1943	15.015	15.167
1944	15.302	15.488
1945	14.309	14.872
1946	14.417	14.906
1947	15.505	15.634
1948	15.482	15.591
1949	14.851	15.106
1950	14.927	15.181
1951	15.945	15.715
1952	14.566	14.331
1953	15.466	15.192
1954	15.686	15.531
1955	15.945	15.560
1956	15.987	15.663
1957	15.029	14.993
1958	14.914	15.026
1959	15.783	15.639
1960	15.749	15.471
1961	16.118	15.671
1962	15.644	15.076
1963	15.217	15.316
1964	15.068	15.143
1965	15.000	15.339
1966	15.088	15.363
1967	15.679	15.767
1968	16.009	15.883
1969	15.578	15.575
1970	15.589	15.759
1971	16.459	16.333
1972	15.447	15.162
1973	15.882	16.049
1974	15.997	15.779
1975	15.609	15.621
1976	15.268	15.193
1977	15.820	15.792
1978	15.512	15.623
1979	16.011	16.103
1980	15.076	15.317
1981	16.543	16.475
1982	15.072	15.238
1983	15.807	15.952
1984	15.335	15.597
1985	15.326	15.632
1986	16.122	16.194
1987	15.359	15.563
1988	16.225	16.089
1989	16.124	16.058
1990	15.524	15.595
1991	15.802	15.897